University of Alberta

Sedimentology and Stratigraphic Architecture of the Cenomanian Bahariya Formation, Western Desert, Egypt

by

Cynthia Ann Hagstrom

©

A thesis submitted to the Faculty of Graduate Studies and Research in partial fulfillment of the requirements for the degree of Master of Science

Department of Earth and Atmospheric Sciences

Edmonton, Alberta

Fall 2004

In compliance with the
Canadian Privacy Legislation
some supporting forms
may have been removed from
this dissertation.

While these forms may be included
in the document page count,
their removal does not represent
any loss of content from the dissertation.

0-612-95759-4

The best way out is always through.

- Robert Frost

Acknowledgments

First and foremost, I would like to thank my supervisor, Dr. George Pemberton. You gave me an amazing project and a taste of what it is like to live and work overseas. Your abundant technical resources and financial support definitely made it easier being a graduate student and gave me the opportunity to do things that I would not have done otherwise. Thank-you to my defense committee, Dr. Charlie Stelck and Dr. David Bundle. Your comments, questions and remarks were greatly appreciated.

This project would not have been possible without the scientific interest and financial support of Apache Oil Company (Egypt); I am very grateful for your support. A special thank-you goes to Fred Wehr, the person who was instrumental in putting this project together. Thank-you for your hospitality, enthusiasm, and patience. I hope to see you one day in Calgary. I would also like to acknowledge financial support from NSERC (Julie Payette Scholarship). Their generosity gave me the freedom to concentrate on school and this thesis. If it were not for them I would still be living at home, driving my parents bananas (or would it be the other way around?)

I would not have survived seven weeks in Egypt without the company of Sean Miller. I enjoyed all of our time together, whether it was walking the streets of Cairo or Amsterdam, trying to direct the local taxi driver to our flat, or chatting on the couch watching Quantum Leap. You were a great work and travel companion and I thank-you for putting up with my eccentricities, being a good sounding board for my ideas, and answering my questions honestly.

To Michelle Spila, the Queen of ichnology/sedimentology – I don't think I can ever repay you for all your help. I would have broken down and given up a long time ago if you had not offered your encouragement, support, and brain full of knowledge. Thank-you for being my encyclopedia, sounding board, and generous editor-in-chief. I could not have finished this thesis without you. If you ever need anything (funding?) you know who to ask.

I would like to thank all the members of the IRG. I've truly enjoyed all of our trips, special events, and time together; you are all very smart and talented. A special thank-you goes out to my editors – Michelle Spila, Curtis Lettley, Dwayne Giggs, and Jennifer Marques. Your time and tact is greatly appreciated and your constructive criticism and comments greatly improved this thesis.

Of course, I must thank my family – Mom, Dad, and Michelle. You've believed in me when I was full of doubt and I can finally tell you for certain that I'm not going to be a life-long student (is that a sigh of relief I hear?) You've supported me in everything I've done and I hope I've made you proud. Finally, to John, thanks for your encouragement, reassurance, and friendship. But most of all, thanks for your patience…I look forward to starting a life with you.

TABLE OF CONTENTS

CHAPTER ONE: INTRODUCTION

1.1 Introductory Remarks 1
1.2 Study Area and Well Control 1
1.3 Regional Stratigraphy 4
1.4 Tectonic Setting 5
1.5 Paleogeography 9
1.6 Previous Work and Interpretations 9
1.7 Objectives 11

CHAPTER TWO: DELINEATION OF FACIES AND FACIES ASSOCIATIONS

2.1 Introduction. 12
2.2 Facies Description and Interpretation 12
2.2.1 Facies 1 – Finely Laminated Mudstone and Sandstone 12
Subfacies 1a: Less Than 40 Percent Sand 12
Subfacies 1b - 40 to 70 Percent Sand 16
Subfacies 1c - Greater Than 70 Percent Sand 18
2.2.2 Facies 2 – Heterolithic Sandstone and Mudstone 20
Subfacies 2a - Lenticular Bedded Mudstone 20
Subfacies 2b - Lenticular to Wavy Bedded Mudstone 20
Subfacies 2c - Wavy to Flaser Bedded Sandstone 22
2.2.3 Facies 3 – Flaser Bedded Sandstone 24
2.2.4 Facies 4 – Sandstone with Mud and Organics 26
2.2.5 Facies 5 – Bioturbated Rippled Sandstone 28
2.2.6 Facies 6a – Burrowed Sandy Mudstone 31
2.2.7 Facies 6b – Burrowed Mottled Sandstone 31
2.2.8 Facies 7 – Rippled Sandstone with Carbonaceous Flasers 33
2.2.9 Facies 8a – Rippled to Flaser Bedded Glauconitic Sandstone 35
2.2.10 Facies 8b – Muddy Rippled to Flaser Bedded Glauconitic Sandstone 38
2.2.11 Facies 9 – Horizontally Bedded to Planar Cross-Bedded Glauconitic Sandstone 40
2.2.12 Facies 10 – Cross-Bedded Glauconitic Sandstone 42
2.2.13 Facies 11 – Structureless Glauconitic Sandstone 45
2.2.14 Facies 12 – Brown Organic Shale 45
2.2.15 Facies 13 – Organic Glauconitic Sandstone 47
2.2.16 Facies 14 – Calcareous Shale with Glauconitic Sandstone Interbeds . . . 49

2.2.17 Facies 15 – Shell Hash 49
2.3 Other Significant Units 51
2.3.1 Sideritized Mud Clast Breccia 51
2.3.2 Carbonate Cemented Sandstone 53
2.4 Facies Association Description and Discussion 55
2.4.1 Facies Association 1 – Brackish Bay 55
2.4.2 Facies Association 2 – Tide-Influenced Delta Front 56
2.4.3 Facies Association 3 – Marine Shoreface 57
2.4.4 Facies Association 4 – Tidal Channel 58
2.4.5 Facies Association 5 – Transgressive Embayment 60
2.5 Summary 62

CHAPTER THREE: DEPOSITIONAL HISTORY AND STRATIGRAPHY

3.1 Introduction 63
3.2 Depositional Environments 63
3.2.1 Tide-Dominated Estuaries 63
3.2.2 Tide-Dominated Deltas 66
3.2.3 Tide-Dominated Estuaries Versus Tide-Dominated Deltas 68
3.2.4 Brackish Bay Versus Embayment 70
3.2.5 Incised Valleys 72
3.2.6 The Shoreface 74
3.3 Cross Sections 75
3.4 Stratigraphic Surfaces 80
3.4.1 The *Glossifungites* Ichnofacies 81
3.4.2 Transgressive Surfaces in the Lower Bahariya Formation 83
3.4.3 Regressive Surfaces in the Lower Bahariya Formation 84
3.5 Lower Bahariya Depositional Stages 85
3.5.1 Stage 1 85
3.5.2 Stage 2 90
3.5.3 Stage 3 90
3.5.4 Stage 4 96
3.6 Sequence Stratigraphic Framework 96
3.7 Summary 98

CHAPTER FOUR: SOFT-SEDIMENT DEFORMATION

4.1 Introduction to Soft-Sediment Deformation 100
4.2 Driving Mechanisms and Triggers 100
4.3 Descriptions of Soft-Sediment Deformation Structures 101

4.3.1 Load-Cast Ripples 101
4.3.2 Load Casts 104
4.3.3 Flame Structures 105
4.3.4 Water Escape Structures 106
4.3.5 Concretions 110
4.3.6 Syn-Sedimentary Faulting and Slump Structures 110
4.3.7 Shrinkage Cracks 113
4.4 Paleoenvironmental Significance 116
4.5 Summary 117

CHAPTER FIVE: CONCLUSIONS

5.1 Conclusions 118

APPENDIX A 132

LIST OF TABLES

CHAPTER TWO: DELINEATION OF FACIES AND FACIES ASSOCIATIONS

Table 2.1 Facies table for the lower Bahariya Formation 13

CHAPTER FOUR: SOFT-SEDIMENT DEFORMATION

Table 4.1 Classification scheme for soft-sediment deformation 101

LIST OF FIGURES

CHAPTER ONE: INTRODUCTION

Figure 1.1 Regional maps showing the location of the study area 2
Figure 1.2 Map of the land currently under lease in the Matruh Basin 2
Figure 1.3 Map of the study area showing location of important oil fields 3
Figure 1.4 Stratigraphic column of the Aptian to Santonian of the Western Desert of Egypt 4
Figure 1.5 Structural regions of the Egyptian continental platform 5
Figure 1.6 The stages of tectonic development that affected the northern Western Desert 7
Figure 1.7 Cretaceous global eustatic and Egyptian relative sea level curves 8
Figure 1.8 Late Cenomanian tectonic plate reconstructions 8
Figure 1.9 Paleogeography of Egypt during the Late Cenomanian 10

CHAPTER TWO: DELINEATION OF FACIES AND FACIES ASSOCIATIONS

Figure 2.1 Finely laminated mudstone and sandstone with less than 40 percent sand (Subfacies 1a) 15
Figure 2.2 Finely laminated mudstone and sandstone with 40 to 70 percent sand (Subfacies 1b) 17
Figure 2.3 Finely laminated mudstone and sandstone with greater than 70 percent sand (Subfacies 1c) 19
Figure 2.4 Lenticular bedded mudstone (Subfacies 2a) 21
Figure 2.5 Lenticular to wavy bedded mudstone (Subfacies 2b) 22
Figure 2.6 Wavy to flaser bedded sandstone (Subfacies 2c) 23
Figure 2.7 Flaser bedded sandstone (Facies 3) 25
Figure 2.8 Sandstone with mud and organics (Facies 4) 27
Figure 2.9 Bioturbated rippled sandstone (Facies 5) 29
Figure 2.10 Trace fossils within bioturbated rippled sandstone (Facies 5) 30
Figure 2.11 Burrowed sandy mudstone (Facies 6a) 32
Figure 2.12 Burrowed mottled sandstone (Facies 6b) 34
Figure 2.13 Rippled sandstone with carbonaceous interbeds (Facies 7) 35
Figure 2.14 Rippled to flaser bedded glauconitic sandstone (Facies 8a) 37
Figure 2.15 Muddy rippled to flaser bedded glauconitic sandstone (Facies 8b) 39
Figure 2.16 Horizontally to planar cross-bedded glauconitic sandstone (Facies 9) and structureless glauconitic sandstone (Facies 11) 41
Figure 2.17 Cross-bedded glauconitic sandstone (Facies 10) 43
Figure 2.18 Brown organic shale (Facies 12) and calcareous shale with glauconitic interbeds (Facies 14) 46
Figure 2.19 Organic glauconitic sandstone (Facies 13) 48
Figure 2.20 Shell hash (Facies 15) 50
Figure 2.21 Sideritized mud clast breccia 52
Figure 2.22 Carbonate cemented sandstone 54

CHAPTER THREE: DEPOSITIONAL HISTORY AND STRATIGRAPHY

Figure 3.1 Physical characteristics of a tide-dominated estuary 65
Figure 3.2 Satellite photograph of the Mary River tide-dominated estuary 65
Figure 3.3 Physical characteristics of a tide-dominated delta 67
Figure 3.4 Satellite photograph of the Fitzroy River tide-dominated delta 67
Figure 3.5 Geomorphic facies showing the evolution of an idealized tide-dominated estuary to delta 69
Figure 3.6 Satellite photograph of Jervis Bay, a coastal embayment 71
Figure 3.7 Schematic diagram depicting the development of an incised valley complex 73
Figure 3.8 Schematic shoreface to shallow marine profile 74
Figure 3.9 Sample well log of the lower Bahariya Formation 76
Figure 3.10 Cross-section A to A 77
Figure 3.11 Cross-section B to B 78
Figure 3.12 Cross section C to C 79
Figure 3.13 Expressions of the *Glossifungites* ichnofacies in the lower Bahariya Formation 82
Figure 3.14 Summary composite litholog for the lower Bahariya Formation 86
Figure 3.15 Distribution of facies during depositional Stage 1 87
Figure 3.16 Isopach map of sand distribution of delta lobe 1 88
Figure 3.17 Isopach map of sand distribution of delta lobe 2 89
Figure 3.18 Isopach map of sand distribution of delta lobe 3 91
Figure 3.19 Facies distribution during depositional Stage 2 92
Figure 3.20 Depositional setting during depositional Stage 3 93
Figure 3.21 Isopach map from datum to regressive surface of erosion 95
Figure 3.22 Depositional setting during depositional Stage 4 97

CHAPTER FOUR: SOFT-SEDIMENT DEFORMATION

Figure 4.1 Load-cast ripples, load casts, and flame structures 102
Figure 4.2 Stages of deformation when a ripple sinks into hydroplastic mud 104
Figure 4.3 Suggested mode of formation of syn-depositional load-cast ripples . . . 104
Figure 4.4 Water escape structures and carbonate concretions 106
Figure 4.5 Soft-sediment deformation due to liquefaction or fluid escape 107
Figure 4.6 Syn-sedimentary faults and slumps 112
Figure 4.7 Syneresis cracks 114

CHAPTER ONE: INTRODUCTION

1.1 INTRODUCTORY REMARKS

The purpose of this study is to provide a detailed sedimentologic description of the Cenomanian lower Bahariya Formation in the vicinity of the Khalda Ridge in the Western Desert of Egypt. This subsurface study focuses on delineating the stratigraphic and depositional architecture of the lower Bahariya Formation through the integration of sedimentology, ichnology, and stratigraphy. The high well density in the study area, combined with good coverage and availability of core, creates an excellent opportunity to examine and describe the sedimentology and ichnology, and create a depositional model for a subsurface unit that has rarely been the subject of such detailed study in the past (e.g. Darwish et al., 1994; Metwalli et al., 2000).

The reason for scientific interest in the Bahariya Formation is its value as a hydrocarbon reservoir in the Western Desert. Based on statistics from 2002, over 50 percent of the wells drilled in the Western Desert to date penetrate and produce hydrocarbons from Cretaceous-aged strata. These strata have been assigned 1727 million barrels of oil equivalent (MMBOE) in reserves. In addition to its reservoir potential, the Bahariya Formation is a hydrocarbon source rock within the basin (Dolson et al., 2001).

The ultimate goal of this study is to contribute to a more complete understanding of the Bahariya Formation. The depositional model developed herein will be applied and become a useful predictive tool for future oil and gas exploration and development of Cretaceous strata within the Western Desert.

1.2 STUDY AREA AND WELL CONTROL

The Bahariya Formation is present in the subsurface throughout the northern Western Desert and extends into southern areas of Egypt (Fig. 1.1A). The current study examines cored intervals from wells along the Khalda Ridge, a structural high within the Matruh Basin (Figs. 1.1 and 1.2; Dolson et al., 2001; Wehr et al., 2002). The study area specifically encompasses a region approximately 100 km^2 centered on four oil pools: Hayat, Yasser, Kenz and Salam (Figs. 1.2 and 1.3).

Over 150 wells have been drilled in these four pools and produce oil and gas from the Bahariya Formation and other Cretaceous reservoirs (Fig. 1.3). Conventional core from the lower Bahariya Formation has been recovered from sixteen of these wells, of which thirteen were examined for this project. Core lengths range between 20 and 60 m, with an

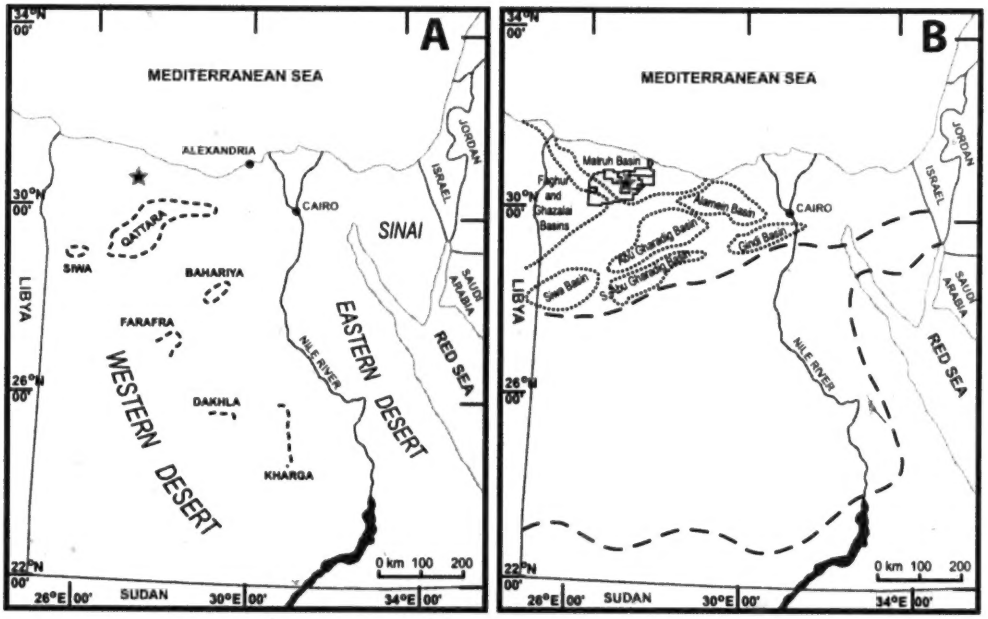

Figure 1.1. Regional maps showing the location of the study area. A) Map of Egypt with study area represented by pink star. Dashed black lines show perimeter of desert oases. B) Map of Egypt showing structural basins (outlined in black) in the northern Western Desert. Land currently under lease is shown in yellow with the study area represented by the pink star. Dashed lines represent the boundaries of the stable and unstable shelves (see Figure 1.5; modified from Dolson et al., 2001).

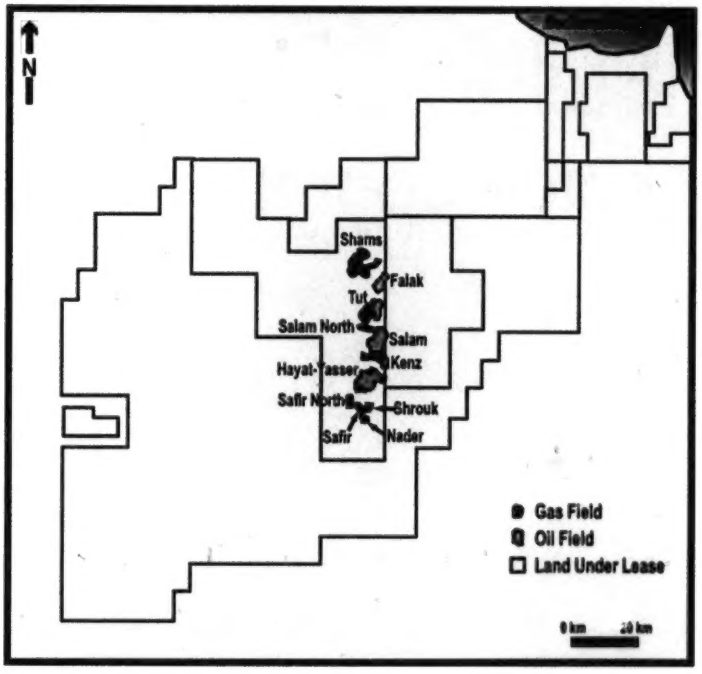

Figure 1.2. Map of the land currently under lease in the centre of the Matruh Basin (yellow). Oil and gas pools along the Khalda Ridge are shown in green and red, respectively. Specifically, this study looks at cored intervals from wells of the Hayat, Yasser, Kenz, and Salam fields (modified from Wehr et al., 2002).

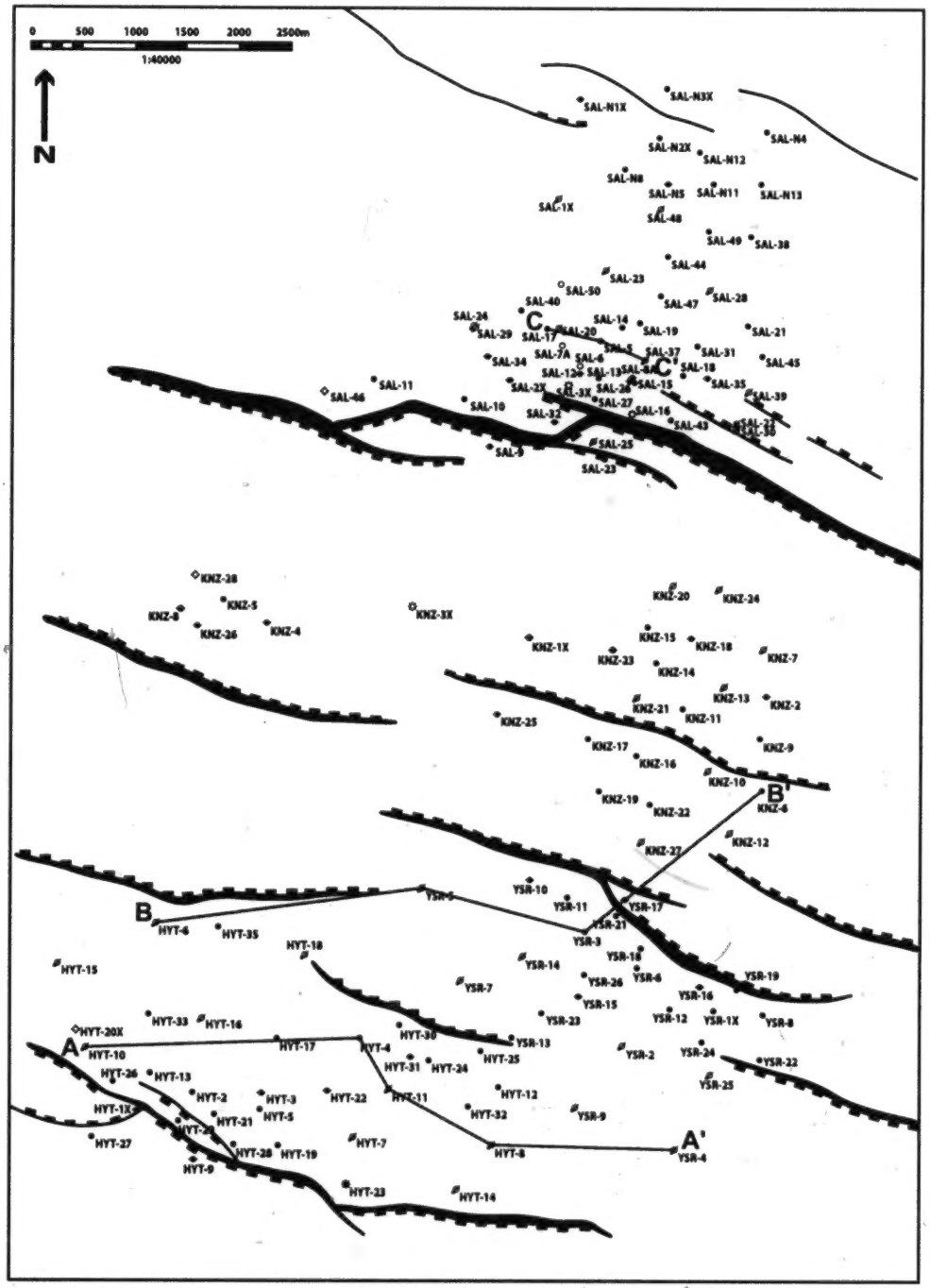

Figure 1.3. Map of the study area showing the relative positions of the Hayat (HYT), Yasser (YSR), Kenz (KNZ), Salam (SAL) oil fields. Cross section lines discussed in Chapter 3 are highlighted in red. Thick black lines indicate location of present-day normal faults. Small black squares present along the faults indicate the direction of the hangingwall.

average of 45 m. In total, about 600 m of core was examined for this study.

1.3 REGIONAL STRATIGRAPHY

The Cenomanian Bahariya Formation conformably overlies sandstones of the Albian Kharita Formation and is located stratigraphically below carbonates of the Cenomanian-Turonian Abu Roash Formation (Fig. 1.4). The Albian represents a regressive phase in Egypt s geological history when shallow marginal marine settings in the northern Western Desert received sediment (Kharita Formation) sourced from an elevated eroding massif to the south (Said, 1990). This regressive phase was followed by a transgressive phase commencing in the Early Cenomanian, when marginal marine clastics and carbonates of the Bahariya Formation were deposited. Transgression continued through to the Turonion when fully marine conditions prevailed, permitting deposition of Abu Roash Formation carbonates (Said, 1990).

In the proximity of the Khalda Ridge, the Bahariya Formation has been informally subdivided into upper and lower units (Fig. 1.4). The lower unit is a clastic dominated succession approximately 60 to 120 m thick, whereas the upper unit is dominated by a mixed carbonate-clastic regime. For a detailed description of the upper unit the reader is

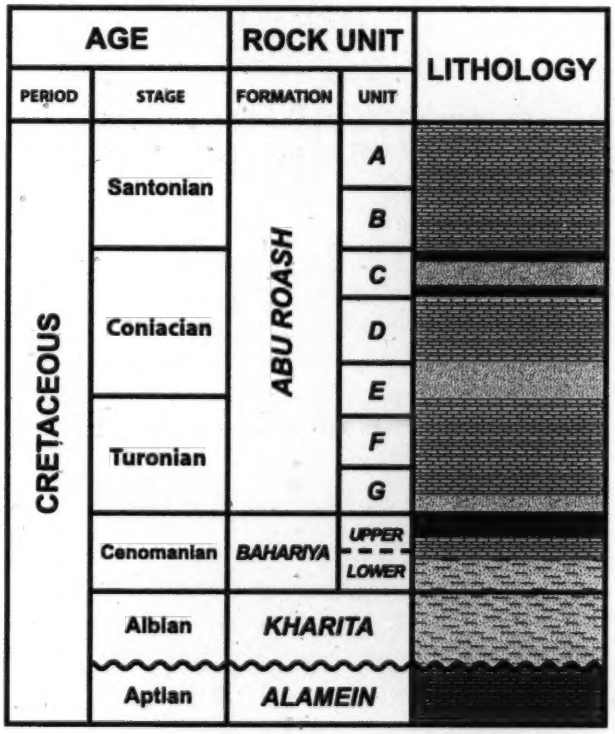

Figure 1.4. Stratigraphic column for the Aptian to Santontion of the northern Western Desert of Egypt (modified from Wehr et al., 2002).

referred to Wehr et al. (2002).

The Bahariya Formation outcrops at the Bahariya Oasis, a large natural depression located in the Western Desert. At this locality, the Bahariya Formation was initially thought to be Early Cenomanian (Stromer, 1914; Blanckenhorn, 1921) to Late Cenomanian in age (Dominik, 1985). However, more recent palynological studies have concluded that in the northern Western Desert, the base of the Bahariya Formation marks the Albian/Cenomanian boundary (El Beialy, 1994).

1.4 TECTONIC SETTING

Egypt occupies part of the large North African continental platform that extends westward from Egypt to the Atlantic Ocean through Libya, northern Algeria, and Morocco (Kerdany and Cherif, 1990). The Egyptian continental platform has historically been subdivided into three regions: the stable and unstable shelves, and the Nubian Shield (Fig. 1.5; Said, 1962; Meshref, 1990). The unstable shelf is located between the Mediterranean coast and stable shelf, where the southern border is an arbitrary line that generally corresponds to the Kattaniya High (Kerdany and Cherif, 1990). The unstable shelf is characterized by a deep mobile basement, a thick sedimentary column, and an overall

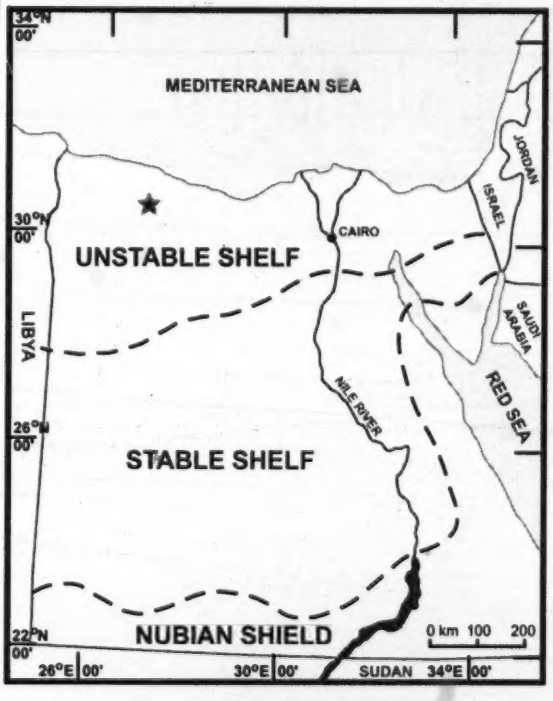

Figure 1.5. The structural regions of the Egyptian continental platform. Pink star indicates study area (modified from Meshref, 1990).

complex structure generated by Mesozoic Tethyan plate movements (Kerdany and Cherif, 1990). The older Mesozoic and Tertiary structures of the unstable shelf in the north Western Desert are hidden from the surface by a blanket of younger Tertiary deposits (Kerdany and Cherif, 1990). The stable shelf, located between the unstable shelf and the Nubian Shield, has a high basement and a sedimentary column less than 1000 m thick. Located in the southern regions of Egypt, the Nubian Shield is an aggregate of terranes and consists of igneous and metamorphic basement rocks (Said, 1962).

Three stages of tectonic development affected the northern portion of the Western Desert: Jurassic rifting, the development of a Cretaceous passive margin, and Syrian Arc Deformation (Fig. 1.6; Dolson at al., 2001).

Triassic/Jurassic Rifting

The break-up of Pangaea and the opening of the proto-Mediterranean/Neotethys Sea in the Late Triassic resulted in rifting of the Egyptian continental margin that continued through the Jurassic and possibly into the Early Cretaceous (Meshref, 1990; Dolson et al., 2001). The Triassic and Jurassic sedimentary record of northern Egypt records the stages of rift development from rift initiation through to post-rift sag (Dolson et al., 2001). The first marine Mesozoic transgression into northern Egypt occurred simultaneously with opening of the Neotethys Sea (Hantar, 1990).

Cretaceous Passive Margin

The Early Cretaceous began with an extended period of thermal sag in which a wide passive continental margin developed across the northern edge of the African Plate (Dolson et al., 2001). During the Cretaceous, the Egyptian portion of the passive margin witnessed a number of transgressive cycles (Fig. 1.7; Said, 1990). South-directed transgressions during the Aptian, Cenomanian, and Coniacian created very shallow seas in northern Egypt, where siliciclastic and carbonate marginal-marine sediments were deposited in tidal, fluvial, and estuarine settings (Said, 1990; Dolson et al., 2001).

A tectonic plate reconstruction for Africa during the Late Cenomanian is shown in Figure 1.8. At this time, the paleo-equator is several hundreds of kilometers north of its present day location. Rifting between South America and Africa has started and the Mid-Atlantic Ridge is visible. The African and Eurasian plates are heading along a collision course as the Neo-Tethys sea is begins to close.

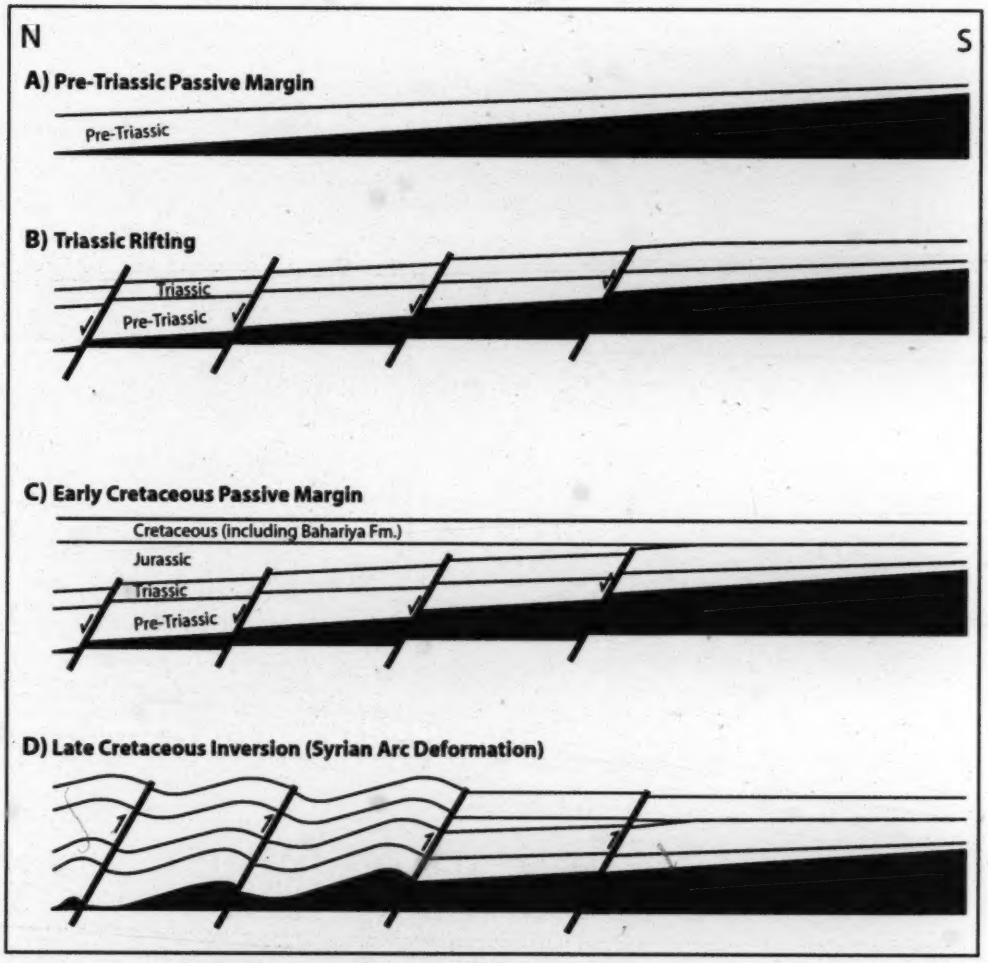

Figure 1.6. The stages of tectonic development that affected the northern portion of the Western Desert (modified from Bauer et al., 2003).

Syrian Arc Deformation

Incipient closure of the Neotethys Sea occurred during the Late Cenomanian to Turonian and resulted in regional uplift of the Egyptian passive margin (Dolson et al., 2001). This uplift caused inversion of the Triassic and Jurassic normal faults and created a series of northeast/southwest trending folds known as "Syrian Arcs" (Moustafa and Khalil, 1990). By the Early Campanian, most of the deformation attributed to rift inversion had ceased and the region was flooded by a Campanian-Maastrichtian transgression (Said, 1990; Dolson et al., 2001). Folds and structural closure associated with the Syrian Arc trends form the majority of productive hydrocarbon traps in Western Desert (Dolson et al., 2001).

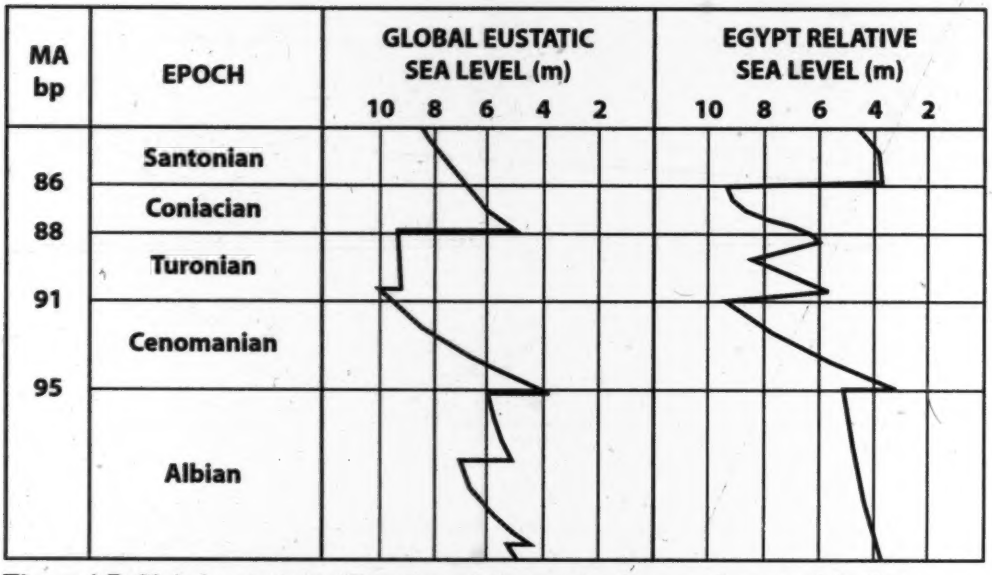

Figure 1.7. Global eustatic and Egyptian relative sea level curves for part of the Cretaceous (modified from Said, 1990).

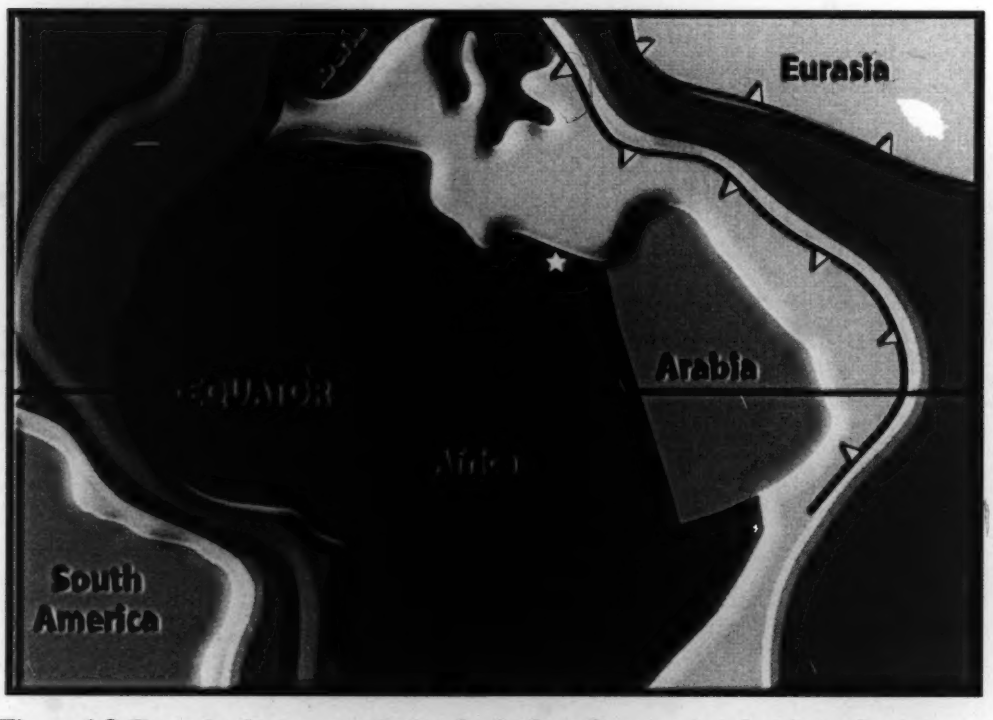

Figure 1.8. Tectonic plate reconstruction for the Late Cenomanian showing paleo-equator. White star indicates study area (modified from Research Center for Marine Geosciences).

1.5 PALEOGEOGRAPHY

Paleogeographical information for the Western Desert during the Cenomanian is scarce (Fig. 1.9). According to Said (1990), marine waters covered most of Egypt during the Early Cenomanian. During the Middle to Late Cenomanian, a transgression pushed southward across Egypt and formed a narrow passageway flanked by structural highs to the west and east. This passageway is thought to have behaved as an estuary where marginal marine conditions prevailed. Sediments of the Bahariya Formation deposited in tidal flat, estuarine, and fluvial settings filled this passageway and contained frequent marine intercalations. Farther south, the Bahariya Formation grades into the Maghrabi Formation, which is distinguished by lesser marine influence. In the Gulf of Suez, shallow marine conditions prevailed and the Raha and Galala Formations were deposited. In northern Sinai, deeper marine conditions existed and the more calcareous sediments of the Halal Formation were laid down.

1.6 PREVIOUS WORK AND INTERPRETATIONS

The Bahariya Formation was first studied in the Bahariya Oasis, where it forms the floor of this large natural depression (for location see Fig. 1.1a). The first descriptions were carried out by Ball and Beadnell (1903), which inspired later detailed work by other authors including Stromer (1914), Blanckenhorn (1921), Said (1962), Akkad and Issawi (1963), Said and Issawi (1963), Soliman et al. (1970), El Hashemi (1978), Soliman and El Badry (1980), Franks (1982), and Dominik (1985).

At the Bahariya Oasis, the Bahariya Formation is a clastic sequence of sandstone, siltstone, and finer grained deposits (Abdalla and El Bassyouni, 1985). The sequence has been divided into three members: the lower fluvatile Gebel Ghorabi, the middle estuarine Gebel Dist, and the upper marine or lagoonal El Heiz (Dominik, 1985; Hantar, 1990). Over time, the environmental interpretations for the Bahariya Formation at the oasis have changed from fluvio-marine (Said and Issawi, 1963; Slaughter and Thurmond, 1974) to deltaic (Soliman and El Badry, 1980), to an estuarine/nearshore setting (Abdalla and El Bassyouni, 1985; Allam, 1986).

With the commencement of drilling for hydrocarbons in the Western Desert in the 1970s, the paleoenvironmental characteristics of the Bahariya Formation in the subsurface have been studied by authors such as Soliman et al. (1970), Soliman and El Badry (1970), Barakat and Arafa (1972), Dia El Din (1974), Baraket et al. (1976), Soliman and El Badry (1980), Phillip et al. (1980), Allam (1986), El Anbaawy and El Shazly (1991), Darwish et

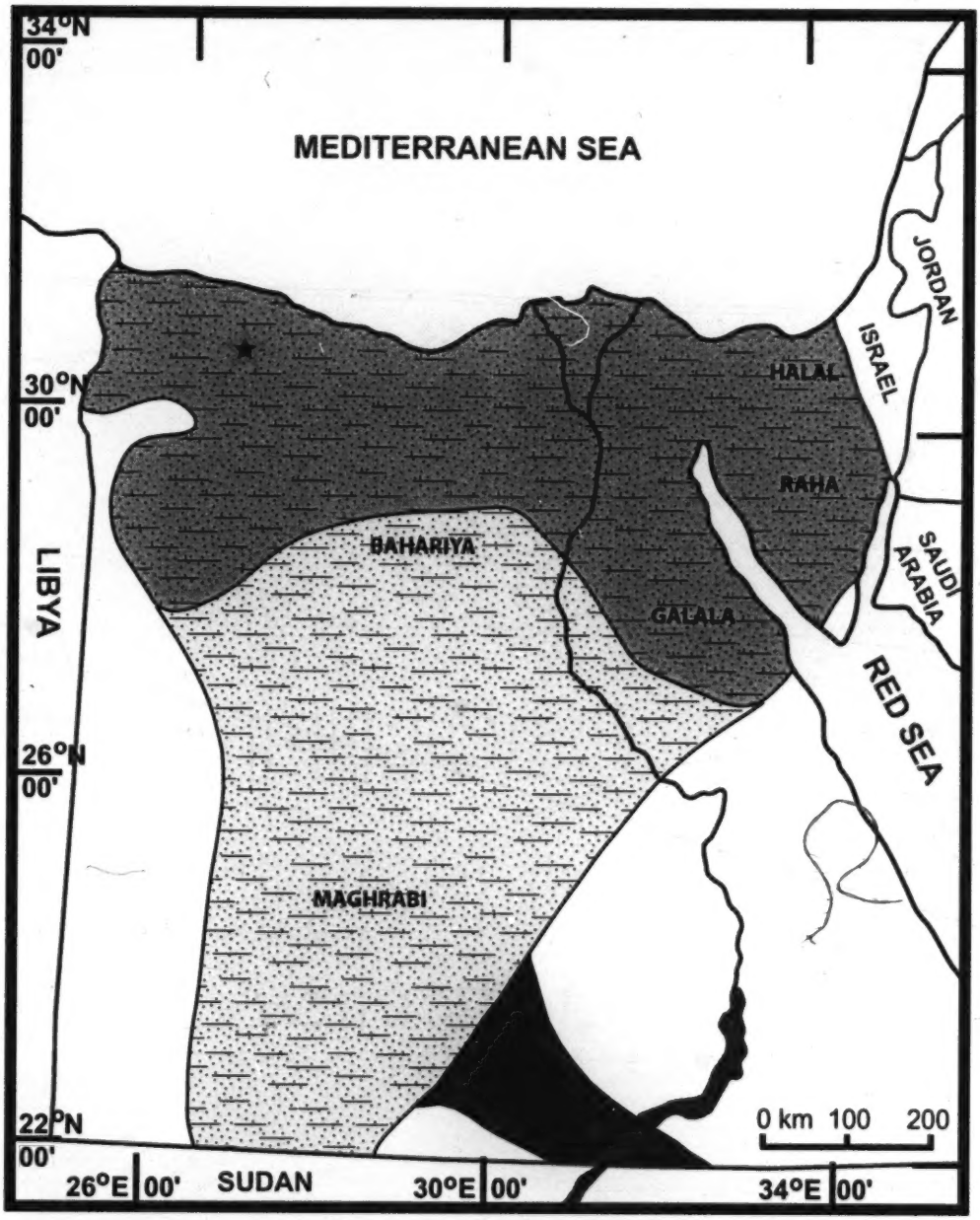

Figure 1.9. Paleogeography of Egypt during the Late Cenomanian. For explanation of formation names in black see section 1.5. Green - open marine deposits; yellow - estuarine deposits; red - fluvial depostis; white - positive areas (modified from Said, 1990).

al. (1994), and Metwalli et al. (2000). Study of lower Bahariya cores from these wells has lead to a shallow marine shelf to tidal flat interpretation (El Sheikh, 1990; Darahem et al., 1990; Metwalli et al., 2000).

1.7 OBJECTIVES

The overall goal of this project is to better understand the facies relationships and depositional setting of the lower Bahariya Formation. Specific objectives of this study are as follows:

1. Subdivision of lower Bahariya Formation into sedimentary facies.
2. Group the individual facies into facies associations that represent genetically related packages of sediment that coexisted within an overall larger depositional system.
3. Construct a genetic stratigraphic framework based on significant stratigraphic surfaces and lateral facies relationships.
4. Create a multi-stage depositional model and reconstruct the changes that occurred in the depositional environment over time.

Objectives 1 and 2 are addressed in Chapter 2, with complete descriptions and interpretations of the sedimentary facies and facies associations. Chapter 3 covers objectives 3 and 4, and includes an explanation of the significant stratigraphic surfaces and descriptions of the general depositional environments and depositional model. In addition to the these objectives, a chapter on the morphology and genesis of soft-sediment deformation structures in the lower Bahariya Formation has also been included (Chapter 4).

CHAPTER TWO: DELINEATION OF FACIES AND FACIES ASSOCIATIONS

2.1 INTRODUCTION

Based on unique physical and biological characteristics observed in core, the lower Bahariya Formation has been divided into fifteen facies. These characteristics include physical and biogenic sedimentary structures, lithologic composition, and grain size. The facies in this chapter are presented in rough depositional order, as many facies occur at more than one stratigraphic level. These facies are subsequently assigned to five facies associations, which are defined as groups of genetically related facies that occur together in complex depositional systems.

Facies interpretations are based on the biologic and hydrodynamic processes that were operating during deposition, as evidenced by the composition and structure of the rock. The distinguishing features and interpretation for each facies are summarized in Table 2.1. Interpretation of the facies associations is based on the distribution and arrangement of facies within the study area, in addition to the character of their constituent facies. The lower Bahariya Formation is divided into five facies associations that represent deposition in marginal-marine to marine settings: brackish bay, tide-influenced delta front, marine shoreface, tidal channel, and transgressive embayment.

A few facies are encountered only rarely in the study area and are located at the base or top of a core. These units have been excluded from the study due to a lack of data and their location outside the interval of principle interest.

2.2 FACIES DESCRIPTION AND INTERPRETATION

2.2.1 Facies 1 – Finely Laminated Mudstone And Sandstone (F1)

Based on sand content, Facies 1 is divided into three intergradational subfacies.

<u>Subfacies 1a - Less Than 40 Percent Sand (F1a)</u>

Description

Subfacies 1a (Fig. 2.1) is limited to the southern portion of the study area and occurs in Hayat-10, Hayat-11, Hayat-8, and Kenz-6. It attains a maximum thickness of about 8 m, although it could be locally thicker as its lower contact is not consistently cored.

This subfacies contains very fine grained sand interlaminated with mud on a

FACIES	LITHOLOGY	SEDIMENTARY STRUCTURES	ICHNOFOSSILS	DEPOSITIONAL ENVIRONMENT
F1	Finely interlaminated fine to very fine grained sandstone and mudstone	lenticular bedding with flat lenses, current ripples, wave ripples, herringbone cross-stratification, syneresis cracks	Pl, Lo, Te, Gy, Th, Si, Sk, Ch, Ar, Be	Brackish Bay
F2	Interbedded fine to very fine grained sandstone and mudstone	Lenticular, wavy and flaser bedding, herringbone cross-bedding, current and wave ripples, syneresis cracks, flat sand lenses, planar bedding	Pl, Lo, Te, Gy, Th	Brackish Bay, Tidal Flat, Tidal Point Bar
F3	Very fine to fine grained sandstone with mudstone laminae	Flaser bedding, herringbone cross-stratification, rare lenticular and wavy bedding	Pl, Pa, Th	Tidal Shoal
F4	Very fine to fine grained sandstone with mudstone beds, mud content less than 15%	Wave ripples, low to high angle planar cross-bedding, rare wavy bedding, hyperpycnal mud flows	Pl, Pa, Th, Te, Sk	Delta Front
F5	Very fine to fine grained sandstone with common thin mud beds	Wave ripples, wavy bedding, syneresis cracks, hyperpycnal muds	Pa, Th, Op, Pl, Ch, Si, Ro, Lo, Be	Delta Front
F6a	Thin mudstone interbedded with thicker sandy bioturbated mudstone	Wave ripples, thinly interbedded planar-bedded sand and mud	Rh, As, Zo, Ch, Pl, Pa, Th	Lower Shoreface (Distal?)
F6b	Fine grained muddy sandstone	Not visible due to abundant bioturbation	Op, Sc, As, Pa	Lower Shoreface (Proximal?)
F7	Very fine to fine grained sandstone	Wave ripples, combined flow ripples, organic rich mud drapes and flasers, herringbone cross-stratification, horizontal bedding	Pa, Sk	Middle Shoreface
F8a	Very fine to fine grained glauconitic sandstone with less than 10% mudstone	Current ripples, horizontal bedding, herringbone cross-bedding, flaser bedding, climbing ripples, wave ripples	Pa, fug, Ro, Di, Sk, Ma, cryptic	Tidal Channel
F8b	Very fine to fine grained glauconitic sandstone with mudstone content between 5% and 30%	Current ripples, wave ripples, horizontal bedding herringbone cross-stratification, wavy and flaser bedding, syneresis cracks	Pl, Pa, Lo, Te	Tidal Shoal, Tidal Channel
F9	Very fine to fine grained glauconitic sandstone	Horizontal bedding, low to high angle planar bedding, current ripples, mud couplets, scour surfaces	Pa, cryptic	Tidal Channel

Table 2.1. Facies table for the lower Bahariya Formation.

FACIES	LITHOLOGY	SEDIMENTARY STRUCTURES	ICHNOFOSSILS	DEPOSITIONAL ENVIRONMENT
F10	Very fine to medium grained glauconitic sandstone	Trough to high angle planar cross-bedding, current ripples, horizontal bedding, herringbone cross-stratification, flaser bedding, scour surfaces	Pa, cryptic	Tidal Channel
F11	Fine grained glauconitic sandstone	None, faint low angle planar cross-bedding	Cryptic?	Tidal Channel
F12	Brown, organic rich shale with thick, very fine grained sandstone interbeds up to 5 cm thick	Ripples, horizontal bedding, syneresis cracks	Pl	Proximal Embayment
F13	Fine to coarse grained organic rich glauconitic sandstone with mudstone	Wave ripples, wavy bedding, horizontal bedding, low to high angle planar cross-bedding	Pa, Pl	High Energy Deposits Within Proximal Embayment
F14	Calcareous shale with fine grained glauconitic sandstone interbeds	Horizontal bedding, ripple cross-bedding, lenticular bedding	Pl, Th, Ch	Distal Embayment
F15	Shell hash in calcareous shale, sandstone or glauconitic matrix	None, common to pervasive disarticulated and articulated oyster shells	None	Transgressive Lag

Table 2.1 ***(Cont.).*** Facies table for the lower Bahariya Formation. Key to abbreviated ichnogenera: Ar: *Arenicolites*, As: *Asterosoma*, Be: *Bergaueria*, Ch: *Chondrites*, cryptic: cryptic bioturbation, Di: *Diplocraterion*, fug: fugichnia, Gy: *Gyrolithes*, Lo: *Lockeia*, Ma: *Macaronichnus*, Op: *Ophiomorpha*, Pa: *Palaeophycus*, Pl: *Planolites*, Rh: *Rhizocorallium*, Ro: *Rosselia*, Sc: *Scolicia*, Si: *Siphonichnus*, Sk: *Skolithos*, Te: *Teichichnus*, Th: *Thalassinoides*, Zo: *Zoophycus*.

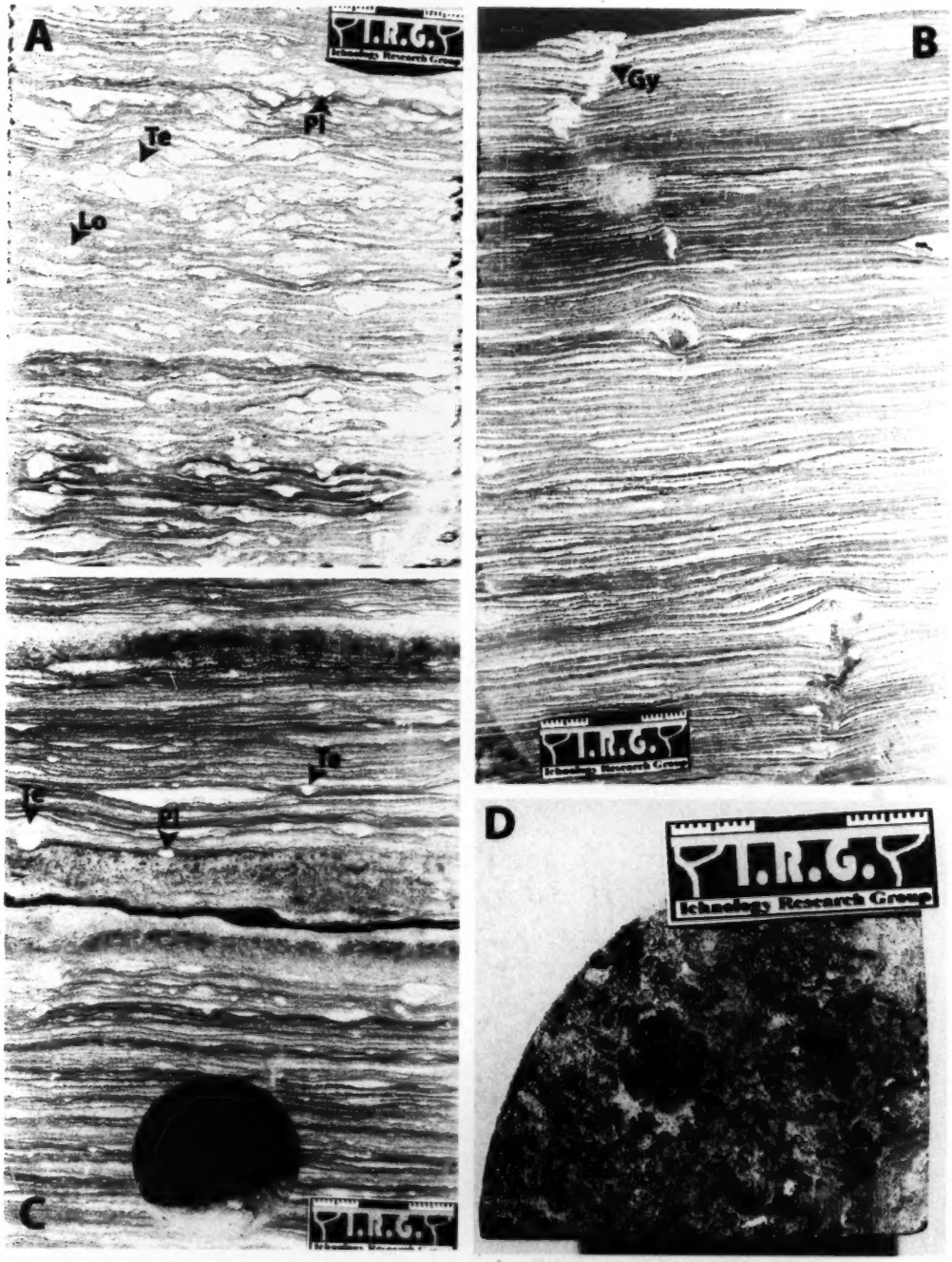

FIGURE 2.1. Finely laminated mudstone and sandstone with less than 40 percent sand (subfacies 1a). A) Moderately bioturbated with *Teichichnus* (Te), *Planolites* (Pl) and *Lockeia* (Lo). B) Sideritized mud laminae and rare bioturbation with *Gyrolithes* (Gy). C) Sideritized sands beds with abundant *Planolites*. D) Bedding plane view showing abundant organic material.

millimetre-scale (Fig. 2.1B). Sedimentary structures include planar lamination, lenticular bedding with flat sand lenses, and rare ripples. Sand laminae and lenses thicker than a few millimetres are typically deformed and sunken into underlying mud. Sand-filled cracks are occasionally present.

Overall, this unit displays rare to moderate bioturbation (Fig. 2.1A). Traces can be grouped into two categories: 1) small burrows less than 1 cm in size that usually occur in large numbers, and 2) large, isolated burrows up to 5 cm long. The most common small ichnogenera are *Planolites*, *Teichichnus*, *Gyrolithes*, *Chondrites* and *Lockeia,* while rare *Thalassinoides* and *Siphonichnus* represent the category of larger trace fossils. Trace fossils and load-cast ripples are easily confused due to similar size and expression in core.

Sideritization and iron staining within this unit is high and is usually focussed on mud beds or sandy beds abundantly bioturbated with *Planolites* (Fig. 2.1C) Disseminated and nodular pyrite is rare and organic matter is locally abundant along bedding planes (Fig. 2.1D). Sideritized mud clast breccias are found within and at the top of this subfacies.

Subfacies 1b - 40 to 70 Percent Sand (F1b)

Description

Subfacies 1b is found throughout the study area but is most common in the Hayat and Yasser fields. Small asymmetric and symmetric ripples and flat sand laminae are the dominant sedimentary structures (Fig. 2.2). The cross-laminae within the asymmetric ripples rarely dip in opposing directions. Lenticular and flaser bedding are also common.

Bioturbation is rare, although some beds show moderate local burrowing. Biogenic structures are small and simple with *Planolites, Chondrites,* and *Lockeia* dominating the trace fossil assemblage (Fig. 2.2A). *Teichichnus*, *Siphonichnus*, *Gyrolithes,* and diminutive *Bergaueria* are less frequently found.

Small-scale syn-sedimentary deformation is restricted to occasional load-cast ripples. Large-scale deformation features, such as pillar structures, contorted bedding, and syn-sedimentary faulting, occur in moderate abundance. Sand lenses occasionally contain nodular and/or disseminated pyrite (Fig. 2.2B). Iron staining and sideritization of mud beds is rare to common. Sand-filled cracks are also rare to common in abundance.

In Hayat-10, a variation of subfacies 1b displays common to abundant bioturbation with a diverse assemblage of *Rhizocorallium*, *Bergaueria*, *Arenicolites*, *Teichichnus*, *Chondrites*, *Planolites,* and *Thallassinoides* (Figs 2.2C, D). Although bioturbation has masked many of the physical sedimentary structures, lenticular bedding and fine sand laminations are visible. Sand-filled cracks are absent, while iron staining is widespread.

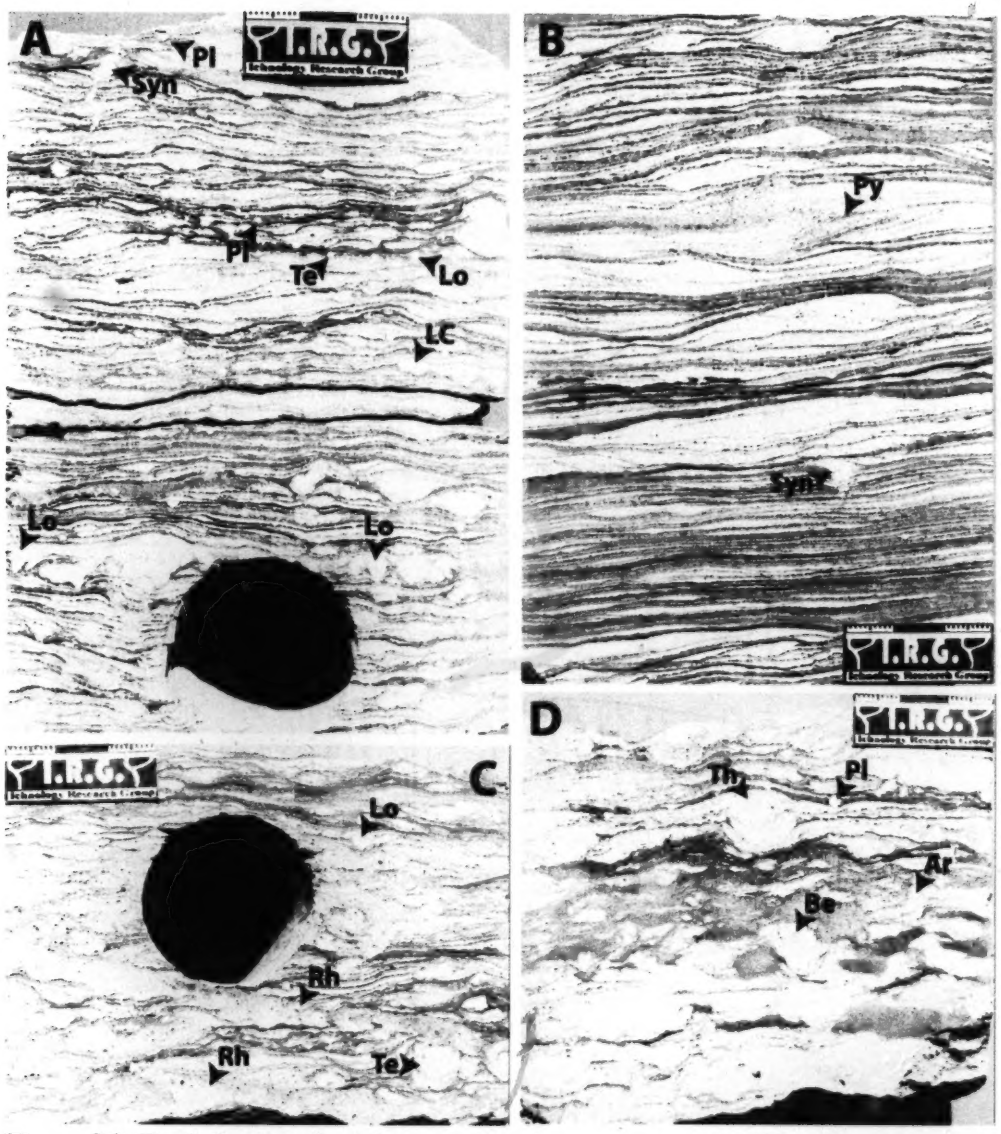

Figure 2.2. Finely laminated mudstone and sandstone composed of 40 to 70 percent sand (subfacies 1b). A and B) Rare to moderate bioturbation with *Planolites* (Pl), *Teichichnus* (Te), *Lockeia* (Lo). Other features include syneresis cracks (Syn), load casts (LC) and pyrite nodules (Py). C and D) variation of subfacies 1b displaying abundant bioturbation with *Lockeia* (Lo), *Rhizocorallium* (Rh), *Teichichnus* (Te), *Planolites* (Pl), *Bergaueria* (Be) and *Arenicolites* (Ar).

Soft-sediment deformation is common in the form of load-cast ripples and syn-sedimentary microfaulting.

Subfacies 1c - Greater Than 70 Percent Sand (F1c)

Description

Facies 1c is found throughout the study area and contains greater than 70 percent very fine grained sand (Fig. 2.3). The dominant sedimentary structures are planar laminated sand and mud beds, and symmetric ripples. Ripple foresets are difficult to distinguish but generally dip in one direction. Rare, thin (less than 5 cm) beds of sandstone with mud and organics (Facies 4) are present.

Bioturbation is moderate in abundance with *Planolites*, *Teichichnus*, *Chondrites*, and *Lockeia* occuring as the most common burrows. *Siphonichnus*, *Arenicolites*, and *Gyrolithes* occur in lesser abundance. Sand-filled cracks are very rare. Deformation is also rare and usually consists of contorted bedding, load-cast ripples, and load casts with flame structures. Syn-sedimentary microfaulting is locally pervasive.

Disseminated and nodular pyrite is common in sand beds. Siderite and iron staining are generally rare to moderate, but locally abundant.

Facies 1 Interpretation

The finely interbedded nature of this facies indicates frequent alternation between bedload and suspension deposition. Asymmetric and symmetric ripples indicate current, and oscillatory or combined flow, respectively. Ripple foreset orientations indicate one dominant flow direction with rare bidirectional transport, which is suggestive of deposition by tidal currents (Nio and Yang, 1991).

There is considerable variation in the sand content of Facies 1. An increase in sand abundance within this facies could be explained by increasing proximity to a point sediment source within the system, or by an overall increase in current or wave energy.

The ichnology of this facies is dominated by a low diversity assemblage of small, simple burrows including *Planolites*, *Teichichnus*, *Lockeia*, and *Chondrites*. These traces were made by trophic generalists and are typical of brackish water environments (Pemberton and Wightman, 1992). Diminutive *Bergaueria* are also common in brackish water settings (Pemberton, pers. comm.).

Sand-filled cracks are attributed to syneresis (Burst, 1965; Plummer and Gostin, 1981). The presence of syneresis cracks along with coexistence of pyrite with siderite are thought to be indicative of organic-rich brackish water settings with fluctuating salinity (Wightman et al., 1987). Siderite formation requries an availability of iron, rapid burial of organic material, and a low supply of water sulfate that allows for methanogenic reactions (Baird et al., 1986). These conditions are met within fresh to brackish water environments,

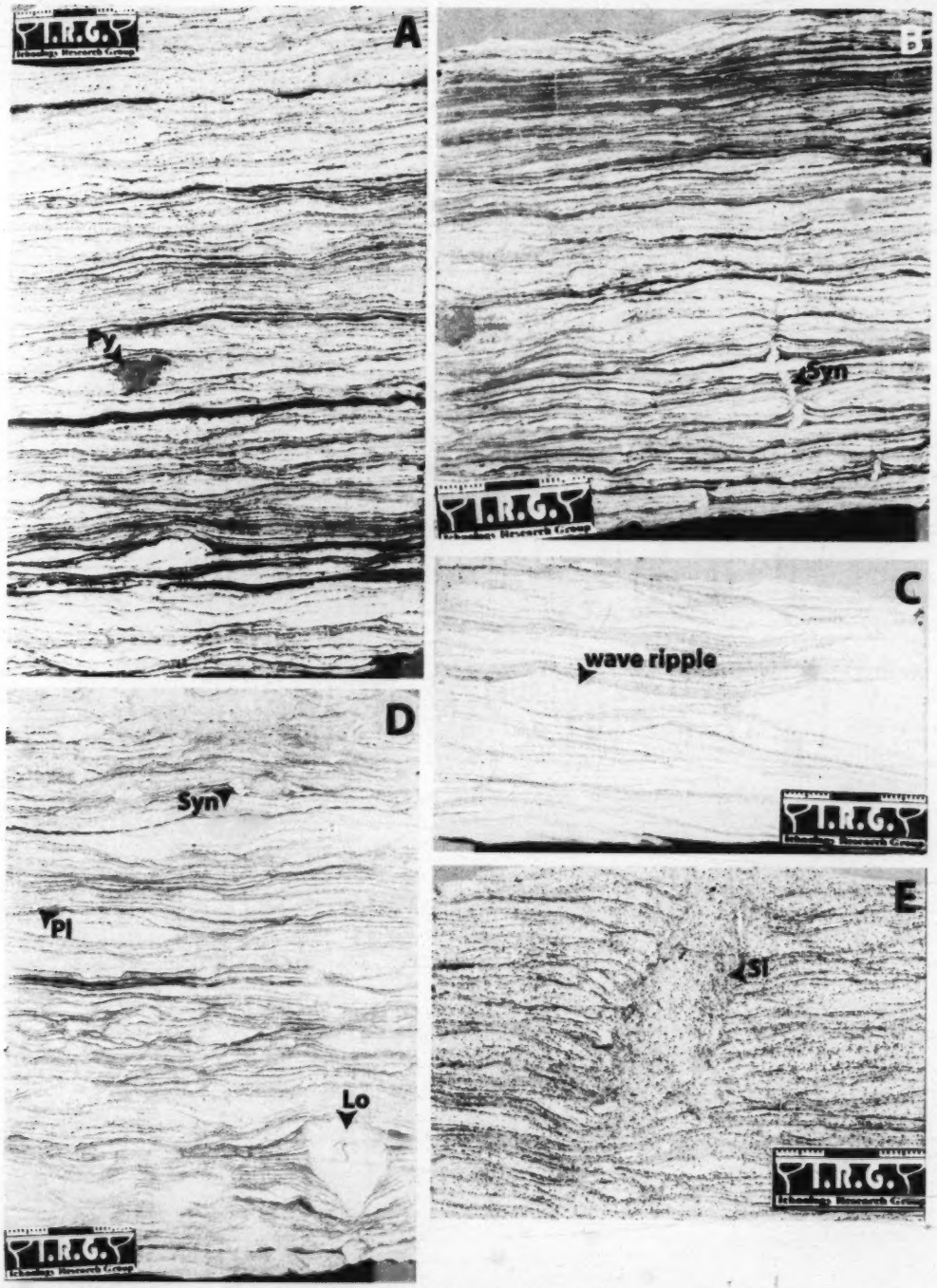

Figure 2.3. Finely laminated mudstone and sandstone with greater than 70 percent sand. Features include A) pyrite nodules (Py); B) syneresis cracks (Syn); and C) wave ripples. Bioturbation is rare and includes D) *Planolites* (Pl), *Lockeia* (Lo); and E) *Siphonichnus* (Si).

where siderite formation most commonly occurs (Baird et al., 1986). The abundance of organic material suggests an overall low energy environment (Wightman et al., 1987).

A variation of subfacies 1b contains a high diversity, high density trace fossil assemblage comprised of traces representing relatively complex behaviour such as *Rhizocorallium*. Such traces are typically associated with more saline water under the influence of fully marine processes (Pemberton et al., 2001).

2.2.2 Facies 2 – Heterolithic Sandstone And Mudstone

Facies 2 contains the range of "tidal" sedimentary structures from lenticular to wavy to flaser bedding (Reineck and Wunderlich, 1968; Reineck and Singh, 1980). The subdivision of this facies is based on the dominant type of bedding.

Subfacies 2a - Lenticular Bedded Mudstone (F2a)

Description

Subfacies 2a is lenticular bedded mudstone and contains less than 40 percent sand (Fig. 2.4). Ripples are less than 2 cm in height and 5 cm in length and usually have asymmetric crests. Most foreset laminae dip in one direction, with rare bidirectional dip. Other sedimentary structures include sharp-based laminations of very fine sand, and flat sand lenses. Mud beds show very fine internal horizontal lamination. Rare beds of Facies 4 are typically sharp-based and less than 5 cm thick.

Bioturbation is rare to moderate in abundance with a trace fossil assemblage consisting of small discrete burrows. *Planolites*, *Lockeia*, *Gyrolithes*, *Chondrites,* and *Teichichnus* are the most common ichnofossils.

Sand-filled cracks are rare to common, and iron and siderite stained mud and sand are occasionally found. Load-cast ripples and load casts are the most widespread soft-sediment deformation structures, with rare syn-sedimentary microfaulting.

Subfacies 2b - Lenticular to Wavy Bedded Mudstone (F2b)

Description

Facies 2b is wavy to lenticular bedded mudstone and contains 40 to 60 percent sandstone (Fig. 2.5). The majority of ripples exhibit symmetrical crests. Ripple foresets dominantly dip in one direction with rare bipolar orientations. Ripple height is less than 2 cm and length is generally less then 5 cm, but can extend the width of the core (9 cm).

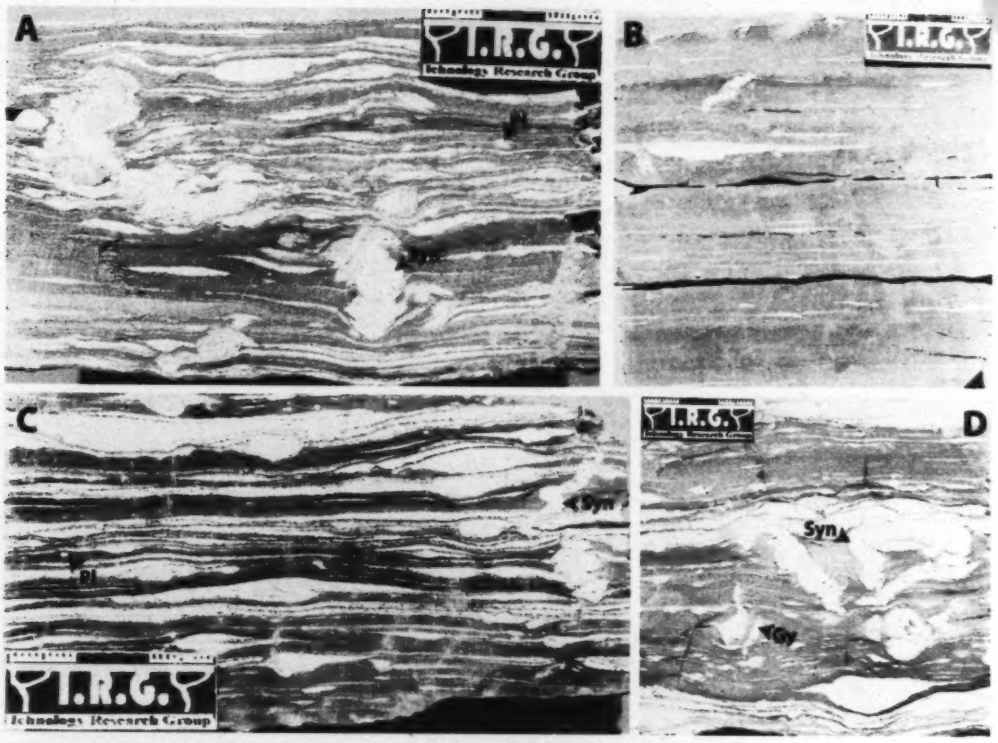

Figure 2.4. Lenticular bedded mudstone (subfacies 2a). A, B, C, D) Trace fossils include *Planolites* (Pl) and *Gyrolithes* (Gy). Syneresis cracks (Syn) are common, as are sideritized mud beds and laminae.

Fine grained, rippled glauconitic sandstone (Facies 8) beds less than 5 cm thick are rare. Parallel bedding is also found in minor abundance.

Trace fossils are rare within this subfacies. *Planolites* and *Lockeia* are the most common with less abundant *Arenicolites*, *Skolithos*, *Gyrolithes*, and *Teichichnus*.

Soft-sediment deformation is ubiquitous with abundant load-cast ripples, load casts with flame structures, and contorted bedding. Syn-sedimentary faults and shearing are commonly associated with contorted bedding. Diminutive sand-filled cracks are intermittently present. Disseminated diagenetic pyrite is found sporadically. Sideritized mud beds and iron stained sand beds are locally abundant.

Hayat-10, Hayat-11, and Yasser-3 contain a unit of lenticular to wavy bedded sandstone 1.5 to 2.5 m thick in which the bedding consistently inclines at an angle of 15 degrees to the horizontal (Fig. 2.5D). Load casts and flame structures dominate this unit, while bioturbation is limited to rare *Planolites* and *Lockeia*. Sand-filled cracks are encountered infrequently.

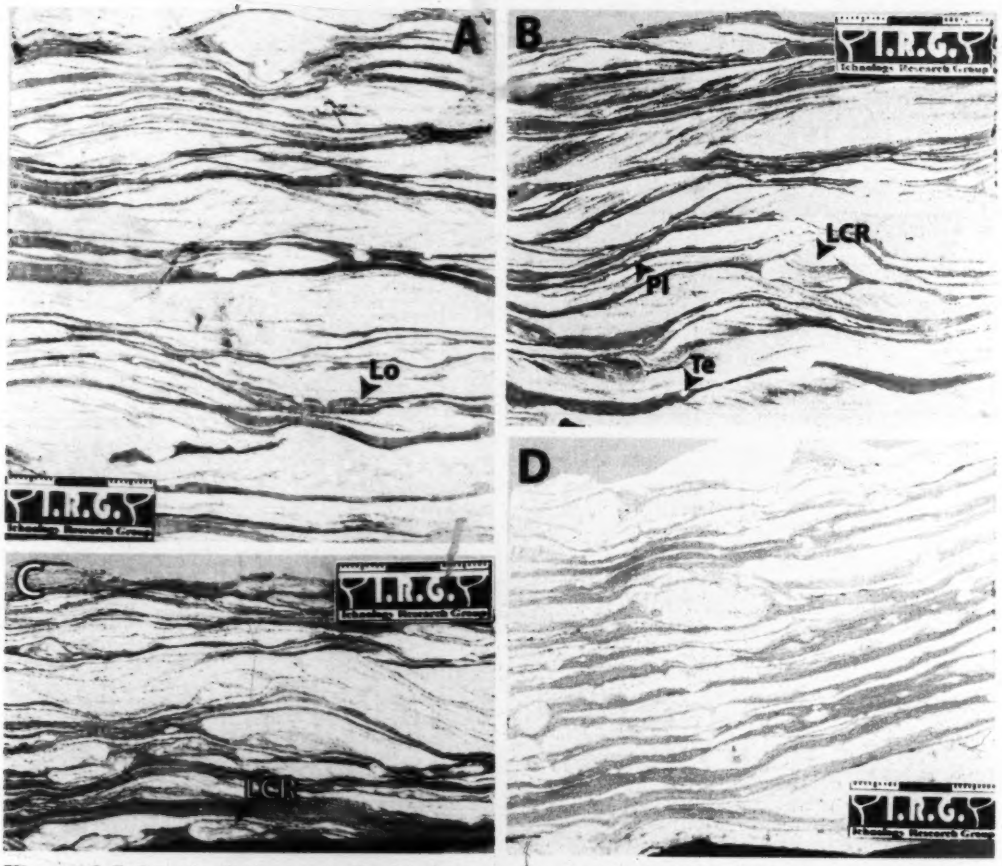

Figure 2.5. Lenticular to wavy bedded mudstone (subfacies 2b). Ichnofossils include A) *Lockeia* (Lo); B) *Planolites* (Pl) and *Teichichnus* (Te). C) Soft-sediment deformation in the form of load-cast ripples (LCR) is common. D) wavy bedded mudstone with depositional dip that is interpreted as a point bar lateral accretion deposit.

Subfacies 2c - Wavy to Flaser Bedded Sandstone (F2c)

Description

Subfacies 2c is characterised by greater than 60 percent sandstone and wavy to flaser bedding (Fig. 2.6). Both asymmetrical and symmetrical crested ripples are present. Herringbone cross-stratification is common. Fine mud laminations and mud beds are also present.

Bioturbation within this unit is rare and the trace fossil assemblage is dominated by *Lockeia* and *Planolites*, with rare *Palaeophycus*, *Teichichnus,* and *Gyrolithes*.

Diminutive sand-filled cracks are rare. Small, sideritized mud rip-up clasts are present

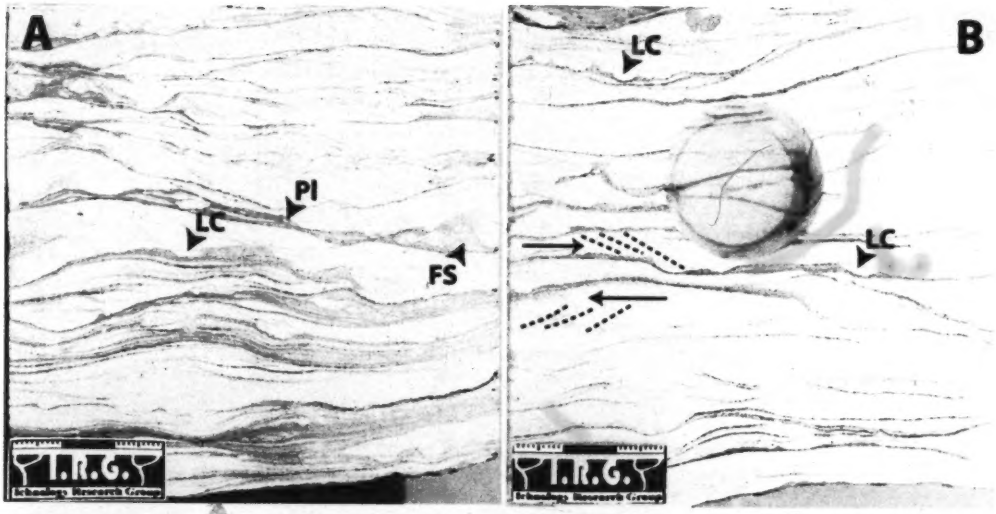

Figure 2.6. Wavy to flaser bedded sandstone (subfacies 2c). A) Load casts (LC) and flame structures (FS) are common. Bioturbation is sparse and usually takes the form of *Planolites* (Pl). B) Dashed lines show the dip of ripple foresets, which suggest bipolar flow directions (arrows).

in beds less than 3 cm thick. Disseminated diagenetic pyrite is found sporadically. Rare glaucony grains are concentrated on ripple foresets. Sideritization of mud beds is locally abundant, while iron staining of sandstone beds is less frequent. Deformation is occasional with local completely deformed and contorted beds. Load-cast ripples and load casts with flame structures are also common.

Facies 2 Interpretation

Symmetric and asymmetric ripples are formed due to wave and current activity, respectively, and their presence demonstrates that sand was being transported into the system via traction currents. A portion of the symmetric ripples were likely produced under combined flow. The presence of herringbone cross-stratification and ripple foresets with bidirectional dip indicate deposition under bipolar currents, likely in a tidal regime.

The trace fossil assemblage is dominated by simple, diminutive burrows such as *Planolites*, *Lockeia*, *Gyrolithes*, *Chondrites*, *Teichichnus*, *Skolithos,* and *Arenicolites*. This low diversity trace fossil suite contains both dwelling and feeding structures and is typical of brackish water settings (Pemberton and Wightman, 1992).

Sand-filled cracks are attributed to syneresis and likely formed when water with a higher salinity than that of the existing sediment moved over the sediment-water interface (Burst, 1965; Donovan and Foster, 1972). The abundant of soft-sediment deformation

indicates a setting with high rates of deposition where sediment cannot easily dewater (Allen, 1982).

Lenticular, wavy and flaser bedding are classically interpreted as tidal features resulting from the alternation of energetic and quiescent conditions (Reineck and Wunderlich, 1968; Reineck and Singh, 1980). Tessier et al. (1995) found that vertical changes between lenticular and wavy to flaser bedding in modern sediments can represent tidal rhythmites: an increase in tidal range from neap to spring causes a change from lenticular and wavy bedding to flaser bedding. The higher tidal ranges are associated with stronger currents that are better able to transport and deposit sand sized particles. Alternatively, the vertical changes in sand abundance could be due to seasonal or storm related variations, or progradation or retrogradation of the sandy subtidal and the mixed sand and mud intertidal zones (Reineck and Wunderlich, 1968; Reineck and Singh, 1980; Weimer et al., 1982).

Willis et al. (1999) described a similar facies which is interpreted to represent subtidal deposition under the influence of weak tide and wave currents. The complex interbedding of sand and mud, and the abrupt transition from sand to mud suggest frequent and rapid alternations in current strength (Reineck and Singh, 1980; Nio and Yang, 1991).

2.2.3 Facies 3 – Flaser Bedded Sandstone (F3)

Description

Facies 3 occurs in approximately half of the wells in the study area. Its thickness ranges from 25 cm to 5 m with an average of 3 m. Although characterised by rippled, very fine to fine grained sand with abundant fine mud laminae or flaser bedding, this facies also contains beds of lenticular to wavy bedded mud and sand (Fig. 2.7). It is also frequently interbedded with heterolithic sandstone and mudstone (Facies 2) and has a gradational relationship with Facies 2c. Ripple morphology ranges from asymmetric to symmetric and shows opposing foreset orientation or herringbone cross-stratification. Facies 3 commonly forms the top sandy unit of a coarsening upward sequence that is bound above and below by a sideritized mud clast breccia.

The trace fossil assemblage is dominated by *Planolites* and *Palaeophycus* with rare *Thalassinoides*. Overall, the abundance of bioturbation is rare to moderate.

Soft-sediment deformation is common within this unit and typically takes the form of contorted bedding and load-cast ripples. Sideritized mud clasts and laminae are found throughout, as are sand-filled cracks within muddier sections. Scour surfaces are frequently found and glaucony grains are occasionally found on ripple foreset laminae.

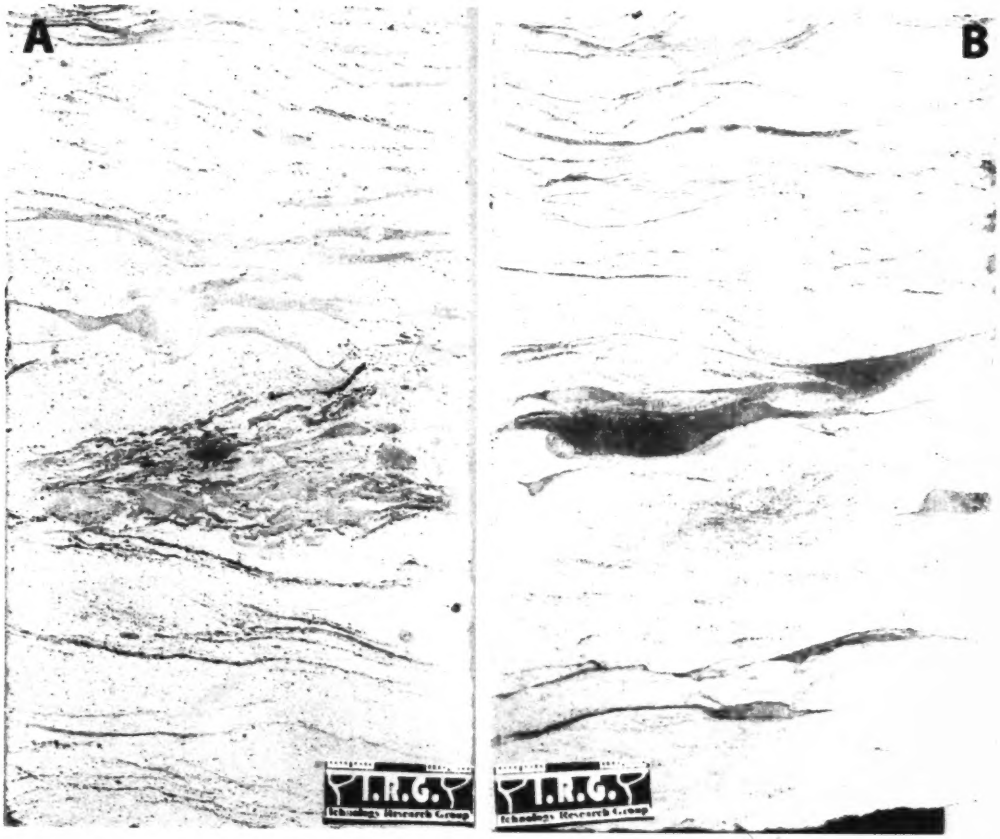

Figure 2.7. Flaser bedded sandstone (Facies 3). A) Sideritized mud intraclasts and mud flasers. B) Thick, sideritized mud flasers and ripples showing bidirectional flow.

Interpretation

Deposition of Facies 3 was strongly influenced by tidal currents, as evidenced by the herringbone cross-stratification. Ripples occasionally have symmetrical crests and are interpreted as current ripples that have been subject to wave modification (combined flow).

Flaser bedding is formed by mud settling out of suspension during slack water periods and is common feature of subtidal deposits (Weimer et al., 1982). The paucity of biogenic structures within this facies suggests a stressed environment (Pemberton and Wightman, 1992). The high amount of soft-sediment deformation coupled with a low amount of mud suggests a relatively high energy depositional environment subject to high sedimentation rates.

2.2.4 Facies 4 – Sandstone With Mud And Organics (F4)

Description

Facies 4 is restricted to the eastern portion of the study area and ranges in thickness from 30 cm to 3.5 m. The main lithology is very fine to lower fine sandstone with common structureless mudstone beds (Fig. 2.8). Primary physical sedimentary structures are generally difficult to distinguish, but symmetrical ripples and small-scale cross-stratification are present, with rare low to high angle planar cross-bedding. Wavy bedding is widespread within muddier sections. The overall mud content of Facies 4 is 15 percent or less, but can be locally abundant.

Disseminated organics and coaly material are common within this facies, as are sideritized mud laminae and mud clasts. Glaucony grains are rarely found on ripple foresets. Pyrite nodules and scour surfaces are rare. Diminutive sand-filled cracks are rare to common in interbedded deposits. Soft-sediment deformation is common and usually expressed as load-cast ripples and load casts.

This facies contains burrowing that is rare to moderate in abundance with trace fossils that are characteristic of a mixed *Cruziana* - *Skolithos* assemblage. Where distinguishable, the most common trace fossils are *Palaeophycus*, *Planolites*, *Skolithos*, *Thalassinoides*, and *Teichichnus*.

This facies displays a gradational relationship with bioturbated ripple bedded sandstone (Facies 5) and finely laminated mudstone and sandstone (Facies 1). In addition, it is commonly hydrocarbon stained.

Interpretation

The centimeter-thick, massive, contorted mud beds were likely deposited through hyperpycnal flow. This type of flow occurs when dense, sediment-laden river water enters a body of less dense water (Bhattacharya and Walker, 1991). The density contrast causes the river water to flow along the floor of the basin. This type of flow is associated with deltaic settings and brings large quantities of fresh water into the basin (Reading and Collinson, 1996). Sand-filled cracks found in this facies are attributed to syneresis (Burst, 1965) and could be associated with salinity fluctuations brought on by the influx of fresh water into the basin.

The symmetrical ripples are either wave or combined flow generated and the small-scale cross-stratification represents lateral migration of these bedforms. Low and high angle planar cross-bedding are created by migrating two-dimensional dunes. The high amount of organic material within this facies suggests close proximity to a fluvial source.

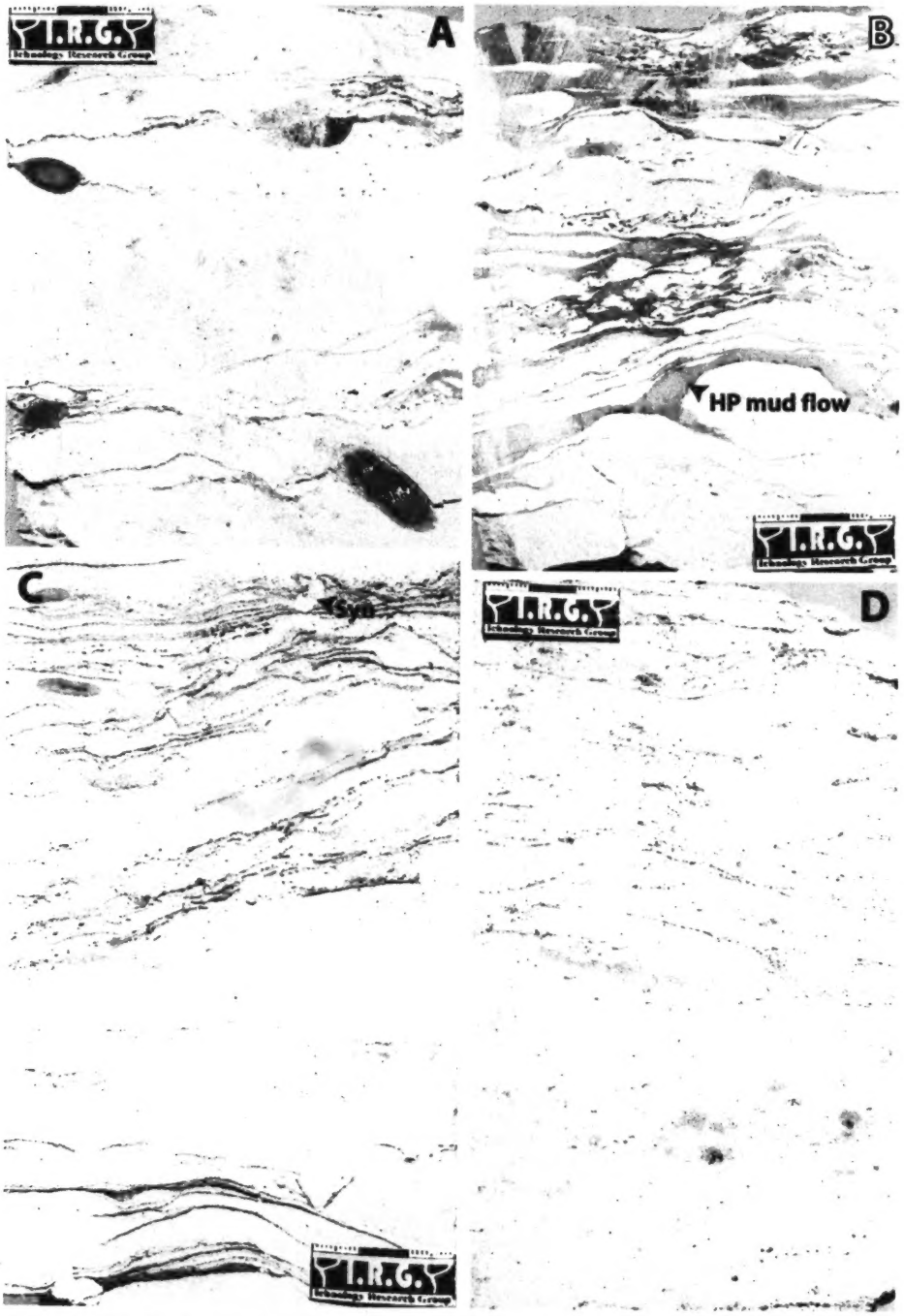

Figure 2.8. Sandstone with mud and organics (Facies 4). A) Sideritized mud clasts in structureless to rippled sandstone. B) Hyperpycnal mud flows in rippled sandstone. C) High angle cross bedding accentuated by organic material along foresets, Syn - syneresis crack. D) Scattered organic material in fine grained sandstone.

The trace fossil assemblage is of low diversity, consists of simple structures constructed by trophic generalists, and contains a mix of vertical and horizontal burrows that are commonly found in the *Cruziana* and *Skolithos* ichnofacies. Such characeristics are typical of brackish water trace fossil suites (Pemberton and Wightman, 1992).

2.2.5 Facies 5 – Bioturbated Rippled Sandstone (F5)

Description

Facies 5 is limited to the eastern half of the study area and occurs in the Hayat-11, Hayat-8, Salam-8, Salam-5, and Salam-17 wells. It ranges in thickness from 50 cm to 6.5 m and is on average 3 m thick. The base of this facies is commonly erosive.

The dominant lithology is very fine to upper fine grained sandstone with common thin mud drapes (Fig. 2.9). Physical structures are difficult to discern but the most prevalent are symmetrical ripples and wavy bedding.

The degree of bioturbation varies from rare to common and consists of a mixed *Cruziana* - *Skolithos* ichnofacies assemblage. The trace fossil suite is dominated by *Palaeophycus*, *Planolites, Thalassinoides,* and *Ophiomorpha* with rare *Chondrites*, *Siphonichnus, Rosselia*, *Lockeia,* and *Bergaueria* (Figs. 2.9C, D and 2.10A-D). In mud-dominated sections, it is often difficult to distinguish between ichnofossils and deformed ripples.

Mudstone intraclasts and laminae within this unit are usually sideritized. Sand-filled cracks are occasionally found. Other diagenetic features include rare disseminated pyrite and locally abundant iron staining (Fig 2.9B). Soft-sediment deformation is rare to moderately abundant.

Interpretation

As foresets are not visible, the symmetrical ripples are interpreted to be formed under either wave or combined flow conditions. Wavy bedding and wavy mudstone laminae within the thick sand beds suggest deposition by both suspension and traction, which could be due to fluctuating energy within the system or episodic sediment input. Small-scale bedforms dominate this facies, which could be the result of a number of factors: 1) a small grain size that restricts bedform dimensions; 2) the overall energy of the system is simply not high enough for larger bedforms to develop; or 3) the depth of flow is too shallow for the development of bedforms larger than ripples.

The trace fossil assemblage within this facies is more diverse than Facies 1 or Facies 2, but is still restricted compared to that characteristic of fully marine environments

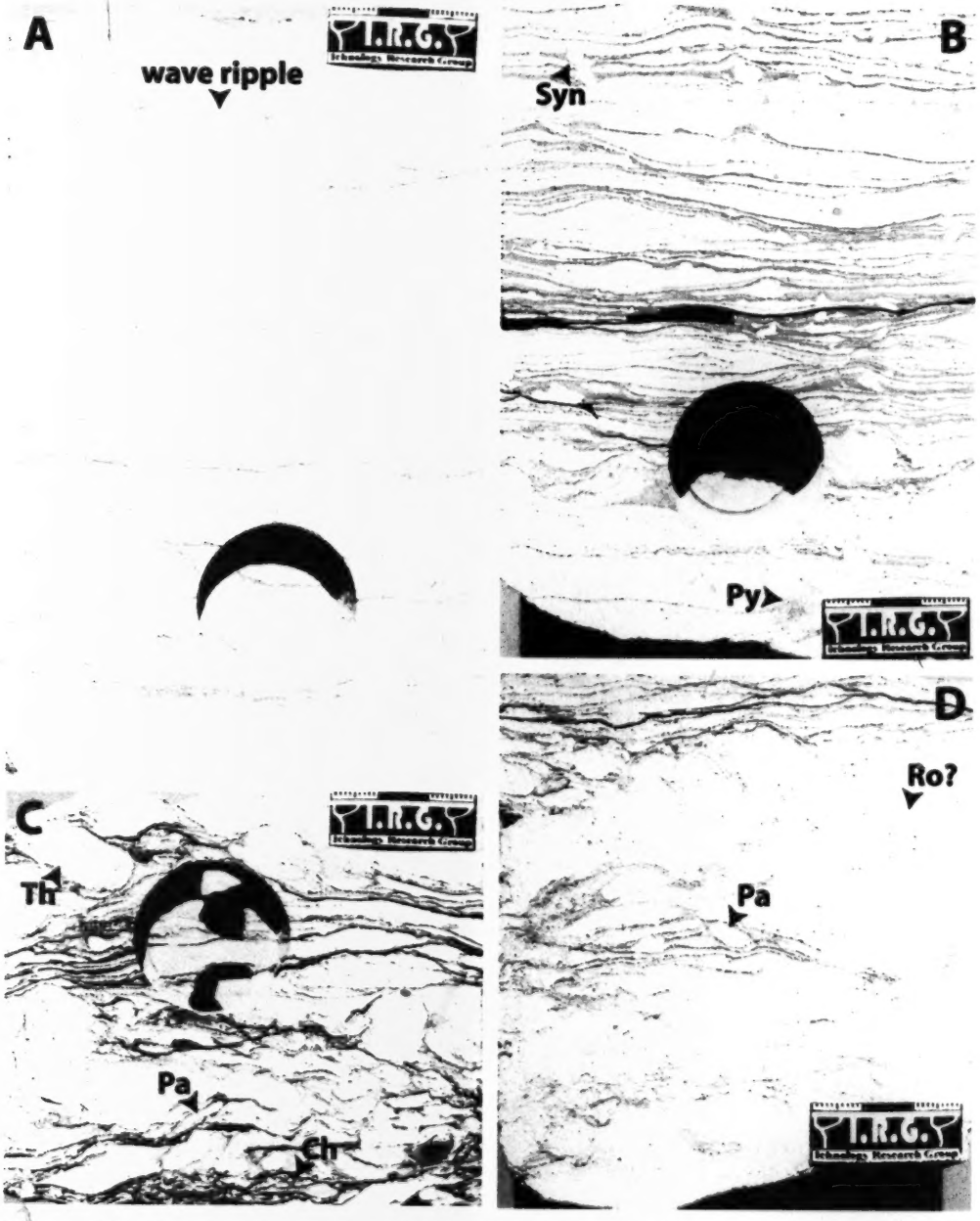

Figure 2.9. Bioturbated rippled sandstone (Facies 5). A) Wave ripples in flaser bedded sandstone. B) Fine mud laminations with syneresis cracks (Syn) and pyrite nodules (Py). C) Abundant bioturbation with *Thalassinoides* (Th), *Palaeophycus* (Pa) and *Chondrites* (Ch). D) Mottled sandstone beds with fine mud laminations with *Palaeophycus* (Pa) and possible *Rosselia* (Ro).

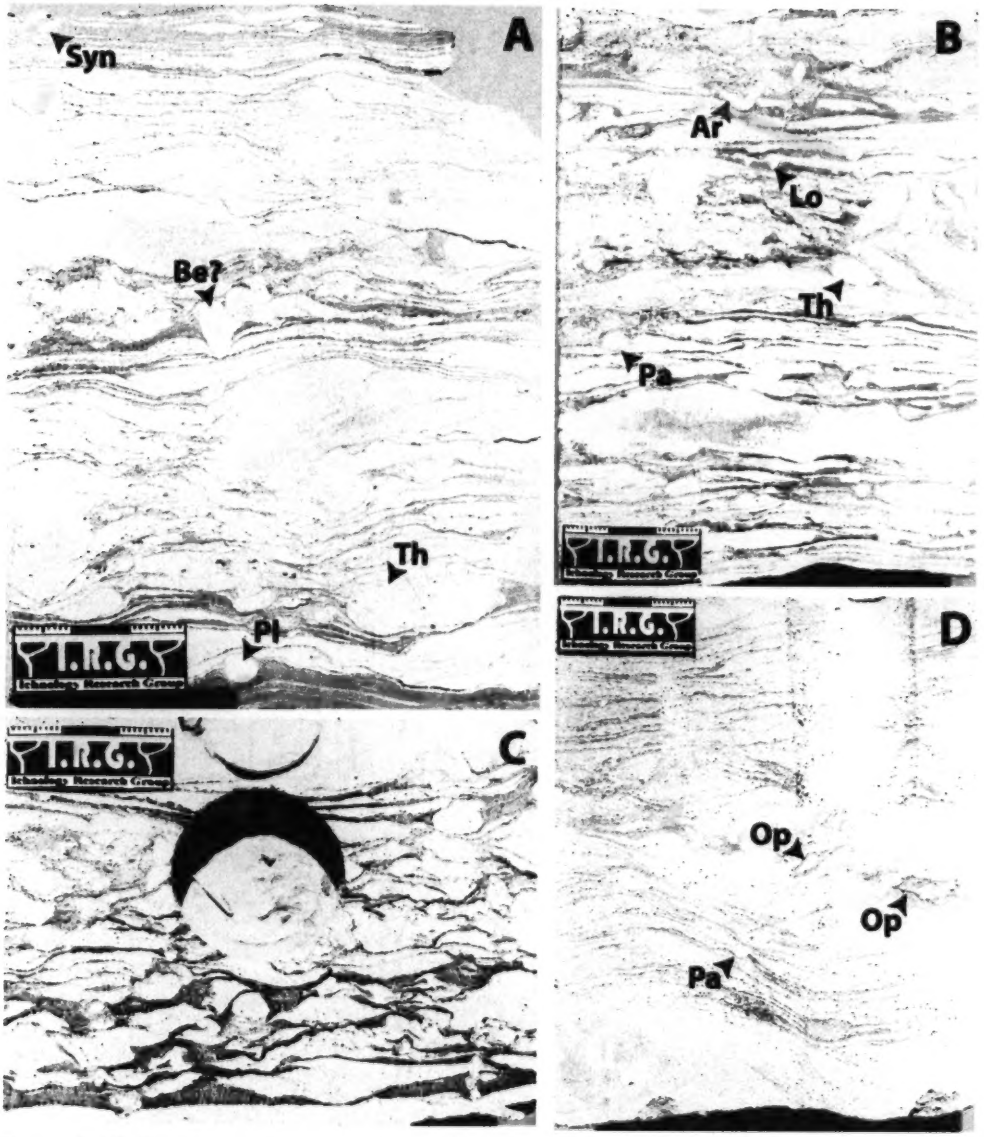

Figure 2.10. Trace fossils in bioturbated rippled sandstone (Facies 5). Be - *Bergaueria*, Th - *Thalassinoides*, Pl - *Planolites*, Pa - *Palaeophycus*, Lo - *Lockeia*, Ar - *Arenicolites*, Op - *Ophiomorpha*. Other features include syneresis cracks (Syn). Photo C shows deformed interbedded sand and hyperpycnal mud beds.

(Pemberton et al., 2001). Most bioturbation is concentrated within the muddier beds and is dominated by deposit feeding structures. The abundant bioturbation within this facies, as compared with Facies 4, suggests conditions that were more hospitable for substrate colonization.

2.2.6 Facies 6a – Burrowed Sandy Mudstone (F6a)

Description

Facies 6a is limited to the northern portion of the study area and is only found in wells of the Salam Field. Its thickness ranges from 50 cm to 1.5 m.

This facies is made up of two interbedded lithologies: thin mudstone beds and thicker sandy bioturbated mudstone beds (Fig. 2.11). Sharp-based sandy bioturbated mudstone units dominate this facies and range in thickness from 10 to 30 cm. Primary sedimentary structures are rare due to the high degree of bioturbation, but when visible, consist of symmetrical ripples with abundant mud laminae, or horizontally laminated mud and sand. The typical sandstone grain size is lower very fine to lower fine. Silt is present in minor amounts. The thin mudstone units are normally between 2 and 8 cm thick and contain rare horizontal sandstone stringers and deformed ripples. The degree of bioturbation ranges from absent to common.

Due to the abundant bioturbation, individual trace fossils are typically difficult to distinguish. The trace fossil assemblage consists of *Rhizocorralium*, *Asterosoma*, *Chondrites*, *Palaeophycus, Thalassinoides,* and *?Zoophycus* (Fig. 2.11B, C, E).

Rare to common siderite and iron stained beds occur, and some ripples have foresets accentuated by glaucony grains. Thin beds of Facies 6b are rarely found.

Interpretation

Ripples with symmetric crests are interpreted as oscillation ripples, which are commonly generated by fair-weather waves (Walker and Plint, 1992; Pemberton et al., 2001). The dominance of mudstone and muddy sandstone suggests a relatively low- energy environment.

The trace fossil assemblage is dominated by traces of the *Cruziana* ichnofacies and consists of mostly deposit and grazing feeders. This ichnofacies is typically developed in poorly sorted, unconsolidated substrates located in moderate energy, shallow waters (Pemberton et al. 1992). Mudstone beds with a paucity of bioturbation could represent low oxygen events (Allison et al., 1995; Taylor et al., 2003).

2.2.7 Facies 6b – Burrowed Mottled Sandstone (F6b)

Description

Facies 6b is limited to wells within the Salam Field and is closely associated with Facies 6a. It obtains a similar thickness of 50 cm to 1.5 m.

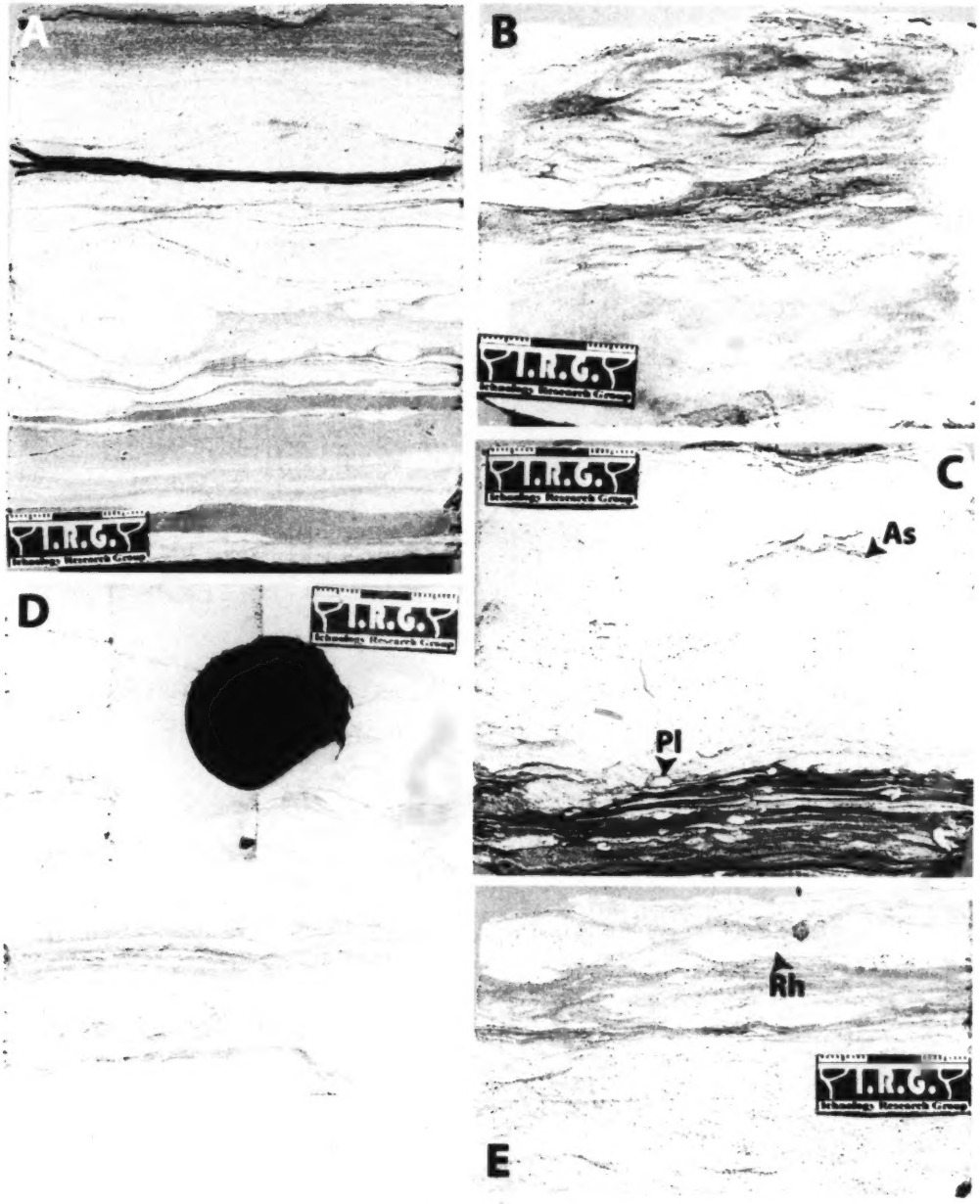

Figure 2.11. Burrowed sandy mudstone (Facies 6a). A) Soft-sediment deformation of sandstone beds in silty mudstone. B) Burrowed mottled sandstone and mudstone. C) *Asterosoma* (As) in mottled sandstone overlying lenticular bedded mudstone with *Planolites* (Pl). D) Interbedded mudstone and sandstone with some soft-sediment deformation. E) *Rhizocorallium* (Rh) in mottled sandstone and mudstone.

Although dominated by lower fine to upper fine grained muddy sandstone, Facies 6b also contains lower medium grained sandstone. Due to abundant bioturbation, physical sedimentary structures are rarely visible (Fig. 2.12). Iron staining is frequent and the unit is occasionally hydrocarbon stained. Glaucony grains and shell fragments are common, whereas thin mudstone beds are scarce.

Bioturbation has completely churned the sediment and the lack of lithologic constrast makes burrow identification difficult. Where discernible, trace fossils include *Ophiomorpha*, *Asterosoma*, *Scolicia*, and *Palaeophycus*.

Interpretation

The lack of sedimentary structures makes an interpretaion of the hydraulic regime difficult, but a higher sand content compared to Facies 6a suggests a relatively higher energy setting. The high abundance of bioturbation, combined with a trace fossil assemblage that is dominated by ichnogenera that show complex behavior patterns, indicates fully marine waters (Pemberton et al., 1992; Pemberton and Wightman, 1992). Members of both the *Cruziana* and *Skolithos* ichnofacies are present.

2.2.8 Facies 7 – Rippled Sandstone With Carbonaceous Flasers (F7)

Description

Facies 7 is an oddity within the study area. It occurs solely in the Salam-5 well and immediately overlies rocks of Facies 6. This very fine to fine grained, oil stained sandstone contains ubiquitous symmetrical ripples with fine grained, organic rich mud flasers (Fig. 2.13). Herringbone cross-stratification and horizontal bedding are occasionally found. Bioturbation is extremely rare, with intermittent *Palaeophycus* and *Skolithos* burrows as the only visible trace fossils. The contact with the underlying unit is marked by a dense, 1 cm thick bed of *Chondrites* or small *Planolites*. Facies 7 contains no glaucony whatsoever but possesses rare sideritized mud intraclasts and mud flasers.

Interpretation

The symmetrical ripples are interpreted as oscillation ripples. The herringbone cross-bedding likely represents the occasional influence of tides within the depositional setting. The deficiency in bioturbation points to a system where a shifting substrate or high sedimentation rate prevented substrate colonization.

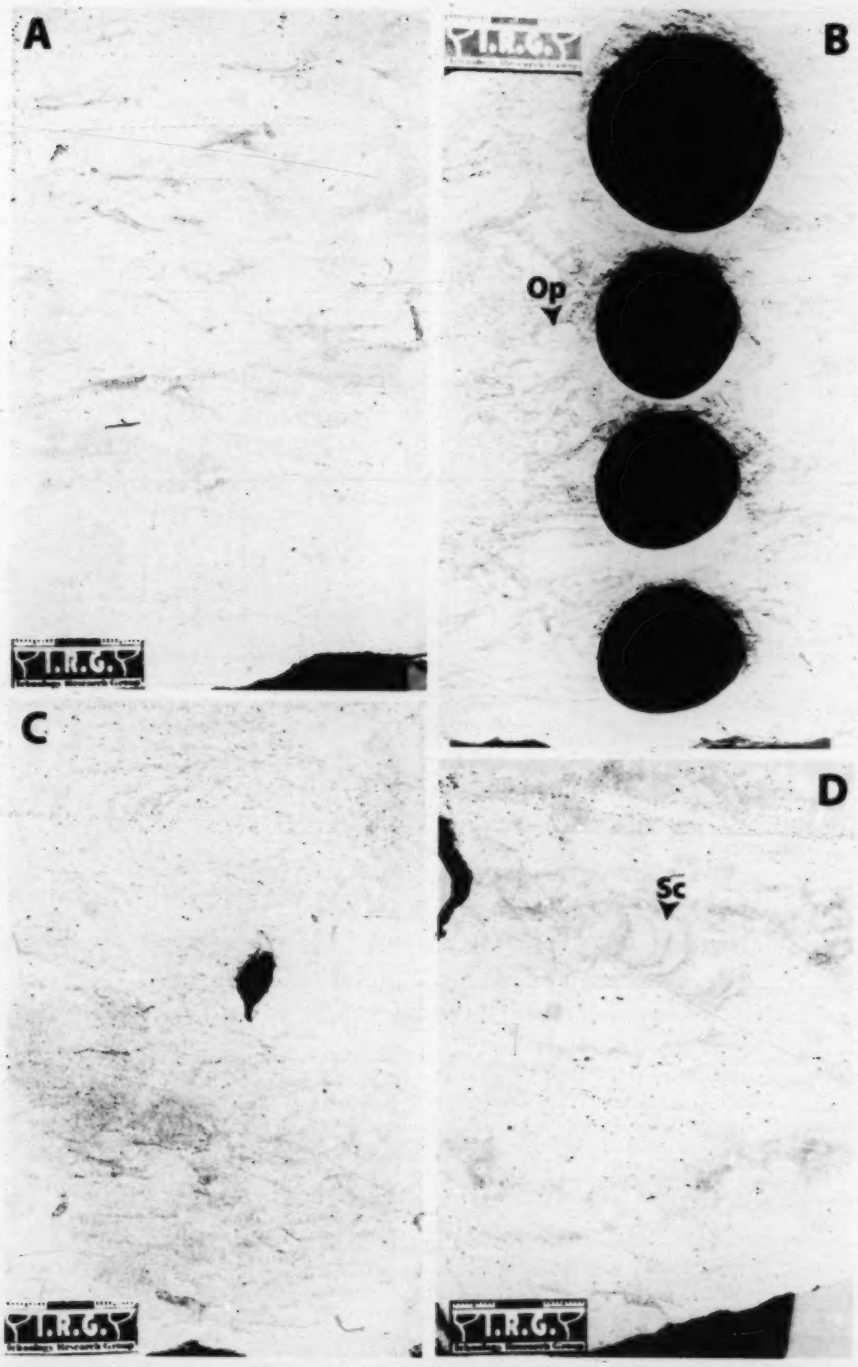

Figure 2.12. Burrowed mottled sandstone (Facies 6b). Abundant bioturbation and mottling (A and C) makes ichnofossil identification difficult, with B) *Ophiomorpha* (Op) and D) *Scolicia* (Sc) as the only discernible burrows. Note the abundant iron staining.

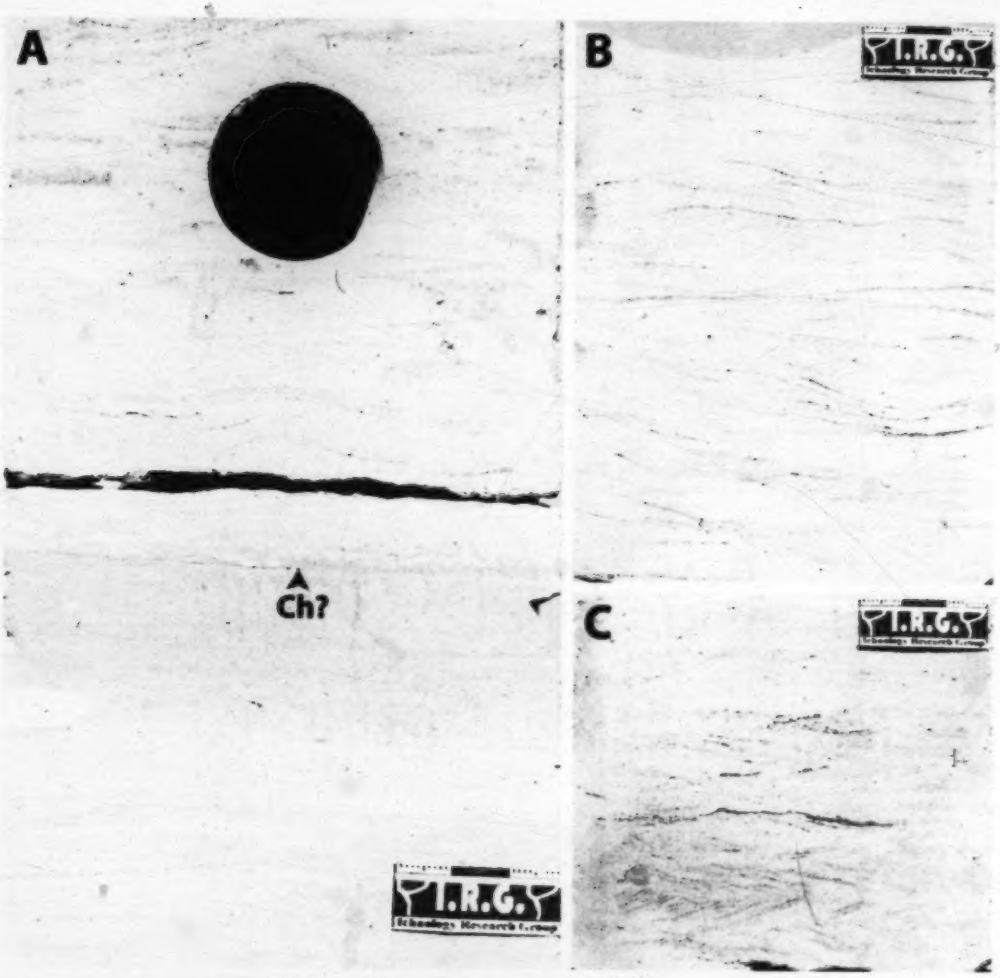

Figure 2.13. Rippled sandstone with carbonaceous flasers (Facies 7). A) The sharp contact between Facies 6a and 7 is demarcated by a dense bed of ?*Chondrites* or small *Planolites* burrows. B) Abundant carbonaceous flasers. C) Herringbone cross-stratification indicating bidirectional flow.

2.2.9 Facies 8a – Rippled To Flaser Bedded Glauconitic Sandstone (F8a)

Description

This facies is very common in the study area and is present in each well at many stratigraphic levels. It is commonly interbedded with the other glaucony-rich facies (Facies 8 through 11) and the heterolithic sandstone and mudstone facies (Facies 2).

The average grain size for this glauconitic sandstone is upper very fine to upper fine. Small-scale cross-bedding is the dominant sedimentary structure with common herringbone cross-stratification. (Fig. 2.14). Ripple height is generally less than 2 cm. Planar horizontal

bedding, symmetrical ripples, and climbing ripples are rare. Scour surfaces are prevalent and may be marked by sideritized mud intraclasts. The overall mud content is less than 10 percent and usually takes the form of mud flasers. Glaucony-rich ripple foresets show possible double mud drapes or tidal lamination.

Overall, the abundance of bioturbation is proportional to the amount of mud within the sediment. *Skolithos*, *Macaronichnus*, and *Palaeophycus* are the most common ichnofossils. Other minor components of the assemblage include *Diplocraterion*, *Arenicolites*, *Rosselia*, and ?*Teichichnus* (2.14A). Occasionally, large indeterminate forms and rare fugichnia appear. Cryptic bioturbation is more prevalent than discrete traces, and tends to make the sedimentary structures appear indistinct.

The glaucony content of this facies varies considerably, but generally imparts a light to dark green tinge to the rocks. It usually accumulates along ripple foresets and horizontal bedding planes. Other diagenetic features include rare disseminated pyrite, scattered sideritized mud clasts, common sideritized mud laminae, and locally abundant iron staining.

The amount of deformation in this facies is low and varies with mud content, as a higher mud content is associated with higher degrees of deformation. Load-cast ripples and flame structures are the most widespread deformation structures. Large-scale dewatering features with calcite deposition in cavities created during water expulsion also occur. This facies is strongly associated with sideritized mud clast breccia development, with breccias present at the base, top, and in the center of the unit.

There are two endmembers within this facies: clean, rippled glauconitic sandstone and flaser bedded glauconitic sandstone. The former contains very little mud and few discrete burrows mostly consisting of *Palaeophycus* and *Skolithos*. Deformation is rare, as are sideritized mud intraclasts. Ripple foresets and herringbone cross-stratification are easy to distinguish. The latter endmember contains common mud flasers and is more heavily bioturbated with large burrows such as *Rosselia*, *Diplocraterion*, *Skolithos* and *Paleophycus*. Ripples are not as well defined and are commonly contorted.

Interpretation

The small-scale cross-bedding is generated by migrating current ripples. Some oscillatory motion is interpreted as well, with some ripples exhibiting foreset terminations that are tangential to lower bounding surfaces. Such ripples also exhibit symmetric crests and irregular bounding surfaces (Boersma, 1970; Harms et al., 1975; Reineck and Singh, 1980).The herringbone cross-stratification was likely formed due to tidal currents (Nio and Yang, 1991). Rare horizontal planar bedding is interpreted to have been deposited under

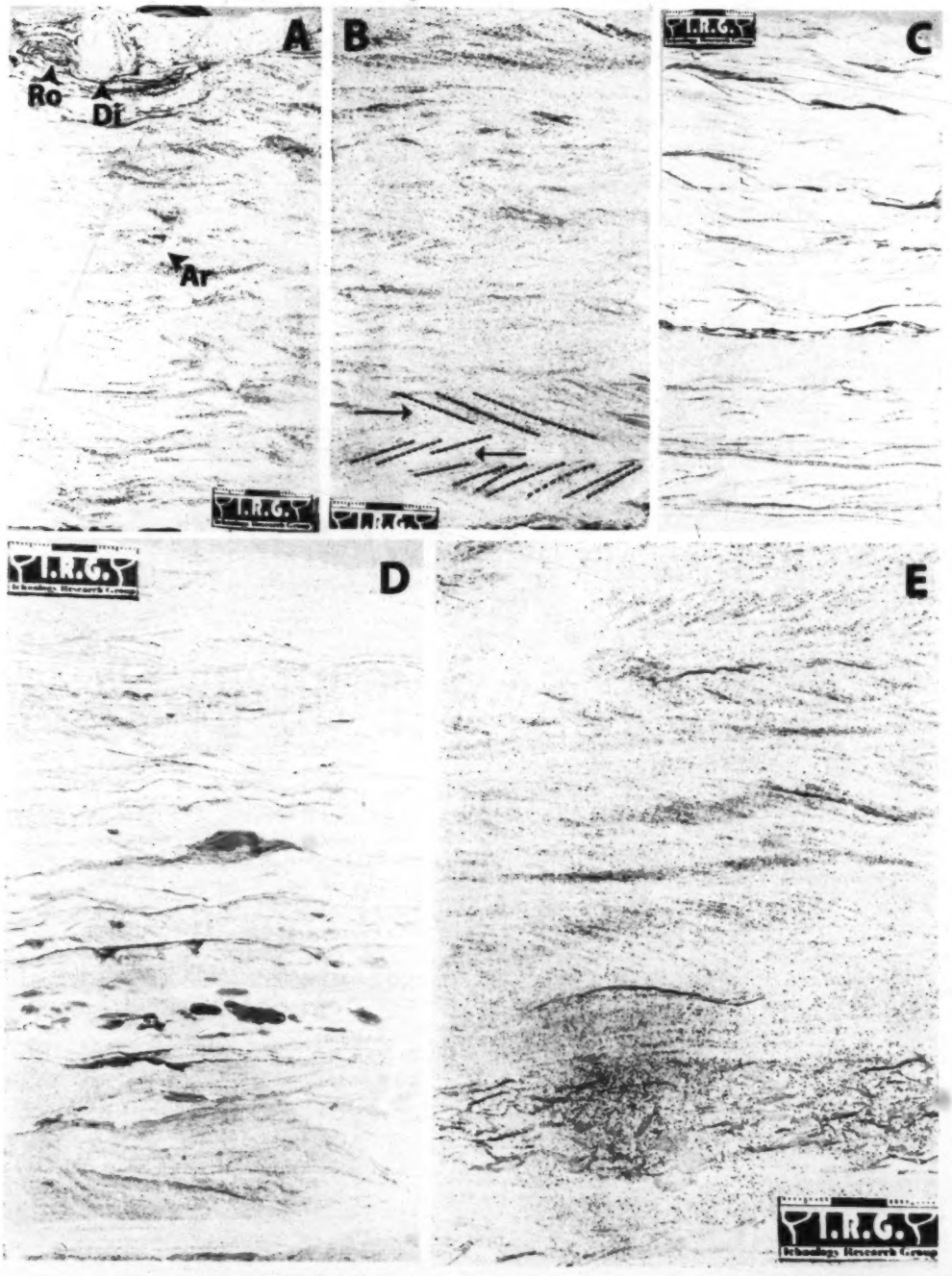

Figure 2.14. Rippled to flaser bedded glauconitic sandstone (Facies 8a). A) Current ripples with *Rosselia* (Ro), *Diplocraterion* (Di) and *Arenicolites* (Ar). B) Herringbone cross-bedding. The dotted lines mark ripple foresets, arrows point in the direction of current flow. C) Flaser bedding. D) Muddier unit with more contorted ripples and sideritized mud clasts. E) Alternating planar bedding and current ripple cross-bedding.

upper plane bed conditions (Harms et al. 1975) at velocities higher than those associated with ripple formation. The repetitively stacked interbedded nature of the planar and current ripple bedding is interpreted to represent deposition under variable or waning tidal flow (Harms et al. 1975).

Mud flasers were likely deposited during low flow or slack water conditions. Occasionally, glaucony grains found along ripple foresets appear to form double mud (glaucony) drapes or tidal bundles (Boersma, 1969; Visser, 1980). Double mud drapes are only found in subtidal depositional settings as two slack water stages are required for their formation (assuming a diurnal tide; Visser, 1980). The general lack of mud within this facies suggests that current velocities were too high for significant mud deposition or mud was deposited but eroded upon ensuing flow.

The overall lack of discrete trace fossils suggests there was environmental stress on the system at the time of deposition. In this case, fluctuating salinity, high sedimentation rate, and a shifting substrate were probably the most significant stresses. Cryptic bioturbation is common in brackish marine settings (Pemberton et al., 2001) and *Macaronichnus* burrows are thought to be indicative of high energy environments (Saunders and Pemberton, 1986).

The glaucony within this (and other) facies is either paratochthonous, transported in from the shelf, or allochthonous and eroded from older rocks that contained primary glaucony; this distinction, however, is beyond the scope of this study. The rocks with the darkest green colour and greatest glaucony content tend to be quite contorted, contain the most mud rip-up clasts, and were probably deposited under higher energy conditions. The difference between the two endmember within this facies is likely a consequence of variation in current energy and mud input into the depositional system.

2.2.10 Facies 8b – Muddy Rippled To Flaser Bedded Glauconitic Sandstone (F8b)

Description

Facies 8b is differentiated from Facies 8a by a different trace fossil assemblage, more soft-sediment deformation, higher mud content, and common iron staining of mud flasers and beds. It occurs at the top of Hayat-8, 11, 4, 6 and Yasser-3 wells and seems to be restricted to the southern portion of the study area. The thickness of this facies ranges between 50 cm and 5 m.

This glauconitic sandstone is dominated by lower fine to upper fine grain sizes and contains symmetrical and asymmetrical ripples, and planar bedding (Fig. 2.15). Herringbone cross-bedding and flaser and wavy bedding occasionally occur. This facies

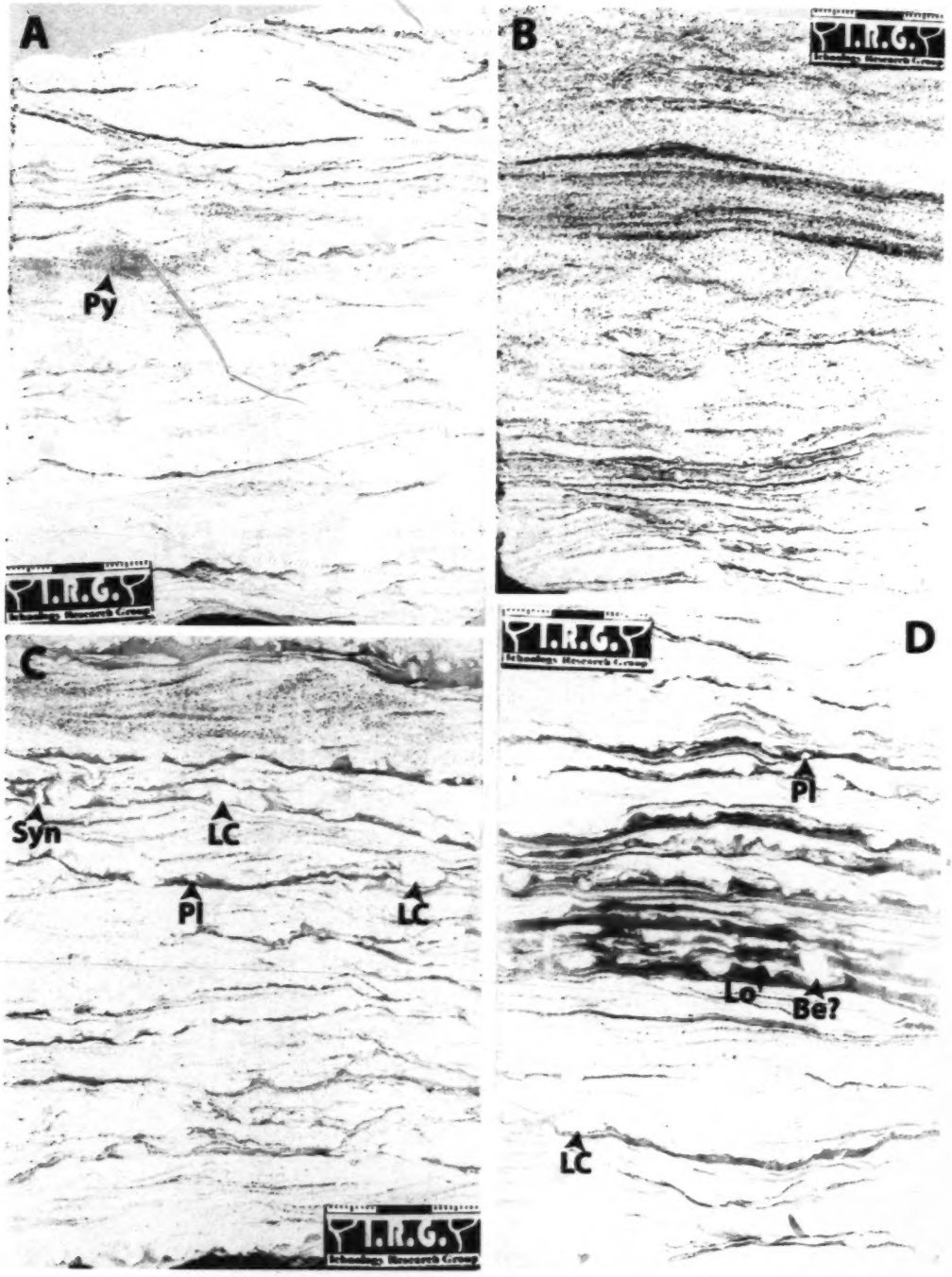

Figure 2.15. Muddy rippled to flaser bedded glauconitic sandstone (Facies 8b). A) Current ripples and pyrite (Py). B) Increase in glaucony content with current ripples and mud drapes. C and D) Common sideritized mud laminae with load casts (LC), syneresis cracks (Syn), *Planolites* (Pl), *Lockeia* (Lo) and possible *Bergaueria* (Be).

is generally muddier than Facies 8a, with a mud content between 5 and 30 percent. Scour surfaces are rare. Bioturbation is rare to moderate and consists of small burrows usually less than 1 cm in size. *Lockeia and Planolites* are the dominant trace fossils with lesser *Teichichnus*, *Palaeophycus,* and *?Bergaueria*.

Load casts and flame structures are common, as are nodular and disseminated pyrite. Sand-filled cracks and water escape structures are rare. Organic debris is abundant on muddy, fissile bedding planes. Most mud laminae and beds within this facies have undergone sideritization or iron staining. Glauconitic material is generally found along ripple foresets, but is less abundant than in Facies 8a.

Interpretation

Small-scale cross-beds are formed by migrating current and wave ripples, of which the former are dominant. A tidal influence is indicated by with the presence herringbone cross-bedding. The rapid change from planar bedding to ripple cross-bedding could indicate currents waning from the upper to lower flow regime, which is also typical of tidal systems (Nio and Yang, 1991). While the ichnofossil assemblage in Facies 8a was typified by traces found in high energy environments, the assemblage in Facies 8b is more common of low-energy brackish settings (Pemberton and Wightman, 1992). Sand-filled cracks are interpreted to be syneresis cracks.

2.2.11 Facies 9 – Horizontally Bedded To Planar Cross-Bedded Glauconitic Sandstone (F9)

Description

Facies 9 is closely associated with the other glauconitic units and it found in most wells within the study area. Its thickness ranges from 30 cm to 3 m.

This facies is characterized by horizontal bedding and low to high angle planar cross-bedding (Fig. 2.16C, D). Ripple cross-stratification is rare. Amalgamation surfaces and scour surfaces are present. The average sandstone grain size is upper very fine to upper fine. Herringbone cross-bedding is present. This facies often exhibits rhythmic bedding of thin glauconitic sandstone laminae. The overall mud content is less than 5 percent.

Bioturbation is rare and dominated by small *Palaeophycus* burrows. Sideritized mud clasts and iron stained sandstone are rare to occasionally present. Rare deformation in the form of slump blocks and syn-sedimentary faults is present.

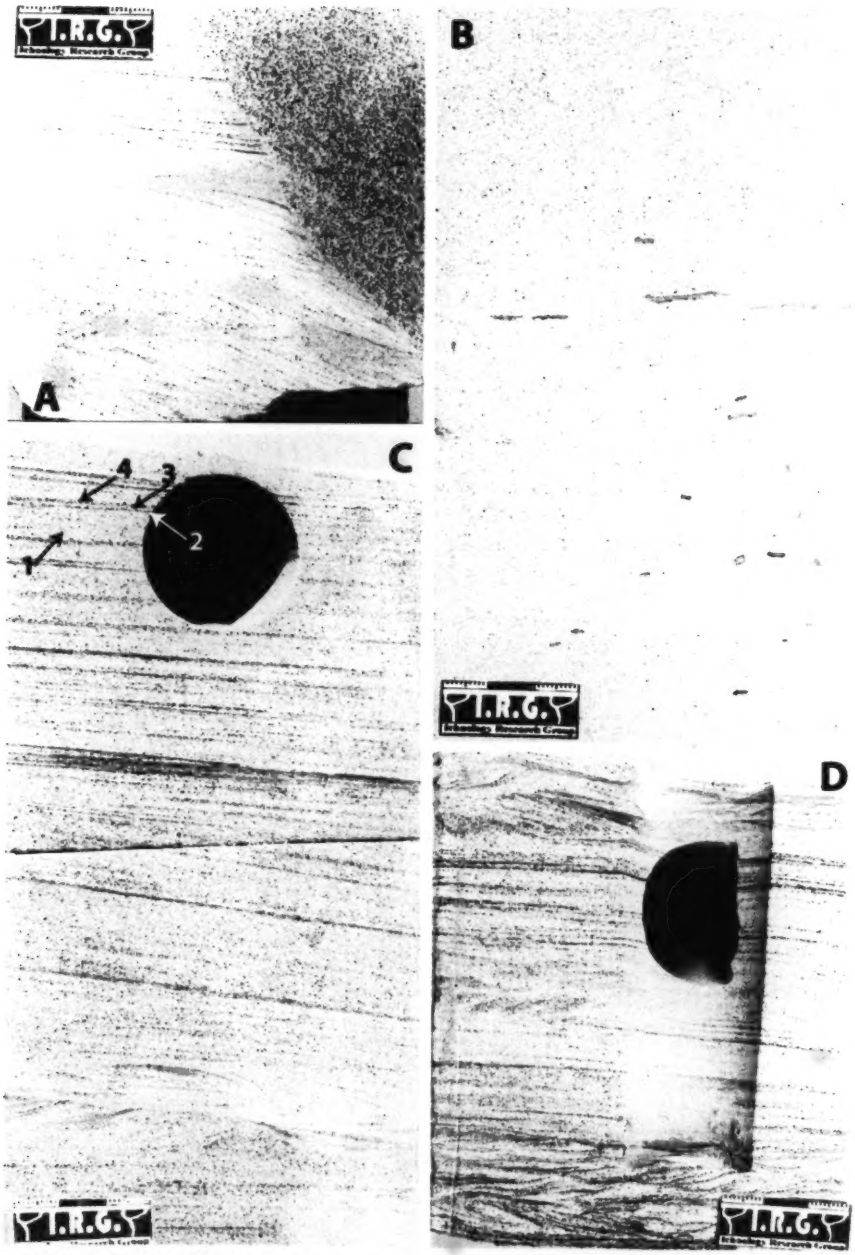

Figure 2.16. Horizontally bedded to planar cross-bedded glauconitic sandstone (Facies 9) and structureless sandstone (Facies 11). A) Structureless sandstone scoured into Facies 8a. B) Facies 11 with sideritized mud clasts. C) Low angle planar cross-bedding with mud couplets (Facies 9): 1- dominant flow sand, 2 - first slack water mud/glaucony lamina, 3 - subordinate flow sand, 4 - 2nd slack water mud/glaucony lamina. D) Glaucony couplets in low angle cross-bedded glauconitic sandstone (Facies 9).

Interpretation

Planar cross-bedding is formed by the migration of two-dimensional dunes. Horizontal bedding is interpreted as deposition within the upper plane bed. Glaucony found along cross-bed foresets occasionally forms double and single mud (glaucony) drapes or tidal bundles (Boersma, 1969; Visser, 1980), where glaucony takes the place of what would normally be mud within the tidal bedding. Again, double mud drapes are only found in subtidal depositional settings as two slack water stages are required (assuming diurnal tide; Visser, 1980). Visser (1980) suggested that tidal bundles and couplets are the most unique and positive diagnostic criteria for identifying ancient subtidal deposits.

A strongly stressed environment is suggested by the paucity of bioturbation. A high sedimentation rate and shifting substrate are the likely culprits.

2.2.12 Facies 10 – Cross-Bedded Glauconitic Sandstone (F10)

Description

Facies 10 is associated with other glauconitic units and is found in most wells within the study area. Its thickness ranges from 30 cm to 5 m with an average of 2.5 m. It commonly forms the base of a fining upward sequence with rippled glauconitic sandstone (Facies 8a) at the top.

This facies is characterised by trough and high angle planar cross-bedding in upper very fine to lower medium grained glauconitic sandstone (Fig. 2.17). Bedform thickness ranges from 5 to 20 cm and is 10 cm on average. Herringbone cross-bedding rarely occurs. Scour surfaces are common and contain glauconitic sandstone rip-up clasts. Cross-bed foresets occasionally show rhythmic alternation of sand beds and glauconitic laminae. Flaser and wavy bedding occur in intermittent muddier sections.

Cryptic bioturbation and rare *Palaeophycus* burrows are the only forms of visible biogenic activity within this facies. The abundance of shell fragments ranges from rare to common. Sideritized mud intraclasts are a major constituent of this facies and accumulate in troughs and along bedding planes. The amount of glauconitic material varies from rare to abundant and gives this facies a range of greenish colours. Red and black diagenetic iron staining is locally abundant. Carbonate cementation occurs locally and organic material is commonly found within muddier sections.

Due to the general lack of mud, soft-sediment deformation is rare. Deformation structures present include flame structures and syn-sedimentary faults. Sideritized mud clast breccia development is often associated with this facies and occurs at the base or within the unit.

Figure 2.17. Trough cross-bedded glauconitic sandstone (Facies 10). Sideritized mud intraclasts are common, as are mud lined troughs. A, B and D) Trough cross-bedding with sideritized mud intraclasts accumulating along troughs. C) Bedform toesets grading upward into foresets.

As with the rippled glauconitic sandstone (F8a), this facies varies between two endmembers: a light green, clean cross-bedded sandstone with occasional sideritized mud clasts, and a dark green muddy glauconitic cross-bedded sandstone with abundant shell fragments and sideritized mud clasts. A cross-bedded oolitic sandstone also occurs in the upper portion of the Hayat-10 well.

Interpretation

Trough cross-bedding forms as a result of migrating three-dimensional dunes, while planar cross-bedding represents migration of two-dimensional dunes (Harms et al., 1975). Herringbone cross-stratification is deposited in a tidal regime.

The abundant mud intraclasts and shelly material are lag deposits. The mud intraclasts were likely eroded from partially lithified mud within the depositional system. This mud probably originated as clay drapes deposited during a tidal slack-water period and were later eroded and incorporated within bedset foresets and between cross-bed sets (Tastet et al., 1986; Allen, 1991).

The suite of trace fossils in this facies demonstrates that accumulation took place under marine or marginal marine conditions, but the low abundance of biogenic structures suggests the presence of an environmental stress upon the system. The migrating dunes that are constantly in motion and the non-cohesive shifting substrate both prevent the development of dwelling and deposit feeding structures (MacEachern and Pemberton, 1994).

As with the rippled glauconitic sandstone, the two endmembers within this facies are likely a consequence of changing current energies and variations in mud input into the depositional system. The oolitic cross-bedded sandstone is a peculiarity within this facies, but its presence gives information about the depositional setting. Carbonate (e.g. oolitic) sand bodies are prominent in high-energy subtidal to intertidal environments in many platform settings (Tucker and Wright, 1990; Wright and Burchette, 1996). Ooids normally form in very shallow, warm, agitated waters that are saturated with respect to calcium carbonate (Wright and Burchette, 1996). Their concentric coatings reflect accretionary growth in environments where both tide and wave action move grains. Tidal current velocities are typically amplified within systems such as tidal channels and therefore there is a great potential for grain movement. If the carbonate content of the water is increased in such a setting, coated grains such as ooids can form with ease (Wright and Burchette, 1996).

2.2.13 Facies 11 – Structureless Glauconitic Sandstone (F11)

Description

Facies 11 is found in the southern portion of the study area. The thickness of individual occurences is less than 2.5 m, but the cumulative thickness in a core varies from 15 cm to 4.3 m. Although it is commonly interbedded and associated with the other glauconitic facies, it is generally found only within the lower half of the main glauconitic unit at the top of each well.

The average grain size of this sandstone is lower to upper fine with rare lower medium. Physical sedimentary structures, when visible, are low angle cross-bedding or horizontal bedding (Fig. 2.16A, B). The bottom and top contacts are usually scoured and sharp, respectively.

Discrete trace fossils are absent, but cryptic bioturbation is present. Accessory components include occasional iron staining and rare sideritized mud clasts and mud laminae.

Interpretation

The apparently structureless glauconitic sandstone beds may be a result of cryptic bioturbation by meiofauna, rapid deposition, or penecontemporaneous liquefaction (MacEachern and Pemberton, 1994). The lower contact of this facies is commonly scoured, suggesting energetic deposition or emplacement. The presence of barely visible sedimentary structures suggests cryptic bioturbation is responsible for at least some occurrences of this facies.

2.2.14 Facies 12 – Brown Organic Shale (F12)

Description

Facies 12 occurs at the tops of most cores and is on average 3 m thick. It is characterized by its brown colour, high fissility, and high organic content in the form of woody material, plant debris, and disseminated organics (Fig. 2.18A, B). Sandstone beds less than 5 cm thick are found occasionally and are usually underlain by sand-filled cracks. The sandstone beds are very fine grained, contain ripple forms and planar laminated silt, and are commonly contorted. Bioturbation is rare to absent and consists of small *Planolites* traces. Sideritized beds less than 3 cm thick are common.

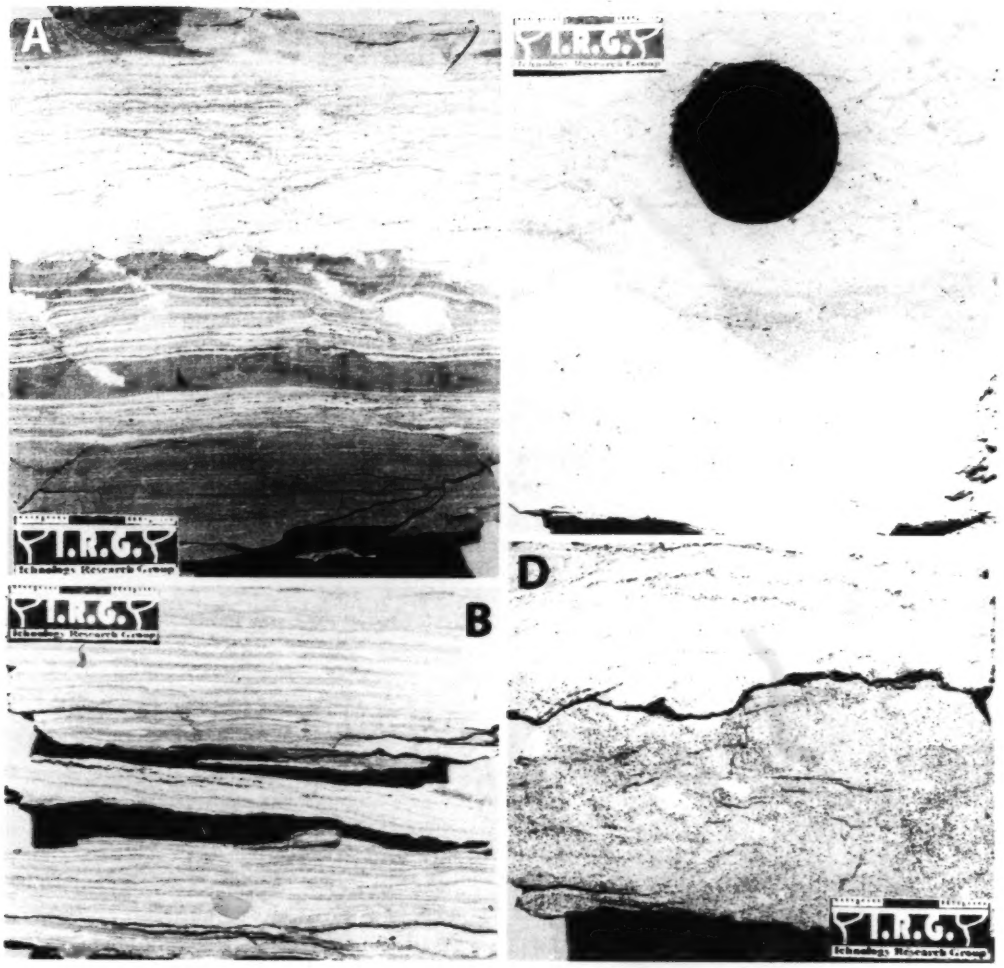

Figure 2.18. Brown organic shale (Facies 12) and calcareous shale with glauconitic sandstone interbeds (Facies 14). A) Facies 12 with syneresis cracks underlying rippled to horizontally bedded contorted sandstone bed. B) Facies 12 with horizontal bedding. C) Facies 14 with abundant bioturbation. D) Calcareous shale with glaucony-filled burrows.

Interpretation

The general lack of bioturbation within this facies suggests the presence of an environmental stress on the system. Otherwise, the burrows are hidden due to a lack of lithologic contrast. Frequent alternations between planar-laminated silt and mud could have been formed in a tidal regime. Sand-filled cracks are attributed to syneresis and underlie rippled, contorted sand beds. The cracks are therefore likely related to the influx of sand into the system and an associated change in salinity. The fine-grained nature of the sediment and the high abundance of organics suggests a quiescent, sheltered environment

near a fluvial source where sediment can rain out of suspension and organic matter can accumulate.

2.2.15 Facies 13 – Organic Glauconitic Sandstone (F13)

Description

Facies 13 is a diagenetically complex unit found in the upper portion of Salam-17, Yasser-3, and Yasser-4. It ranges in thickness from 10 cm to 2 m and commonly occurs as interbeds within brown organic shale (Facies 12).

This unit is poorly sorted with an average grain size of lower fine to upper medium with common coarser sized grains and clasts. Local fining and coarsening upward grain size trends are visible. A wide range of sedimentary structures is present and includes symmetrical and asymmetrical ripples, horizontal bedding, and low to high angle planar cross-bedding (Fig. 2.19). Mudstone beds and flasers are a significant component of this facies and can also take the form of wavy and lenticular mudstone beds. Dark green and purple beds rich with glaucony are typical of this facies.

Although bioturbation ranges from rare to common, individual burrows are difficult to identify. *Planolites* and *Palaeophycus* are the most frequent identifiable ichnofossils. Mudstone beds are typically sideritized and iron stained. Abundant organic and coalified material collects on bedding planes. Shell fragments are rare. Diagenetic reactions have imposed a purple to black tinge on the rocks. Sideritized mud clasts are occasionally found and can be up to 3 cm in size. Generally, the unit appears contorted and deformed, although discrete soft-sediment deformation structures are rare.

Interpretation

Facies 13 contains a wide range of sedimentary structures that are formed under a variety of flow conditions. Ripple cross-bedding represents migrating current and wave ripples, while low to high angle planar cross-bedding is created by migrating two-dimensional dunes. The abundance of mud laminae indicates common deposition from suspension. The large grain size and high amount of soft-sediment deformation implies a high energy environment.

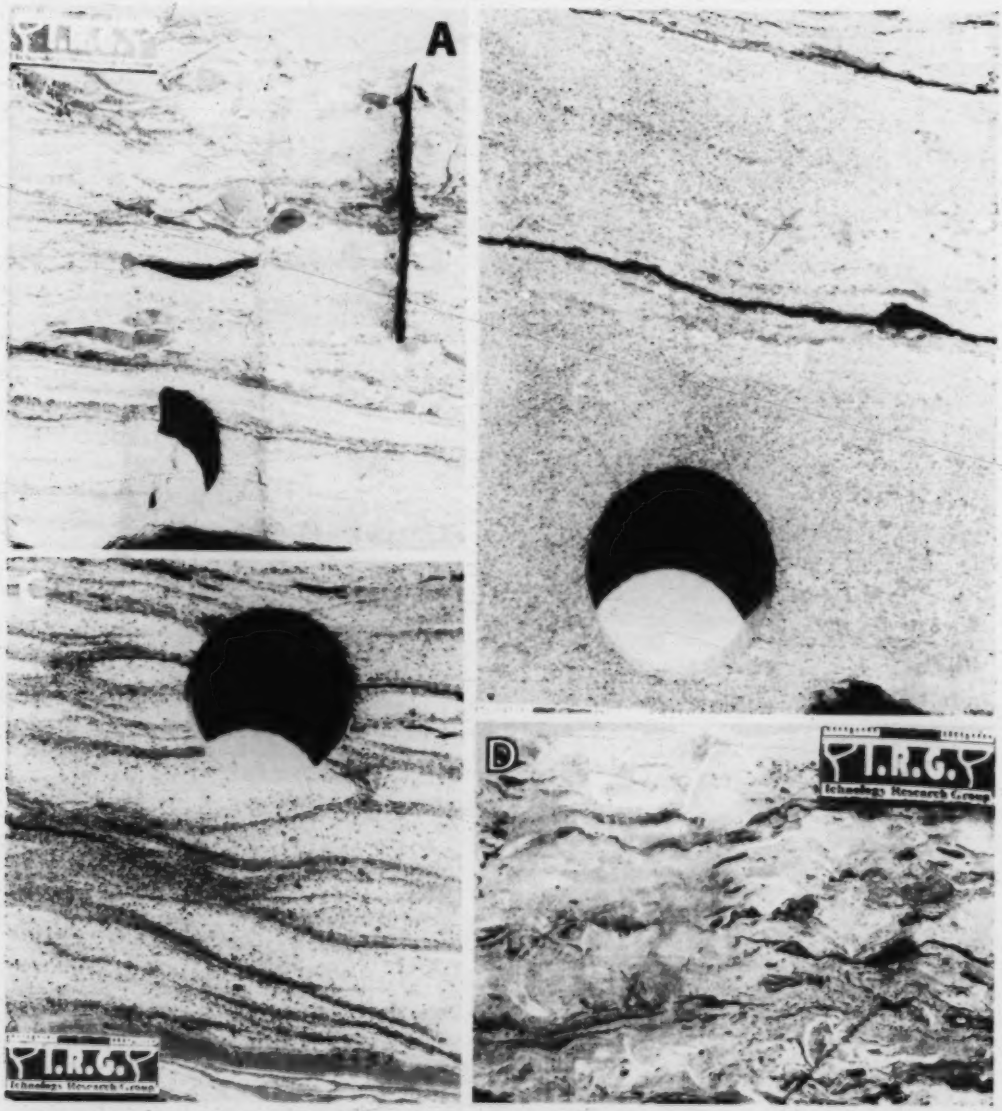

Figure 2.19. Organic glauconitic sandstone (Facies 13). A) Low angle planar bedding with organic rich beds and sideritized mud intraclasts. B) Purple low angle planar bedded coarse grained sandstone with glauconitic and organic material. C) Wavy bedded sandstone and glaucony beds with abundant carbonaceous debris. D) Shell and coal rich sandstone.

2.2.16 Facies 14 – Calcareous Shale With Glauconitic Sandstone Interbeds (F14)

Description

Facies 14 underlies Facies 15 and ranges in thickness from 60 cm to 3.5 m. It occurs at the top of most cores.

This facies is composed of calcareous shale with glauconitic sandstone interbeds (Fig. 2.18C, D). The interbeds are 3 to 5 cm thick and generally contain ripple cross-bedding and planar bedding. The shale occasionally contains millimetre-scale horizontal lamination and lenticular bedding. There is little visual lithologic contrast between the shale and the glaucony-rich ripples and sand units.

Burrowing is moderate to abundant, but usually the lack of lithologic contrast makes the trace fossils difficult to decipher. *Planolites, Thalassinoides,* and *Chondrites* are present; otherwise, the rocks have a mottled appearance and trace fossil identification is difficult. In some cases there appears to be complete homogenization of the sediment by the activity of benthic organisms (Fig. 2.18C).

Disseminated pyrite and pyrite nodules are moderately abundant, while diagenetic reactions have imparted a purple colour to the rocks. There is an overall upward increase in glaucony content.

Interpretation

The presence of carbonate within this facies suggests a transition from a siliclastic dominated regime to a system where carbonate generation has commenced. The abundant bioturbation with a restricted suite of traces indicates an environment where benthic organisms are flourishing but in a somewhat stressed (i.e. not fully marine) environment. The occasional ripple bedded glauconitic sandstone is evidence of some current or wave activity. The fine-grained nature of the sediment signifies that most deposition was from suspension.

2.2.17 Facies 15 – Shell Hash (F15)

Description

Facies 15 occurs at the top of most core within the study area and consists of individual shell hash beds, up to 60 cm thick, interbedded with calcareous shale (Fig. 2.20). The shell beds contain disarticulated and articulated *Exogyra* oyster shells in a matrix of shale, fine-grained sandstone, or glaucony. Siderite and limestone are present in varying amounts. Bioturbation is rare, as are visible sedimentary structures.

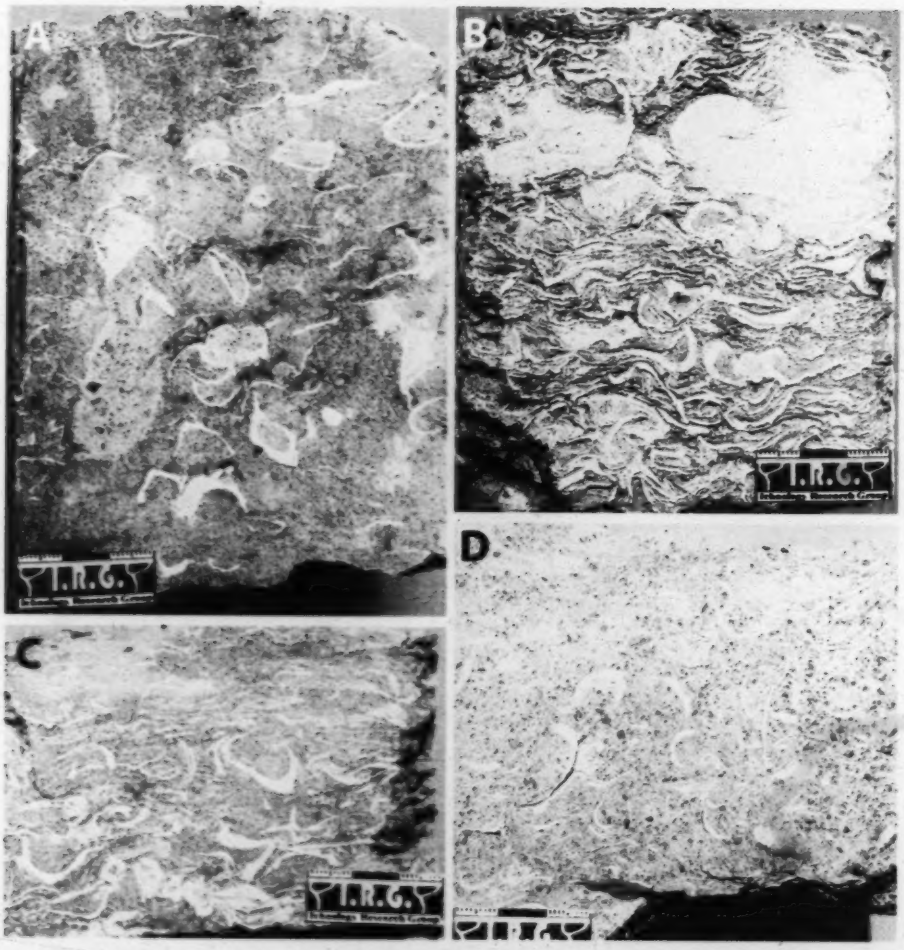

Figure 2.20. Shell hash (Facies 15). A) Glaucony rich matrix. B and C) Matrix of calcareous shale. D) Coarse-grained sandstone matrix.

Interpretation

The abundant shells were likely deposited during a high energy event. Concentrations of coarse shell fragments can be found where large surfaces are undergoing erosion or where channels are eroding and migrating laterally (Reineck and Singh, 1980). Oysters growing on the banks of tidal channels can be reworked into lag deposits upon transgression within the bay (Weimer et al., 1982). However, the abundance of carbonate within this facies and the presence of the marine oyster *Exogyra* (Fairbridge and Jablonski, 1979) suggests a shallow marine depositional setting.

2.3 OTHER SIGNIFICANT UNITS

2.3.1 Sideritized Mud Clast Breccia

Description

This unit is not considered to be a facies on its own due to its limited thickess and sporadic nature, but it is a significant component of many facies and therefore deserves attention. It consists of abundant, poorly sorted sideritized mud clasts in a mudstone or sandstone matrix (Fig. 2.21). The clasts range in size from 3 mm to 10 cm, while the average sand matrix grain size ranges from upper fine to lower medium. Both matrix and clast supported varieties occur and the unit as a whole ranges in thickness from 3 to 60 cm.

The mud clasts are occasionally imbricated. Shelly and coaly material is rare to common. Iron and siderite staining is common to locally abundant. The basal contact is consistently scoured. Although bioturbation within the unit is generally rare or difficult to discern, it is commonly associated with the *Glossifungites* ichnofacies (see discussion in Chapter 3).

Interpretation

In the lower Bahariya Formation, most sideritized mud clast breccias are developed where there is a facies change within the sedimentary succession. As such, they commonly represent lag deposits. In other cases, breccias are found within homolithic units and have little stratigraphic importance, aside from representing local erosion and accumulation.

Often the mud clasts within this unit are imbricated, suggesting deposition under unidirectional flow. Unlithified mud clasts are normally very brittle and do not survive intact when transported over long distances (Reineck and Singh, 1980). As such, these clasts were probably ripped up from within the depositional system. The variation in rounding and sorting could be due to varying current energy and transport distance. Baker et al. (1995) described "mud balls" from the Fly River delta and interpret them as rip-up clasts that have been rounded through transport. These balls are associated with channel deposits within the tide-dominated delta and could be analogous to the rip-up clasts seen in the lower Bahariya Formation.

Sideritization is a chemical reaction that occurs early in a sediment's diagenetic history. For this reason, the mud clasts within the breccias were probably already sideritized prior to erosion, transport, and deposition.

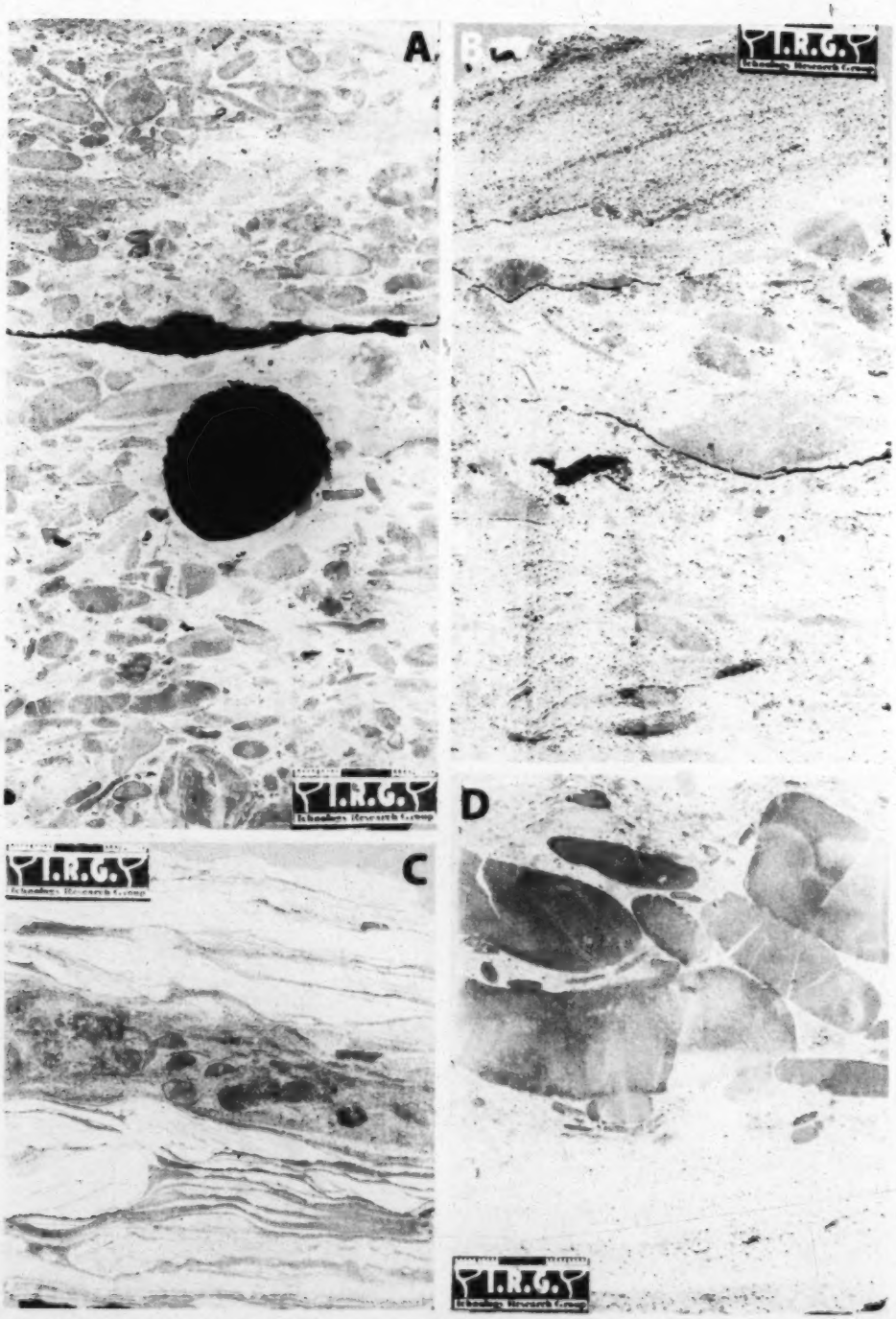

Figure 2.21. Sideritized mud clast breccia. A) Clast supported conglomerate. B) Overlain by sandstone with high angle planer cross-bedding. C) Thin unit within deformed wavy bedded sandstone and mudstone. D) Large imbricated clasts within fine grained sandstone.

2.3.2 Carbonate Cemented Sandstone

Description

Another important unit is the carbonate cemented sandstone. The average thickness of this unit is approximately 60 cm, while ranging from 15 cm to 1.8 m. It is found in about half the wells in the study area.

This unit consists of lower fine to lower medium sandstone with abundant carbonate allochems (Fig. 2.22). The allochems are typically bivalve and oyster shells and crinoid ossicles with an average size of lower medium to very coarse. Crude low angle planar cross-bedding and horizontal bedding are the only sedimentary structures. Iron staining is moderate to abundant with common sideritized mud clasts and glauconitic grains. Organics, mudstone laminae, and carbonaceous material are widespread. This unit contains no clear bioturbation. Calcareous veins and moldic porosity are occasionally found.

Interpretation

Shelly material is commonly deposited as a lag during sea level rise or fall, such as along flooding surfaces (Ketzer et al., 2003). The concentration of carbonate bioclasts is itself the likely source for carbonate cement in this unit (Ketzer et al., 2003). Also, transgression may significantly reduce siliciclastic input into the system, increasing carbonate production. Many of the calcite cemented sandstone units can be correlated between wells and likely represent significant stratigraphic surfaces (see discussion in Chapter 3).

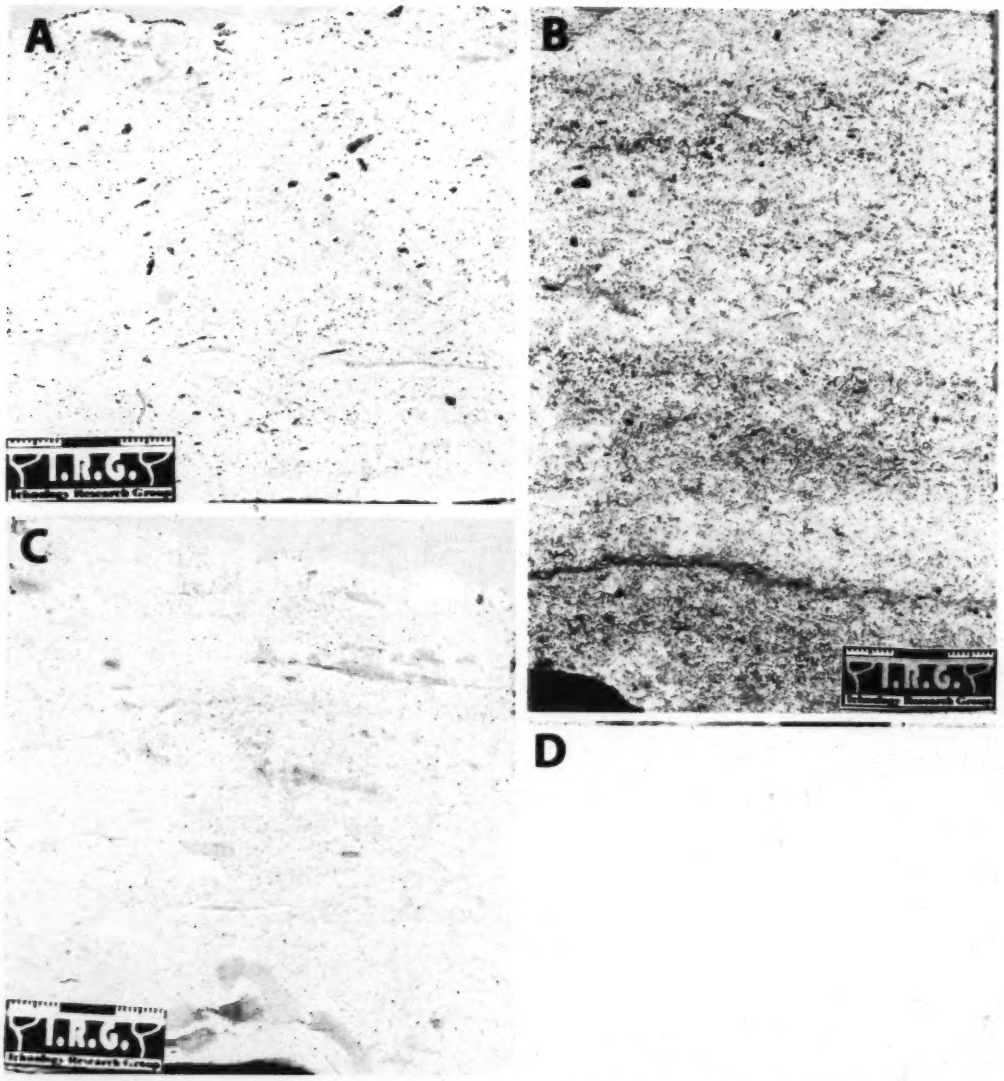

Figure 2.22. Carbonate cemented sandstone. A) Abundant shelly material and moldic porosity. B) Abundant shelly material. C) Shelly material and sideritized mud intraclasts. D) Allochems such as crinoid ossicles.

2.4 FACIES ASSOCIATION DESCRIPTION AND DISCUSSION

2.4.1 Facies Association 1 – Brackish Bay (FA1)

Finely laminated mudstone and sandstone (F1) and heterolithic sandstone and mudstone (F2) are the dominant facies within FA1, with flaser bedded sandstone (F3) occuring less frequently. Facies Association 1 can be up to 10 m thick and is commonly bound at the base and top by a sideritized mud clast breccia. It interfingers with all other facies associations.

Discussion

Facies Association 1 represents a brackish bay depositional system with a range of subenvironments from brackish bay, tidal shoal or bar, tidal point bar, to tidal flat. The major portion of sedimentation within this association is likely subtidal. Because it is difficult to distinguish between brackish bay and tidal flat deposits, there is likely a mixture of both within this association.

Facies 1 is interpreted to represent deposition within a quiescent, tide-influenced shallow bay due to its finely laminated nature, broad lateral extent and trace fossil assemblage. The finely laminated nature of Facies 1a and 1b closely resembles tidal bedding described from the tidal flats of the North Sea (Reineck, 1972; Reineck and Singh, 1980). Although abundant in modern environments, the preservation potential of tidal flat sediments in the rock record is low and is commonly restricted to a thin veneer of sediment overlying channel deposits (Weimer et al., 1982). The typical trace fossils found in tidal flats are vertical burrows such as *Arenicolites* and *Skolithos*, morphologies that reflect suspension feeding behaviour in deep domiciles (Pemberton et al., 2001). The broad lateral extent of Facies 1 combined with an abundance of horizontal and deposit feeding burrows precludes a tidal flat interpretation. The thinly laminated nature of the facies is likely due to a low energy tidal influence within the bay.

Facies 2 is also represents deposition mainly in a tide-influenced brackish bay, but includes tidal flat deposits. A variation of Facies 2b containing 1.5 to 2.5 m thick successions of lenticular to wavy bedded sandstone and mudstone with depositional dip is interpreted as tidal point bar deposits (e.g. Smith, 1987).

Facies 3 was deposited subtidally, probably as a tidal shoal or bar. The herringbone cross-bedding indicates deposition by tidal currents and the presence of mud flasers suggests periods of current activity alternating with periods of quiescence (Nio and Yang, 1991). The coarsening upward successions from Facies 1A & B and 2A & B, into Facies

1c and 2c, and finally into Facies 3 probably record the progradation of these subtidal sand bars into a lower energy bay setting (Allen, 1991; Rossetti, 1998).

Overall, the presence of locally abundant soft-sediment deformation suggests periods of rapid sedimentation within the bay (Allen, 1982). The stressed, low density, low diversity ichnologic assemblage is indicative of colonization in brackish water (Pemberton and Wightman, 1992). Both tide and wave energies are present, which is also common in bays and on tidal flats (Weimer et al., 1982). The presence of syneresis cracks, which are indicative of changing salinities at the sediment-water interface, supports a brackish bay interpretation. Siderite and pyrite are commonly found in brackish bay sediments where a high amount of organic matter and an influx of fresh water create reducing conditions at the sediment-water interface (Wightman et al., 1987; Rossetti, 1998).

2.4.2 Facies Association 2 – Tide-Influenced Delta Front (FA2)

Facies Association 2 is found throughout the study area and is composed of numerous repeating coarsening upward successions containing up to six different facies: finely laminated mudstone and sandstone (F1c) or lenticular bedded mudstone (F2a) at the base, grading upward into sandstone with mud and organics (F4), bioturbated rippled sandstone (F5), or flaser bedded sandstone (F3). The top and basal contacts of FA2 are commonly scoured and mantled by sideritized mud clast breccias. FA2 ranges in thickness from 2.5 to 12 m and is closely associated with FA1 and FA3.

Discussion

Based on the high organic content, hyperpycnal muds, and ichnofossil assemblage, FA 2 is interpreted as a tide-influenced delta. The coarsening upward sequences represent prograding delta lobes, with Facies 1c and Facies 2 as the muddy distal deltaic deposits and Facies 3, 4, and 5 representing sandy proximal delta front deposits.

The coarsening upward sequences containing Facies 4 represent the most active portion of the delta front. The lack of bioturbation combined with the high degree of deformation indicate high sedimentation rates, while the abundance of organic material suggests a proximity to terrestrial input. Facies 5 is also deposited within the delta front, but under sedimentation rates that were slower than for Facies 4, which allowed for substrate colonization by benthic organisms. Facies 3 shows slightly more tidal influence than either Facies 4 or Facies 5 and could represent distributary/tidal channel or bar deposits on the subaqueous delta plain.

Distal delta front or prodelta deposits (F1c and F2) closely resemble the background

brackish bay deposits, although they are occasionally slightly more deformed. A tide-dominated delta is considered to be a brackish water bay-like environment that contains a number of subenvironments such as distributary/tidal channels, delta plain, etc. (Pemberton et al., 2001), so an abundance of brackish-water bay fill deposits within such a system should be expected. For the lower Bahariya Formation, the only actual difference between the brackish bay and prodelta deposits is their stratigraphic location and association: the prodelta muds are located at the base of coarsening upward successions that grade into delta front distributary bars (FA2), while brackish bay deposits are associated with tidal channel and bar sediments (FA1).

Delta fronts are made up of sheet sediment flows that move and erode along the sediment-water interface and deposit sand bodies with a scoured or eroded basal contact (Reading and Collinson, 1996). The lack of tidal features within this tide-dominated delta front (F4 and F5) is somewhat problematic. It is possible that formation of tidal structures was disrupted by wave action (Williams, 1991), or the presence of ebb- and flood-dominated channels on the delta front created channel bedforms related solely to unidirectional flow, which could have been also affected by wave action (Caston, 1972; Gastaldo et al., 1995). The sand distribution of the delta lobes (see chapter 3) suggests an increase in wave energy over time, which could explain the abundance of wave-generated structures in certain facies. It is interesting to note that tidal sedimentary structures are not found in the some subtidal deposits of the tide-dominated Fly River Delta (Baker et al., 1995). This is thought to be due to low sediment accumulation rates, current speeds that are not conducive to the preservation of tidal rythmites, or the erosion of sediments by waves or currents (Dalrymple and Makino, 1989; Nio and Yang, 1991; Baker et al., 1995).

2.4.3 Facies Association 3 – Marine Shoreface (FA3)

Burrowed mottled sandstone and mudstone (Facies 6a), burrowed muddy sandstone (Facies 6b), rippled sandstone with organic rich flasers (Facies 7), and a variation of Facies 1b make up Facies Association 3. This association is of limited thickness and restricted to the wells in the Salam Field, with thin intervals preserved in Hayat-11 and Hayat-10. It is bound at its base and top by discontinuity surfaces. FA3 overlies FA2 and is overlain by FA4 or FA1. Its maximum thickness is 8 m.

Discussion

Facies Association 3 is interpreted as lower to middle shoreface deposits. The interbedded character of Facies 6a, combined with the presence of oscillation ripples

and a trace fossil suite dominated by burrows belonging to the *Cruziana* ichnofacies, is characteristic of the lower shoreface (Walker and Plint, 1992; Pemberton and MacEachern, 1995). Facies 6b is deposited in slightly higher energy conditions than Facies 6b and the presence of members of the *Skolithos* ichnofacies indicates some shifting and unstable substrates with enough suspended food to allow for suspension feeding. Facies 6 could represent distal (F6a) and proximal (F6b) components of the lower shoreface.

The transition from Facies 6 to Facies 7 is abrupt but conformable. Facies 7 was deposited under much higher energy conditions than Facies 6, and therefore probably corresponds to the middle shoreface, as this portion of the shoreface is characerized by high wave energy (Reinson, 1984; Pemberton et al., 2001). According to Pemberton et al. (2001), when storm influence is negligible, fair-weather oscillatory waves dominate the lower and middle shoreface. The middle shoreface is also under the influence of tidal processes, which explains the presence of herringbone cross-stratification within Facies 7. Although the *Skolithos* ichnofacies typically dominates the middle shoreface, bioturbation within this zone can be extremely variable. Sedimentologically, middle shoreface sands tend to be well sorted, fine to medium grained with only minor shale and silt layers (Pemberton et al., 2001).

The lack of visible storm beds or bedding associated with storm processes suggests that the shoreface during this time was under weak storm influence. The fair-weather *Cruziana* ichnofacies dominates such a succession and a change from the *Cruziana* suite to a *Skolithos* suite may be taken to correspond to a change from lower shoreface to middle shoreface (MacEachern and Pemberton, 1992). If present, thin, storm generated sandstones, especially those less than 15 cm thick, tend to be thoroughly bioturbated or obliterated by biogenic reworking (Wheatcroft, 1990; MacEachern and Pemberton, 1992).

A variation of Facies 1b contains a high diversity, high density trace fossil suite containing *Rhizocorallium, Bergaueria, Teichichnus, Chondrites,* and *Thalassinoides*. These traces are not found in any of the other brackish bay deposits and indicate a change of environmental parameters. Such traces are more typical of the fully marine *Cruziana* ichnofacies. Therefore, this unit is interpreted to represent sediment deposited during a marine incursion into the bay and is likely the proximal equivalent of the marine shoreface within sheltered portions of the embayment.

2.4.4 Facies Association 4 – Tidal Channel (FA4)

Facies Association 4 is very common within the study area and erosively overlies strata of FA1 and FA3. It consists of upper very fine to medium grained, large- to small-

scale cross-stratified, structureless and rhythmically bedded sandstone (F8 to F11) with lenticular to wavy bedded mud (F2b and c). Stacked amalgamations of Facies 8 through 11 display a sharp-based, fining upward character that ranges in total thickness from 3 to 15 m. Facies 9, 10, and 11 are generally found at the base of these fining upward sequences, with Facies 8 and 2 at the top. Not every facies is present within each succession and there is an abundance of Facies 8. Glaucony is the dominant accessory mineral and is found almost exclusively within this association.

Discussion

Facies Association 4 is interpreted as stacked amalgamations of fining-upward tidal channel deposits. These sediments reflect a prevalence of deposition from currents and the tidal influence within this association is great, as evidenced by the large number of tide generated sedimentary structures. The overall fining upward succession from high energy trough and planar cross-bedded sands (F9 and 10) to lower energy ripple cross-bedded sands (F8) to lenticular and wavy mudstone (F2) follows Allen's (1970) fluvial model for deposition on a point bar with an upwards decline in flow strength (typical channel succession). Although this is a tidally influenced channel, there is no evidence of inclined heterolithic stratification (IHS; Thomas et al. 1987). The tidal channel interpretion is further supported by the presence of tidal bedding and double mud drapes (F9). These sedimentary features can only form in subtidal channels, as they required two slack-water periods during the diurnal tidal cycle.

Tidal channels are associated with composite bedforms such as sand waves, which are found adjacent to or within the channels (Allen, 1980; Ashley, 1990; Dalrymple, 1992). These large-scale bedforms migrate downstream and contain dunes or mega-ripples with superimposed smaller bedforms that change their orientation with the tidal flow (Ashley, 1990). Subsequently, bedforms typically created under different hydraulic regimes are found in close association, and this could explain the alternation between trough cross-bedding with ripple cross-lamination in Facies 10. Futhermore, for fine to medium grained sand, a small decrease in current velocity can quickly cause a major change in bedform morphology (from ripples to dunes to planar horizontal bedding; Ashley, 1990).

The trace fossil assemblage within FA3 contains a low diversity and low abundance of ichnofossils. *Palaeophycus, Macaronichnus*, *Skolithos,* and escape structures are the dominant forms, and their presence precludes a fluvial origin for these channel deposits. Both *Skolithos* and *Macaronichnus* are indicative of high energy conditions: *Skolithos* is created by a suspension feeding organism that requires a certain level of water turbitiy and suspended food to survive (Pemberton et al., 2001). *Macaronichnus* is typically found in

high-energy subtidal (usually foreshore) zones (Saunders and Pemberton, 1986).

Facies Association 4 closely resembles Meckel's (1975) estuarine channel deposits from the Holocene Colorado River Delta. Although the estuarine channels of his study are finer grained and are dominated by parallel lamination instead of trough and ripple cross-bedding, both systems contain abundant mud intraclasts, the same range of sedimentary structures that decrease in scale upward, and rare bioturbation.

MacEachern and Pemberton (1994) described a similar channel facies association within the Cretaceous Viking Formation of Alberta. They interpret their association to reflect a number of depositional settings including tidal channels, tidal inlets, or marine-influenced lowstand channels. Mud clasts and shell lags are abundant in channel deposits and a channel lag of up to 3 metres thick is not uncommon (Reineck and Singh, 1980).

The major occurrences of glaucony within the study area is concentrated within the tidal channel deposits. Its provenance is unknown, but because it is associated with the channel deposits, it is likely derived from older strata that the channels eroded into (allochthonous glaucony; Amorosi, 1995). Alternatively, tidal currents transported the glaucony grains from the shelf into the embayment where it was concentrated in the high energy channel deposits (parautochthonous glaucony; Amorosi, 1995).

Facies 2a and 2b commonly overlie and are interspersed within tidal channel deposits and could represent deposits associated with channel abandonment (channel-fill). Typically, fluvial channel-fill deposits consist of clay and silt sized sediment with rare sand beds and common organic material (Reineck and Singh, 1980). In the case of the lower Bahariya Formation, channel abandonment deposits would closely resemble the surrounding bay deposits, as the abandoned channel would be filled with brackish bay waters after the tidal channel was cut off. As such, it would be very difficult to fully differentiate between brackish bay and abandoned channel fill deposits.

2.4.5 Facies Association 5 – Transgressive Embayment (FA5)

Facies Association 5 is a complex, but predictable, sequence of up to six facies. Facies 2 (heterolithic sandstone and mudstone) occurs at the base and is typically overlain by Facies 8b (muddy rippled to flaser bedded glauconitic sandstone). This in turn is overlain by brown organic shale (F12) with beds of organic glauconitic sandstone (F13). This is overlain by calcareous shale with glauconitic interbeds (F14) and finally a shell hash unit (F15). Not all the wells have core that intersects FA5, resulting in an incomplete dataset and a great range in thickness for this succession. Two complete successions are found within the study area and are 6 and 14 m thick.

Discussion

FA5 has an overall fining upward character and is interpreted as a sequence of embayment deposits lain down during a time of overall sea level rise. The carbonate content and degree of bioturbation increase upward, while the grain size and organic content decrease upward, suggesting a landward shift in facies (Van Wagoner et al., 1990).

Muddy, rippled to flaser bedded glauconitic sandstone (F8b) is deposited under lower energy conditions than Facies 8a, which is attested to by a higher mud content and a dissimilar trace fossil assemblage. The trace fossil suite in Facies 8a indidcates the presence of a shifting, unstable substrate, while the assemblage in Facies 8b contains more deposit feeding traces, which require a more stable substrate. The trace fossil assemblage in Facies 8b is therefore more characteristic of a low-energy brackish setting than a high-energy tidal channel (Pemberton and Wightman, 1992). As such, Facies 8b was likely deposited as a tidal shoal with some possible associated channel deposits.

The fine grained nature of Facies 12, brown organic shale, is indicative of low-energy conditions. The rippled, fine grained sandstone beds represent periods of weak wave and current activity. The sand beds are underlain by syneresis cracks, which form as a result of large fluctuations in salinity at the sediment-water interface (Burst, 1965; Plummer and Gostin, 1981). Therefore, the sand beds must be associated with an influx of saline water into a less saline body of water. One possibility is that storm activity introduced saline water in association with higher energy conditions and coarser sediment into a more brackish water setting, forming syneresis cracks beneath the sandstone beds. The trace fossil assemblage is of low abundance and diversity, which is generally characteristic of brackish water settings (Pemberton and Wightman, 1992). The above evidence suggests that deposition of Facies 12 was in a proximal position to land within a large, quiescent embayment.

Facies 13, organic glauconitic sandstone, is a hodgepodge of fine to coarse sandstone, shale, glaucony, intraclasts, and coalified organic matter. The large variety of sedimentary structures suggests variable hydraulic conditions were active during its deposition. It occurs as thin interbeds within Facies 12, or as thick units associated with Facies 8b. The lack of visible bioturbation indicates a setting that was inhospitable for organism colonization. This facies is therefore interpreted as storm or high energy deposits within an otherwise quiescent embayment, proximal to land.

Calcareous shale with glauconitic interbeds (Facies 14) is interpreted as a distal embayment deposit. The lack of organic matter and high carbonate content suggests a position far from siliciclastic input. The fine grained nature of sediment is indicative of a quiet depositional setting, while rippled glauconitic sandstone beds were formed during

periods of higher energy. The presence of abundantly bioturbated units within this facies indicate hospitable conditions within more saline portions of the embayment.

The shell hash unit (Facies 15) contains debris of the oyster *Exogyra*. This organism was restricted to shallow marine habitats (less than 50 m water depth) and can be abundant in Late Cretaceous rocks (Fairbridge and Jablonski, 1979; Reiss, 1984). The variable lithology of the matrix, from limestone to sandstone to glaucony, suggests that high energy currents picked up and deposited sediment from a number of sediment source areas. This facies is therefore interpreted as a transgressive lag, likely deposited when the shoreline transgressed the quiet embayment.

2.5 SUMMARY

Within the study area, the lower Bahariya Formation was divided into fifteen facies that record varying tidal and wave influence. These facies were then grouped into five facies associations that represent distinctive marginal-marine and marine depositional systems. Tidal currents dominate the marginal-marine settings (brackish bay, delta, and tidal channel), while waves dominate the marine environments (shoreface). Chapter 3 elaborates on the interpretations made in this chapter and places these facies associations into a depositional model.

CHAPTER THREE: STRATIGRAPHY AND DEPOSITIONAL MODEL

3.1 INTRODUCTION

Building on the sedimentologic and ichnologic descriptions of the fifteen facies and five facies associations proposed in Chapter 2, this chapter further elaborates on the characteristics of each depositional system comprising the lower Bahariya Formation. Following a brief review of the morphological and ecological parameters governing each depositional environment, several stratigraphic cross sections are presented. These illustrations serve to delineate the distribution of facies, facies associations, and key stratigraphic surfaces within the study area. As depicted in the cross sections, three main types of stratigraphic surfaces are recognized. Their nature, sequence stratigraphic implications, and unique association with the *Glossifungites* ichnofacies are discussed. Based on the evidence presented in this and previous chapters, a four stage depositional model is proposed. The depositional stages are presented in a series of paleogeographic maps that illustrate the morphology of the depositional setting and place it in a regional context.

3.2 DEPOSITIONAL ENVIRONMENTS

Lower Bahariya strata were deposited in various marine and marginal marine depositional environments ranging from a tide-dominated delta and estuary to the shoreface. A definition of each environment is provided, along with a brief description of the morphological, sedimentological, ecological, and stratigraphic factors commonly associated with known modern analogues and ancient examples. Because marginal marine settings commonly contain similar sub-environments, misuse of terms and confusion of depositional system architecture is commonplace. As such, it is important to clearly differentiate one depositional setting from another.

3.2.1 Tide-Dominated Estuaries

An estuary is the seaward portion of a drowned river valley that receives sediment from both fluvial and marine sources, and contains facies influenced by tide, wave and fluvial processes. It extends from the landward limit of tidal facies to the seaward limit of coastal facies (Dalrymple et al., 1992; Boyd et al., 1992).

Over the past decade, modern estuaries have become popular research subjects in

the hope that these studies will lead to a better understanding of estuarine sequences in the rock record. Present-day estuaries are best developed on mid-latitude coastal plains with wide continental shelves undergoing marine submergence (Reinson, 1992). These estuaries originated as fluvial incised valleys that formed during the Late Pleistocene fall in global eustatic sea level (Allen and Posamentier, 1993). Therefore, following the principle of uniformitarianism, it is assumed that most ancient estuaries were located in incised valleys that formed as a result of relative sea level fall.

The classification of modern-day estuaries is based on the interaction of the tidal prism with fluvial discharge, which together are responsible for generating specific circulation types and sedimentary response patterns (Reinson, 1992). Although estuary morphology is largely dependent on the tidal range, incipient basin configuration also imparts an influence (Hayes, 1975; Harris, 1988). Thus, estuary classification is based on wave or tide dominance, with a gradation in morphology from lagoonal, partially closed, and open-ended (wave-dominated), to tidal (tide-dominated) as tidal range increases. The categories important to this study are open-ended estuaries, which do not have barrier bar at their mouths and occur in mesotidal to low macrotidal regimes with intermediate to high freshwater input, and tidal estuaries, which are typically funnel shaped, have large tidal prisms, and are found along macrotidal coastlines (tidal range: microtidal: < 2 m; mesotidal: 2 - 4 m; macrotidal: > 4 m; Reinson, 1992).

Tide-dominated estuaries contain both marine and fluvial sediment sources and are infilled by progradation of the landward margin (Boyd et al., 1992; Dalrymple, 1992). The gross geomorphology of modern tide-dominated estuaries consists of a network of tidal channels separated by tidal sand banks, intertidal flats, salt marshes, and salt flats (Fig. 3.1; Heap et al., 2004). A true tripartate facies distribution is absent in these systems due to the lack of a coarse-grained barrier and low-energy central basin.

The mouth of many tide-dominated estuaries contains elongate sand bars that are oriented parallel to the axis of the system and separated by ebb- and flood-dominated channels (Fig. 3.2; Dalrymple et al., 1990; Dalrymple, 1992). Lateral shifting of these bars produces a fining-upward succession because channel speeds are greatest in the channel bottom and decrease upward towards the bar crest. These bars grade landward into estuarine tidal flats and marshes that are dissected by tidal channels and creeks containing lateral accretion point bar deposits (Clifton, 1982). Tidal flat areas pass landward into coarse grained alluvial plain deposits (Dalrymple et al., 1990; Boyd et al., 1992; Dalrymple, 1992).

Based on this description of the sedimentologic and geomorphologic characteristics of tide-dominated estuaries, the facies associations within the lower Bahariya Formation

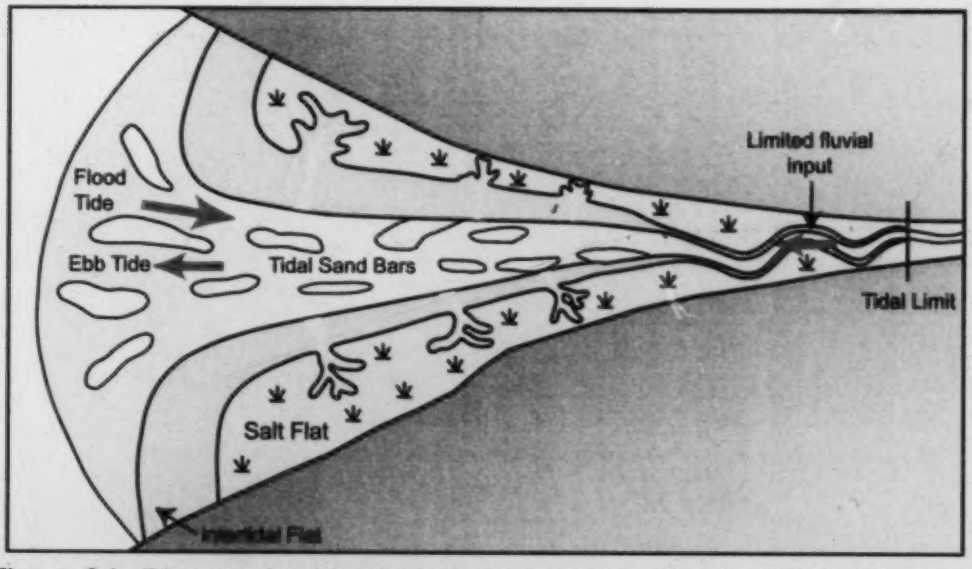

Figure 3.1. Diagram showing physical characteristics of a tide-dominated estuary (modified from Geoscience Australia [c]).

Figure 3.2. Satellite photograph of a tide-dominated estuary (the mouth of the Mary River) on eastern coast of Australia. Note the well developed tidal channels and bars (from NASA).

that correspond to such a system are the brackish bay (FA1) and tidal channel (FA4) associations.

3.2.2 Tide-Dominated Deltas

Deltas are defined as "discrete shoreline protuberances formed where rivers enter oceans, semi-enclosed seas, lakes, or lagoons and supply sediment more rapidly than it can be distributed by basinal processes" (Elliot, 1986, p. 113). They are subdivided into three categories based on the dominant process that controls their morphology, and are either river-, wave-, or tide-dominated (Galloway, 1975; Bhattacharya, 1992). Tide-dominated deltas are usually found at the head of embayments where the tidal range is amplified, or adjacent to narrow straits with high tidal current speeds (Dalrymple, 1992). Like their wave- and river-dominated counterparts, tide-dominated deltas contain three main sub-environments (Fig. 3.3): delta plain (dominated by rivers), delta front (zone of interaction between fluvial and basinal processes) and prodelta (zone of quiet sedimentation where basinal processes dominate).

The delta plain of tide-dominated deltas can be subdivided into two areas: tidal (distributary) channels and tidally influenced interdistributary areas. Tidal channels are usually slightly sinuous, exhibit a funnel shape, and contain mid-channel tidal sand ridges and sandwaves (Fig. 3.4). Interdistributary areas contain intertidal flats that grade seaward into tidal bars, but may also encompass bays, marshes, swamps, and salt flats (Reading and Collinson, 1996; Heap et al., 2004).

Basinward of the delta plain is the delta front, where sediment-laden fluvial water enters the basin and is consequently affected by basinal processes (Reading and Collinson, 1996). Because tidal processes dominate in this region, there is an abundance of tidal channels and tidal sand (distributary) bars. These bars are oriented at a high angle to the strike of the shoreline, may have relief of 15 to 20 m, and are often associated with small ebb or flood tidal deltas. They decrease in height away from distributary channels and pass outward into the distal delta front and prodelta.

In a deltaic system, the finest grain sizes are generally found in the prodelta. Heterolithic mudstone, siltstone, and sandstone are common tide-dominated prodelta sediments. Physical sedimentary structures include lenticular and wavy bedding, current ripples, and both graded and massive beds. Soft-sediment failure can be pervasive. Tide-dominated prodelta sediments can show tidal cyclicity (Bhattacharya and Walker, 1991) and contain sharp-based graded beds emplaced by flood-generated hyperpycnal flow (Reading and Collinson, 1996). Just as prodelta deposits of a delta prograding onto the

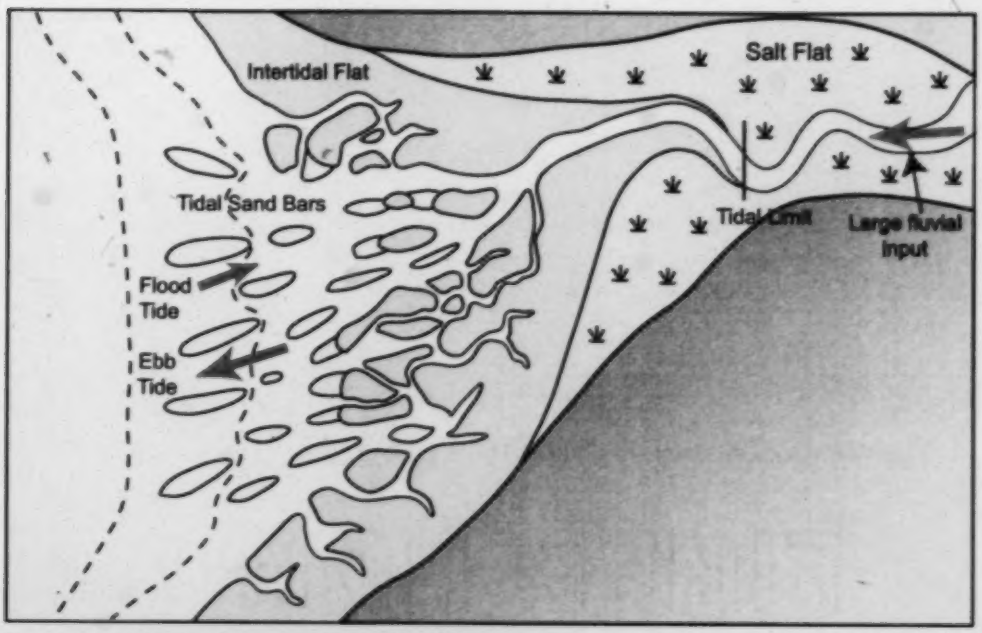

Figure 3.3 (above). Diagram showing physical characteristics of a tide-dominated delta (modified from Dalrymple, 1992).

Figure 3.4 (below). Satellite photograph of the Fitzroy River tide-dominated delta located on the western coast of Australia (from NASA).

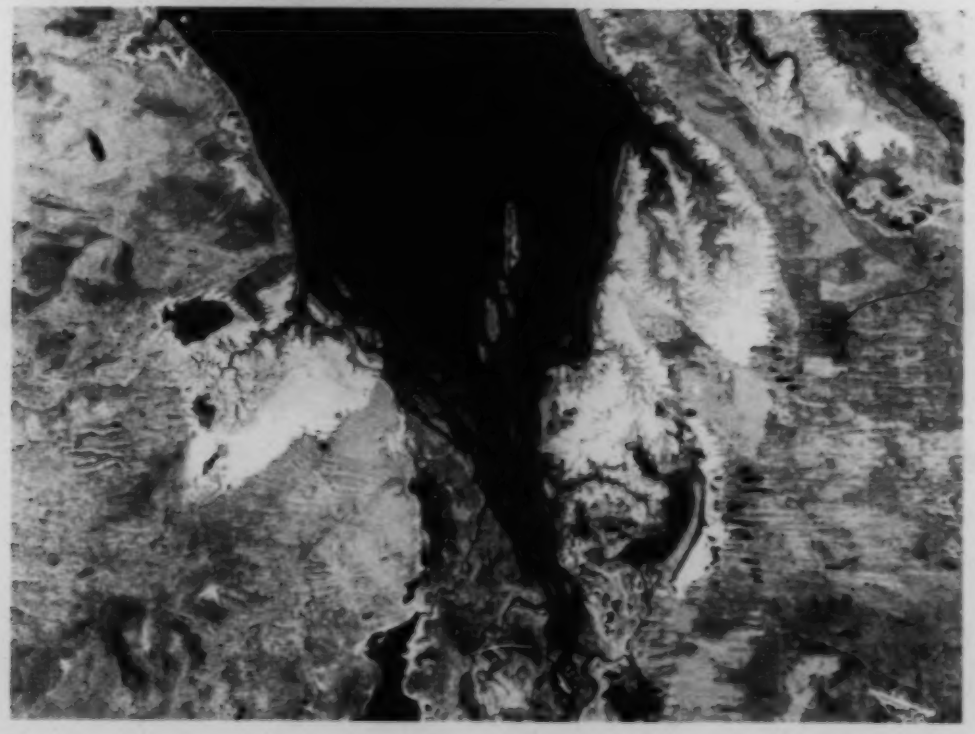

shelf are difficult to distinguish from the shelf-mud environment (Reineck and Singh, 1980), a tide-dominated prodelta prograding into an embayment will closely resemble the surrounding brackish bay environment.

Progradation of the active distributaries within a tide-dominated delta produces a gradational, coarsening upward succession from prodelta muds into interbedded sands, silts, and muds of the delta front. This is overlain by fine- to medium-grained sand of the tidal ridge (distributary mouth bar) deposits of the upper delta front (Reading and Collinson, 1996) or subaqueous delta plain (Dalrymple, 1992). The tidal ridge deposits merge landward into sandy channel fill (Coleman and Wright, 1975). On the delta plain, the tidal sand bars are gradationally overlain by an upward-fining succession of tidal flat and marsh sediments. Erosionally based tidal creeks may cut through this sequence (Dalrymple, 1992).

Examples of modern tide-dominated deltas include the Klang-Langat delta in Malaysia (Coleman et al., 1970), the Colorado River delta in California (Meckel, 1975), and the Yangtze River delta in China (Hori et al., 2001). Ancient examples include the Frontier Formation of Wyoming (Willis et al., 1999) and the Clearwater Formation of Alberta (McCrimmon and Arnott, 2002).

Based on the sedimentologic, geomorphologic, and ecologic characteristics of tide-dominated deltas described herein, the facies associations within the lower Bahariya Formation that represent such a system are the brackish bay (FA1), tidal channel (FA4), and tide-influenced delta front (FA2) associations.

3.2.3 Tide-Dominated Estuaries Versus Tide-Dominated Deltas

Based on the previous discussions of sections 3.2.1 and 3.2.2, it is apparent that the morphologic and sedimentologic differences between tide-dominated estuaries and deltas are few. Basinward, they both contain tidal sand bars separated by tidal channels; landward, they both contain tidal flats or marshes cut by tidal creeks. Sedimentary facies in either system can include cross-bedded medium grained sand with reactivation surfaces, tidal bundles, and bipolar paleocurrents, parallel-laminated (upper flow regime) fine sand, and heterolithic deposits with tidal rhythmites (Dalrymple, 1999). Because tide-dominated deltas and estuaries are so morphological similar, it is difficult to explicitly assign certain facies associations to either system.

In fact, controversy has arisen over whether tide-dominated deltas and estuaries can actually be differentiated. Reading and Collinson (1996) state that in order for a system to be deltaic, sediment must be largely derived from the river that feeds it, rather

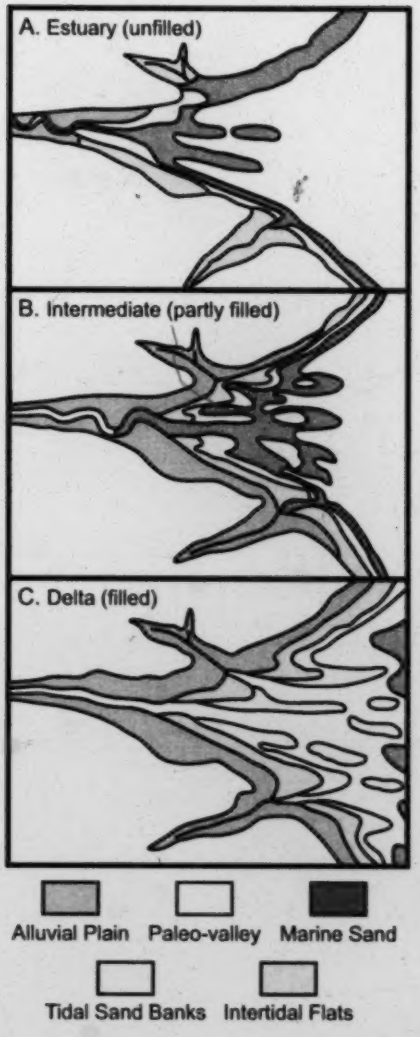

Figure 3.5. Geomorphic facies showing the idealized evolution (A through C) of a tide-dominated estuary into a tide-dominated delta (after Harris, 1988; Dalrymple et al., 1992; Woodroffe et al., 1993). As the estuary evolves, there is a basinward movement of facies and growth of the tidal sand banks (modified from Heap et al., 2004).

than from marine sources. Therefore, because most modern tide-dominated deltas are found almost exclusively in transgressive settings, which are dominated by marine sediment input, they are actually all tidal estuaries. Although Dalrymple (1992, 1999) admited that the distinction between tide-dominated deltas and estuaries is not well documented and that many tide-dominated deltas may actually be estuaries, he believed fervourently that tide-dominated deltas do exist. In addition, he suggested that the key to their differentiation is in their stratigraphic organization, rather than their sedimentologic characteristics.

Several authors agree with Dalrymple, and furthermore believe that under sea level stillstand, with sufficient direct river influence, tide-dominated estuaries evolve into tide-dominated deltas (Fig. 3.5; Boyd et al., 1992; Dalrymple et al., 1992; Roy et al., 2001; Heap et al., 2004). However, knowing exactly when an estuary becomes a delta is not clear without knowledge of the sedimentary deposits or long-term sediment influx (Heap et al., 2004).

According to Dalrymple (1999), tide-dominated deltas are typically progradational, while estuaries are transgressive in nature. As such, tidal ravinement surfaces will underlie estuarine channel and sand bar deposits, while elongate deltaic distributary mouth bars should gradationally overlie prodelta muds. Estuaries are commonly associated with incised valleys, display a tributary channel pattern, and have the coarsest sand at the head and mouth. Conversely, deltas need not be associated with incised valleys, show a distributary channel pattern, and contain sands that show a unidirectional seaward-fining trend. When the morphology of the fluvial source to the system is available, it is suggested by Dalrymple et al. (1992) that the straight-meandering-straight river morphology be used

to differentiate between a delta and an estuary. When the river meanders, the net bedload transport in the region seaward of the meanders is landward, and the system is therefore estuarine.

3.2.4 Brackish Bay Versus Embayment

The terms brackish bay and embayment are used often within this study, and as such there is a need to explain and differentiate between the two systems. A brackish bay is defined as a physically restricted, low energy setting within an overall higher energy, complex depositional system. An example would be the central basin within a wave-dominated estuary or an interdistributary bay within a deltaic setting. Brackish bay deposits are usually widespread within estuarine and deltaic systems and tend to represent background sedimentation. Because the water within these bays is truly brackish, the deposits are characterized by a low diversity suite of trace fossils from the *Cruziana* and *Skolithos* ichnofacies. Brackish bays are constantly subjected to changes in salinity and variable rates of sedimentation, which are extensively reflected in their sedimentologic characteristics. Facies Association 1 (brackish bay) represents these types of deposits within the lower Bahariya Formation.

An embayment is defined as a topographic depression or indentation in the country rock along a shoreline (Fig. 3.6; Roy et al., 1980; Hudson, 1991). It is geomorphologically simple compared to other coastal waterway types, such as estuaries or deltas. Embayment morphology ranges from wide and rounded to highly indented with convoluted shorelines, and also includes narrow, tapered drowned river valley systems (Albani and Johnson, 1974; Perillo, 1995; Riggs et al., 1995; Geoscience Australia [a]). Embayments have wide, unconstricted entrances that permit free water and sediment exchange with the ocean (Hudson, 1991). In the long term, river input is small compared to the total volume of water contained within the embayment (Hudson, 1991; Geoscience Australia [a]). Overall, tide and wave energies vary, although the smooth, gentle basinward slope of the embayment floor tends to accentuate incoming tidal energy, causing a tide-dominated regime even on microtidal coasts (Clifton, 1982; Cooper, 2001; Geoscience Australia [a]).

Environmental conditions within embayments are transitional between true estuarine environments and the coastal ocean (Roy et al., 2001; Geoscience Australia [a]). Parameters such as salinity, turbidity and water temperature are dependent on the strength of tide and wave energy, the amount of river input, ocean circulation patterns, and climate. Generally, embayments are characterized by low nutrient levels, dominantly subtidal habitats, and salinity greater than that of brackish bays, but not quite fully marine

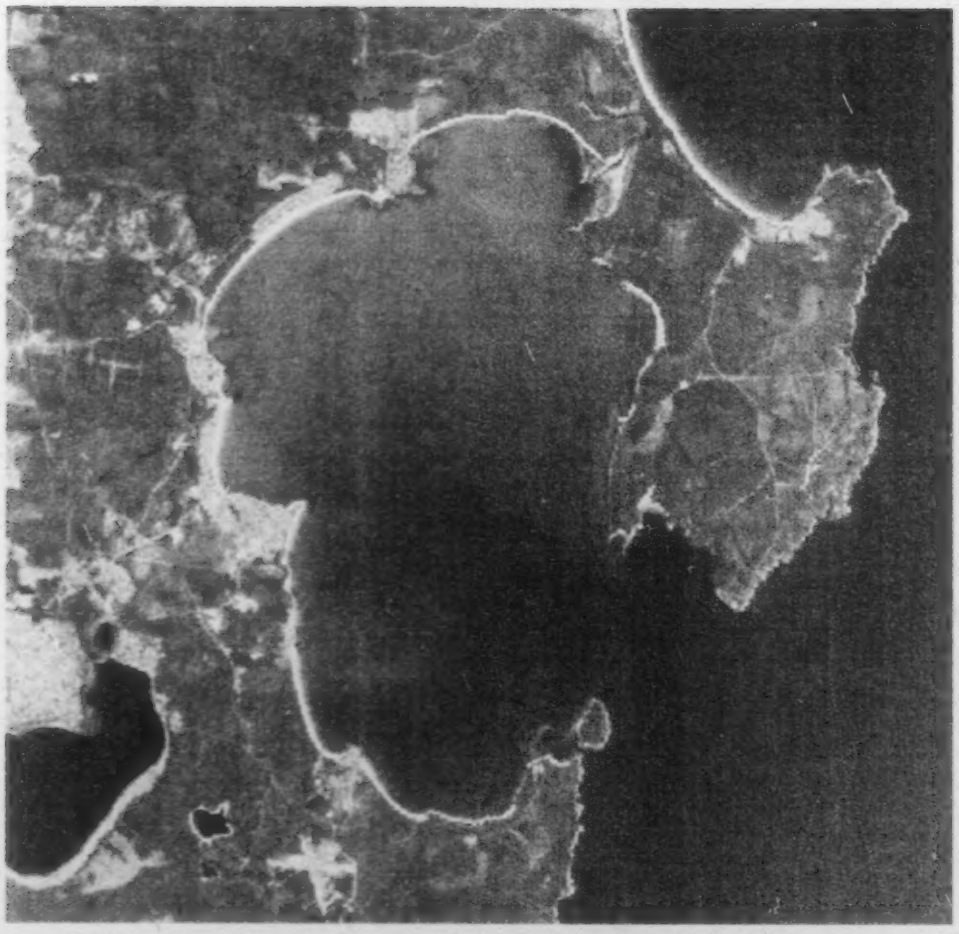

Figure 3.6. Satellite photograph of Jervis Bay, eastern Australia, a modern analogue for intervals interpreted as embayment deposits within this study (from Geoscience Australia [b]).

(Geoscience Australia [a]). A number of environmental stresses that occur rarely within open ocean habitats, such as changing salinity or varying sedimentation rate, may occur frequently in embayment settings, causing a restricted diversity or limited abundance of the highly variable biota found within its subenvironments (Nelson et al., 1980; Howard and Nelson, 1982; Dethier, 1992; Roy et al., 2001).

Strata of the lower Bahariya Formation are interpreted to represent the development of a tide-dominated delta and/or estuary along the margin of a large embayment. Deposits of Facies Associations 1, 2, and 4 (brackish bay, delta front, and tidal channel) represent the tide-dominated delta/estuary within this embayment. Sediments deposited within the embayment environment proper, as described above, are formally denoted as Facies

Association 5 (transgressive embayment). It is uncertain if the coastal waters "outside" the embayment (represented by Facies Association 3 (marine shoreface) are fully marine or are themselves parts of the embayment system. However, during the Late Cenomanian, it is known that the paleo-coastline of northern Egypt was highly embayed (see Fig. 1.9; Said, 1990).

3.2.5 Incised Valleys

As previously mentioned, most modern estuaries are contained within incised valleys. An incised valley is defined as a "fluvially eroded, elongate topographic low that is typically larger than one channel form and is characterized by an abrupt seaward shift in depositional facies across a regionally mappable sequence boundary at the base" (Zaitlin et al., 1994, p. 47). Incised valleys are closely linked to sea level rise and fall, and fit easily into a sequence stratigraphic framework (see Fig. 3.7). The basic features of an incised valley include: 1) a negative topographic valley that erodes into and truncates underlying strata; 2) valley base and walls that represent a sequence boundary that may be later modified by transgression to form an amalgamated transgressive and regressive surface (TS/RSE), or using sequence stratigraphic terminology, a combined flooding surface and sequence boundary (FS/SB; Van Wagoner et al., 1990). The sequence boundary may be associated with a pebble lag or burrows of the *Glossifungites* ichnofacies, which subtend from the surface into older strata (MacEachern and Pemberton, 1992); 3) basal valley fill that represents an erosional juxtaposition of landward facies over basinward facies; and 4) depositional markers within the incised valley fill that onlap the valley walls (Zaitlin et al., 1994). All these features must be visible to establish the existence of a true incised valley; however, studies with limited data or of limited aerial extent will rarely confirm the presence of each of these features.

A thick (6 to 18 m) succession of Facies Association 4 (tidal channel) located in the upper half of each cored interval (see Figs. 3.9 - 3.11) is interpreted to represent an incised valley fill on the grounds that 1) this sequence was deposited on a surface that was incised by rivers (see section 3.5.3) into the underlying strata of Facies Association 2 and 3 (delta front and marine shoreface); 2) this surface is an amalgamated transgressive-regressive surface (TS/RSE) that is demarcated by a sideritized mud clast breccia and/or burrows representing the *Glossifungites* ichnofacies (see section 3.4); and 3) there is an erosional juxtaposition of landward facies (tidal channels - FA4) over basinward facies (marine shoreface - FA3).

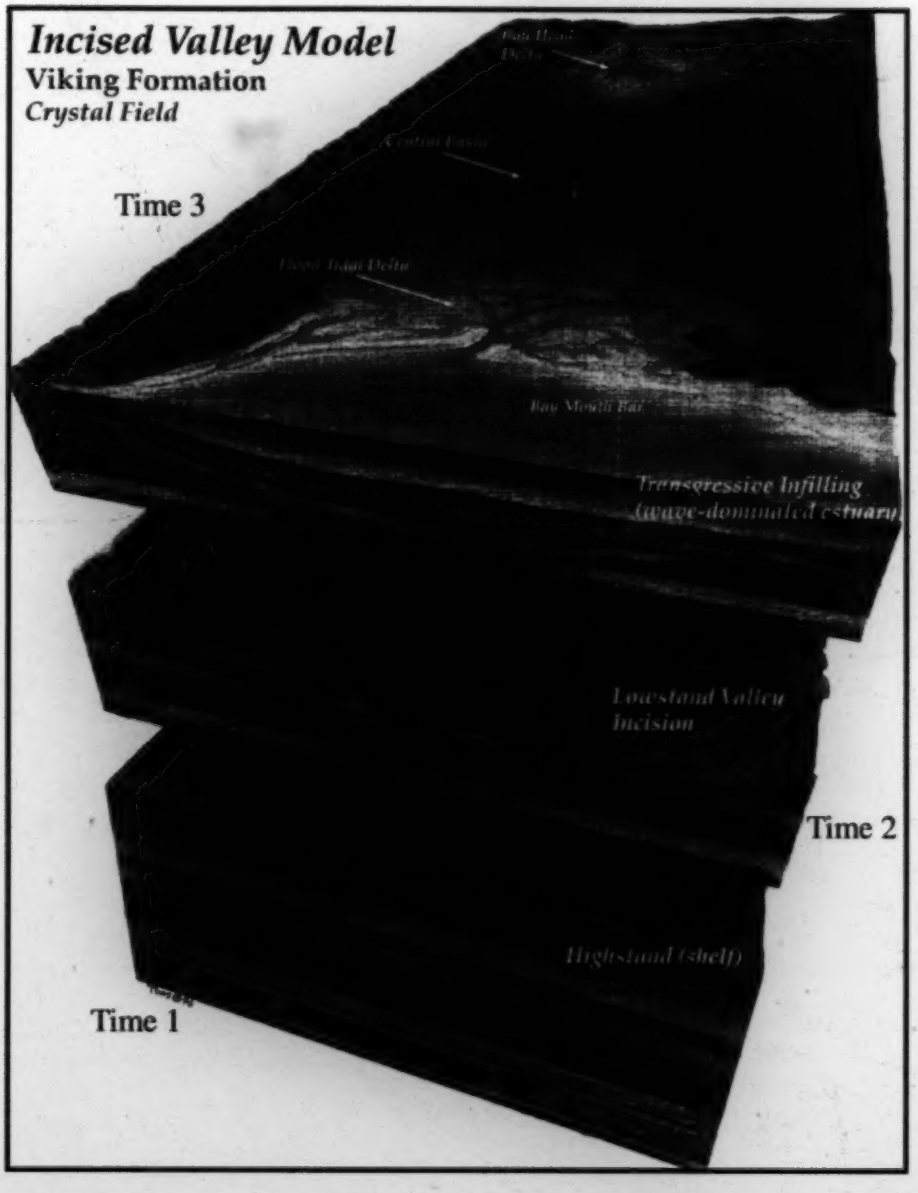

Figure 3.7. Schematic diagram depicting the development of an incised valley complex. Model is developed for the Lower Cretaceous Crystal Field, Viking Formation, Alberta. Time 1 contains prograding shoreline parasequences comprising the highstand systems tract. Time 2 represents the lowstand systems tract where relative sea-level fall initiated the lowering of base level and an incised valley is cut into underlying deposits by rivers. Time 3 represents the transgressive systems tract where, upon relative sea level rise, the incised valley becomes a wave-dominated estuary and is filled by sediment deposited in numerous, localized subenvironments (modified from Pemberton et al., 2001).

3.2.6 The Shoreface

In known literature, the division and classification of the shoreface environment varies, but it is usually considered to be the continuously submerged portion of the shoreline. The shoreface is commonly divided into upper, middle and lower zones, although the middle unit is sometimes indistinguishable (Fig. 3.8). The mean low tide level demarcates the upper limit of the shoreface (Davis, 1978; Walker and Plint, 1992; Pemberton et al., 2001) whereas the lower limit has been defined as either the storm wave base (Reineck and Singh, 1980) or fair-weather wave base (Walker and Plint, 1992; Reading and Collinson, 1996; Pemberton et al., 2001). The shoreface is found at depths ranging from 5 to 15 m and is the zone of maximum sediment movement along the shoreline (Howard and Reineck, 1981; Walker and Plint, 1992). Wave energy is the dominant physical process due to the influence of both fair-weather and storm-weather waves. During fair weather, oscillatory and shoaling waves affect the lower shoreface, while breaker/surf zone processes are active in the upper shoreface (Reading and Collinson, 1996). While the upper and lower divisions are based on sedimentologic criteria, the middle shoreface is commonly identified based on ichnologic characteristics (Pemberton and MacEachern, 1995).

As summarized from Pemberton et al. (2001) and Walker and Plint (1992), a prograding shoreline creates a sandying upward succession of offshore, shoreface, foreshore, and backshore deposits. The offshore is characterized by burrowed, silty mudstone with rare wave ripples and hummocky cross-stratification. The lower shoreface contains higher amounts of hummocky cross-stratification and wave ripples, with some burrowed muddy sandstone. Both the offshore and lower shoreface are characterized by trace fossils of the *Cruziana* ichnofacies. In strongly storm-dominated shorelines, the middle shoreface consists of both swaley and hummocky cross-stratified sandstone. In low storm-influenced

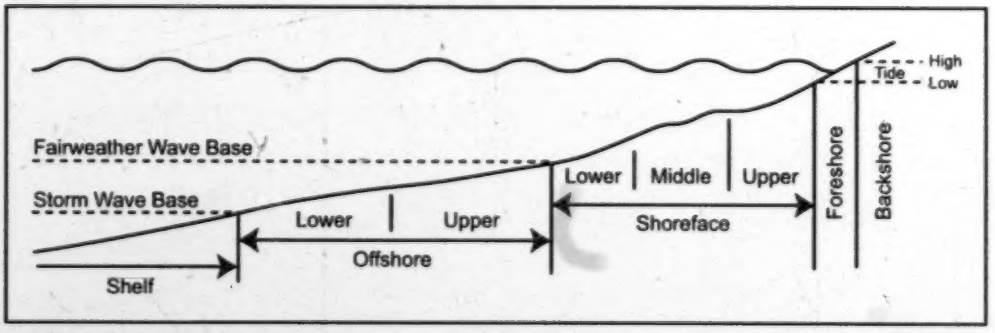

Figure 3.8. Schematic shoreface to shallow marine profile depicting the foreshore, backshore, shoreface, offshore and shelf, with fair-weather and storm wave base (modified from Walker and Plint, 1992).

settings, oscillation ripples are the dominant sedimentary structure. The upper shoreface is characterized by trough cross-bedded sandstone. Both the middle and upper shoreface are dominated by burrows representing the *Skolithos* ichnofacies. The foreshore is confined to the intertidal zone and contains swash-zone cross stratification with rare bioturbation. The backshore is extremely variable and may contain many different types of sediment and physical sedimentary structures.

In the lower Bahariya Formation, Facies Association 3 (marine shoreface) represents sedimentation in the shoreface environment. While deposits representing the lower and middle shoreface are the only sediments preserved, it is very likely that sediment deposited in other divisions of the shoreface (i.e. upper shoreface or foreshore) was originally deposited and later removed by erosion (see section 3.5.3).

3.3 CROSS SECTIONS

In order to determine the depositional architecture and history of the lower Bahariya Formation, three stratigraphic cross sections were constructed (for cross section locations see Figure 1.3). The datum for each cross section is a flooding surface observed on wells logs, and is located approximately 9 to 15 m higher than the top of the cored intervals (Fig. 3.9). The stratigraphic surfaces discussed in section 3.4 are labelled on each cross section. In addition, the facies associations (as determined in Chapter 2) and depositional stages (as established in section 3.5) are highlighted.

Cross section A to A' is oriented west to east through the southern part of the Hayat and Yasser fields (Fig. 3.10). The western half of the cross section is oriented along dip, while the eastern half is oriented along strike. Three prograding delta lobes of Stage 1 (S1) are visible, although in some wells lobes 2 and 3 are partially removed by the overlying regressive surface of erosion (RSE). Any marine shoreface deposits originally deposited during Stage 2 are also removed by the RSE, except for thin (less than 1 m) beds in Hayat-10 and 11. Deposits of Stage 3 become thinner and muddier towards the east.

Cross section B to B' runs approximately west to east through the northern portion of the Hayat and Yasser fields, then northeast into the Kenz field (Fig. 3.11). The western half of the cross-section is a dip-section, while the eastern half is a strike-section. The two uppermost delta lobes of S1 are present and are more mud-dominated than their counterparts farther south. The RSE is extremely undulatory and the absence of any marine deposits (FA3) suggests regression was accompanied by significant erosion. Deposits of Stage 3 (S3) remain somewhat uniform in thickness across the section, although they seem slightly muddier towards the east.

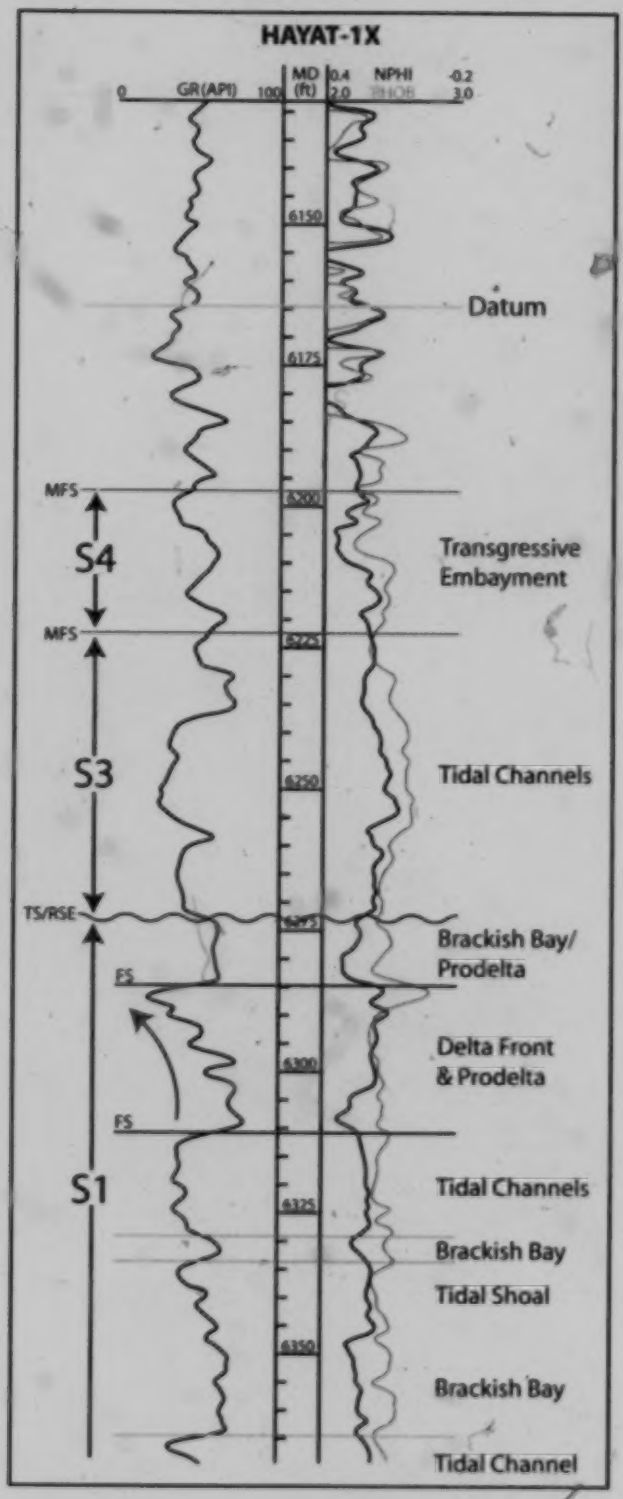

Figure 3.9. Sample well log of the lower Bahariya Formation. For well location see Figure 1.3. Red arrow indicates coarsening upward succesion. Datum is shown in green and interpreted depositional environments are written on the right-hand side of the log. MD - measured depth (feet); GR - gamma ray; NPHI - neutron porosity; RHOB - bulk density; FS - marine flooding surface; MFS - major marine flooding surface; TS/RSE - amalgamated transgressive-regressive surface; S1, S3, S4 - depositional stages 1, 3 and 4 (Stage 2 is not preserved in this well).

Stratigraphic Cross Section

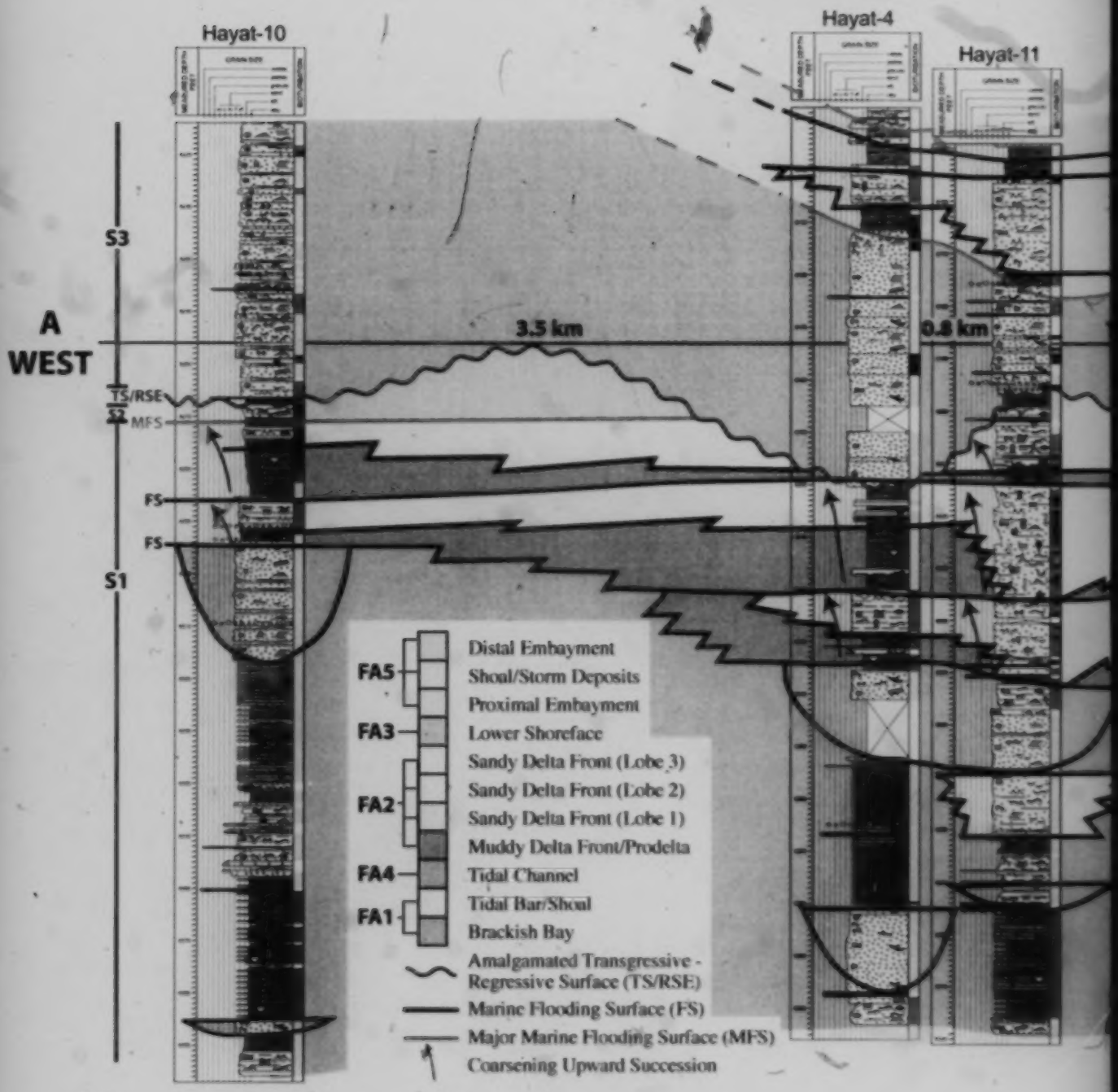

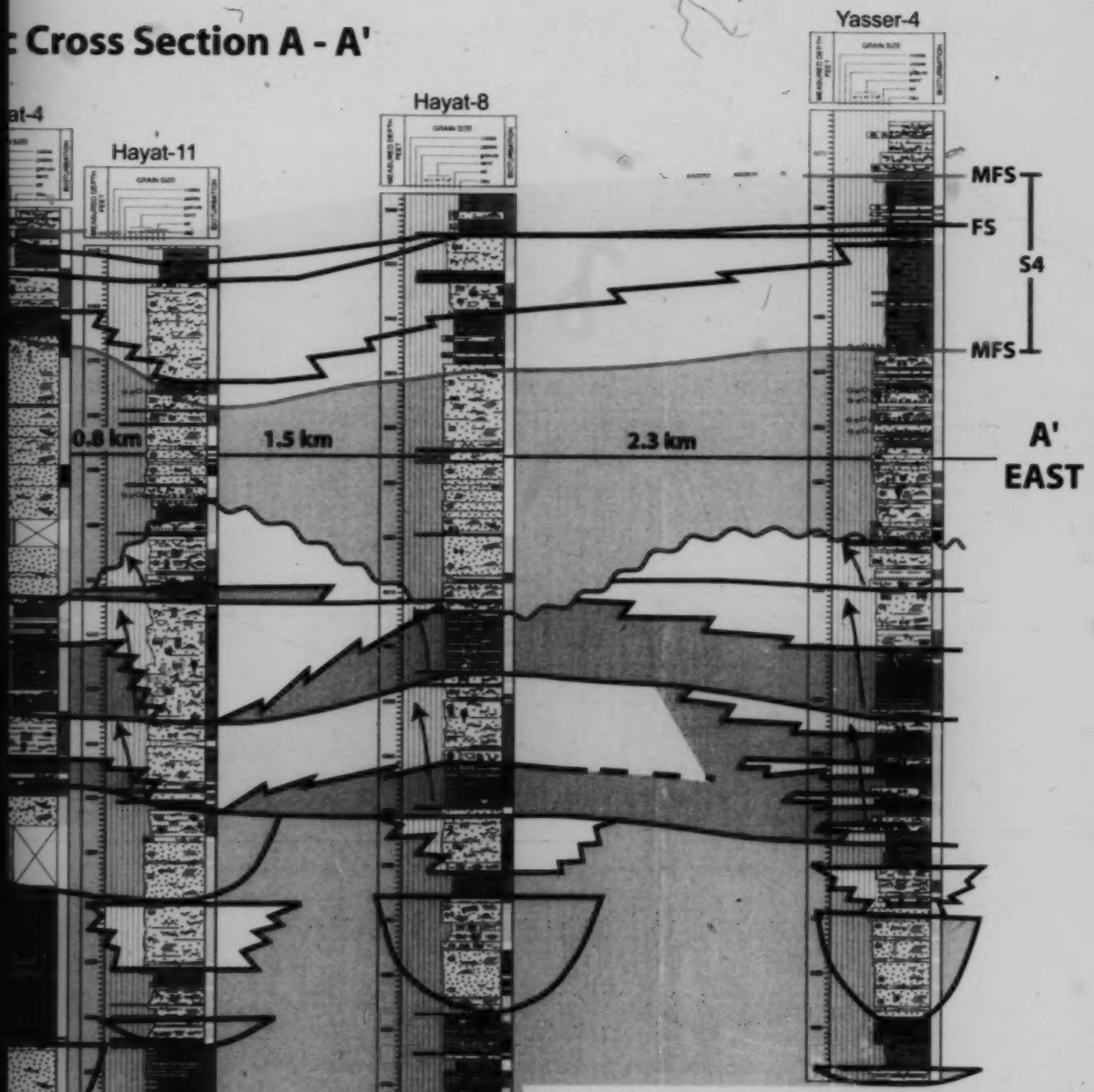

Figure 3.10. Stratigraphic cross section A to A'. See text for discussion of cross section characteristics and relationships. The datum is a flooding surface located stratigraphically above the section recorded in these core (See Fig. 3.9). For section location see Figure 1.3. For litholog symbols see Appendix A.

Stratigraphic Cross Secti

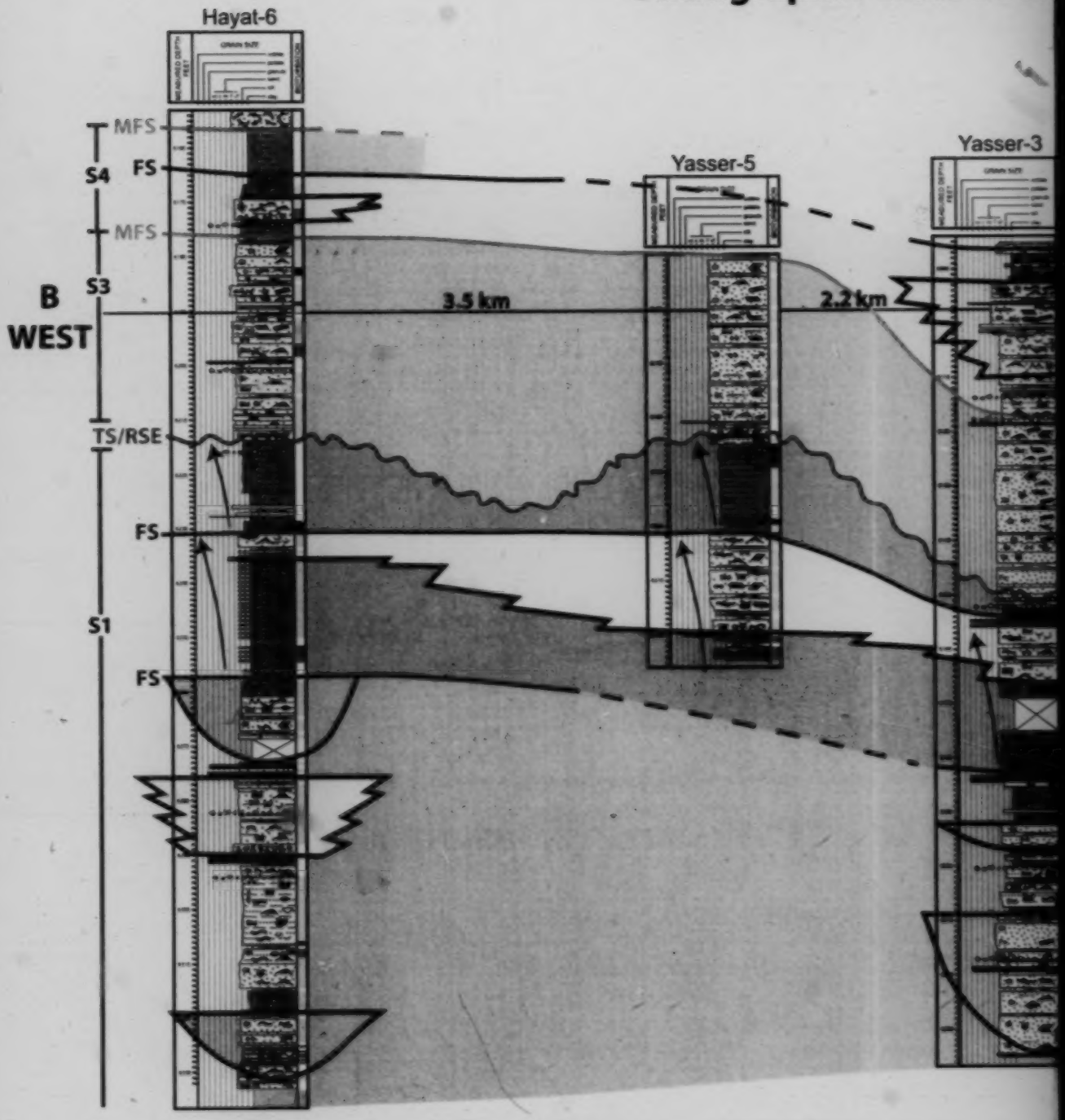

Cross Section B - B'

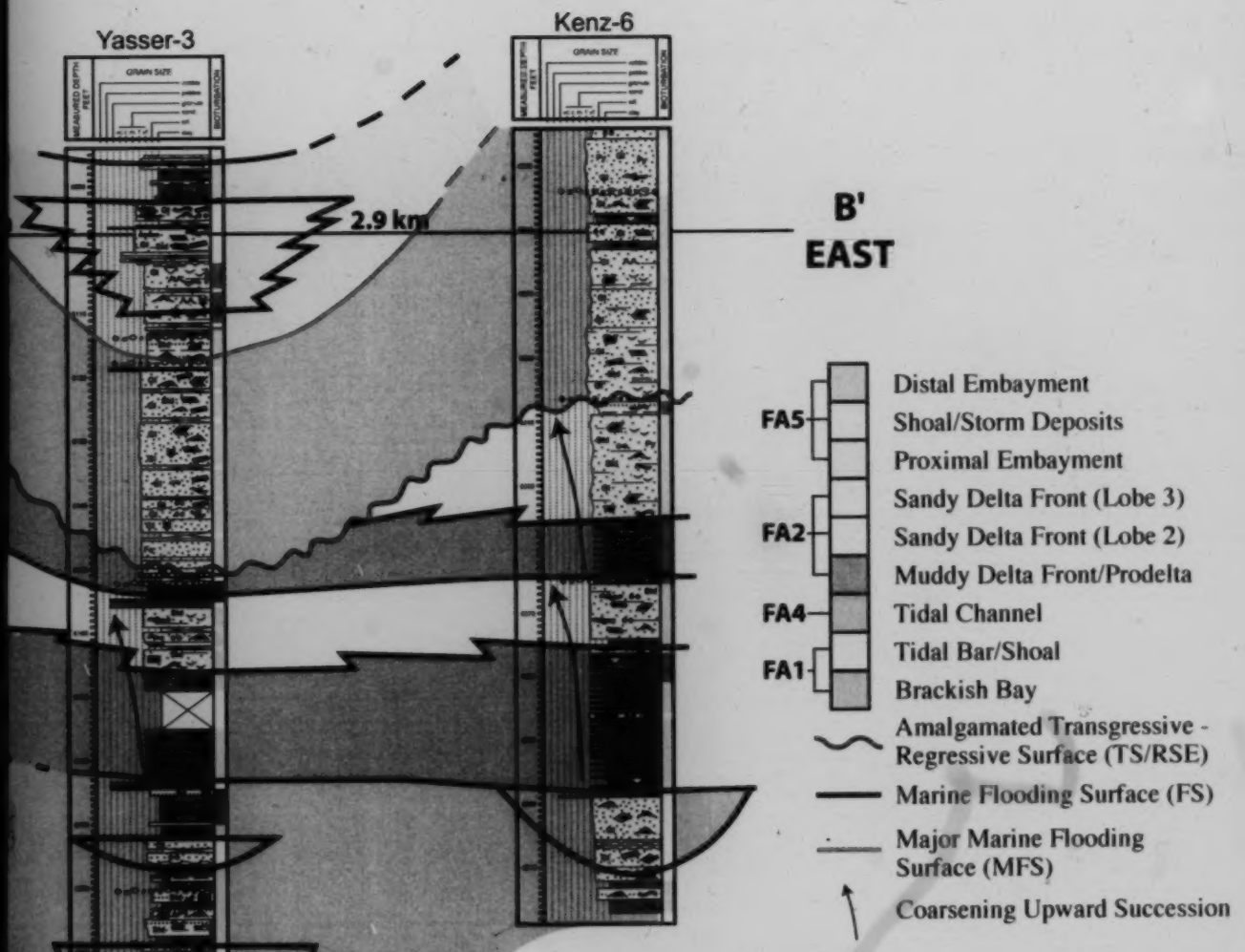

Figure 3.11. Stratigraphic cross section B to B'. See text for discussion of cross section characteristics and relationships. The datum is a flooding surface located stratigraphically above the section recorded in these cores (e.g. see Fig. 3.9). For litholog symbols see Appendix A. Location of cross section is shown in Figure 1.3.

Stratigraphic Cross Section C - C'

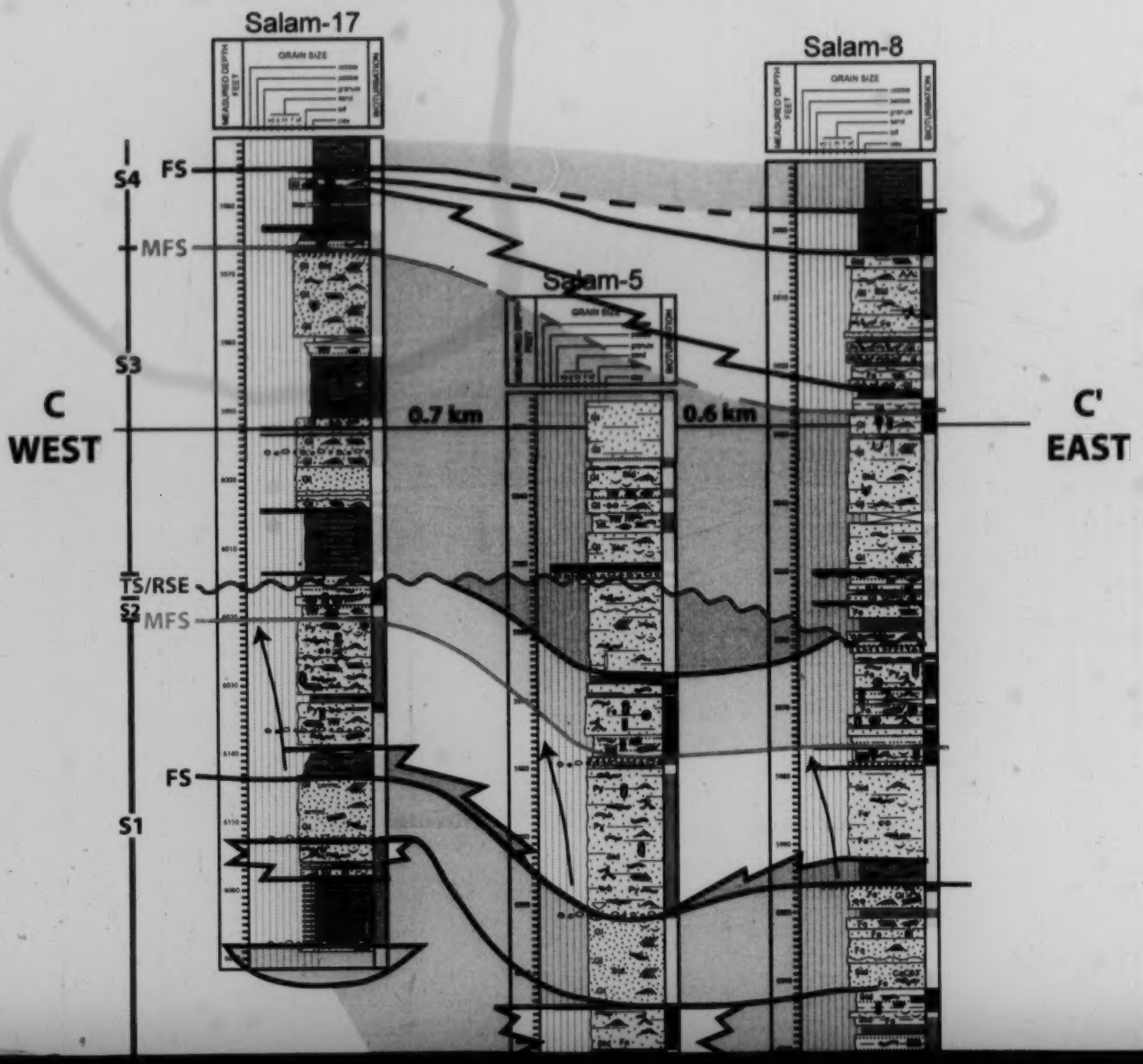

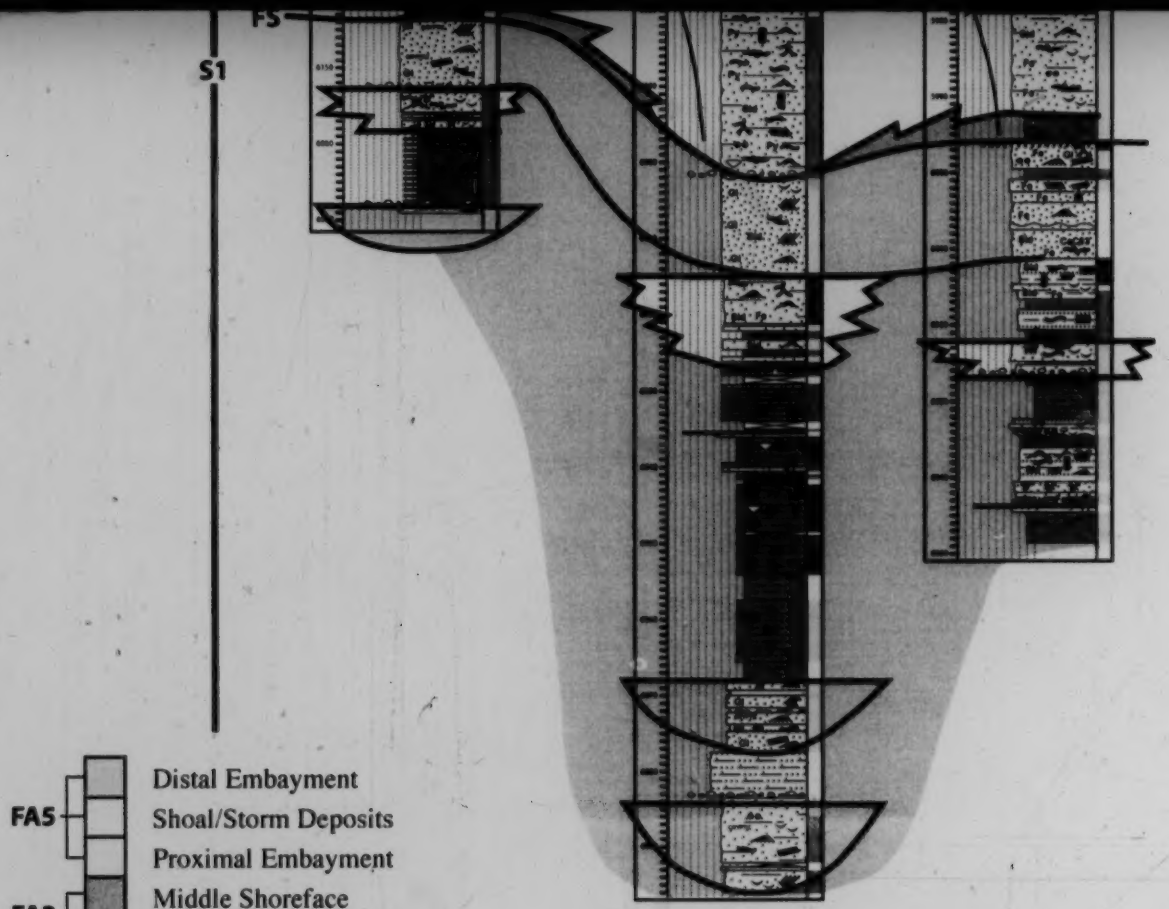

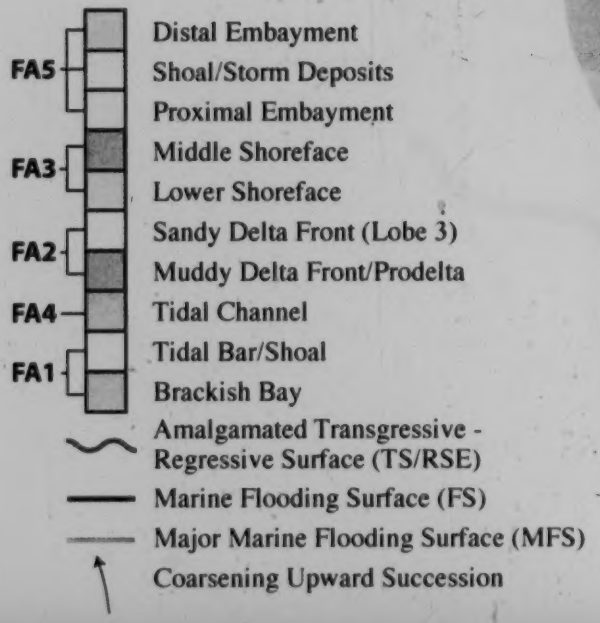

Figure 3.12. Stratigraphic cross section C to C'. See text for discussion of the cross section characteristics and relationships. The datum is a flooding surface located stratigraphically above the section recorded in these core (see Fig. 3.9). Location of cross section is shown in Figure 1.3. For litholog symbols see Appendix A.

Cross section C to C' is a strike-section oriented from west to east through the centre of the Salam field (Fig. 3.12). Only the uppermost delta lobe (lobe 3) is visible, which is extremely sandy compared to delta lobes south of the Salam field. Significant thicknesses (up to 8 m) of S2 (marine shoreface) are preserved. Sediments of S3 are thinner than in the southern portion of the study area and are significantly muddier. In the Salam-17 well, thick (up to 3 m) brackish bay deposits (FA1) are found associated with the tidal channel deposits (FA4), suggesting that the tidal channels in this area were less common or did not incise as deeply as in other areas.

3.4 STRATIGRAPHIC SURFACES

Determining the depositional history of a stratigraphic succession is largely dependent on the identification of stratigraphic surfaces. Many different genetic stratigraphic approaches have been developed, such as allostratigraphy (NACSN, 1983), sequence stratigraphy (Wilgus et al., 1988; Van Wagoner et al., 1990), and genetic stratigraphic sequences (Galloway, 1989). Despite their differences, each is dependant on the identification of stratigraphic surfaces such as bounding discontinuities, unconformities, or flooding surfaces (MacEachern et al., 1992). Discontinuities divide a stratigraphic succession into genetically related strata so that Walther's Law can be applied. Outlining the origin of the discontinuity is also important in resolving depositional environments and determining the allocyclic controls on depositional systems (MacEachern et al., 1992).

The lower Bahariya Formation has been previously described as stacked estuaries with numerous erosion/onlap surfaces (Wehr et al., 2002). With analysis of the facies distributions and key surfaces present in the study area, a more detailed stratigraphic model is herein presented. The strata in the study area contain a number of stratigraphic breaks that can be regionally traced. Analysis of the facies above and below these discontinuities reveals that they separate fundamentally different depositional environments. Two general types of surfaces are found in the lower Bahariya Formation: transgressive surfaces and amalgamated transgressive and regressive surfaces. In core, these surfaces are commonly represented by sideritized mud clast breccias and carbonated cemented sandstones (described in Chapter 2).

3.4.1 The *Glossifungites* Ichnofacies

The three types of discontinuities identified in the lower Bahariya Formation are commonly associated with the firm-ground *Glossifungites* ichnofacies. The *Glossifungites* assemblage belongs to a group of substrate controlled ichnofacies, including the *Teredolites* and *Trypanites* ichnofacies, which represent burrowing in woody and hard substrates, respectively (Bromley et al., 1984).

The *Glossifungites* suite is associated with firm or semi-lithified substrates, usually dewatered, cohesive muds. The burrows are sharp walled, unlined, robust, vertical to subvertical dwelling structures of suspension feeding organisms, such as *Diplocraterion*, *Skolithos*, *Psilonichnus,* and *Arenicolites*, or deposits feeding organisms, such as firmground *Thalassinoides* and *Rhizocorallium* (Fig. 3.13). The unlined nature of these traces supports the presence of a firm substrate because open, unlined vertical shafts and horizontal networks cannot be maintained in muddy, soupy substrates. In addition, scratch marks are often found on the burrow walls, further indicating a firm substrate. The traces often contain a fill that contrasts with the surrounding host sediment and is similar to the deposits that overlie the bed junction (MacEachern et al., 1992).

In siliciclastic settings, most firmground assemblages are a result of erosional exhumation of dewatered and compacted substrates, and therefore correspond to erosional discontinuities. Organisms producing a *Glossifungites* suite of trace fossils colonize the substrate during a depositional hiatus between the erosional event that exhumed the substrate and subsequent deposition of the overlying unit. A crosscutting relationship between the pre-exhumation softground assemblage and the post-exhumation firmground assemblage is commonly recognized. By analyzing the relationships between the softground trace fossil assemblage, the *Glossifungites* assemblage, and the overlying softground trace fossil assemblage, it is possible to make interpretations regarding the origin of the surface and the mechanisms responsible for its formation (MacEachern et al., 1992).

Transgressive surfaces are contacts across which there is evidence of an increase in water depth. These surfaces are commonly eroded by wave or tide activity in marine or marginal-marine environments upon relative sea-level rise, and as such are often demarcated by the *Glossifungites* ichnofacies. Firm ground dwelling organisms colonize the substrate after it is cut but prior to significant deposition of the overlying unit.

Lowstand or regressive surfaces of erosion are produced during relative lowstand of sea level as a result of subaerial exposure and/or erosion. This results in the widespread development of dewatered and firm substrates ideal for organism colonization. In the case of an incised valley, subaerial exposure at the valley base exposes a firm substrate

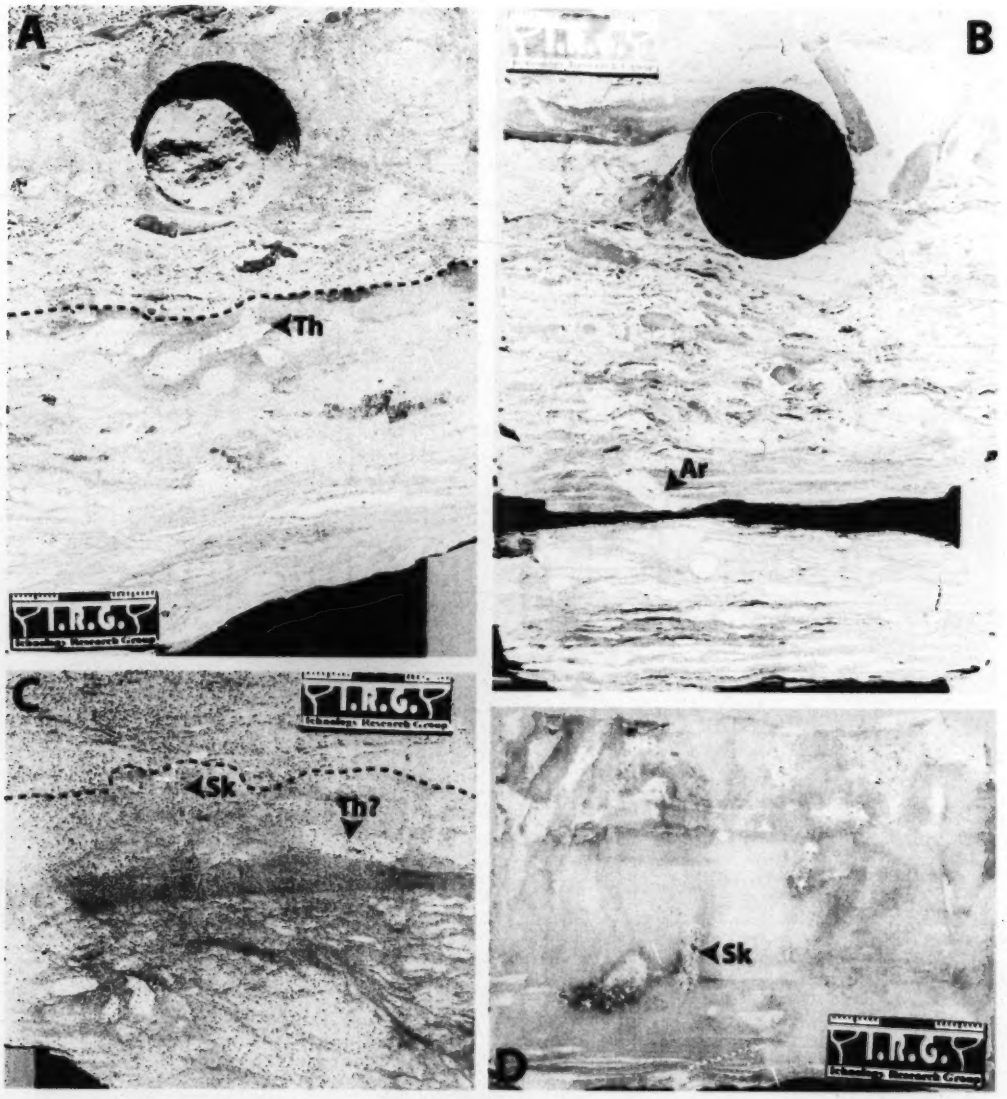

Figure 3.13. Expressions of the *Glossifungites* ichnofacies in the lower Bahariya Formation. A) Distal delta front with firmground *Thalassinoides* overlain by marine shoreface (transgressive surface of erosion). B) Brackish bay facies with *Arenicolites* overlain by estuarine facies (regressive surface of erosion and transgressive surface). C) *Skolithos* and *Thalassinoides* demarcating a transgressive-regression surface underlain by brackish bay facies and overlain by estuarine tidal channel facies. D) *Skolithos* burrows subtending from a discontinuity (transgressive surface) within proximal embayment deposits. Note the sideritization associated with the surface.

that is subject to marine or marginal marine conditions upon ensuing transgression. The transgression into the valley redistributes the lowstand sediments (if present) and colonization of this exhumed substrate by organisms is then made possible. In this case, the surface would represent an amalgamated regressive and transgressive surface (TS/RSE) and would be demarcated by the *Glossifungites* ichnofacies (MacEachern et al., 1992). These burrows would be filled with the same sediment that overlies the discontinuity, which is commonly estuarine or marginal marine in origin. The presence of the *Glossifungites* ichnofacies below the sequence boundary in an incised valley can help determine if the fill is associated with lowstand fluvial conditions or transgressive marginal marine conditions. The presence of this trace fossil assemblage indicates that the valley did not fill with sediment until transgression ensued (MacEachern et al., 1992); its absence suggests the presence of fluvial lowstand deposits (Savrda, 1991).

Although the presence of the *Glossifungites* ichnofacies aids in identifying significant surfaces in general, the real key to differentiating between lowstand/regressive and transgressive surfaces is the examination of the facies that occur above and below the surface in question. If more proximal facies overlie more distal facies, then the surface represents regression; alternatively, if more distal facies overlie proximal facies, then the surface represents transgression.

3.4.2 Transgressive Surfaces in the Lower Bahariya Formation

Transgressive surfaces, also known as flooding surfaces, represent an abrupt increase in relative sea level. In sequence stratigraphy, there are both marine and major marine flooding surfaces, which describe the amount of relative deepening. As the names suggest, marine flooding surfaces represent small-scale deepening and separate parasequences, while major marine flooding surfaces represent a much larger scale of deepening and separate parasequence sets (Van Wagoner et al., 1990).

The lower Bahariya Formation contains both types of flooding surfaces. They are usually mantled by a sideritized mud clast breccia. Marine flooding surfaces occur at the base of coarsening upward sequences within the upper portion of the lower Bahariya depositional Stage 1 (see Section 3.5). Three major marine flooding surfaces occur within the study area and are located at: 1) the boundary between Stages 1 and 2, where shoreface deposits overlie estuarine/deltaic sediments; 2) the boundary between Stages 2 and 3, where estuarine deposits overlie a regressive surface of erosion; and 3) the boundary between Stages 3 and 4, where proximal embayment facies overlie estuarine tidal channel deposits (See Figs. 3.10 - 3.12 for surface placements). Burrows representing the *Glossifungites*

ichnofacies are usually found just below the major marine flooding surfaces, suggesting transgression was accompanied by erosion. Therefore, these surfaces could also be called transgressive surfaces of erosion.

3.4.3 Regressive Surfaces in the Lower Bahariya Formation

One major regressive surface, associated with significant erosion, can be traced throughout the study area. This surface truncates a large portion of both Stages 1 and 2, and superimposes estuarine deposits on top of shoreface deposits. There is no direct evidence within the study area for subaerial exposure at this surface, so it cannot technically be called a Type 1 sequence boundary (Van Wagoner et al., 1990). However, there could be evidence of exposure in rocks adjacent to the study area towards the south, in a landward direction.

The regressive surface in the Hayat and Yasser fields is designated by a sideritized mud clast breccia and is subtended by burrows of the *Glossifungites* ichnofacies. The presence of these sharp-walled burrows suggests that after the regressive surface was cut into the underlying marine deposits, there was a depositional hiatus that allowed organisms to colonize the firm substrate; the hiatus was then followed by estuarine sedimentation. The lack of significant sediment accumulation between regression and transgression, in addition to the presence of the *Glossifungites* ichnofacies, supports the classification of this surface as an amalgamated transgressive-regressive surface.

In the Salam field, a carbonate-cemented sandstone unit, underlain by burrows of the *Glossifungites* ichnofacies, demarcates the transgressive-regressive surface. The presence of these burrows suggests that the sandstone was deposited during transgression, rather than regression. Siliciclastic deposits with diagenetic alterations involving calcite, dolomite, and siderite are commonly linked to flooding surfaces (Ketzer et al., 2003). Such surfaces are the locus of carbonate cementation because of the high amount of carbonate bioclasts, and long residence time of the substrate at shallow depths on the sea floor. Furthermore, lags associated with transgressive surfaces can have proximal and distal components (Ketzer, 2002): the lags in proximal settings are rich in mud clasts (as in the Hayat, Yasser, and Kenz fields) while lags associated with distal settings are rich in carbonate bioclasts (as in the Salam field).

3.5 LOWER BAHARIYA DEPOSITIONAL STAGES

Based on the identified stratigraphic surfaces and lateral vertical facies relationships, the lower Bahariya Formation is divided into four significant depositional stages (S1 through S4). Major marine flooding surfaces and/or regressive surfaces separate each depositional stage. A sample composite litholog summarizing these relationships is given in Figure 3.14. An approximate representation of the study area is shown in red on each paleogeographic map, and is oriented with basinward towards the north/northwest and landward towards the south/southeast.

3.5.1 Stage 1 (S1)

During Stage 1, the study area was part of a tide-influenced brackish bay containing prograding delta lobes (Fig. 3.15). It is difficult to say for certain if the succession is entirely estuarine or deltaic; however, the abundance of tidal channels and bay deposits with rare tidal bars (FA1 and 4) suggests the lower portion of S1 acted like a tide-dominated estuary. The upper portion of S1 contains noticeable prograding, coarsening-upward sequences (FA2) and exhibits many features commonly found in deltaic systems. As such, the study area during the closing stages of S1 contained a prograding tide-dominated delta. Because similar facies and facies successions are found within both tide-dominated estuaries and deltas, it is difficult to pinpoint the exact nature of the depositional system during this stage. However, the most probable interpretation for Stage 1 is that of a tide-dominated estuary evolving into a tide-dominated delta, as illustrated in Figure 3.5.

The delta lobes found in the upper part of S1 move progressively northward (basinward) over time. Each lobe is a coarsening-upward succession interpreted as a parasequence (a relatively conformable succession of genetically related beds bounded by marine flooding surfaces that are upward-shallowing; Van Wagoner et al., 1990).

Gross sand isopach maps of the three delta lobes show their general morphology and aereal extent (Figs. 3.16 through 3.18). Lobe 1 occurs only in the Hayat and Yasser fields and grades basinward into tidal channel and brackish bay sediments (Fig. 3.16). The net sand distribution in this lobe is similar to deltas with low wave energy and medium tidal energy (Coleman and Wright, 1975).

Lobe 2 is present in all wells except for those north of the Kenz field (Fig. 3.17). The net sand distribution shows a delta lobe configuration under moderate wave influence and high tidal influence (Coleman and Wright, 1975). The major sand depocenter for lobe 2 has moved north compared to lobe 1 and is located in the Kenz field.

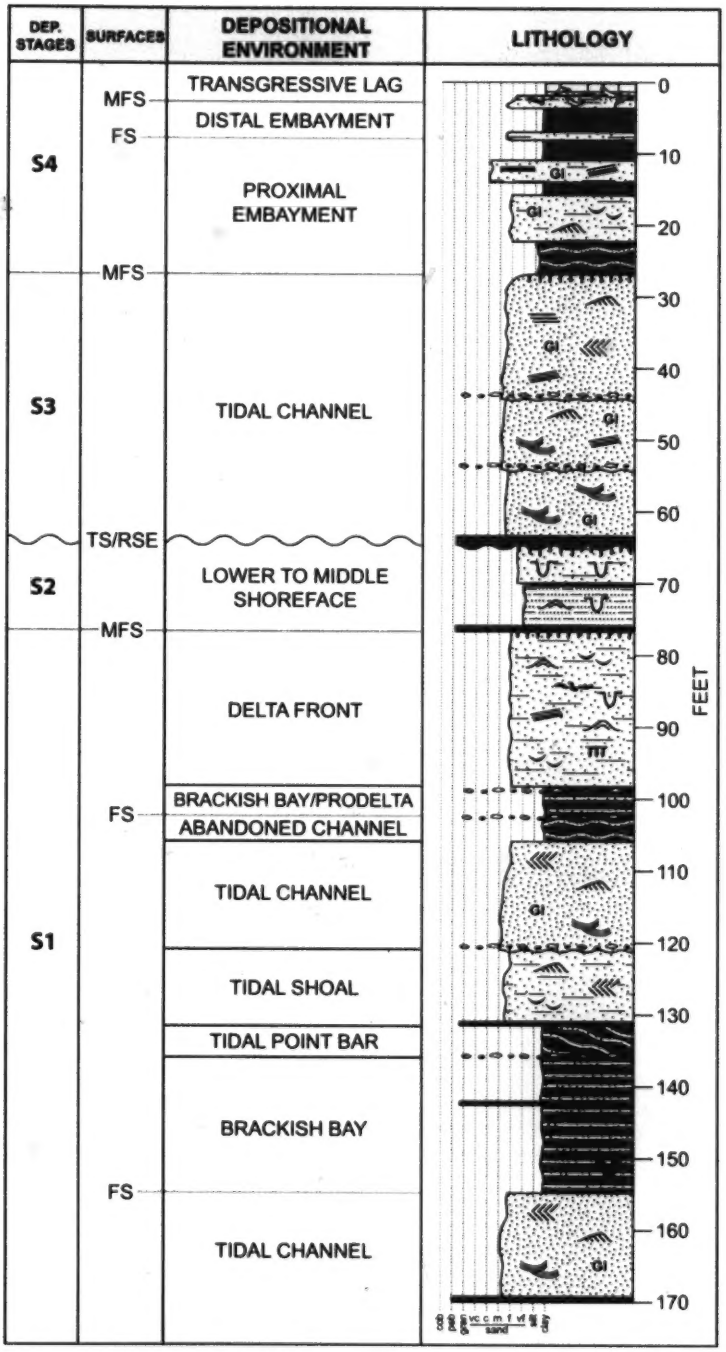

Figure 3.14. Summary composite lithology for the lower Bahariya Formation. For legend of symbols see Appendix A. FS - marine flooding surface; MFS - major marine flooding surface; TS/RSE - regressive surface of erosion; S1, S2, S3, S4 - depositional stages 1 through 4, respectively.

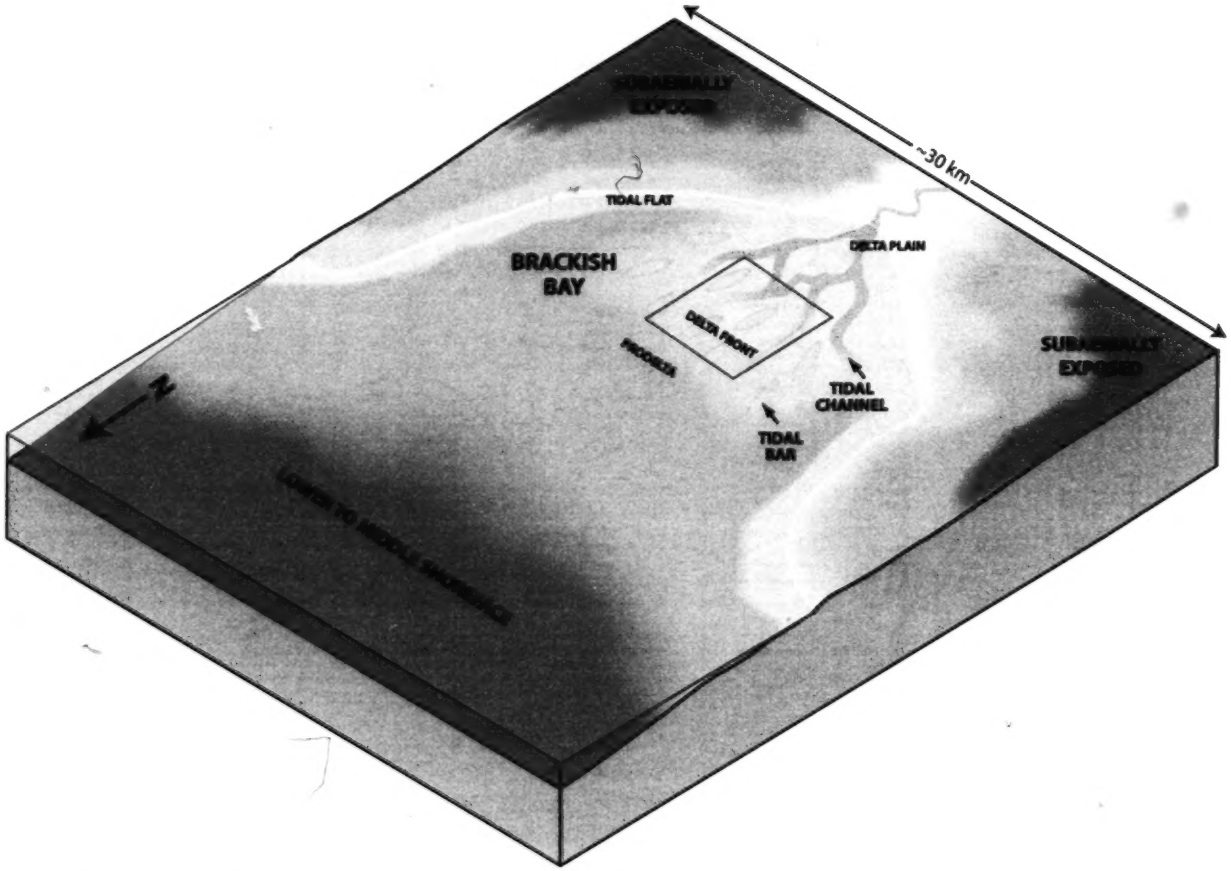

Figure 3.15. Distribution of facies during lower Bahariya Stage 1. Although estuarine conditions may have been present, the area is depicted as a tide-dominated delta prograding into a brackish bay. Red squares denotes approximate location of study area.

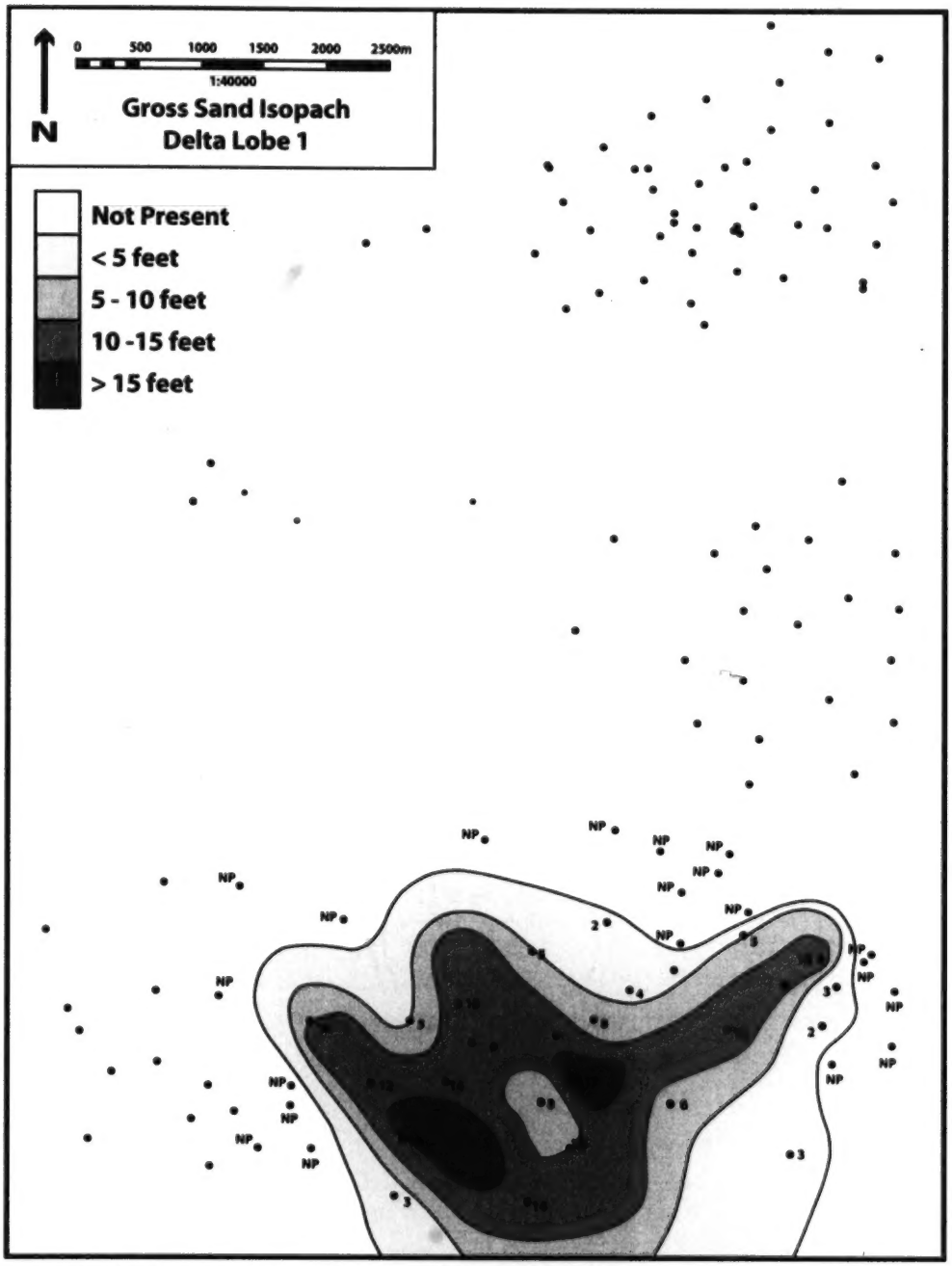

Figure 3.16. Gross sand isopach map of delta lobe 1. Lobe 1 is restricted to the southern portion of the study area and exhibits finger-like protrusions of sand, likely related to tidal action. Isopach values were measured directly from wire-line logs. Measured depths on the logs are recorded in imperial units, so for sake of simplicity, these units were used on the isopach map.

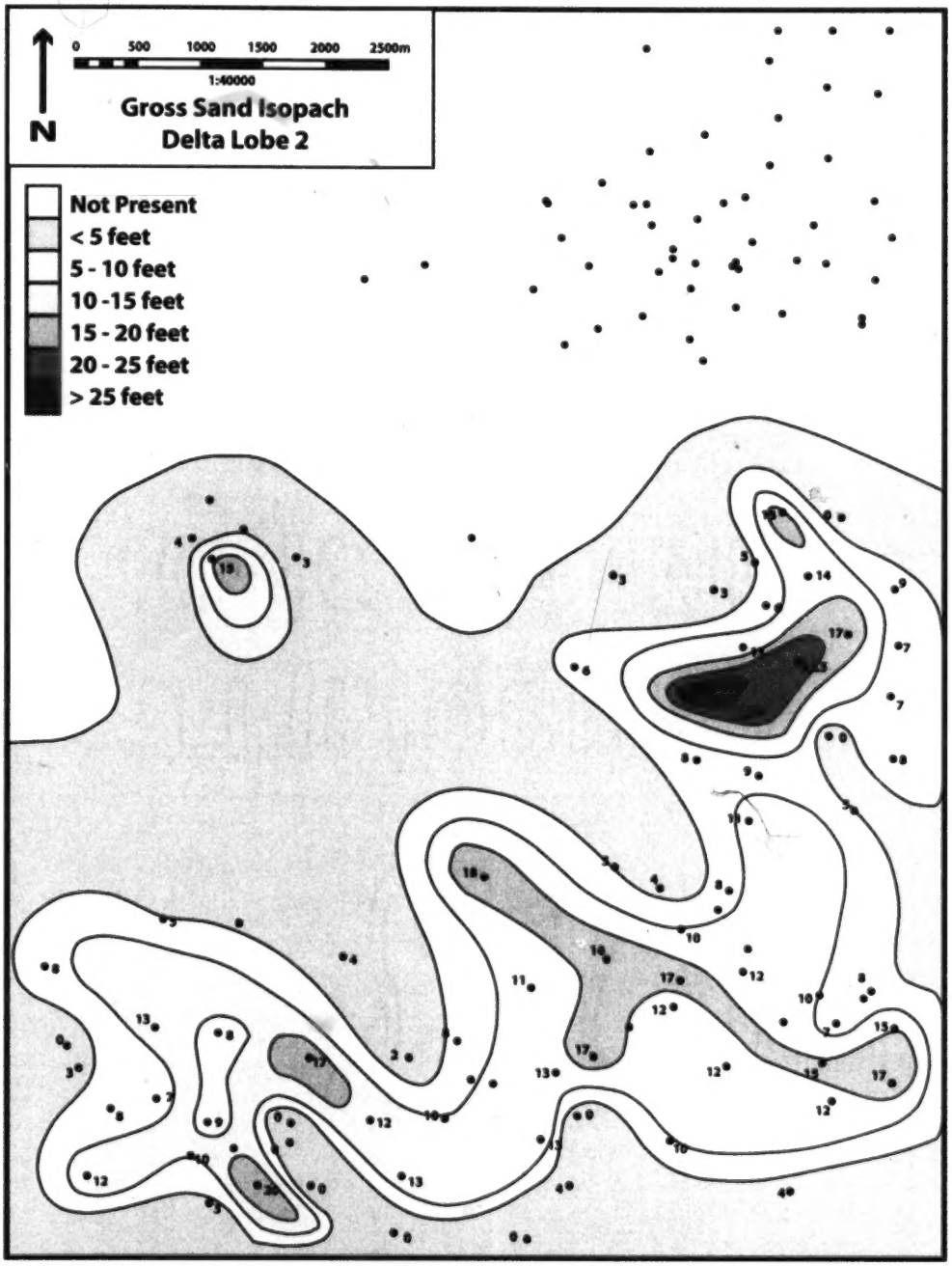

Figure 3.17. Gross sand isopach map of delta lobe 2. This lobe covers the southern half of the study area and exhibits linear sand bodies that are almost certainly related to tidal action. Isopach values were measured directly from wire-line logs. Measured depths on the logs are recorded in imperial units, so for sake of simplicity, these units were used on the isopach map.

Sediments of lobe 3 occur throughout the study area, except where they are eroded out from above in the southern portions of Hayat and Yasser (Fig. 3.18). Mud-dominated sediment is concentrated in the Hayat and Yasser fields, while sandy sediment dominates the Kenz and Salam fields. The depocenter of lobe 3 has moved even farther north compared to lobe 2, suggesting an overall progradation of the delta towards the north and west. The paucity of linear sand trends on the lobe 3 gross sand isopach map suggests a limited tidal influence. South of the Salam field, the top portion of lobe 3 is likely partially eroded and therefore the validity of the isopach map in this area is questionable. Overall, the changes in delta lobe sand distribution suggest a slight increase in wave energy over time.

3.5.2 Stage 2 (S2)

Following a significant rise in relative sea level at the end of Stage 1, a large marine embayment is created and marine sediments (FA3) are deposited in the study area during Stage 2 (Fig. 3.19). A major marine flooding surface, or transgressive surface of erosion, separates S1 and S2. Marine deposits of S2 are rarely preserved because they are commonly eroded by channel incision during Stage 3. In the northern parts of the study area (Salam and northern Kenz), these sediments show a coarsening upward, progradational character from lower to middle shoreface and essentially correspond to a parasequence. In the southern portion of the study area, Hayat-10 and 11 are the only wells that contain marine deposits. Although they were deposited in a marine environment, the sediments in Hayat-10 are not typical shoreface deposits. Based on the ichnologic and sedimentologic information presented in Chapter 2, this unit was likely deposited in a relatively more restricted portion of the marine embayment, landward of the middle and lower shoreface. Due to a lack of data, it is difficult to determine the exact layout of the depositional environments in the southern portion of the study area; to say where the shoreface ends and the restricted marine areas begin is speculative.

3.5.3 Stage 3 (S3)

A significant drop in relative sea level near the end of Stage 2 allowed for the development of a discontinuity between S2 and S3 (Fig. 3.20) This discontinuity is an amalgamated transgressive-regressive surface that truncates underlying deposits of S1 and S2, and separates these underlying distal facies from the overlying proximal facies of S3. The sediments of S3 were deposited in a tide-influenced estuary and consist of thick (generally 6 to 18 m) tidal channel deposits (FA4) with minor brackish bay sediments

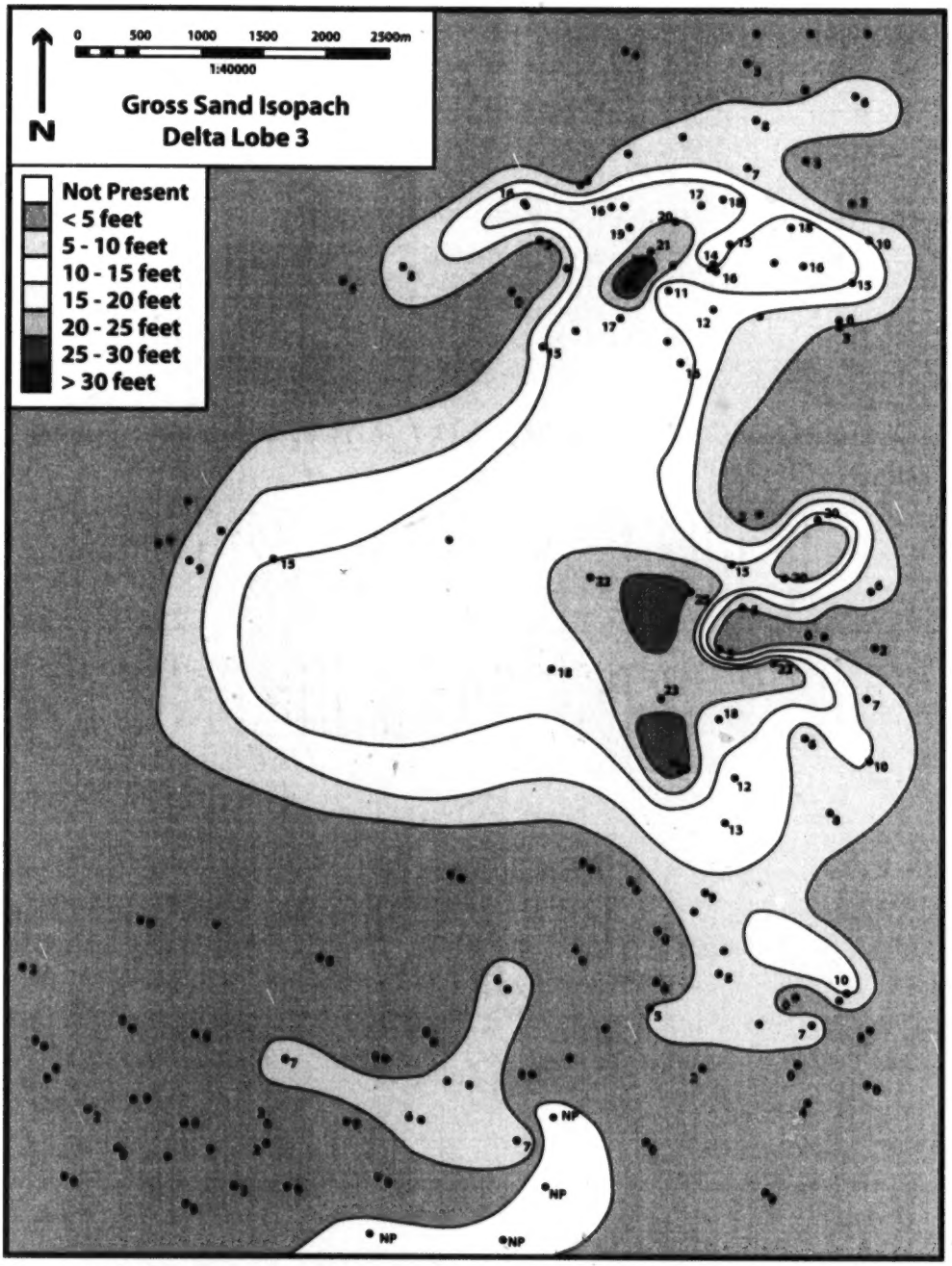

Figure 3.18. Gross sand isopach map of delta lobe 3. This lobe covers the entire study area except in southern Hayat where it is eroded out from above. The sand distribution seems relatively random but is centered on the Salam and Kenz fields. Isopach values were measured directly from wire-line logs. Measured depths on the logs are recorded in imperial units, so for sake of simplicity, these units were used on the isopach map.

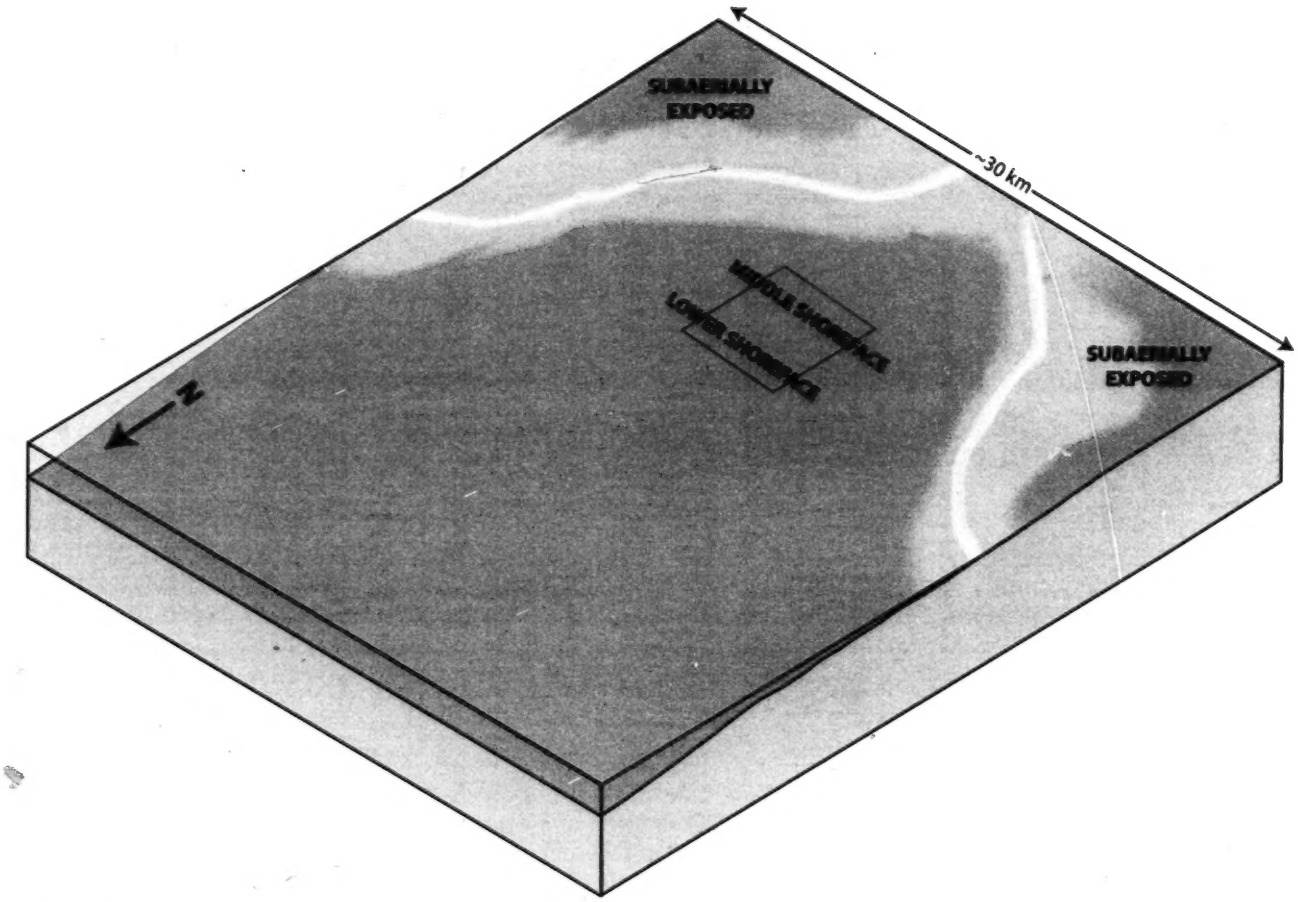

Figure 3.19. Depositional facies during lower Bahariya Stage 2. A marine shoreface covered the study area during Stage 2, following a major relative rise in sea level after Stage 1. Red squares deonotes the approximate location of the study area.

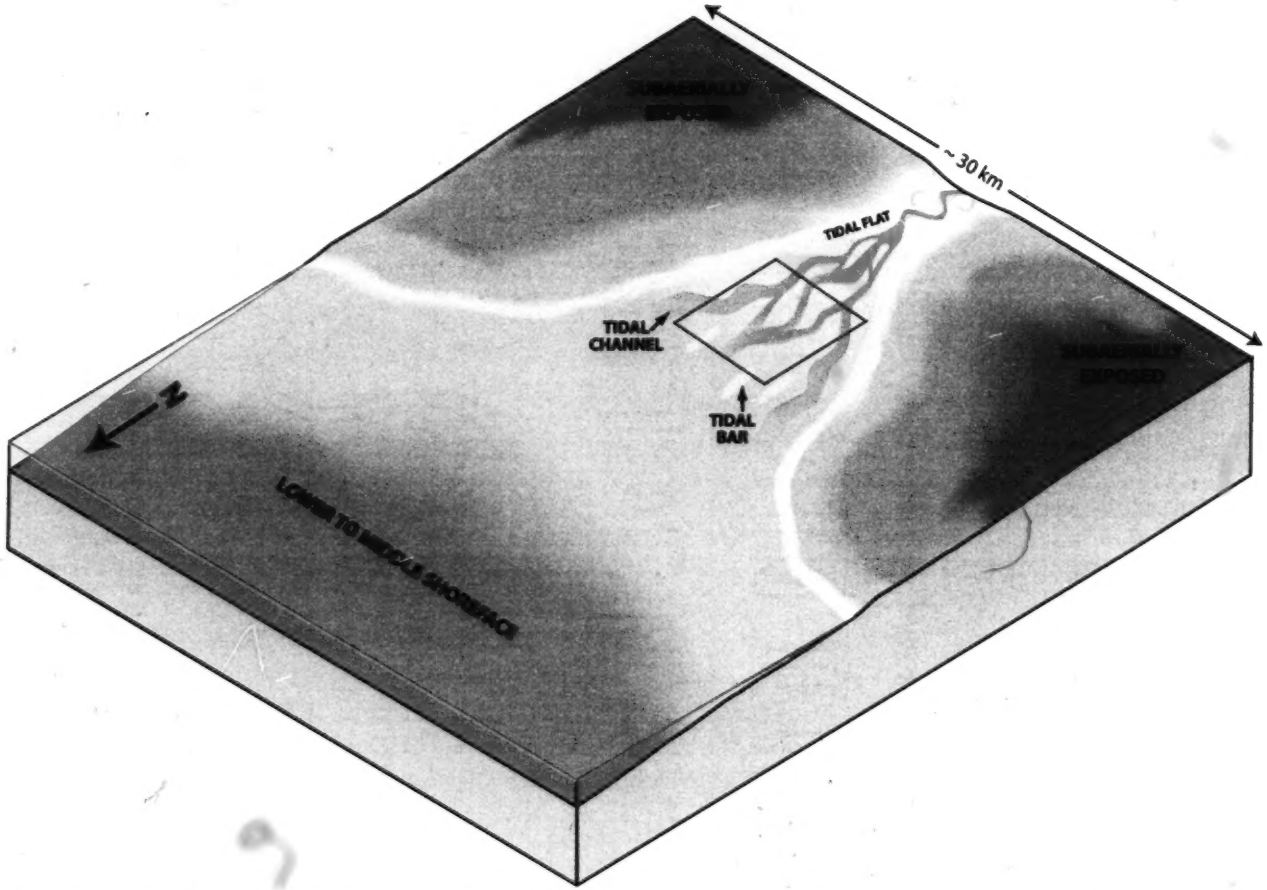

Figure 3.20. Depositional setting during lower Bahariya Stage 3. Following a drop in relative sea level late in Stage 2, tide-dominated estuarine conditions persisted within an incised valley system (see text). Red square deonotes the approximate location of the study area.

(FA1).

A classic example of a transgressive-regressive surface (where estuarine deposits overlie marine sediments) occurs in the Cretaceous Viking Formation of the Western Canadian Sedimentary Basin (MacEachern et al., 1992). In the case of the Viking Formation, the succession is interpreted as an incised valley system (Zaitlin et al., 1994). A drop in relative sea level and subsequent lowering of base level caused fluvial systems to incise a large, wide valley into the underlying progradational shoreline succession. This erosion created a regressive surface of erosion, or sequence boundary. The valley was then transformed into an estuarine system upon subsequent relative sea level rise, and the regressive surface thus became a transgressive surface (TS/RSE). The estuarine deposits are likely related to transgression, although they could have been deposited during relative sea level lowstand near the basinward portion of the valley (MacEachern et al., 1992).

Accordingly, S3 of the lower Bahariya Formation represents an incised valley system. An isopach map of the strata between the datum and the discontinuity at the base of Stage 3, shows thicks and thins that correspond to lows and highs on the discontinuity surface, respectively (Fig. 3.21). This map reveals a low trending sinuously through the study area from south to north. This sinuous to branching low represents a valley system with main channels and distributaries that incised into underlying deposits during lowstand. In addition, the transgressive-regressive surface is demarcated by the *Glossifungites* suite of trace fossils. The organisms responsible for these burrows would have colonized the substrate during a depositional hiatus after relative sea level fall and substrate exhumation by fluvial incision, but before any significant estuarine sedimentation.

It is uncertain whether the estuarine valley fill was deposited during lowstand or transgression. Because the organisms responsible for the burrows of the *Glossifungites* ichnofacies are only found in marine or brackish water, the presence of these burrows at the base of the valley suggests that the valley was inundated with marine water at some point after fluvial incision. While it is possible that estuarine conditions existed in the basinward portions of the incised valley during sea level lowstand, permitting substrate colonization and deposition of estuarine facies (Pemberton and MacEachern, 1995), the presence of an amalgamated transgressive-regressive surface at the valley base indicates that the valley did not fill until transgression. The lack of fluvial deposits in S3 suggests that either the valley served as a zone of sediment bypass during lowstand and possessed no fluvial deposits, or any lowstand deposits were subsequently eroded and reworked during transgression by tidal scour associated with rapid sea level rise.

In typical incised valley fill successions, continuing transgression transposes more distal estuarine facies above proximal estuarine facies. For example, fluvial bayhead

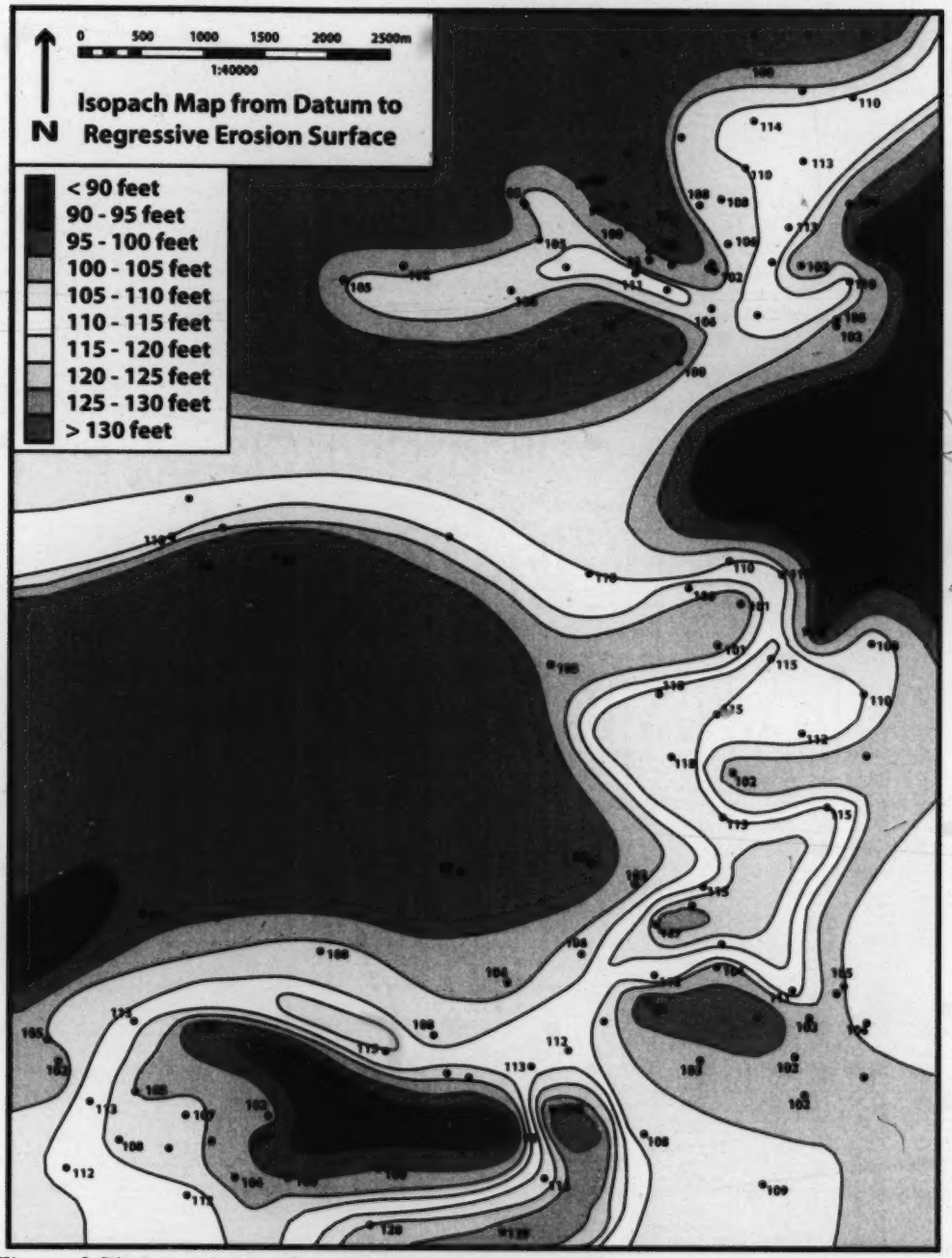

Figure 3.21. Isopach map fron datum to regressive surface of erosion. Thicks represent structural lows on the regressive surface and are shown in blue; thins represent structural highs on the regressive surface and are coloured red. Note the sinuous to branching low areas trending through the study area. Isopach values were measured directly from wire-line logs in imperial units, so for the sake of simplicity, these units were used on the isopach map.

delta sands are commonly overlain by brackish bay muds, which are in turn overlain by barrier bar sands. This is not the case in S3, as tide-dominated estuaries lack the seaward-basinward facies distributions that are typical of wave-dominated estuaries. Because tidal channels and bay sediments are found throughout tide-dominated estuaries, there is rarely a tripartite facies distribution, and a unique succession of proximal to distal facies will not be present. However, the tidal channel successions of S3 grade upward into the more basinward deposits of Stage 4 (proximal embayment, then distal embayment), indicating continued relative sea level rise.

3.5.4 Stage 4 (S4)

Relative sea level rise continued into Stage 4, resulting in the development of a shallow marine embayment (Fig. 3.22). There is minimal fluvial input into the system and the area is inundated with marine water. Sedimentation during this time occurred first in a proximal embayment setting with shoal, channel, and storm deposits in an organic rich shale. Following a small rise in relative sea level, distal embayment settings persisted, with rare current activity depositing glauconitic sandstone and shell beds in a calcareous shale (FA5). Shell hash beds at the top of this succession likely represent a lag deposit associated with another significant rise in relative sea level (major marine flooding surface). The juxtaposition of distal over proximal facies suggests continued relative sea level rise throughout S4.

3.6 SEQUENCE STRATIGRAPHIC FRAMEWORK

Although sequence stratigraphy was originally developed for use with seismic data on passive, continental margin successions (Van Wagoner et al., 1990), it is becoming commonplace to apply it to marginal-marine settings. This study has taken mainly an allostratigraphic approach to genetic stratigraphy. For the sake of completion, the stratigraphy and depositional stages of the lower Bahariya will be loosely placed in a sequence stratigraphic framework. For definitions of terminologies used in this section the reader is referred to Van Wagoner et al. (1990).

It is unclear whether relative sea level during S1 is falling, rising, or at a stand-still. Although deltas are generally formed during sea level fall and estuaries during sea level rise, there are many examples of deltas and estuaries occurring during transgression and regression, respectively (Dalrymple, 1999). The three delta lobes are composed of parasequences that prograde basinward, which is characteristic of sea level stillstand or

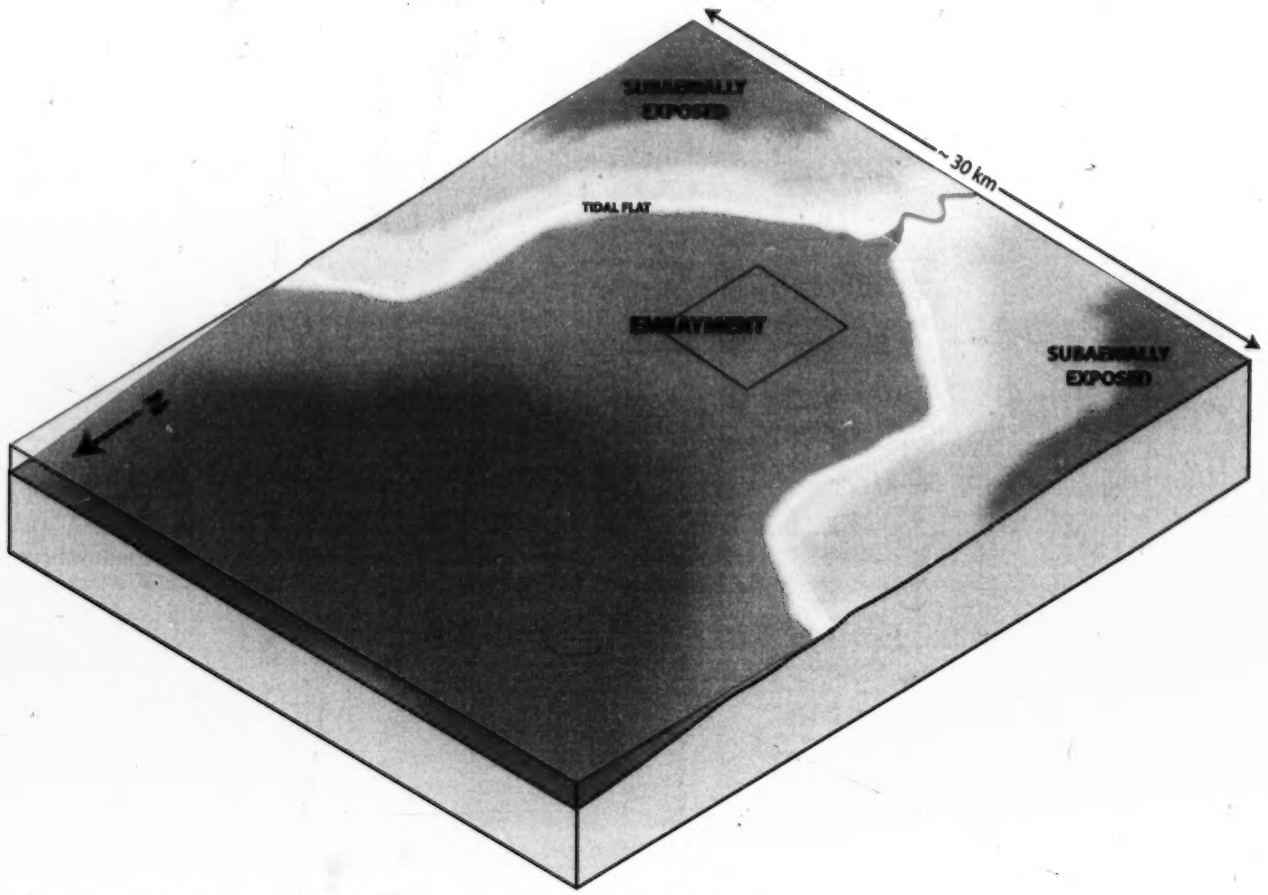

Figure 3.22. Paleogeography during lower Bahariya Stage 4. Due to decreasing fluvial input and increasing relative sea level, the tide-dominated estuarine valley system of S3 has been flooded and turned into a marine embayment. Red square denotes the anticipated location of the study area.

fall. As such, at least the upper portion of S1 comprises part of the highstand systems tract (HST).

A significant increase in relative sea level occurs between S1 and S2 and is interpreted as a major marine flooding surface, which typically separates parasequence sets. In the lower Bahariya Formation, the major marine flooding surface separates the underlying delta lobe parasequences from the overlying shoreface parasequence deposited during S2. Sea level is likely at a stillstand or slowly falling, placing these deposits in the highstand systems tract as well.

Stage 3 fits effortlessly into a sequence stratigraphic context. In sequence stratigraphy, the amalgamated transgressive-regressive surface of erosion (TS/RSE) that truncates the S2 shoreface parasequence is called an amalgamated flooding surface-sequence boundary (FS/SB), despite the lack of evidence for subaerial exposure. The estuarine deposits of S3 overlying the FS/SB were deposited in the incised valley upon transgression and represent the initial stages of the transgressive systems tract (TST).

Stage 4 was deposited under continued relative sea-level rise and although individual parasequences are not visible, it likely represents part of the TST. Stage 4 contains a minor marine flooding surface at its base and a major marine flooding surface at its top.

In summary, the lower Bahariya Formation represents two partial sequences. S1 and S2 make up the first partial sequence consisting of the highstand systems tract. The base of S3 is a sequence boundary, and together S3 and S4 represent the second partial sequence consisting of LST and TST. The sea level changes affecting this rock succession are on a much smaller scale than the 1st order changes shown by the global eustatic sea level curve in Figure 1.7. Tectonic movement likely plays a minor role in changing relative sea level as the area is underlain by a stable, passive continental margin. Except for the significant drop in sea level at the base of S3, autocyclic controls such as sediment supply and local subsidence are the probable driving forces behind the relative sea level changes throughout most of the succession, especially in the deltaic portions of S1.

3.7 SUMMARY

The lower Bahariya Formation consists of a complex association of marginal marine and marine deposits. Transgressive and regressive surfaces associated with abrupt relative sea level rise and fall, respectively, are found throughout the succession and are commonly associated with the *Glossifungites* ichnofacies, sideritized mud clast breccias, and carbonate cemented sandstones. These surfaces naturally divide the lower Bahariya Formation into four depositional stages that record the change in depositional setting

from tide-dominated estuary/delta, to lower and middle shoreface, to incised valley with estuarine fill, and finally, to marine embayment.

CHAPTER FOUR: SOFT-SEDIMENT DEFORMATION

4.1 INTRODUCTION

All sediments can be deformed non-tectonically during deposition or shortly after burial. Structures produced by the deformation of unlithified or "soft" sediment are consequently called soft-sediment deformation structures. Early deformation modifies the original sedimentary structures produced during deposition. In some cases, many of the original structures are recognizable, while in other cases the sedimentary structures have been modified or completely destroyed (Collinson, 1994). The nature of the deformation structure is controlled by sediment characteristics, such as porosity, packing arrangement, density, and permeability (Reineck and Singh, 1980).

The lower Bahariya Formation contains a great quantity and variety of soft-sediment deformation structures, including load casts, load-cast ripples, pillars, sediment dykes, homogenized bedding, syn-sedimentary faults and slumps, shrinkage cracks, and concretions. This chapter provides a summary of the general kinematics and driving mechanisms of deformation within soft sediment, a description of the deformation structures within the lower Bahariya Formation, a review of relevant literature, and a discussion of the paleoenvironmental significance of such features.

4.2 DRIVING MECHANISMS AND TRIGGERS

The forces found at the sediment-water interface that cause soft-sediment deformation are relatively weak in ordinary geological terms. Therefore, at the time of deformation, the deposits must be either in a liquid-like state or solids of insignificant yield strength (Allen, 1982). Due to high initial porosity and loose packing arrangement, most soft-sediment deformation occurs in fine grained sand to mud sized sediment (Mills, 1983; Collinson, 1994). Grain cohesion, sediment permeability, and rate of deposition are some of the parameters that control sediment response to stress (Mills, 1983).

The dominant mechanisms responsible for soft-sediment deformation are: 1) liquefaction or fluidization (Lowe, 1975; Allen, 1982; Owen, 1987; Owen, 1996); 2) gravitationally unstable vertical profiles of sediment bulk density, also known as reverse density gradients (Allen, 1982; Mills, 1983); 3) slumping or slope failure (Reineck and Singh, 1980; Allen, 1982; Mills, 1983); 4) shear stress (Allen, 1982; Mills, 1983); and 5) unevenly distributed confined loads (Owen, 1987). Many of these mechanisms require a change in sediment state from solid to liquid-like, which is often initiated by an external

event or trigger. Such triggers include pore-pressure build-up during seismic shaking, fluctuation in pore pressure due to wave passage, groundwater movements, and impacts (Allen, 1982; Owen, 1987).

Many different classification schemes for soft-sediment deformation structures have been proposed (Table 4.1; e.g. Pettijohn and Potter, 1964; Elliot, 1965; Lowe, 1975; Allen, 1977; Brenchley and Newall, 1977; Allen, 1982; Owen, 1987). These are based on either the geometry of the deformation structure, kinematics of deformation, or origin of the deforming stress. No agreement has been made on how to formally classify these types of structures.

4.3 DESCRIPTION OF SOFT-SEDIMENT DEFORMATION STRUCTURES

4.3.1 Load-Cast Ripples

Description

The deformation structures most commonly found in the lower Bahariya Formation are related to loading, of which load-cast ripples are the most prevalent. They are usually less than 3 cm in width and 1 cm in height, although loaded ripples with larger dimensions do occur (Fig. 4.1A-C). The ripples consist of very fine grained sand, and sink into an

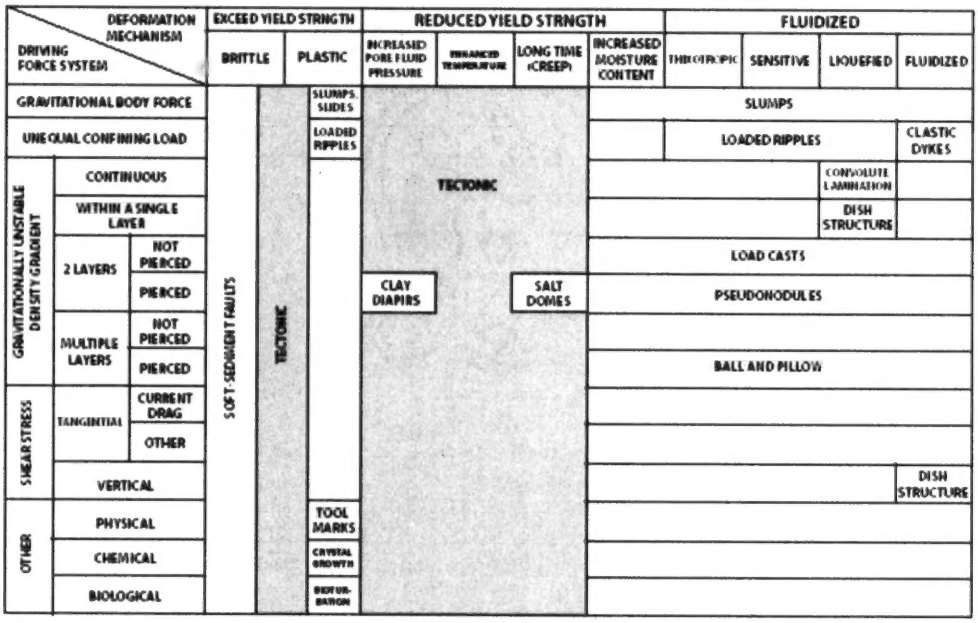

TABLE 4.1. Parameters affecting the formation of soft-sediment deformation (modified from Owen, 1987).

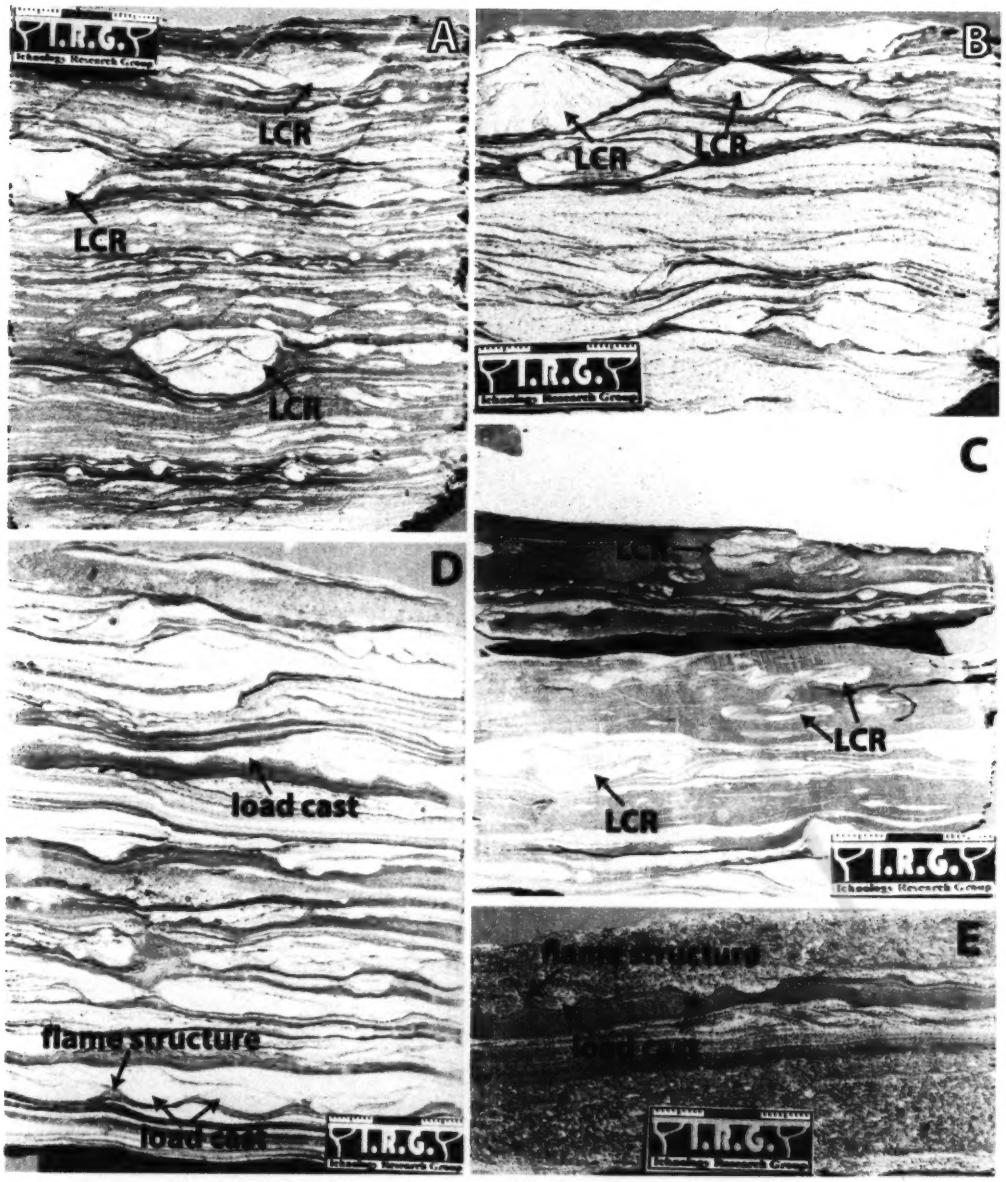

FIGURE 4.1. Photographs A through C show load-cast ripples (LCR). Photographs D and E show load casts and flame structures. Way up for all photographs is indicated by the scale bar.

underlying mud layer. The internal foreset laminae of the ripples are often contorted. A defined minimum thickness of mud is not required for deformation, although a higher overall bed mud content tends to result in a higher degree of deformation. The load-cast ripples range in morphology from slightly sunken to completely overturned and contorted.

In some specimens, the ripples are completely isolated from other ripples in the mud and resemble ball and pillow structures. Loaded ripples occur dominantly in heterolithic sandstone and mudstone (Facies 2) and rarely in other interbedded sand and mud facies (Facies 1, 3, 4 and 5). The degree to which the ripples have been deformed changes their crest profile (e.g. from symmetrical to asymmetrical, or vice versa), therefore making sedimentological analysis difficult.

Literature Review

According to Allen (1982) there are three varieties of load-cast ripples: 1) postdepositional, involving incomplete ripple marks; 2) syndepositional, involving a sequence of ripple marks; and 3) syndepositional, where one ripple grows continuously. All three types occur in the lower Bahariya Formation.

Postdepositional load-cast ripples appear as a row of plano-convex or biconvex lenses of coarse silt or sand embedded in mud (Fig. 4.2; Dzulynski and Kotlarczyk, 1962; Dzulynski, 1963; Allen, 1982). The lenses are usually less than 10 cm in width and rarely thicker than 1 cm. The mud in the trough between two ripples is effectively unloaded, whereas the mud beneath the ripples is loaded to an extent proportional to the local ripple height and sand bulk density. Dzulynski and Kotlarczyk (1962) suggest that these structures result from the differential loading of a hydroplastic substrate.

Syndepositional load-cast ripples are described by Dzulynski and Kotlarczyk (1962), Dzulynski (1963), and Dzulynski and Walton (1965) as cylindrical masses of sand or coarse silt that occur in rows along the plane of bedding (Fig. 4.3). In cross section, they display a radial internal structure of laminated sand wedges and mud fingers. The sand wedges are believed to be caused by the loading of a number of ripples into weak mud, one after the other at much the same site. Each new ripple presses downward and forward the previous ripples until a radial structure becomes developed. They also suggest that once weakened, the mud tends to remain of reduced strength, permitting further deformation.

Owen (1987) attributes the formation of load-cast ripples to an unevenly distributed confining load where there is relief on sediment surface. Upon liquidization, the lower layer loses its bearing capacity and the sandy load sinks into the muddy substrate.

Load-cast ripples are differentiated from ball and pillow structures by their lack of concentricity in all sections (Dzulynski and Kotlarczyk, 1962). Ball and pillow structures are essentially load casts that have broken off and separated from their originating sand bed and descended into an underlying mud layer (Kuenen, 1965; Reineck and Singh, 1980). They do not occur within the lower Bahariya Formation.

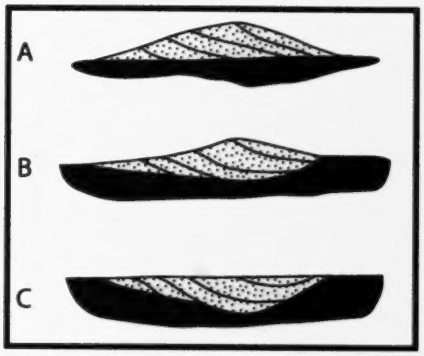

FIGURE 4.2 (above). Various stages of deformation (A through C) due to ripples sinking into a hydroplastic substrate (modified from Dzulynski and Kotlarczyk, 1962).

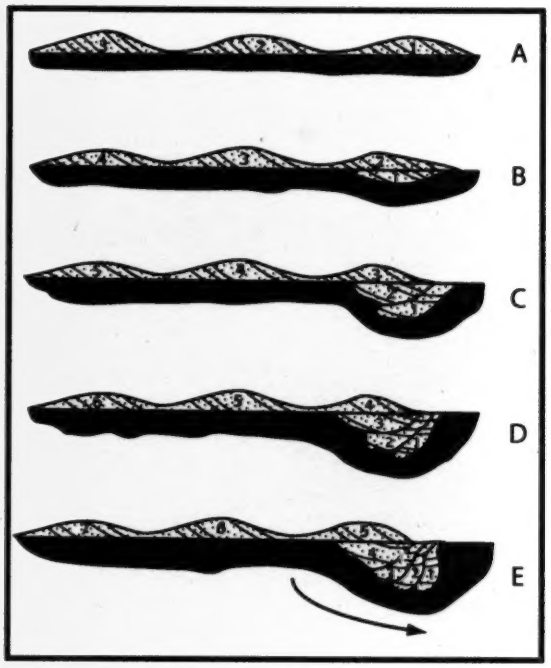

FIGURE 4.3 (right). Suggested mode of formation of syn-depositional load-cast ripples (modified from Dzulynski and Kotlarczyk, 1962).

4.3.2 Load Casts

Description

Load casts are occasionally found in the lower Bahariya Formation, dominantly within heterolithic sandstone and mudstone (Facies 2) and flaser bedded sandstone (Facies 3), and to a lesser extent in finely laminated mudstone and sandstone (Facies 1), rippled glauconitic sandstone (Facies 8), and bioturbated rippled sandstone (Facies 5). They are bulbous protrusions located at the base of centimeter-thick sand beds that overlie relatively thinner mud beds (Fig. 4.1D, E). The requisite sand bed thickness for their formation within the lower Bahariya Formation is at least 5 mm. Internal laminations within the load casts, where visible, are usually parallel to the edges of the protrusion and may show convolute lamination.

Literature Review

In the literature, load casts are described as swellings that vary in shape from slight bulges, to deep or shallow round sacks and knobby bodies, to highly irregular protuberances. They are generally found as sole markings preserved on the lower side of a sand layer that overlies a mud layer (Reineck and Singh, 1980; Allen, 1982). The underlying mud layer is distorted and bent downward beneath the load protuberance (Reineck and Singh,

1980). The bulges vary in height from a few millimeters to several decimeters. In vertical section, load casts commonly display contorted internal lamination. Close to the edge of the protuberance, the internal laminations tend to be oriented parallel to the margin, while the laminations in the core of the structure are more intensely disturbed and approach convolute lamination (Collinson, 1994).

Allen (1982) recognized load casts as one of the most common type of soft-sediment deformation structure in unstable, discontinuous layered systems. A horizontal layer of dense fluid overlying a layer of light fluid is unstable in the field of gravity, as the potential energy of the system is not at a minimum (Allen, 1982). Such a system is created when a sand layer is deposited over a hydroplastic mud layer (Reineck and Singh, 1980). The unequal loading created by the presence of the sand is adjusted by vertical movements. This causes the sand layer to sink into the mud, or the mud layer to push upward into the sand, creating load casts and flame structures, respectively (Kelling and Walton, 1957; Reineck and Singh, 1980).

Load casts are not a unique indicator for any specific environmental setting, as the only requirement for their genesis is unequal loading caused by the deposition of a sand layer over a hydroplastic mud layer (Reineck and Singh, 1980). They can be found in fluvial, deltaic, turbidite, and shallow marine deposits (Allen, 1982). They are also found in shallow water environments where continuous, rapid mud deposition is interrupted by occasional sand deposition, as in the channels of muddy intertidal flats (Reineck and Singh, 1980).

4.3.3 Flame Structures

Description and Review

As load casts are relatively rare within the sediments of the lower Bahariya Formation, flame structures are accordingly rare. They are related to load structures and take the form of curved, pointed tongues of mud that project upward into an overlying sand layer (Fig. 4.1D, E; Walton, 1956; Reineck and Singh, 1980). Due to unequal loading and liquefaction, the mud layer projects upward into the sand layer, while the sand layer sinks into the underlying mud layer. Its origin has also been attributed to shear stress (Mills, 1983).

4.3.4 Water Escape Structures

Description

Within the lower Bahariya Formation, there are a number of soft-sediment deformation structures attributed to water escape: pillars (Fig. 4.4A-C), soft-sediment intrusions and dykes (Fig. 4.5A), and beds displaying intense liquefaction (Fig. 4.5C, D).

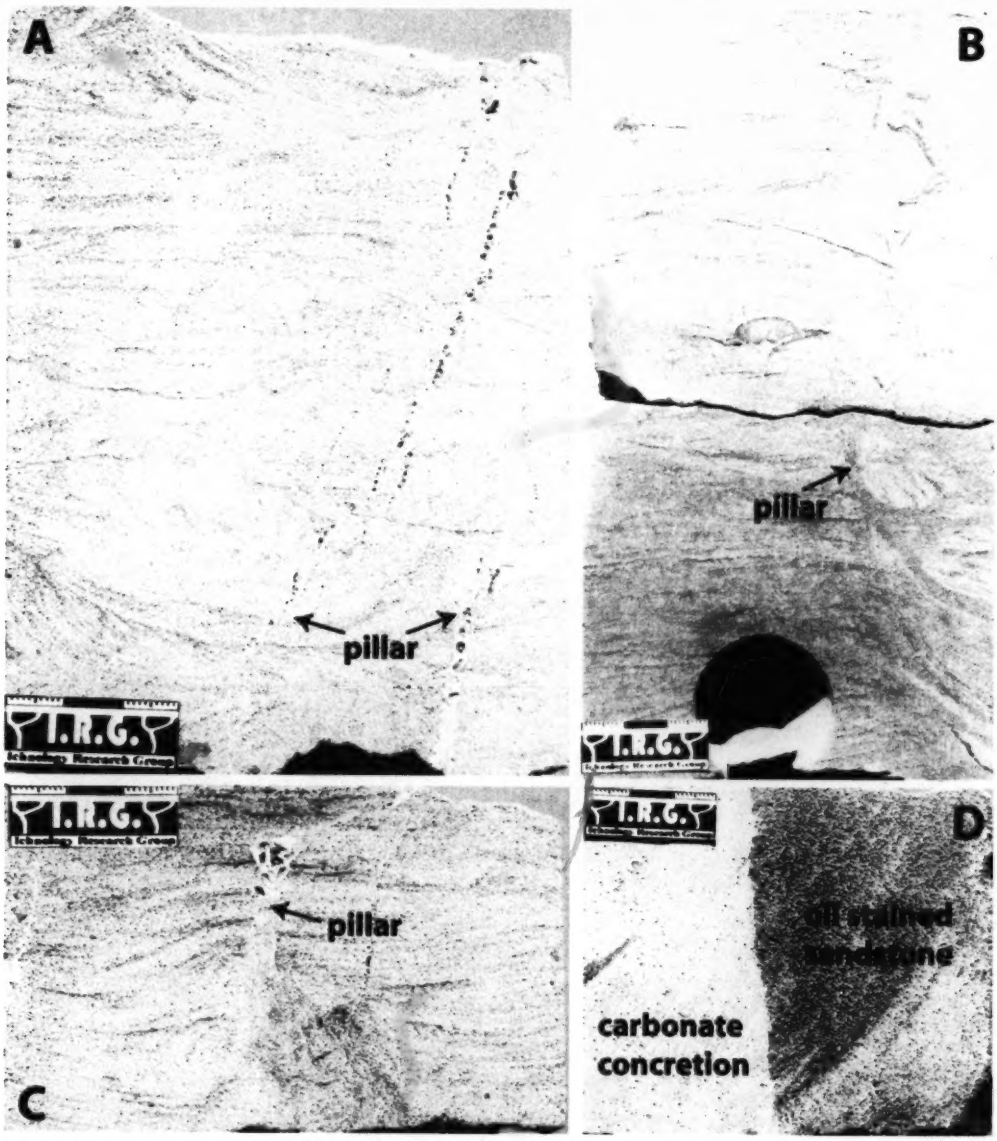

FIGURE 4.4. Water escape structures and concretions. A - C) Water escape pillars in rippled glauconitic sandstone (Facies 8a);. D) Carbonate concretion in fine grained, oil stained sandstone.

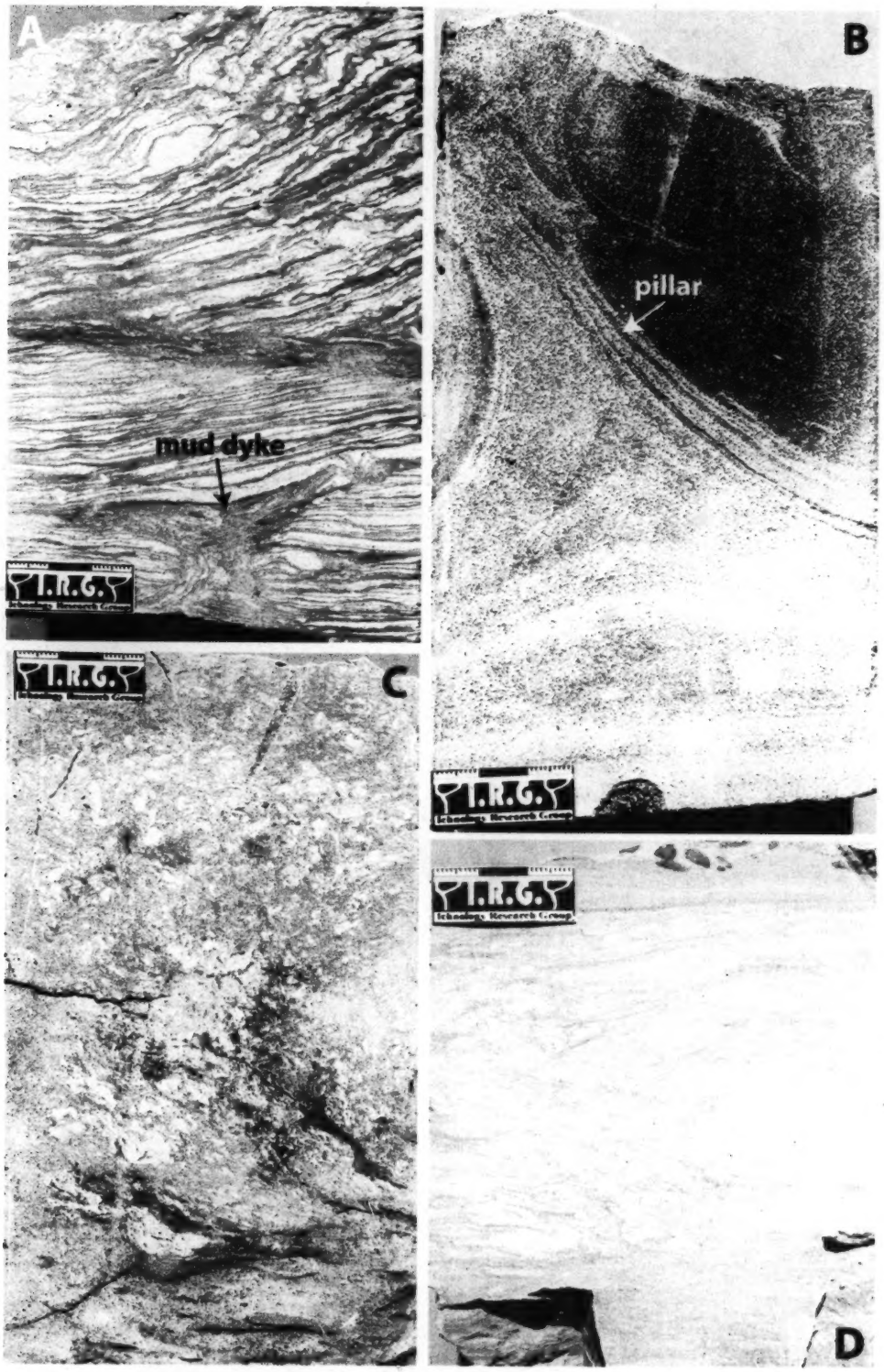
A
mud dyke
B
pillar
C
D

FIGURE 4.5 (previous page). Soft sediment deformation due to liquefaction and/or fluid escape. A) Soft-sediment intrusion in the form of the mud dyke. B) Water escape pillar in sandstone strongly affected by diagenesis. C and D) Intense liquefaction (liquefaction layers) resulting in contorted bedding.

The pillars are limited to fine grained, rippled glauconitic sandstone (Facies 8a). They are narrow, vertical to slightly inclined channels of massive sand that crosscut primary sedimentary structures. Individual structures range from 5 to 10s of centimeters in height, while their thickness is difficult to determine due to limited width of the core (Fig. 4.4). These structures are occasionally associated with strong chemical diagenetic effects (Fig. 4.5B), and calcite cementation along pore space created along fluid pathways. Affected sedimentary units contain both single and multiple vertical channels, and are identified as type B pillar structures of Lowe (1975).

Many cores contain interbedded very fine grained sand and mud units that have undergone intense liquefaction (Fig. 4.5C, D). The affected beds range in thickness from 10 cm to 1 m, and are characterized by highly contorted, sinuous, or patchy interbedded sand and mud layers.

An example of soft-sediment intrusion occurs in the form of a dyke (Fig. 4.5A). It is approximately 4 cm high and is comprised of interlaminated very fine grained sand and mud that was pushed vertically upward. The sediment came to rest and spread out laterally under a 0.5 cm thick sand lamination. Coincidentally, the dyke is located about 4 cm below a soft-sediment shear zone.

Literature Review

Soft-sediment deformation structures related to water escape are usually formed in loose, unconsolidated sediment as a result of pore water escape from sediment undergoing compaction. Water escape causes the rearrangement of existing laminae, or the genesis of entirely new structures (Lowe, 1975; Reineck and Singh, 1980; Owen 1996). The formation of water escape structures is controlled by grain size, hydrodynamic instability, sediment packing arrangement, cohesive strength, and permeability (Reineck and Singh, 1980). Although they are most common in high porosity, medium to fine grained sand that was deposited quickly, water escape structures are also associated with rapidly deposited interlaminated sand and mud (Lowe, 1975; Reineck and Singh, 1980; Owen, 1987; Owen 1996).

Lowe (1975) described three processes of water escape: 1) seepage – the slow upward movement of pore water without disturbance of the sediment grains; 2) liquefaction – the upward movement of pore water that causes the grains in a loosely packed framework

to become suspended in their own fluid, resulting in a temporary loss of sediment strength. Liquefaction occurs within a closed system and no external source of fluid is required. As the pore fluid is displaced upward, a more tightly packed, grain-supported framework is produced in its wake; and 3) fluidization – a process that occurs when interstitial fluid moves upward through a granular medium at such a rate that the upward drag force on the sediment grains exceeds their particle weight. The grains are lifted and the framework is destroyed, erasing all primary sedimentary structures.

Fluidization and liquefaction are the most common deformation mechanisms within unconsolidated, water-saturated sands. It is assumed that they play a role in the formation of many soft-sediment deformation structures, including dish and pillar structures, individual pillars, and soft-sediment dykes and folds (Lowe, 1995; Owen 1996). Water escape structures are commonly produced in settings that are characterized by 1) episodic deposition of fine to medium grained sand from currents of declining velocity at high mean and instantaneous sedimentation rates; 2) alternating sand and mud sedimentation; or 3) overall high mean sedimentation rates (Lowe, 1975).

Lowe's (1975) type B individual pillars are described as vertical to steeply inclined zones of homogenous or faintly structured sand. They range in height from a few millimeters to many metres. Some pillars are small, irregular patches of massive sand, while others display simple streamlined shapes or shapes with sinuous to undulating boundaries. They can form under a variety of conditions, but commonly within 1) zones of high permeability; 2) zones associated with large pebbles, chunks of plant matter, clay chips, or blocks of impermeable silt and sand that trap fluid and force confined flow at their margins; 3) above zones acting as restricted fluid escape routes; for instance at the base of a sand unit that overlies mud or clay layers; and 4) directly above zones of water escape in underlying layers.

Clastic dykes, also known as soft-sediment intrusions, are tabular bodies that cut across sedimentary strata. They are composed of extraneous gravel, sand, silt, or mud that penetrate the host strata from above or below, commonly along cracks. Under favourable conditions, almost any unconsolidated or easily deformed material could invade a crack and solidify to form a clastic dyke (Reineck and Singh, 1980).

Soft-sediment intrusions are related to liquefaction and fluidization (Lowe, 1975). Under sufficient pressure, clastic material in a liquefied form can easily rise, founder, or be forcefully injected into surrounding strata. The pressure required for injection can be produced by the load of overlying sediments, accumulated gas pressure, or hydrostatic pressure. The possible trigger mechanisms for sediment liquefaction include shock waves and slumping (Reineck and Singh, 1980; Lowe, 1975). Soft-sediment intrusions cannot

be assigned to any particular environment and are known to occur in deep-sea, shallow-marine, and non-marine sediments (Reineck and Singh, 1980).

Intensely liquefied beds, also known as liquefaction layers, show severely deformation primary structures, nearly complete homogenization, or water escape structures formed by the redistribution of grains during water escape and resedimentation. Individual layers of sediment can be liquefied either during deposition or post-deposition. Distinguishing sediments deposited in a liquid-like state from those liquefied post-depositionally is difficult, however most liquefied layers form as a result of post-depositional liquefaction (Lowe, 1975).

4.3.5 Concretions

Description

The Salam-8 well intersects a 1 m thick bed of massive sandstone displaying unique characteristics: the (relative) right half of the bed is porous and oil stained, while the left half of the bed is completely cemented by carbonate and contains no hydrocarbon stain (Fig. 4.4D). This well is interpreted to have intersected the interface between a carbonate concretion and the surrounding porous sandstone.

Literature Review

In general, concretions of any mineralogy found in clastic rocks are formed by mineral precipitation from pore water, rather than in-situ chemical reactions, which is normally the case in carbonate rocks (Collinson and Thompson, 1982). Most calcite concretions form during early diagenesis from alkaline pore waters (Collinson and Thompson, 1982). They range in diameter from a few centimeters to 3 m. Concretions in sandstone are commonly larger than those found in silt or clay, as sand has greater permeability and allows greater transport of material in solution (Pettijohn et al., 1987).

4.3.6 Syn-Sedimentary Faulting and Slump Structures

As syn-sedimentary faults and slump structures are typically genetically related, they are herein dealt with jointly.

Description

Two types of syn-sedimentary faulting occur within the lower Bahariya Formation and generally affect sediment belonging to Facies 1 and 2 (Fig. 4.6).

1. Medium-scale normal faults affecting beds approximately 10 cm thick (Fig. 4.6A, B). Because the faults extend beyond the edges of the core, the amount of displacement is indeterminable. Fault dip is between 30 and 45 degrees. Shearing of the sediment along the fault plane is common. Occasionally, closely spaced shear fractures occur within these fault zones.
2. Small-scale conjugate pairs of imbricate normal faults with longer main faults that together create a horst and graben configuration (Fig. 4.7C). The amount of vertical displacement on the smaller faults is less than 3 cm, while the displacement on the main faults is indeterminable. All faults dip between 30 and 45 degrees. Sediment shearing along or adjacent to the fault plane is absent.

Literature Review

Faulting in recently deposited sediment is common both in otherwise undeformed and deformed sequences. Both normal and reverse faults occur, although extensional faults are much more common. Fault displacement can be up to a few meters, but is usually on the scale of a few millimeters to centimeters. The extensional stress field may be due to contemporaneous tectonic activity or mass movement of sediment on slope (Collinson, 1994).

Most syn-sedimentary faulting is caused by 1) the action of gravity along steep basin slopes; 2) shock waves from earthquakes; or 3) a sudden release of stress through hydraulic fracturing caused by the build-up of pore fluid pressures as sediment is added to a horizontal pile. Overall, faulting is common to mixed mud and sand facies where density contrasts lead to the development of instabilities (Pickering, 1983).

Reineck and Singh (1980) defined slump as a general term that includes all the syn-sedimentary deformation structures resulting from the movement and displacement of previously deposited layers under the action of gravity. Slumping is associated with areas of rapid sedimentation where steeper slopes develop, and sediment susceptible to liquefaction is deposited (Reineck and Singh, 1980; Owen, 1987). Slumping can cause the break-up and transportation of sedimentary layers, producing a chaotic mixture of different sediment types (Fig. 4.6D). Plastic deformation, brittle fracture, brecciated horizons, injection phenomena, and small-scale faults are usually associated with slumping (Reineck and Singh, 1980). Dzulynski (1963) classified slumps into coherent and incoherent; the

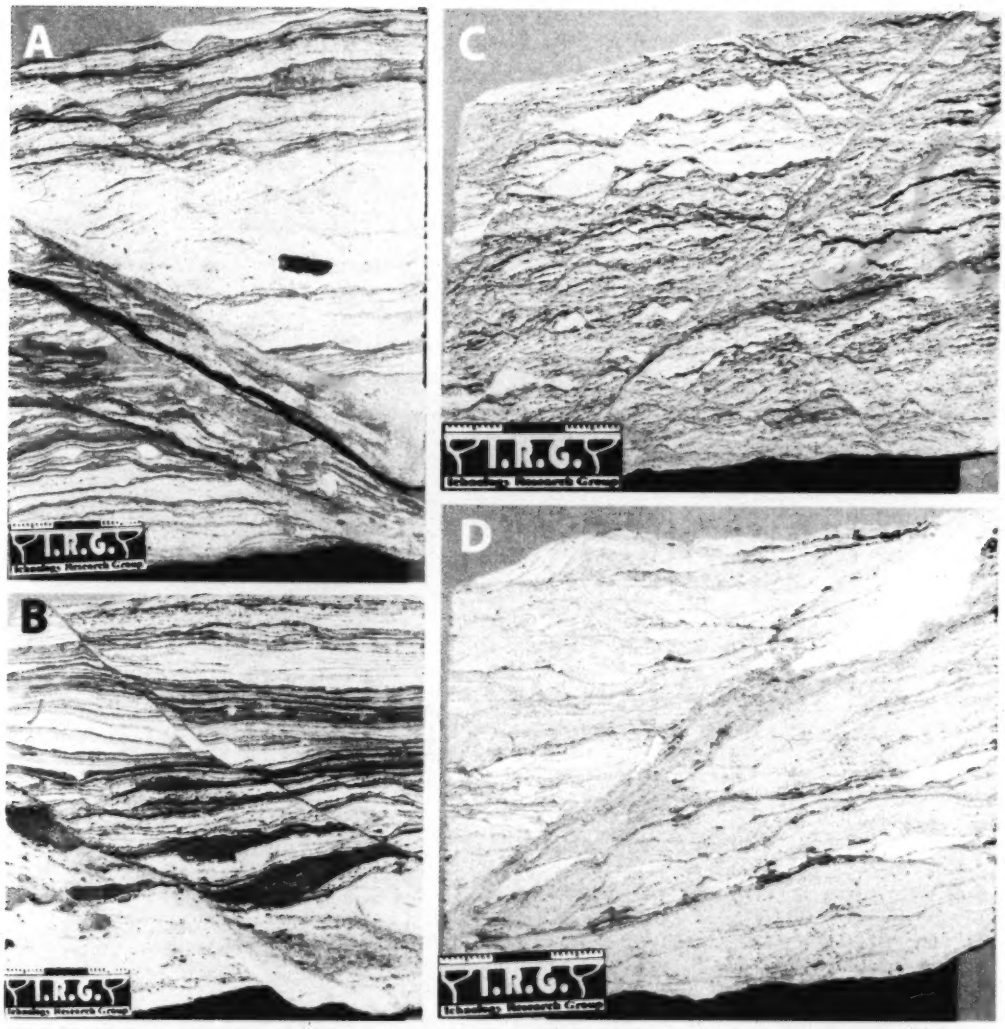

FIGURE 4.6. Soft-sediment faults and slumps. A and B) Medium-scale normal faults (Type 1). C) Small-scale conjugate pairs of normal faults (Type 2). D) Possible slump plane.

former is characterized by the general preservation of original primary sedimentary structures with minimal mixing of sediment, while the latter exhibits extensive mixing of deformed bedding within a mass of unconsolidated sand, silt, and mud, and often contains tight folds. Mills (1983) described five features that can be used to differentiate slumps from other structures: rotational slip surfaces, pull aparts, slump balls, basal slickensides, and plastic thickening.

The most common cause of slumping in unconsolidated sediments is slope oversteepening. This frequently occurs on point bars in tidal creeks and river channels.

Oversteepening may be a depositional response, perhaps related to liquefaction, or may occur as a result of erosional undercutting by water currents (Mills, 1983).

Type 1 faults of the lower Bahariya Formation are similar to the isolated normal faults of Pickering (1983). He suggested that they formed in response to tensile stresses developed on oversteepened slopes, or due to escaping pore fluids. Early faults are seldom mineralized and are commonly associated with smearing of sediment along the fault surface (Collinson, 1994). As such, Type 1 faults are interpreted to have occurred shortly after sediment deposition, likely due to slumping brought on by liquidization on an oversteepened slope.

Type 2 faults were likely created late in the compaction history of the sediment, as shown by the lack of sediment smearing or evidence for growth faulting. The crispness of the faults suggests that the sediment was probably relatively lithified and compacted prior to deformation. Occasionally, Type 2 faults occur in association with Type 1 faults, and are therefore likely associated with slope failure or slumping.

Type 2 faulting affects a 4.5 m thick unit of Facies 1 in Hayat-4 (Fig. 4.6C). The facies above and below this unit show no signs of deformation. It is most probable that the faulting of this unit originated from a single deformation event. Ground motion associated with a localized seismic event could have triggered this faulting, causing slope failure, sediment foundering under a heavy load, or deformation associated with upstream bank collapse and subsequent downstream movement of sediment. It is also possible that deformation is associated with channel processes, such as flooding or slumping on a large scale.

4.3.7 Shrinkage Cracks

Description

Shrinkage cracks are very common in facies consisting of interbedded sandstone and mudstone (F1 and F2 dominantly, less common in F3, F4, and F5). In vertical profile, they are crenulated, sinuous sand-filled structures that vary in dimension (Fig. 4.7). Two different morphologies occur within the lower Bahariya Formation:

1. Long, thin cracks less than 2 mm wide. The average length is 1 to 3 cm, but varies between 3 and 10 cm. They are usually vertical to slightly inclined and are generally solitary forms (Fig. 4.7A).
2. Short, thick cracks between 2 mm and 1 cm wide and less than 3 cm long. Their orientation varies from vertical to inclined to occasionally horizontal, and they

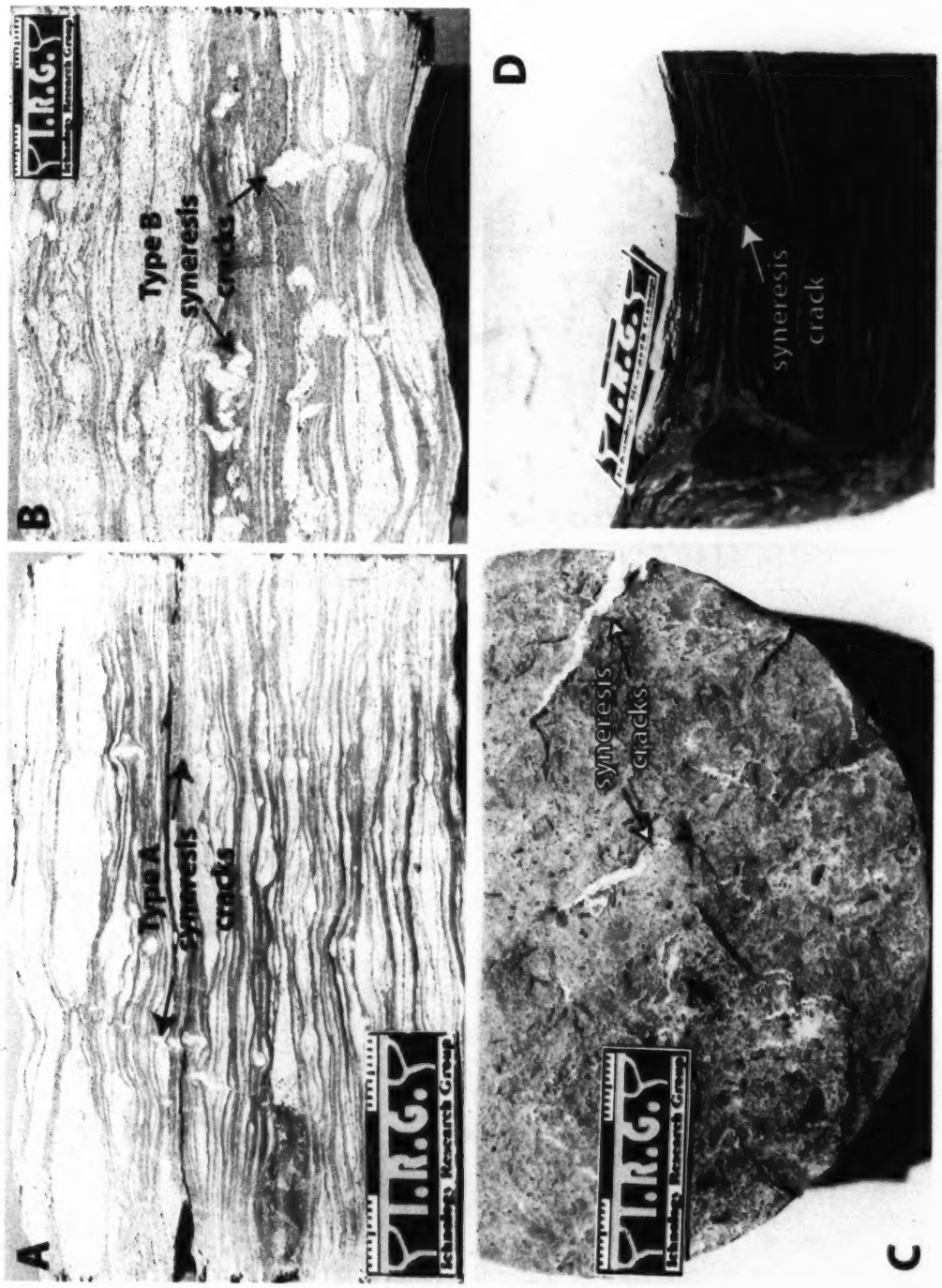

Figure 4.7. Syneresis cracks. A) Type A syneresis cracks. B) Type B syneresis cracks. C) Spindle-shaped syneresis cracks on a muddy bedding plane with disseminated organic material. D) Type B syneresis crack in cross section and plan view.

generally occur in clusters. The individual cracks within clusters commonly exhibit opposing inclinations (Fig. 4.7B).

All cracks within the lower Bahariya Formation usually taper downward in thickness and rarely taper upward or become bulbous at their bottom terminations. They cross-cut and are overlain by both sand and mud layers. Occasionally, cracks are associated with beds showing strong deformation. Differential compaction of the sand infill and the surrounding mud host is common.

Literature Review

Desiccation cracks are straight or variously curved in plan view and are characterized by well-developed polygonal patterns. Polygonal areas between cracks are commonly concave-upward. In vertical section, they taper downwards, and range in width up to several centimeters and depth up to several decimeters. They are typically infilled by coarser-grained material, usually sandstone.

Dessication cracks are formed by the sustained drying of a water-saturated mud layer exposed to the surface, such a river bed, lake floor, lagoon, or tidal flat. Dessication cracks are often associated with other evidence of exposure, such as raindrop prints or animal tracks (Reineck and Singh, 1980; Collinson, 1994).

Syneresis cracks are sand-filled, sinuous to spindle or lenticular shaped structures in plan view (Plummer and Gostin, 1981; Collinson, 1994). In vertical section, they are lenticular or V-shaped (Burst, 1965) or parallel sided (Pratt, 1998). They typically taper downward but can also taper upward, and have margins that are straight, curved, lobate or ragged (Pratt, 1998). Cracks range from straight to strongly crumpled and have vertical, oblique, or stepwise orientations (Pratt, 1998). Like dessication cracks, they can develop polygonal patterns over time (Plummer and Gostin, 1981; Collinson, 1994). The sand or silt infill is usually derived from overlying beds (Pratt, 1998).

Syneresis cracks form in muddy substrates in subaqueous settings in response to: 1) tensional stresses produced within the sediment by water loss and accompanying decrease in volume induced by changes in salinity of the surface water; 2) sediment compaction; or 3) contractions due to changes in temperature (Plummer and Gostin, 1991). Some authors believe that syneresis cracks are induced by earthquake ground motion (Pratt, 1998) while others have related their synthesis to the formation of gypsum crystals (Astin and Rogers, 1991).

Both dessication and syneresis cracks can be deformed shortly after formation (Pratt, 1998). Under continuous compaction, the original V to lenticular shaped cracks

become bulbous or ptygmatically folded (Bradley, 1930; Donovan and Foster, 1972). Crack deformation can lead to the formation of new secondary cracks accompanied by lateral injection of coarse material along bedding planes, and upward movement in the form of clastic dykes (Donovan and Foster, 1972). Bradley (1930) describes differential compaction between the sand-filled cracks and mud host. The tops of some cracks stand up and form sharply defined ridges above the upper surface of the cracked bed. He summarizes that a greater grain size difference between the crack infill and host sediment results in a larger amount of differential compaction around the top of the crack. Where cracks are squashed or folded, a bed thickness reduction of up to 50% or 80% can be inferred (Bradley, 1930; Donovan and Foster, 1972).

Shrinkage cracks have considerable environmental significance. The presence of dessication cracks indicates subaerial exposure, which may have important stratigraphic implication. The presence of syneresis cracks is often associated with the influx of saline water into brackish-water settings, which is typical of brackish bay, estuarine, and deltaic environments.

Based on their morphology and mode of occurrence, both types of cracks found within the lower Bahariya Formation are interpreted as syneresis cracks. It is unclear why two different morphologies exist; perhaps each was formed under a unique combination of sediment and water characteristics .

4.4 PALEOENVIRONMENTAL SIGNIFICANCE

The presence of soft-sediment deformation structures provides the geologist more information regarding the rock's early consolidation history than the actual depositional environment (Allen, 1982). Deformation structures are not specific to any particular environment because the hydraulic conditions responsible for their development can be found in a variety of settings (Mills, 1983). They tend to occur frequently in water lain sediments where high sedimentation rates prevail and promote loose packing of sand and silt. Such settings include deltas, river floodplains, deep water basins affected by turbidity currents, and storm-influenced shallow marine environments (Allen, 1982). It is interesting to note that most deformation structures described in the literature are reported from turbidite and fluvial sequences (Brenchley and Newall, 1977). Shrinkage cracks are the only forms of soft-sediment deformation that can provide unique information regarding the depositional environment (see Section 4.3.7).

4.5 SUMMARY

A large variety of soft-sediment deformation structures are found in the lower Bahariya Formation. Most of these structures are related to fluidization and liquefaction, either as the triggers for deformation or the deformation mechanisms themselves. Most deformation features are associated with rapidly deposited sediment with high porosity and water saturation. The presence of syn-sedimentary deformation in a rock succession gives more information about the early consolidation history of the rock than about the specific depositional environment. To retrieve as much information as possible about the original depositional setting, soft-sediment deformation structures should be studied in association with other lithologic, paleontological, and structural data (Mills, 1983).

CHAPTER 5: CONCLUSIONS

1. The Cenomanian lower Bahariya Formation was deposited in a shallow embayment located on a tide-influenced, passive continental margin undergoing overall transgression during the Cenomanian.

2. Based on its sedimentologic and ichnologic characteristics, the lower Bahariya Formation was divided into five facies associations: brackish bay, tidal channel, tide-influenced delta front, marine shoreface, and transgressive embayment.

3. The high amount of soft-sediment deformation combined with an overall low diversity trace fossil assemblage suggests that the overall depositional setting was subject to a number of environmental stresses including a variable sedimentation rate, fluctuating salinity, and shifting substrates.

4. Both transgressive and amalgamated transgressive-regressive surfaces were identified based on the presence of the *Glossifungites* ichnofacies, sideritized mud clast breccias, and carbonate cemented sandstones.

5. The lower Bahariya Formation is divided into four depositional stages:
   - Stage 1: Tide-dominated delta/estuary with brackish bay, tidal channel, and delta front deposits
   - Stage 2: Lower to middle shoreface
   - Stage 3: Incised valley with tide-dominated estuarine fill consisting of tidal channel and brackish bay deposits
   - Stage 4: Marine embayment with transgressive embayment deposits

   Transgressive surfaces separate Stages 1 and 2, as well as Stages 3 and 4, whereas an amalgamated transgressive-regressive surface separates Stages 2 and 3.

REFERENCES

Abdalla, A.Y. and El Bassyouni, A.A. 1985. Primary sedimentary structures and sedimentary environments of the Bahariya Formation, "Lower Cenomanian," Bahariya Oasis, Egypt. Annals of the Geological Survey of Egypt, v. 15, p. 267-274.

Akkad, S.E. and Issawi, B. 1963. Geology and iron ore deposits of Bahariya Oasis. Geological Survey of Egypt, Paper 18, 300 p.

Albani, A.D. and Johnson, B.D. 1974. The bedrock topography and origin of Broken Bay, New South Wales. Journal of the Geological Society of Australia, v. 21, p. 209-214.

Allam, A.M. 1986. A regional and paleoenvironmental study on the Upper Cretaceous deposits of the Bahariya Oasis, Libyan Desert, Egypt. Journal of African Earth Science, v. 5, p. 407-412.

Allen, G.P. 1991. Sedimentary processes and facies in the Gironde Estuary: a recent model for macrotidal estuarine systems. In: Clastic Tidal Sedimentology. D.G. Smith, G.E. Reinson, B.A. Zaitlin and R.A. Rahmani (eds.). Canadian Society of Petroleum Geologists, Memoir 16, p. 29-40.

Allen, G.P. and Posamentier, H.W. 1993. Sequence stratigraphy and facies model of an incised valley fill: the Gironde estuary, France. Journal of Sedimentary Petrology, v. 63, p. 378-391.

Allen, J.R.L. 1970. Studies in fluvatile sedimentation: a comparison of fining-upwards cyclothems, with special reference to coarse-member composition and interpretation. Journal of Sedimentary Petrology, v. 40, p. 298-323.

Allen, J.R.L. 1977. The possible mechanics of convolute lamination in graded sand beds. Journal of the Geological Society of London, v. 134, p. 19-31.

Allen, J.R.L. 1980. Sand waves: a model of origin and internal structure. Sedimentary Geology, v. 26, p. 281-328.

Allen, J.R.L. 1982. Sedimentary Structures: Their Character and Physical Basis. Elsevier, Amsterdam: Developments in Sedimentology 30B, 663 p.

Allison, P.A., Wignall, P.B. and Brett, C.E. 1995. Palaeo-oxygenation: effects and recognition. In: Marine Paleoenvironmental Analysis From Fossils. D.W.J. Bosence and P.A. Allison (eds.). Geological Society Special Publications, v. 83, p. 97-112.

Amorosi, A. 1995. Glaucony and sequence stratigraphy: a conceptual framework of distribution in siliciclastic sequences. Journal of Sedimentary Research, v. B65, p. 419-425.

Ashley, G.M. 1990. Classification of large-scale subaqueous bedform: a new look at an old problem. Journal of Sedimentary Petrology, v. 60, p. 160-172.

Astin, T.R. and Rogers, D.A. 1991. "Subaqueous shrinkage cracks" in the Devonian of Scotland reinterpreted. Journal of Sedimentary Petrology, v. 61, p. 850-859.

Baird, G.C., Sroka, S.D., Shabica, C.W., and Kuecher, G.J. 1986. Taphonomy of middle Pennsylvanian Mazon Creek area fossil localities, northeast Illinois: significance of exceptional fossil preservation in syngenetic concretions. Palaios, v. 1, p. 271-285.

Baker, E.K., Harris, P.T., Keene, J.B. and Short, S.A. 1995. Patterns of sedimentation in the macrotidal Fly River delta, Papua New Guinea. In: Tidal Signatures in Modern and Ancient Sediments. B.W. Flemming and A. Bartholomae (eds.). Special Publication of the International Association of Sedimentologists, v. 24, p. 193-211.

Ball, J. and Beadnell, H.J.L. 1903. Bahariya Oasis: its topography and geology. Egypt. Surv. Dept., 84 p.

Barakat, M.G. and Arafa, A. 1972. Lithofacies and biofacies of Early-Upper Cretaceous in Mersa Matruh well no. 1, Western Desert, Egypt. 8th Arab Petroleum Congress, Algiers, Paper No. 69 (B-3), p. 1-27.

Barakat, M.G., Sadek, A. and Arafa, A.A. 1976. Microfacies analysis of the Cretaceous sediments in the north Western Desert, Egypt. Bulletin of the Faculty of Science, Cairo University, 49, p. 447-467.

Bauer, J., Kuss, J. and Steuber, T. 2003. Sequence architecture and carbonate platform configuration (Late Cenomanian - Santonian), Sinai, Egypt. Sedimentology, v. 50, p. 387-414.

Bhattacharya, J.P. 1992. Deltas. In: Facies Models: Response to Sea Level Change. R.W. Walker and N.P. James (eds.). Geological Association of Canada, p. 157-177.

Bhattacharya, J.P. and Walker, R.G. 1991. Allostratigraphic subdivision of the Upper Cretaceous Dunvegan, Shaftesbury and Kaskapau Formations in the northwestern Alberta subsurface. Bulletin of the Canadian Society of Petroleum Geologists, v. 39, p. 145-164.

Blanckenhorn, M. 1921. Handbuch der regionalen Geologie, Aegypten. Carl Winters, Heidelberg, 244 p.

Boersma, J.R. 1969. Internal structures of some tidal megaripples on a shoal in the Westerschelde estuary, the Netherlands. Geologie en Mijnbouw, v. 48, p. 409-414.

Boersma, J.R. 1970. Distinguishing features of wave-ripple cross-stratification and morphology. Ph.D. Thesis, University of Utrecht, 65 p.

Boyd, R., Dalrymple, R. and Zaitlin, B.A. 1992. Classification of clastic coastal depositional environments. Sedimentary Geology, v. 80, p. 139-150.

Bradley, W.H. 1930. The behavior of certain mud crack casts during compaction. American Journal of Science, v. 20, p. 136-144.

Brenchley, P.J. and Newall, G. 1977. The significance of contorted bedding Upper Ordovocian sediments of the Olso region, Norway. Journal of Sedimentary Petrology, v. 47, p. 819-833.

Bromley, R.G., Pemberton, S.G. and Rahmani, R. 1984. A Cretaceous woodground: the Teredolites ichnofacies, Journal of Paleontology, v. 58, p. 488-498.

Burst, J.F. 1965. Subaqeously formed shrinkage cracks in clay. Journal of Sedimentary Petrology, v. 35, p. 348-353.

Caston, V.N.D. 1972. Linear sand banks in the southern North Sea. Sedimentology, v. 18, p. 63-78.

Clifton, H.E. 1982. Estuarine deposits. In: Sandstone Depositional Environments. P.A. Scholle and D. Spearing (eds.). American Association of Petroleum Geologists, Memoir 31, p. 179-189.

Coleman, J.M., Gagliano, S.M. and Smith, W.G. 1970. Sedimentation in a Malaysian high tide tropical delta. In: Deltaic Sedimentation: Modern and Ancient. J.P. Morgan (ed.). Society of Economic Paleontologists and Mineralogists, Special Publication 15, p. 185-197.

Coleman, J.M. and Wright, L.D. 1975. Modern river deltas: variability of processes and sand bodies. In: Deltas: Models of Exploration. M.L. Broussard (ed.). Houston Geological Society, p. 99-149.

Collinson, J.D. 1994. Sedimentary deformational structures. In: The Geological Deformation of Sediments. A. Maltman (ed.). Chapman & Hall, p. 95-125.

Collinson, J.D. and Thompson, D.B. 1982. Sedimentary Structures. George Allen & Unwin (Publishers) Ltd. London, United Kingdom, 194 p.

Cooper, J.A.G. 2001. Geomorphological variability among microtidal estuaries from the wave dominated South African coast. Geomorphology, v. 40, p. 99-122.

Dalrymple, R.W. 1992. Tidal depositional systems. In: Facies Models: Response to Sea Level Change. R.G. Walker and N.P. James (eds.). Geological Association of Canada, p. 195-218.

Dalrymple, R. W., 1999. Tide-dominated deltas: do they exist or are they all estuaries? American Association of Petroleum Geologists, Annual meeting program, San Antonio, Texas, April 11-14, 1999.

Dalrymple, R.W., Knight, R.J., Zaitlin, B.A. and Middleton, G.V. 1990. Dynamics and facies model of a macrotidal sand-bar complex, Cobequid Bay-Salmon River Estuary (Bay of Fundy). Sedimentology, v. 37, p. 577-612.

Dalrymple, R.W. and Makino, Y. 1989. Description and genesis of tidal bedding in the Cobequid Bay-Salmon River estuary, Bay of Fundy, Canada. In: Sedimentary Facies in the Active Plate Margin. A. Taira and F. Masuda (eds.). Terra Scientific Publication Company, Tokyo, p. 151-177.

Dalrymple, R.W., Zaitlin, B.A. and Boyd, R., 1992. Estuarine facies models: conceptual basis and stratigraphic implications. Journal of Sedimentary Petrology, v. 62, p. 1130-1146.

Darahem, M., Paradisi, C. and Moinard, L. 1990, Evaulation of the Bahariya Formation from high resolution logging. 10th Egyptian General Petroleum Company Exploration and Production Seminar, p. 290-315.

Darwish, M., Abu Khadra, A.M. and Abd El Hamied, M.L. 1994. Sedimentology, environmental conditions and hydrocarbon habitat of the Bahariya Formation, Central Abu El Gharadig Basin, Western Desert, Egypt. 12th Egyptian General Petroleum Company Exploration and Production Conference, v. 1, p. 429-449.

Davis, R.A.Jr. 1978. Beach and nearshore zone. In: Coastal Sedimentary Environments. Davis, R.A.Jr. (ed.). Springer-Verlag, New York, New York, p. 237-285.

Dethier, M.N. 1992. Classifying marine and estuarine natural communities: an alternative to the Cowardian system. Natural Areas Journal, v. 12, p. 90-98.

Dia El Din, M. 1974. Stratigraphic and structural studies on Abu Gharadig oil and gas field. 4th Petrol. Explor. Seminar, Egyptian General Petroleum Corporation, Cairo.

Dolson, J.C., Shann, M.V., Matbouly, S., Harwood, C., Rashed, R. and Hammouda, H. 2001. The petroleum potential of Egypt. In: Petroleum Provinces of the Twenty-First Century. M.W. Downey, J.C. Threet and W.A. Morgan (eds.). American Association of Petroleum Geologists, Memoir 74, p. 453-482.

Dominik, W. 1985. Stratigraphie und Sedimentologie (Geochemie, Schwermineralanayse) der Oberkreide von Bahariya und ihre Korrelation zum Dakhla Becken (Western Desert, Agypten). Berl. Geowiss. Abh., v. 50, p. 153-176.

Donovan, R.N. and Foster, R.J. 1972. Subaqueous shrinkage cracks from the Caithness Flagstone Series (Middle Devonian) of northeast Scotland. Journal of Sedimentary Petrology, v. 42, p. 309-317.

Dzulynski, S. 1963. Directional structures in flysch. Studia Geol. Pologne, v. 12, p. 1-136.

Dzulynski, S. and Kotlarczyk, J. 1962. On load-casted ripples. Annales de la Societe Geologique de Pologne, v. 32, p. 147-160.

Dzulynski, S. and Walton, E.K. 1965. Sedimentary features of flysch and greywackes. Develoments in Sedimentology, Elsevier, Amsterdam, v. 7, 274 p.

El Anbaawy, M.I. and El Shazly, S.A. 1991. Sedimentation pattern and diagenesis of the Bahariya Formation in Abu El Gharadig oilfield, north Western Desert, Egypt. Bulletin of the Faculty of Science, Cairo University, v. 59, p. 193-223.

El Beialy, S.Y. 1994. Palynological evidence for the age and depositional environment of the Cretaceous Bahariya Formation, Northwestern Desert, Egypt. Sci. Geol., Bull., v. 47, p. 51-65.

El Hashemi, M.M. 1978. Sedimentologie et paleogeographie des series detritiques de l'Egypte occidentale, du Cambrien au Cenomanien. Diss. Inst. Geol. Univ. Louis Pasteur.

El Sheikh, M. 1990. Reservoir geology of the Bahariya Formation in the Meileiha development lease. 10th Egyptian General Petroleum Company Exploration and Production Seminar, Cairo, 14 p.

Elliot, R.E. 1965. A classification of subaqueous sedimentary structures based on rheological and kinematic parameters. Sedimentology, v. 5, p. 193-209.

Elliot, T. 1986. Deltas. In: Sedimentary Environments and Facies. H.G. Reading (ed.). Blackwell Scientific Publications, Oxford, p. 113-154.

Fairbridge, R.W. and Jablonski, D. 1979. The Encyclopedia of Paleontology. Dowden, Hutchinson and Ross, Inc. Stroudsburg, Pennsylvania, 886 p.

Franks, G.D. 1982. Stratigraphical modelling of Upper Cretaceous sediments of the Bahariya Oasis. 6th Egyptian General Petroleum Corporation. Exploration Seminar, March 1982, Cairo.

Galloway, W.E. 1975. Process framework for describing the morphologic and stratigraphic evolution of deltaic depositional systems. In: Deltas: Models of Exploration. M.L. Broussard (ed.). Houston Geological Society, p. 87-98.

Galloway, W.E. 1989. Genetic stratigraphic sequences in basin analysis; II, Application to Northwest Gulf of Mexico Cenozoic basin. American Association of Petroleum Geologists, Bulletin 73, p. 143-154.

Gastaldo, R.A., Allen, G.P. and Huc, A.-Y. 1995. The tidal character of fluvial sediments of the modern Mahakam River delta, Kalimantan, Indonesia. In: Tidal Signatures in Modern and Ancient Sediments. B.W. Flemming and A. Bartholomae (eds.). Special Publication of the International Association of Sedimentologists, v. 24, p. 171-181.

Geoscience Australia (A). Embayments and drowned river valleys. OzEstuaries. http://www.ozestuaries.org/conceptual_mods/cm_emb.htm, (June 2004).

Geoscience Australia (B). Online GIS. OzEstuaries. http://www.ozestuaries.org/gis/index.htm (June 2004).

Geoscience Australia (C). Physical characteristics of an Australian tide-dominated estuary. OzEstuaries. http://www.ozestuaries.org/conceptual_mods/TDE_physical.html (June, 2004).

Hantar, G. 1990. North Western Desert. In: The Geology of Egypt. R. Said (ed.) A. A. Balkema, Rotterdam, Netherlands, p. 293-319.

Harms, J.C., Southard, J.C., Spearing, D.R. and Walker, R.G. 1975. Depositional Environments as Interpreted from Primary Sedimentary Structures and Stratification Sequences. Society of Economic Paleontologists and Mineralogists, Short Course 2, 161 p.

Harris, P.T. 1988. Large-scale bedforms as indicators of mutually evasive sand transport and the sequential infilling of wide-mouthed estuaries. Sedimentary Geology, v. 57, p. 273-298.

Harris, P.T., Pattiaratchi, C.B., Cole, A.R. and Keene, J.B. 1992. Evolution of subtidal sand banks in Moreton Bay, eastern Australia. Marine Geology, v. 103, p. 225-247.

Hayes, M.O. 1975. Morphology of sand accumulations in estuaries. In: Estuarine Research. L.E. Cronin (ed.). Academic Press, New York, v. 2, p. 3-22.

Heap, A.D., Bryce, S. and Ryan, D.A. 2004. Facies evolution of Holocene estuaries and deltas: a large-sample statistical study from Australia. Sedimentary Geology, in press.

Hori, K., Saito, Y., Zhao, Q., Cheng, X., Wang, P., Sato., and Li, C. 2001. Sedimentary facies and Holocene progradation rates of the Changjiang (Yangtze) delta, China. Geomorphology, v. 41, p. 233-248.

Howard, J.D. and Nelson, C.H. 1982. Sedimentary structures on a delta-influenced shallow shelf, Norton Sound, Alaska. Geologie en Mijnbouw, v. 61, p. 29-36.

Howard, J.D. and Reineck, H.E. 1981. Depositional facies of high energy beach-to-offshore sequence, comparision with low energy sequence. Bulletin of the American Association of Petroleum Geologists, v. 65, p. 807-830.

Hudson, J.P. 1991. Late Quaternary evolution of Twofold Bay, southern New South Wales. Unpublished thesis, University of Sydney.

Kelling, G. and Walton, E.K. 1957. Load-cast structures: their relationship to upper-surface structures and their mode of formation. Geological Magazine, v. 94, p. 481-491.

Kerdany, M.T. and Cherif, O.H. 1990. Mesozoic. In: The Geology of Egypt. R. Said (ed.) A. A. Balkema, Rotterdam, Netherlands, p. 407-438.

Ketzer, J.M. 2002. Diagenesis and sequence stratigraphy: an integrated approach to constrain evolution of reservoir quality sandstones. Ph.D. Thesis, Department of Earth Sciences, Uppsala University, Sweden.

Ketzer, J.M., Holz, M., Morad, S. and Al-Aasm, I.S. 2003. Sequence stratigraphic distribution of diagenetic alterations in coal-bearing, paralic sandstones: evidence from the Rio Bonito Formation (early Permian), southern Brazil. Sedimentology, v. 50, p. 855-877.

Kuenan, P.H. 1965. Value of experiments in geology. Geol. Mijnbouw, v. 44, p. 22-36.

Lowe, D.R. 1975. Water-escape structures in coarse-grained sediments. Sedimentology, v. 22, p. 157-204.

MacEachern, J.A. and Pemberton, S.G. 1992. Ichnological aspects of Cretaceous shoreface successions and shoreface variability in the Western Interior Seaway of North America. In: Applications of Ichnology to Petroleum Exploration. S.G. Pemberton (ed.). Society of Economic Paleonotologists and Mineralogists, Core Workshop 17, p. 57-84.

MacEachern, J.A. and Pemberton, S.G. 1994. Ichnological aspects of incised-valley fill systems from the Viking Formation of the Western Canada Sedimentary Basin, Alberta, Canada. In: Incised-valley Systems: Origin and Sedimentary Sequences. R.W. Dalrymple, R. Boyd and B.A. Zaitlin (eds.). Society of Economic Paleontologists and Mineralogists, Special Publication 51, p. 129-157.

MacEachern, J.A., Raychaudhuri, I., and Pemberton, S.G. 1992. Stratigraphic applications of the Glossifungites ichnofacies: delineating discontinuities in the rock record. In: Applications of Ichnology to Petroleum Exploration. S.G. Pemberton (ed.). Society of Economic Paleonotologists and Mineralogists, Core Workshop 17, p. 169-198.

McCrimmon, G.G. and Arnott, R.W.C. 2002. The Clearwater Formation, Cold Lake, Alberta: a world class hydrocarbon reservoir hosted in a complex succession of tide-dominated deltaic deposits. Bulletin of Canadian Petroleum Geology, v. 50, p. 370-392.

Meckel, L.D. 1975. Holocene sand bodies in the Colorado delta area, northern Gulf of California. In: Deltas: Models of Exploration. M.L. Broussand (ed). Houston Geological Society, p. 239-265.

Meshref, W.M. 1990. Tectonic framework. In: The Geology of Egypt. R. Said (ed.) A. A. Balkema, Rotterdam, Netherlands, p. 113-155.

Metwalli, M.H., Saad, M.K. and Ali, T.A. 2000. Effect of depositional environments on reservoir capacity of upper Bahariya Formation, Meleiha oilfields, North Western Desert, Egypt. Sedimentology of Egypt, v. 8, p. 105-118.

Mills, P.C. 1983. Genesis and diagnostic value of soft-sediment deformation structures – a review. Sedimentary Geology, v. 35, p. 83-104.

Moustafa, A.R. and Khalil, M.H. 1990. Structural characteristics and tectonic evolution of north Sinai fold belts. In: The Geology of Egypt. R. Said (ed.) A. A. Balkema, Rotterdam, Netherlands, p. 381-389.

NASA. Earth Science Applications Directorate. https://zulu.ssc.nasa.gov/mrsid/mrsid.pl (June 2004).

Nelson, C.H., Rowland, R.W., Stoker, S.W. and Larsen, B.R. 1980. Interplay of physical and biological sedimentary structures of the Bering epicontinental shelf. In: Geological, geochemical and geotechnical observations on the Bering Shelf, Alaska. M.C. Larsen, C.H. Nelson and D.R. Thor (eds.). U.S. Geological Survey, Open File Report, p. 1-51.

Nio, S.D. and Yang, C.S. 1991. Diagnostic attributes of clastic tidal deposits: as review. In: Clastic Tidal Sedimentology. D.G. Smith, G.E. Reinson, B.A. Zaitlin and R.A. Rahmani (eds.). Canadian Society of Petroleum Geologists, Memoir 16, p. 3-27.

North American Commission on Stratigraphic Nomenclature (NACSN). 1983. North American stratigraphic code. American Association of Petroleum Geologists Bulletin, v. 67, p. 841-875.

Owen, G. 1987. Deformation processes in unconsolidated sands. In: Deformation of Sediments and Sedimentary Rocks. M.E. Jones and R.M.F. Preston (eds.). Geological Society Special Publication, 29, p. 11-24.

Owen, G. 1996. Experimental soft-sediment deformation: structures formed in the liquefaction of unconsolidated sands and some ancient examples. Sedimentology, v. 43, p. 279-293.

Pemberton, S.G. and MacEachern, J.A. 1995. The sequence stratigraphic significance of trace fossils: examples from the Cretaceous foreland basin of Alberta, Canada. In: Sequence Stratigraphy of Foreland Basin Deposits. J.C. VanWagoner and G.T. Bertram (eds.). American Association of Petroleum Geologists, Memoir 64, p. 429-475.

Pemberton, S.G., MacEachern, J.A. and Frey, R.W. 1992. Trace fossils facies models: environmental and allostratigraphic significance. In: Facies Models: Response to Sea Level Change. R.G. Walker and N.P. James (eds.). Geological Association of Canada, p. 47-72.

Pemberton, S.G. and Wightman, D.M. 1992. Ichnological characteristics of brackish water deposits. In: Applications of Ichnology to Petroleum Exploration. S.G. Pemberton (ed.). Society of Economic Paleontologists and Mineralogists, Core Workshop 17, p. 141-167.

Pemberton, S.G., Spila, M., Pulham, A.J., Saunders, T., MacEachern, J.A., Robbins, D. and Sinclair, I.K. 2001. Ichnology and Sedimentology of Shallow to Marginal Marine Systems. Geological Association of Canada, Short Course Notes 15, 343 p.

Perillo, G.M.E. 1995. Definitions and geomorphologic classifications of estuaries. In: Geomorphology and Sedimentology of Estuaries. G.M.E Perillo (ed.). Developments in Sedimentology, v. 53, p. 17-47.

Pettijon, F.J. and Potter, P.E. 1964. Atlas and Glossary of Primary Sedimentary Structures. Springer-Verlag, New York.

Pettijohn, F.J., Potter, P.E. and Siever, R. 1987. Sand and Sandstone. Springer-Verlag, New York. 553 p.

Phillip, G., Metwalli, H. and Wali, A.M. 1980. Cretaceous sandstones as oil and gas reservoirs and their petrographic characteristics in Northern Western Desert, Egypt. Geologia, v. 6, p. 59-77.

Pickering, K.T. 1983. Small scale syn-sedimentary faults in the Upper Jurassic 'Boulder Beds.' Scottish Journal of Geology, v. 19, p. 169-181.

Plummer, P.S. and Gostin, V.A. 1981. Shrinkage cracks: dessication or syneresis? Journal of Sedimentary Petrology, v. 51, p. 1147-1156.

Pratt, B.R. 1998. Syneresis cracks: subaqueous shrinkage in argillaceous sediments caused by earthquake-induced dewatering. Sedimentary Geology, v. 117, p. 1-10.

Reading, H.D. and Collinson, J.D. 1996. Clastic Coasts. In: Sedimentary Environments: Processes, Facies and Stratigraphy. H.G. Reading (ed.). Blackwell Science, Oxford. 688 p.

Reineck, H.E. 1972. Tidal Flats. In: Recognition of Ancient Sedimentary Environments. J.K. Rigby and W.K. Hamblin (eds.). Society of Economic Paleontologists and Mineralogists, Special Publication 16, p. 146-159.

Reineck, H.E. and Singh, I.B. 1980. Depositional Sedimentary Environments. Springer-Verlag, New York, 551 p.

Reineck, H.E. and Wunderlich, F. 1968. Classification and origin of flaser and lenticular bedding. Sedimentology, v. 11, p. 99-104.

Reinson, G.E. 1984. Barrier-island and associated strand-plain systems. In: Facies Models. R.G. Walker (ed.). Geoscience Canada, Reprint Series 1, Geological Association of Canada, p. 119-140.

Reinson, G.E. 1992. Transgressive barrier island and estuarine systems. In: Facies Models: Response to Sea Level Change. R.W. Walker and N.P. James (eds.). Geological Association of Canada, p. 179-194.

Reiss, Z. 1984. Stratigraphy of phosphate deposits in Israel. Geological Survey of Israel, Bulletin, v. 34, p. 1-23.

Research Center for Marine Geosciences. ODSN plate tectonic reconstruction service. Ocean Drilling Stratigraphic Network. http://www.odsn.de/odsn/services/paleomap/paleomap/html. (March 2004).

Riggs, S.R., Cleary, W.J. and Snyder, S.W. 1995. Influence of inherited geologic framework on barrier shoreface morphology and dynamics. Marine Geology, v. 126, p. 213-234.

Rossetti, D.D.F. 1998. Facies architecture and sequential evolution of an incised-valley estuarine fill: the Cujupe Formation (Upper Cretaceous to ?Lower Teritary), Sao Luis Basin, Northern Brazil. Journal of Sedimentary Research, v. 68, p. 299-310.

Roy, P.S., Thom, B.G. and Wright, L.D. 1980. Holocene sequences on an embayed high-energy coast: an evolutionary model. Sedimentary Geology, v. 26, p. 1-19.

Roy, P.S., Williams, R.J., Jones, A.R., Yassini, R., Gibbs, P.J., Coates, B., West, R.J., Scanes, P.R., Hudson, J.P. and Nichol, S. 2001. Structure and function of southeast Australian estuaries. Estuarine, Coastal and Shelf Science, v. 53, p. 351-384.

Said, R. 1962. The Geology of Egypt. Elsevier Publishing Company, Amsterdam. 377 p.

Said, R. 1990. Cretaceous paleogeographic maps. In: The Geology of Egypt. R. Said (ed.) A.A. Balkema, Rotterdam, Netherlands, p. 439-449.

Said, R. and Issawi, B. 1963. Geology of the northern plateau, Bahariya Oasis, Egypt. Geological Survey of Egypt, 41 p.

Saunders, T. and Pemberton, S.G. 1986. Trace fossils and sedimentology of the Appaloosa Sandstone: Bearpaw-Horseshoe Canyon Formation transition, Dorothy, Alberta. Canadian Society of Petroleum Geologists Field Trip Guide Book, 117 p.

Savrda, C.E., 1991. Ichnology in sequence stratigraphic studies: an example from the Lower Paleocene of Alabama. Palaios, v. 6, p. 39-53.

Slaughter, B.H. and Thurmond, J.T. 1974. A Lower Cenomanian (Cretaceous) Ichthyofauna from the Bahariya Formation of Egypt. Annals of the Geological Survey of Egypt, v. 4, p. 25-40.

Smith, D.G. 1987. Meandering river point bar lithofacies models: modern and ancient examples compared. In: Recent Developments in the Fluvial Sedimentology. F.G. Ethridge, R.M. Flores and M.D. Harvey (eds.). Society of Economic Paleontologists and Mineralogists, Special Paper 39, p. 83-91.

Soliman, S.M. and El Badry, O. A. 1970. Nature of Cretaceous sedimentation in Western Desert, Egypt. American Association of Petroleum Geologists, Bulletin, v. 54, 12, p. 2349-2370.

Soliman, S.M. and El Badry, O. A. 1980. Petrology and tectonic framework of the Cretaceous, Baharia Oasis, Egypt. Egyptian Journal of Geology, v. 24, p. 11-51.

Soliman, S.M., Faris, M.I. and El Badry, O. 1970. Lithostratigraphy of the Cretaceous formations in the Bahariya Oasis, Western Desert, Egypt. Seventh Arab Petroleum Conference, Kuwait, II, Paper 59 (B-3).

Stromer, E. 1914. Die topographie und geologie der strecke Gharag-Baharije, nebst Ausfuhrungen uber die geologische Geschinchte Aegyptens. Aby. bayr. Akad. wissensch. Math. Naturw, v. 11, p. 1-78.

Tastet, J.P., Fenies, H. and Allen, G.P. 1986. Facies, sequences et geometrie d'une barre tidale estuarienne; le banc de Trompeloup dans l'estuaire de la Gironde. Bulletin de l'Institut de Geologie du Bassin d'Aquitaine, Bordeaux, v. 39; p. 165-184.

Taylor, A., Goldring, R. and Gowland, S. 2003. Analysis and application of ichnofabrics. Earth Science Reviews, v. 60, p. 227-259.

Tessier, B., Archer, A.W., Lanier, W.P. and Feldman, H.R. 1995. Comparison of ancient tidal rhythmites (Carboniferous of Kansas and Indiana, USA) with modern analogues (the Bay of Mont-Saint-Michel, France). In: Tidal Signatures in Modern and Ancient Sediments. B.W. Flemming and A. Bartholomae (eds.). Special Publication of the International Association of Sedimentologists, 24, p. 259-271.

Thomas, R.G., Smith, D.G., Wood, J.M., Visser, J., Calverley-Range, E.A. and Koster, E.H. 1987. Inclined heterolithic stratification – terminology, description, interpretation and significance. Sedimentary Geology, v. 53, p. 123-179.

Tucker, M.E. and Wright, V.P. 1990. Carbonate Sedimentology. Blackwell Scientific Publications, Oxford. 496 p.

Van Wagoner, J.C., Mitchum, R.M., Campion, K.M., Rahmanion, V.D. 1990. Siliciclastic sequence stratigraphy in well logs, core and outcrops. American Association of Petroleum Geologists, Methods in Exploration Series No. 7, 55 pp.

Visser, M.J. 1980. Neap-spring cycles reflected in Holocene subtidal large-scale bedform deposits: a preliminary note. Geology, v. 8, p. 543-546.

Walker, R.G and Plint, A.G. 1992. Wave- and storm-dominated shallow marine systems. In: Facies Models: Response to Sea Level Change. R.W. Walker and N.P. James (eds.). Geological Association of Canada, p. 219-238.

Walton, E.K. 1956. Limitations of graded bedding and alternative criteria of upward sequence in the rocks of the southern uplands. Edinburgh Geological Society Transactions, v. 16, p. 262-271.

Wehr, F., Youle, J. and Pemberton, S.G. 2002. Sequence stratigraphy and sedimentology of the Bahariya Formation, Khalda Concession, Western Desert, Egypt. American Association of Petroleum Geologists conference, Cairo, abstract.

Weimer, R.J., Howard, J.D. and Lindsay, D.R. 1982. Tidal flats and associated tidal channels. In: Sandstone Depositional Environments. P.A. Scholle and D. Spearing (eds.). American Association of Petroleum Geologists, Memoir 31, p. 191-245.

Wheatcroft, R.A. 1990. Preservation potential of sedimentary event layers. Geology, v. 18, p. 843-845.

Wightman, D.M., Pemberton, S.G., and Singh, C. 1987. Depositional modeling of the Upper Mannville (Lower Cretaceous), east central Alberta: implications for the recognition of brackish water deposits. In: Reservoir Sedimentology. R.W. Tillman and K.J. Weber (eds.). Society of Economic Paleontologists and Mineralogists, Special Publication 40, p. 189-220.

Wilgus, C.K., Hastings, B.S. Kendall, C.G.St.C., Posamentier, H.W., Ross, C.A., and Van Wagoner, J.C. (eds.). 1988. Sea-level Changes: An Integrated Approach. Society of Economic Paleontologists and Mineralogists, Special Publication 42, 407 p.

Williams, G.E. 1991. Upper Proterozoic tidal rhythmites, South Australia: sedimentary features, deposition, and implications for the Earth's paleorotation. In: Clastic Tidal Sedimentology. D.G. Smith, G.E. Reinson, B.A. Zaitlin, and R.A. Rahmani (eds.). Canadian Society of Petroleum Geologists, Memoir 16, p. 161-178.

Willis, B.J., Bhattacharya, J.P., Gabel, S.L. and White, C.D. 1999. Architecture of a tide-influenced river delta in the Frontier Formation of central Wyoming, USA. Sedimentology, v. 46, p. 667-688.

Woodroffe, C.D., Mulrennan, M.E. and Chappell, J. 1993. Estuarine infill and coastal progradation, southern van Diemen Gulf, northern Australia. Sedimentary Geology, v. 83, p. 257-275.

Wright, V.P. and Burchette, T.P. 1996. Shallow-water carbonate environments. In: Sedimentary Environments: Processes, Facies and Stratigraphy. H.G. Reading (ed.). Blackwell Science, Oxford. 688 p.

Zaitlin, B.A., Dalrymple, R.W. and Boyd, R. 1994. The stratigraphic organization of incised-valley systems associated with relative sea-level change. In: Incised-Valley Systems: Origin and Sedimentary Sequences. R.W Dalrymple, R. Boyd, and B.A. Zaitlin (eds.). Society of Sedimentary Geology, Special Publication 51, p. 45-60.

APPENDIX A

CORE LOGS

HAYAT-4
HAYAT-6
HAYAT-8
HAYAT-9
HAYAT-10
HAYAT-11
KENZ-6
SALAM-5
SALAM-8
SALAM-17
YASSER-3
YASSER-4
YASSER-5

TABLE OF SYMBOLS

PHYSICAL STRUCTURES

- Fine Lamination
- Planar Parallel Lamination
- Low Angle Stratification
- High Angle Stratification
- Trough Cross Stratification
- Bipolar Ripple Lamination
- Aggradation Ripple
- Current Ripple
- Wave Ripple
- Combined Flow Ripple
- Lenticular Bedding
- Flaser Bedding
- Wavy Bedding
- Contorted Bedding
- Syneresis Crack
- Microfault
- Water Escape Structure
- Load Cast/Flame Structure
- Load-Cast Ripple
- SLUMP Slump Structure

LITHOLOGY

- Sand
- Interbedded Shale and Sand
- Shaley Sand
- Shale
- Muddy Sand
- Mud Clast Breccia
- Interbedded Sand and Shale
- Calcareous Sand

TRACE FOSSILS

- *Arenicolites*
- *Asterosoma*
- *Chondrites*
- CRYPTIC Cryptic Bioturbation
- *Diplocraterion*
- Fugichnia
- *Gyrolithes*
- *Lockeia*
- *Macaronichnus*
- *Ophiomorpha*
- *Palaeophycus*
- *Planolites*
- *Rhizocorallium*
- *Rosselia*
- *Scolicia*
- *Siphonichnus*
- *Skolithos*
- *Teichichnus*
- *Thalassinoides*

CONTACTS

- Sharp
- Erosive
- Gradational
- Firmground

LITHOLOGIC ACCESSORIES

- Bioclastic Debris
- Oyster Shells
- Coated Grain
- Carbonaceous Debris
- Woody Debris
- Coal Laminae
- Py Pyrite
- Sid Siderite
- Gl Glaucony
- Fe Iron Staining
- Sideritized Mud Clasts
- Mud Clast Lag

BIOTURBATION

- Abundant
- Common
- Moderate
- Rare
- Absent

HYDROCARBON STAIN

- Abundant
- Common
- Moderate
- Rare
- Absent

Hayat-4

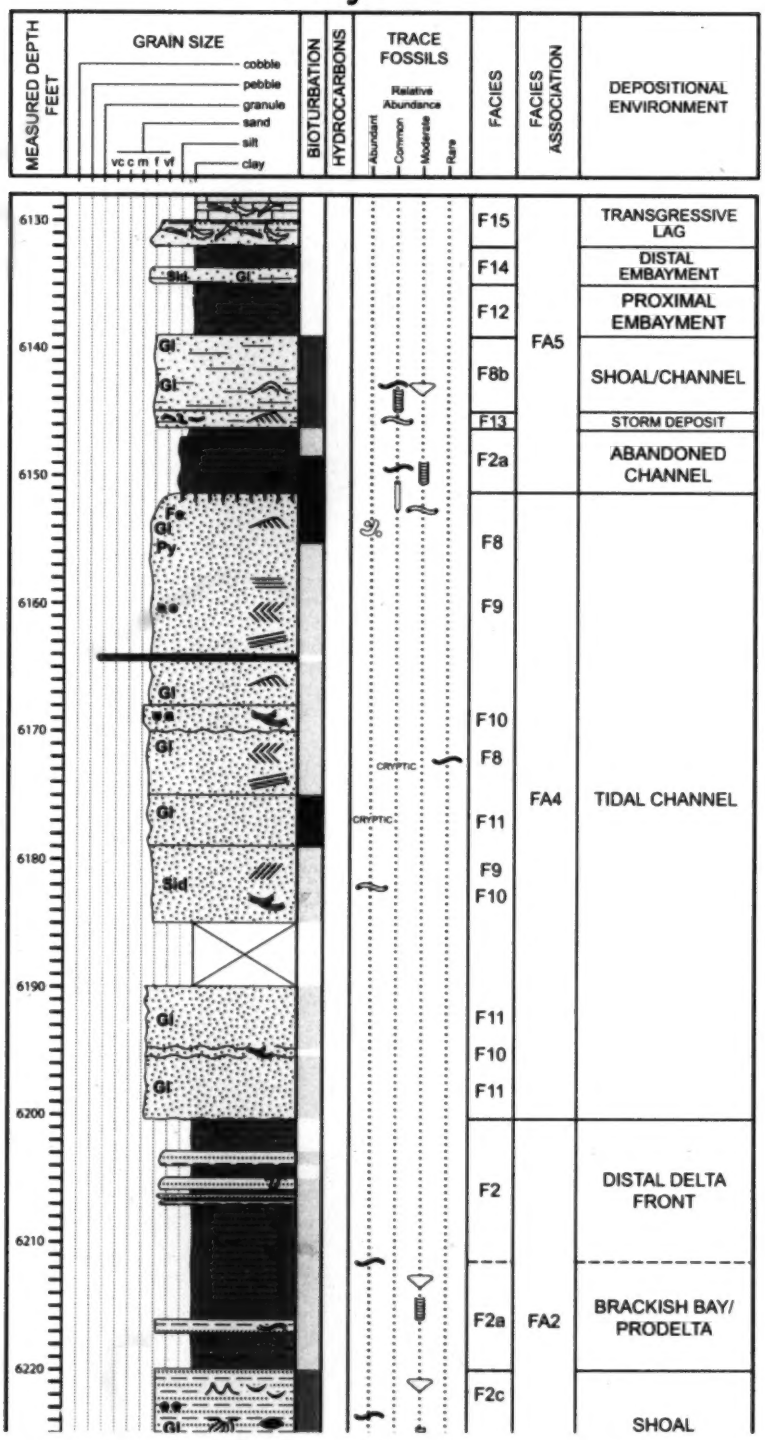
MEASURED DEPTH FEET
GRAIN SIZE
cobble
pebble
granule
sand
silt
clay
vc c m f vf
BIOTURBATION
HYDROCARBONS
TRACE FOSSILS
Relative Abundance
Abundant
Common
Moderate
Rare
FACIES
FACIES ASSOCIATION
DEPOSITIONAL ENVIRONMENT
6130
6140
6150
6160
6170
6180
6190
6200
6210
6220
Sid
Gl
Fe
Py
CRYPTIC
F15
F14
F12
F8b
F13
F2a
F8
F9
F10
F11
F2
F2a
F2c
FA5
FA4
FA2
TRANSGRESSIVE LAG
DISTAL EMBAYMENT
PROXIMAL EMBAYMENT
SHOAL/CHANNEL
STORM DEPOSIT
ABANDONED CHANNEL
TIDAL CHANNEL
DISTAL DELTA FRONT
BRACKISH BAY/ PRODELTA
SHOAL

Hayat-4 cont.

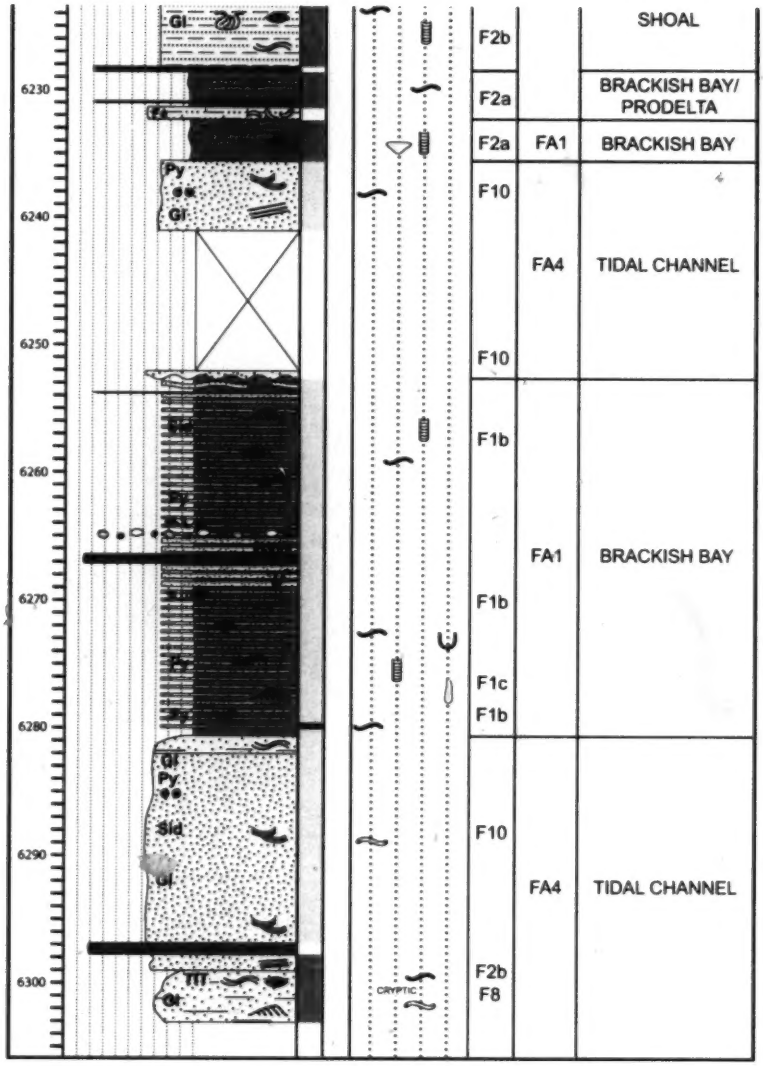
6230
6240
6250
6260
6270
6280
6290
6300
Gl
Py
Gl
Py
Gl
Py
Sid
Gl
Gl
CRYPTIC
F2b
F2a
F2a
F10
F10
F1b
F1b
F1c
F1b
F10
F2b
F8
SHOAL
BRACKISH BAY/ PRODELTA
FA1
BRACKISH BAY
FA4
TIDAL CHANNEL
FA1
BRACKISH BAY
FA4
TIDAL CHANNEL

Hayat-6

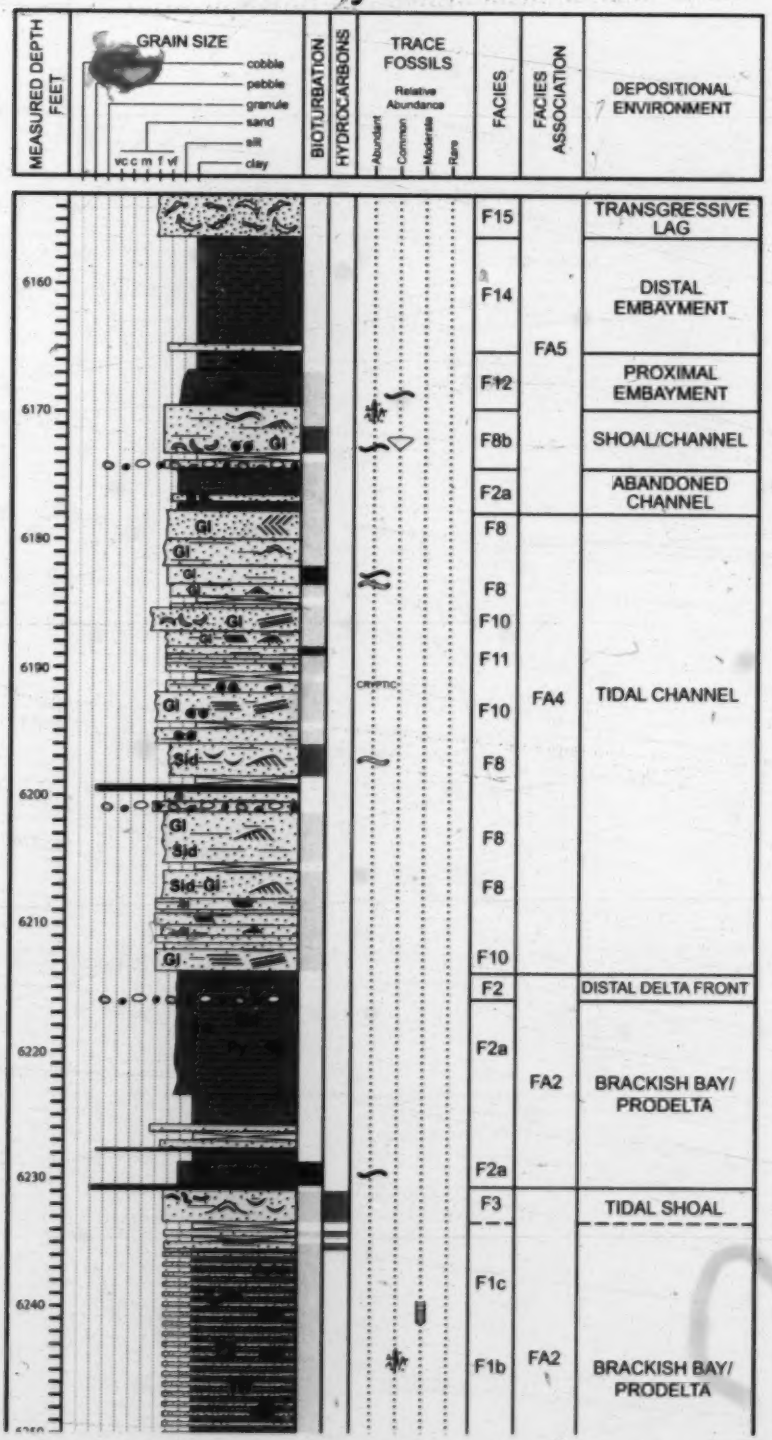
MEASURED DEPTH FEET
GRAIN SIZE
cobble
pebble
granule
sand
silt
clay
vc c m f vf
BIOTURBATION
HYDROCARBONS
TRACE FOSSILS
Relative Abundance
Abundant
Common
Moderate
Rare
FACIES
FACIES ASSOCIATION
DEPOSITIONAL ENVIRONMENT
6160
6170
6180
6190
6200
6210
6220
6230
6240
Gl
Sid
CRYPTIC
F15
TRANSGRESSIVE LAG
F14
DISTAL EMBAYMENT
FA5
F12
PROXIMAL EMBAYMENT
F8b
SHOAL/CHANNEL
F2a
ABANDONED CHANNEL
F8
F10
F11
FA4
TIDAL CHANNEL
F2
DISTAL DELTA FRONT
FA2
BRACKISH BAY/ PRODELTA
F3
TIDAL SHOAL
F1c
F1b

Hayat-6 cont.

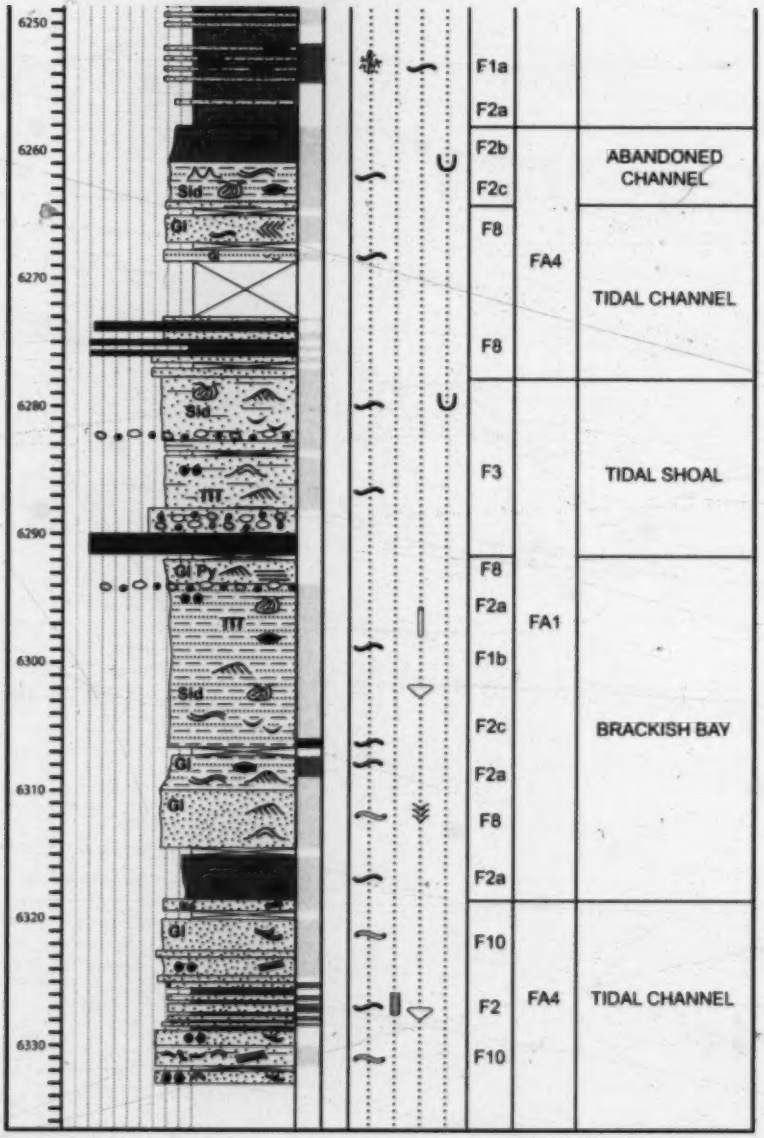
6250
6260
6270
6280
6290
6300
6310
6320
6330
Sid
Gl
Sid
TTT
Gl Py
TTT
Sid
Gl
Gl
Gl
F1a
F2a
F2b
F2c
F8
F8
F3
F8
F2a
F1b
F2c
F2a
F8
F2a
F10
F2
F10
FA4
FA4
FA1
FA4
ABANDONED CHANNEL
TIDAL CHANNEL
TIDAL SHOAL
BRACKISH BAY
TIDAL CHANNEL

Hayat-8

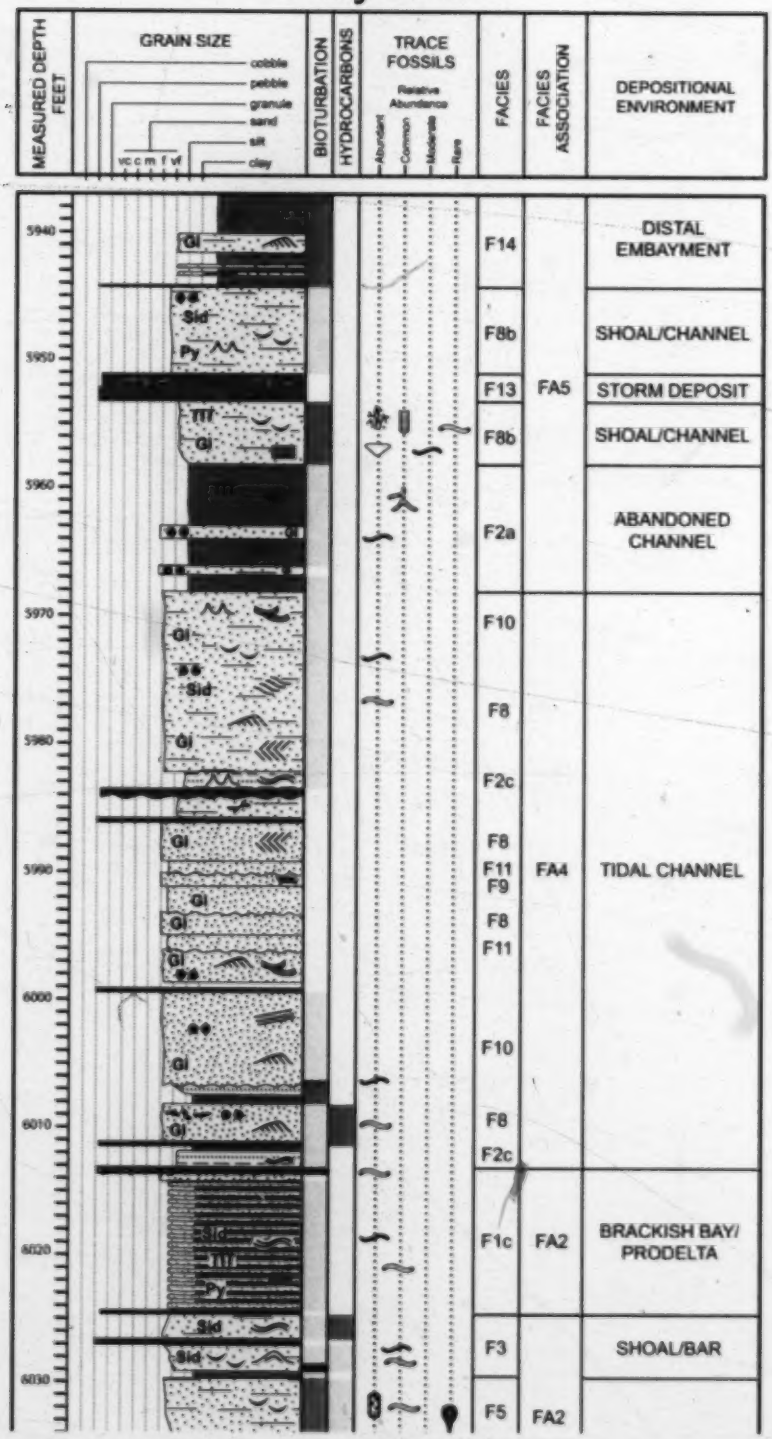
MEASURED DEPTH FEET
GRAIN SIZE
cobble
pebble
granule
sand
silt
clay
vc c m f vf
BIOTURBATION
HYDROCARBONS
TRACE FOSSILS
Relative Abundance
Abundant
Common
Moderate
Rare
FACIES
FACIES ASSOCIATION
DEPOSITIONAL ENVIRONMENT
5940
5950
5960
5970
5980
5990
6000
6010
6020
6030
Gl
Sid
Py
F14
DISTAL EMBAYMENT
F8b
SHOAL/CHANNEL
F13
FA5
STORM DEPOSIT
F8b
SHOAL/CHANNEL
F2a
ABANDONED CHANNEL
F10
F8
F2c
F8
F11
F9
FA4
TIDAL CHANNEL
F8
F11
F10
F8
F2c
F1c
FA2
BRACKISH BAY/ PRODELTA
F3
SHOAL/BAR
F5
FA2

Hayat-8 cont.

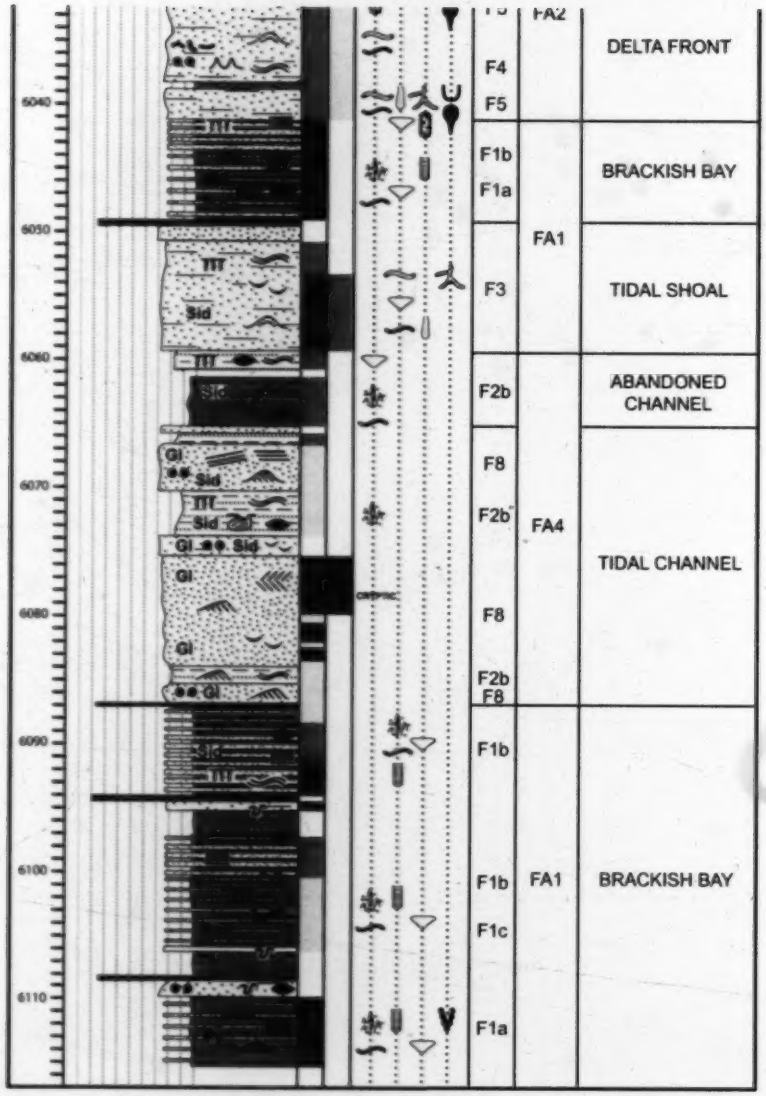
6040
6050
6060
6070
6080
6090
6100
6110
Sid
Gl
Slc
F4
F5
F1b
F1a
F3
F2b
F8
F2b
F8
F1b
F1b
F1c
F1a
FA2
FA1
FA4
FA1
DELTA FRONT
BRACKISH BAY
TIDAL SHOAL
ABANDONED CHANNEL
TIDAL CHANNEL
BRACKISH BAY

Hayat-9

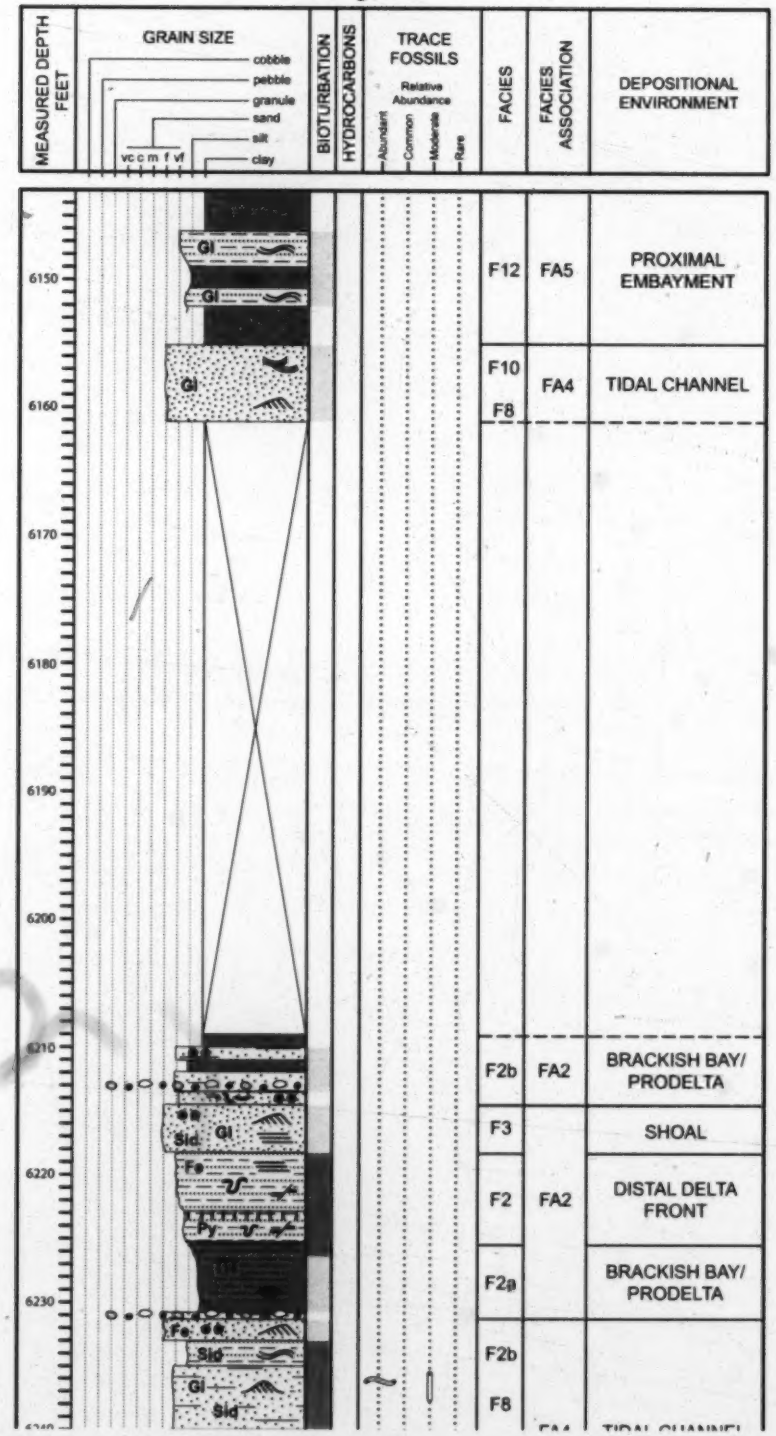
MEASURED DEPTH FEET
GRAIN SIZE
cobble
pebble
granule
sand
silt
clay
vc c m f vf
BIOTURBATION
HYDROCARBONS
TRACE FOSSILS
Relative Abundance
Abundant
Common
Moderate
Rare
FACIES
FACIES ASSOCIATION
DEPOSITIONAL ENVIRONMENT
6150
6160
6170
6180
6190
6200
6210
6220
6230
Gl
Sid.
Fe
Py
F12
FA5
PROXIMAL EMBAYMENT
F10
F8
FA4
TIDAL CHANNEL
F2b
FA2
BRACKISH BAY/ PRODELTA
F3
SHOAL
F2
DISTAL DELTA FRONT
F2a
BRACKISH BAY/ PRODELTA
F2b
F8
TIDAL CHANNEL

Hayat-9 cont.

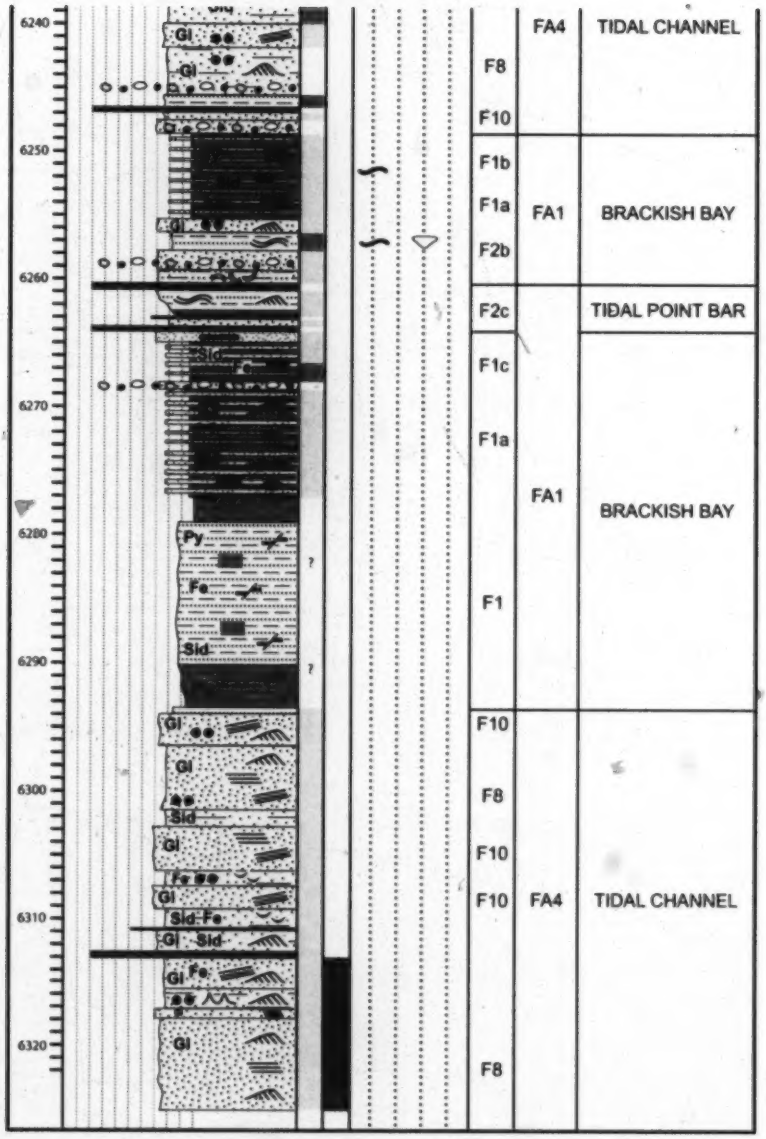
6240
6250
6260
6270
6280
6290
6300
6310
6320
Gl
Sid
Py
Fe
F8
F10
F1b
F1a
F2b
F2c
F1c
F1
FA4
FA1
TIDAL CHANNEL
BRACKISH BAY
TIDAL POINT BAR

Hayat-10

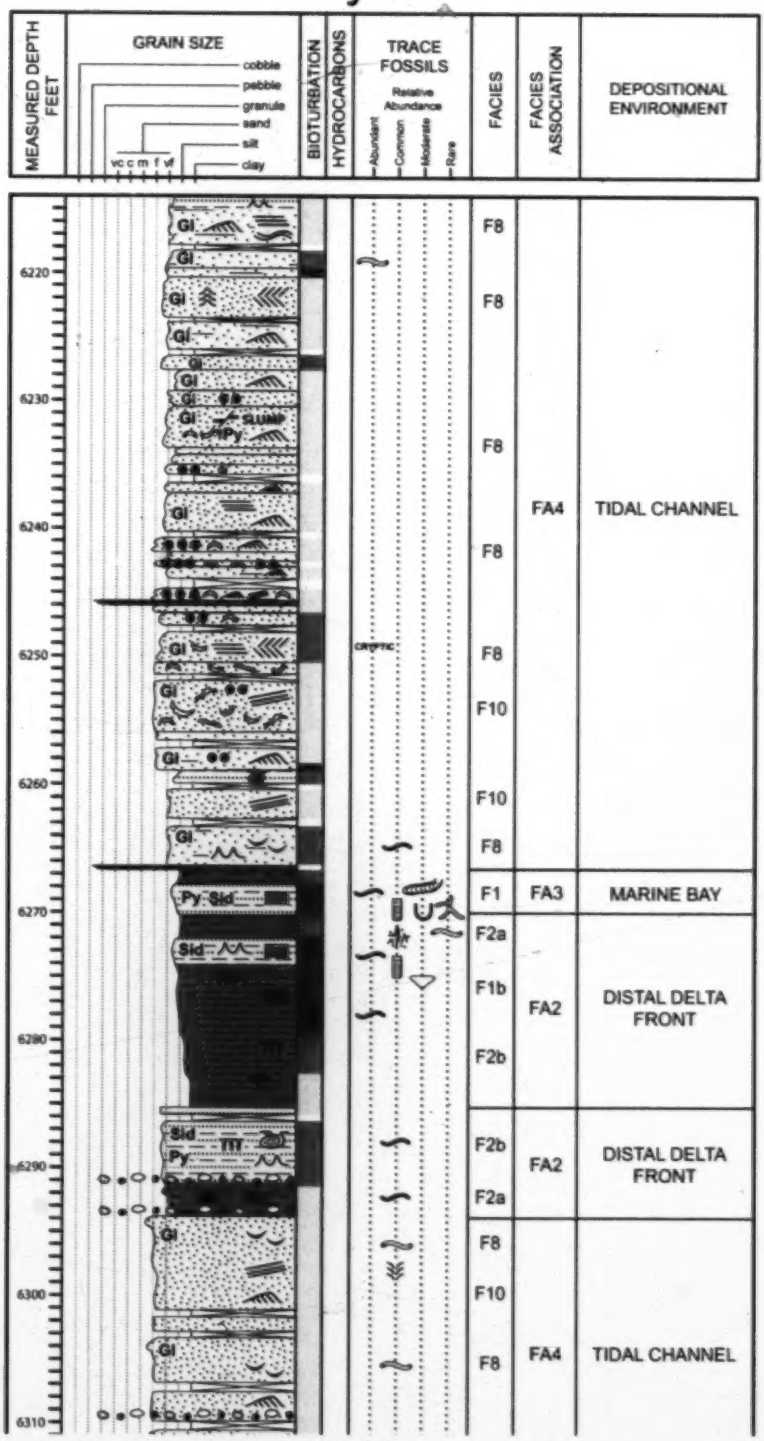
MEASURED DEPTH FEET
GRAIN SIZE
cobble
pebble
granule
sand
silt
clay
vc c m f vf
BIOTURBATION
HYDROCARBONS
TRACE FOSSILS
Relative Abundance
Abundant
Common
Moderate
Rare
FACIES
FACIES ASSOCIATION
DEPOSITIONAL ENVIRONMENT
6220
6230
6240
6250
6260
6270
6280
6290
6300
6310
Gl
SLUMP
Py
CRYPTIC
Py Sid
Sid
TTT
F8
F10
F1
F2a
F1b
F2b
FA4
FA3
FA2
TIDAL CHANNEL
MARINE BAY
DISTAL DELTA FRONT

Hayat-10 cont.

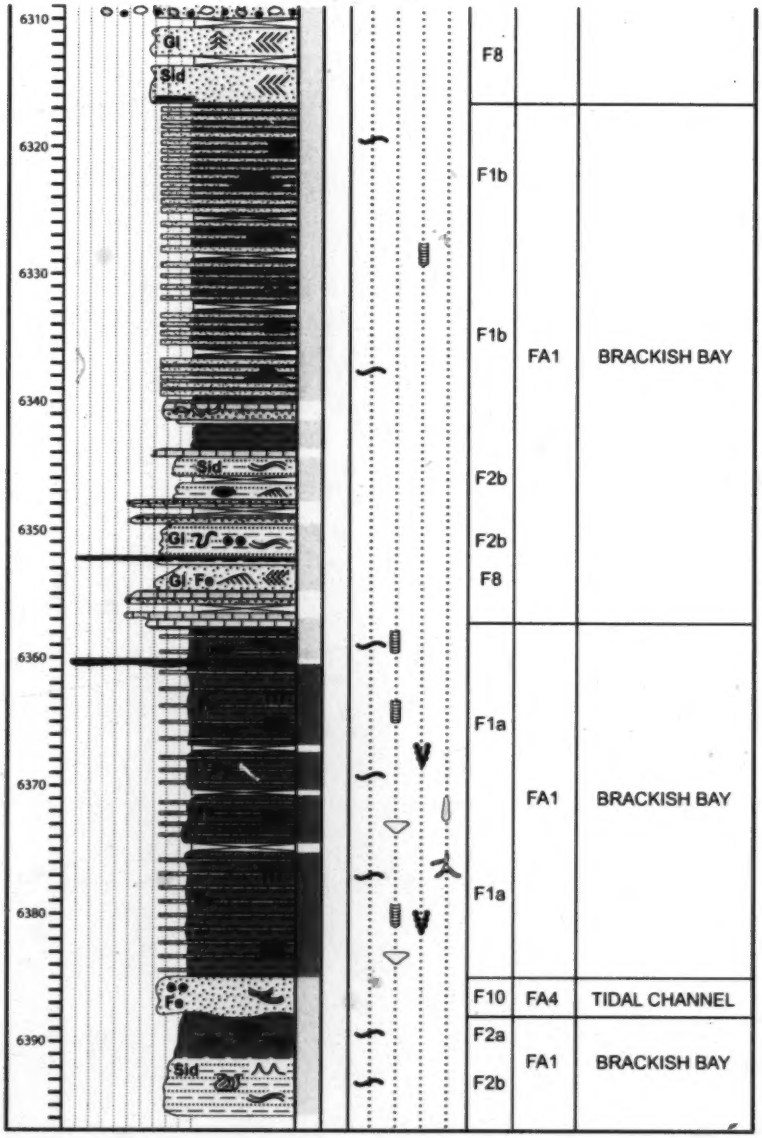

Hayat-11

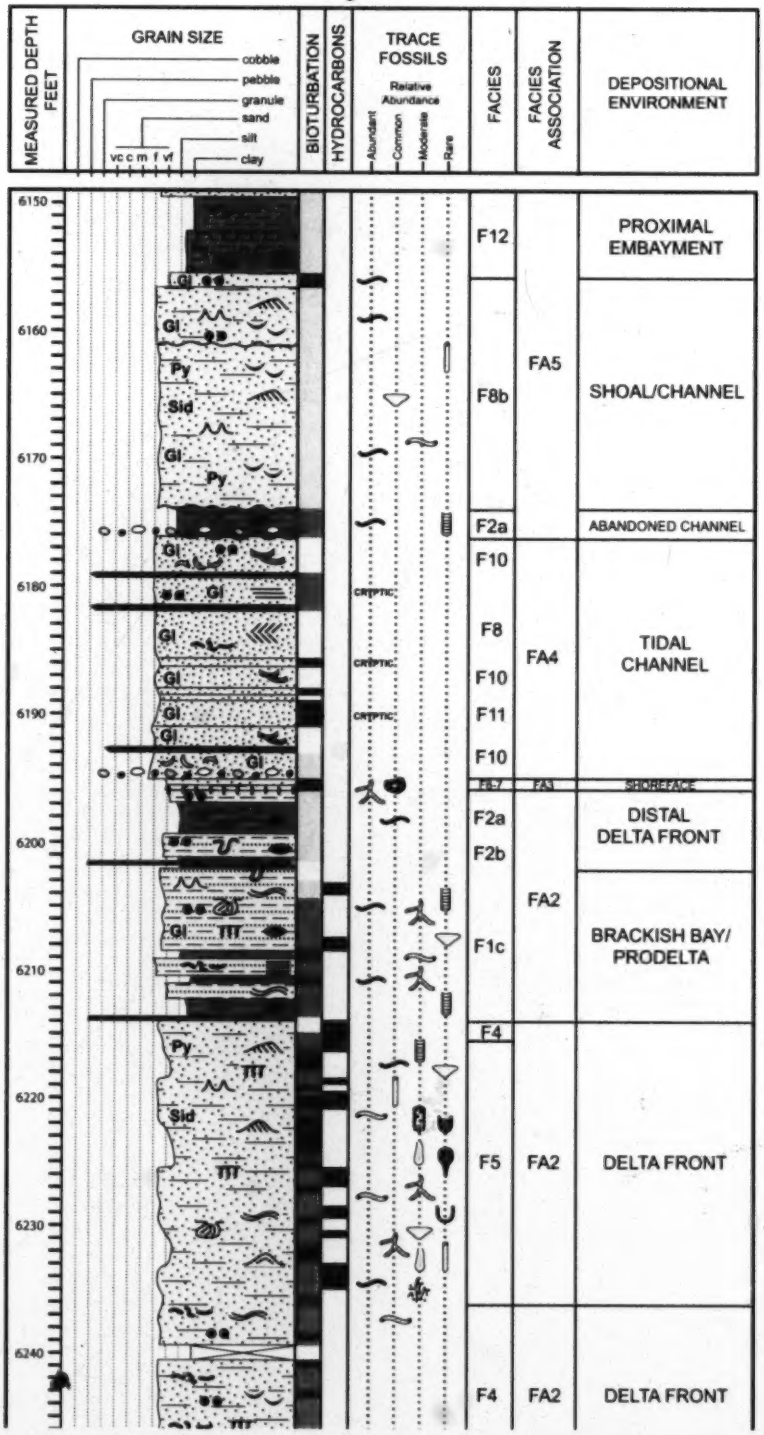
MEASURED DEPTH FEET
GRAIN SIZE
cobble
pebble
granule
sand
silt
clay
vc c m f vf
BIOTURBATION
HYDROCARBONS
TRACE FOSSILS
Relative Abundance
Abundant
Common
Moderate
Rare
FACIES
FACIES ASSOCIATION
DEPOSITIONAL ENVIRONMENT
6150
6160
6170
6180
6190
6200
6210
6220
6230
6240
Gl
Py
Sid
TTT
CRYPTIC
F12
PROXIMAL EMBAYMENT
F8b
FA5
SHOAL/CHANNEL
F2a
ABANDONED CHANNEL
F10
F8
F10
F11
F10
FA4
TIDAL CHANNEL
F6-7
FA3
SHOREFACE
F2a
F2b
DISTAL DELTA FRONT
F1c
FA2
BRACKISH BAY/ PRODELTA
F4
F5
FA2
DELTA FRONT
F4
FA2
DELTA FRONT

Hayat-11 cont.

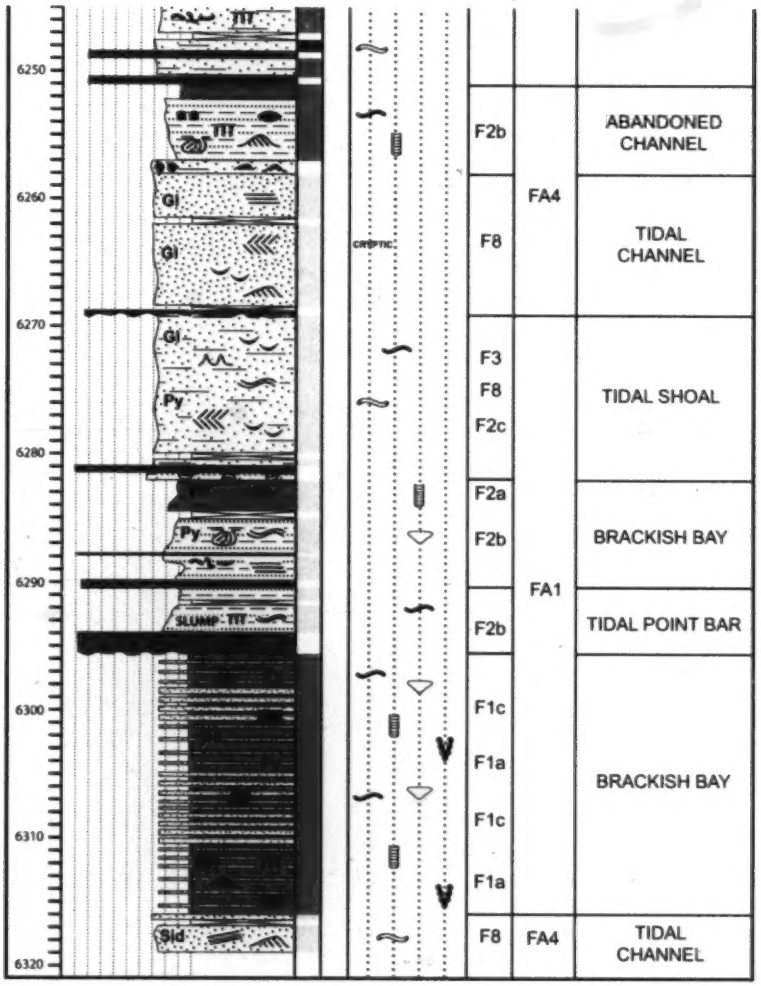

Kenz-6

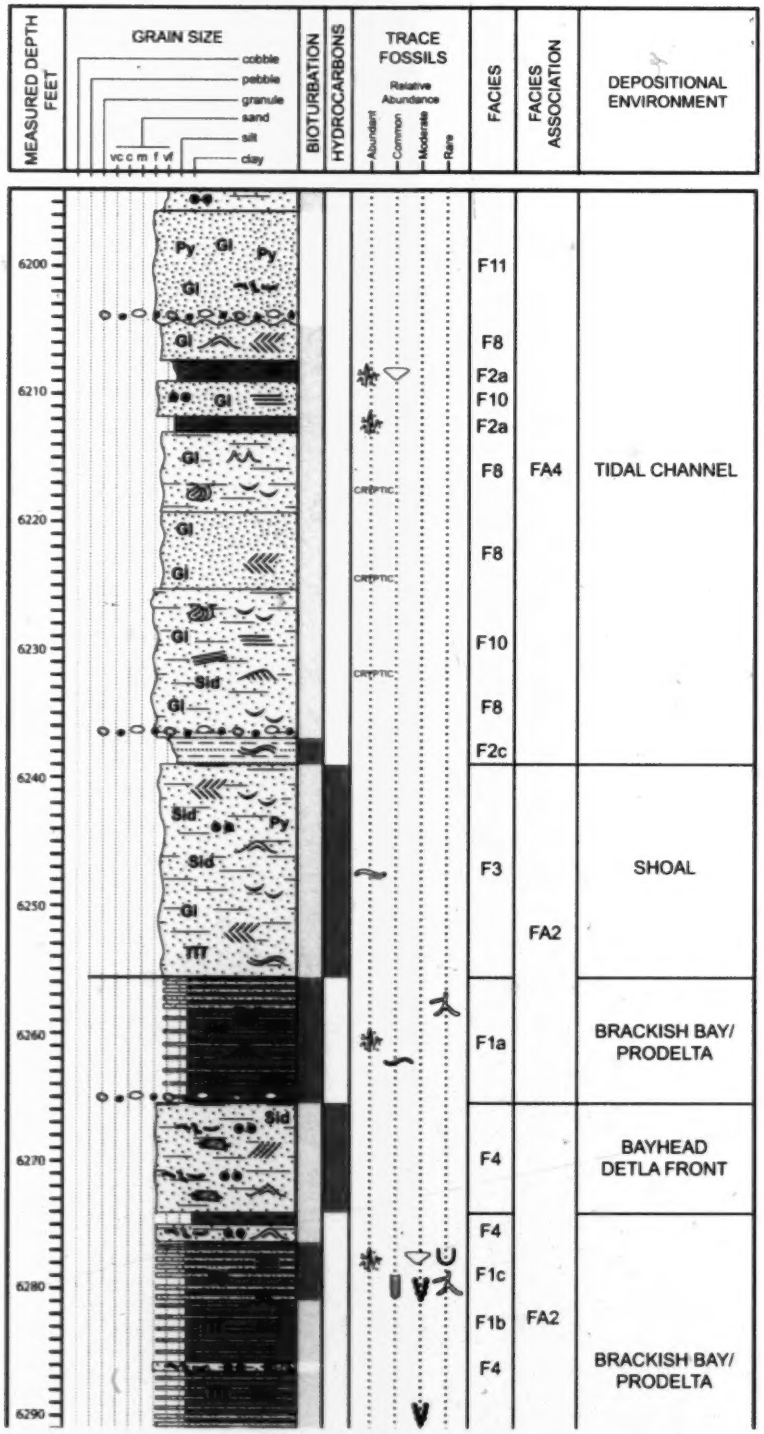
MEASURED DEPTH FEET
GRAIN SIZE
cobble
pebble
granule
sand
silt
clay
vc c m f vf
BIOTURBATION
HYDROCARBONS
TRACE FOSSILS
Relative Abundance
Abundant
Common
Moderate
Rare
FACIES
FACIES ASSOCIATION
DEPOSITIONAL ENVIRONMENT
6200
6210
6220
6230
6240
6250
6260
6270
6280
6290
Py
Gl
Sid
TIT
CRYPTIC
F11
F8
F2a
F10
F2a
F8
F8
F10
F8
F2c
F3
F1a
F4
F4
F1c
F1b
F4
FA4
FA2
FA2
TIDAL CHANNEL
SHOAL
BRACKISH BAY/ PRODELTA
BAYHEAD DETLA FRONT
BRACKISH BAY/ PRODELTA

Kenz-6 cont.

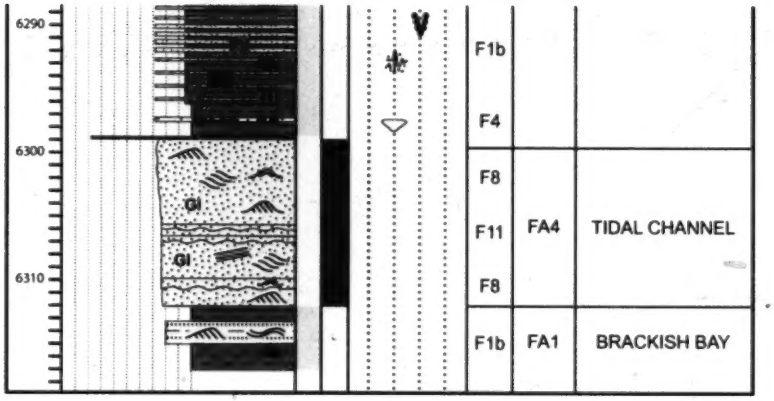
6290
6300
6310
Gl
Gl
F1b
F4
F8
F11
F8
FA4
TIDAL CHANNEL
F1b
FA1
BRACKISH BAY

Salam-5

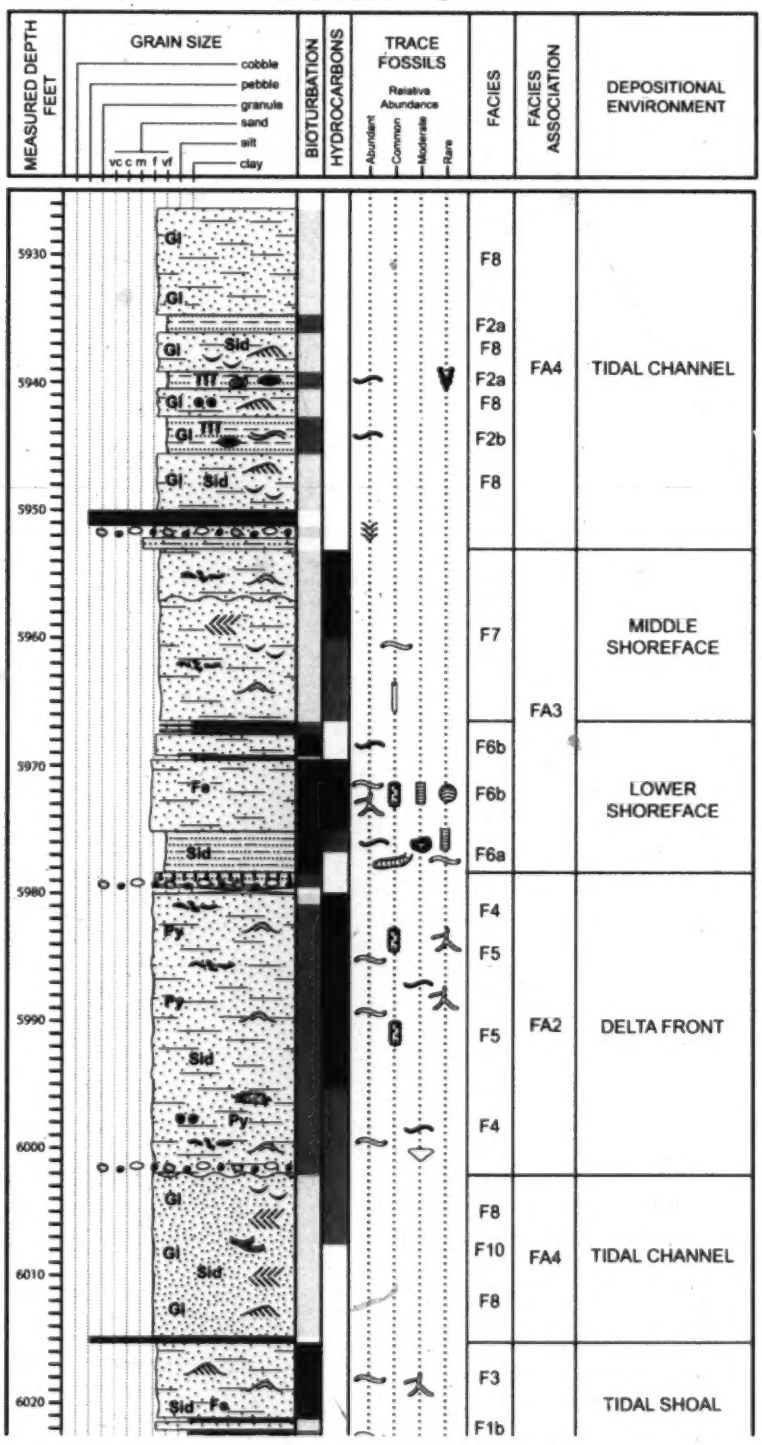
MEASURED DEPTH FEET
GRAIN SIZE
cobble
pebble
granule
sand
silt
clay
vc c m f vf
BIOTURBATION
HYDROCARBONS
TRACE FOSSILS
Relative Abundance
Abundant
Common
Moderate
Rare
FACIES
FACIES ASSOCIATION
DEPOSITIONAL ENVIRONMENT
5930
5940
5950
5960
5970
5980
5990
6000
6010
6020
Gl
Sid
Fe
Py
F8
F2a
F2b
F7
F6b
F6a
F4
F5
F10
F3
F1b
FA4
FA3
FA2
TIDAL CHANNEL
MIDDLE SHOREFACE
LOWER SHOREFACE
DELTA FRONT
TIDAL SHOAL

Salam-5 cont.

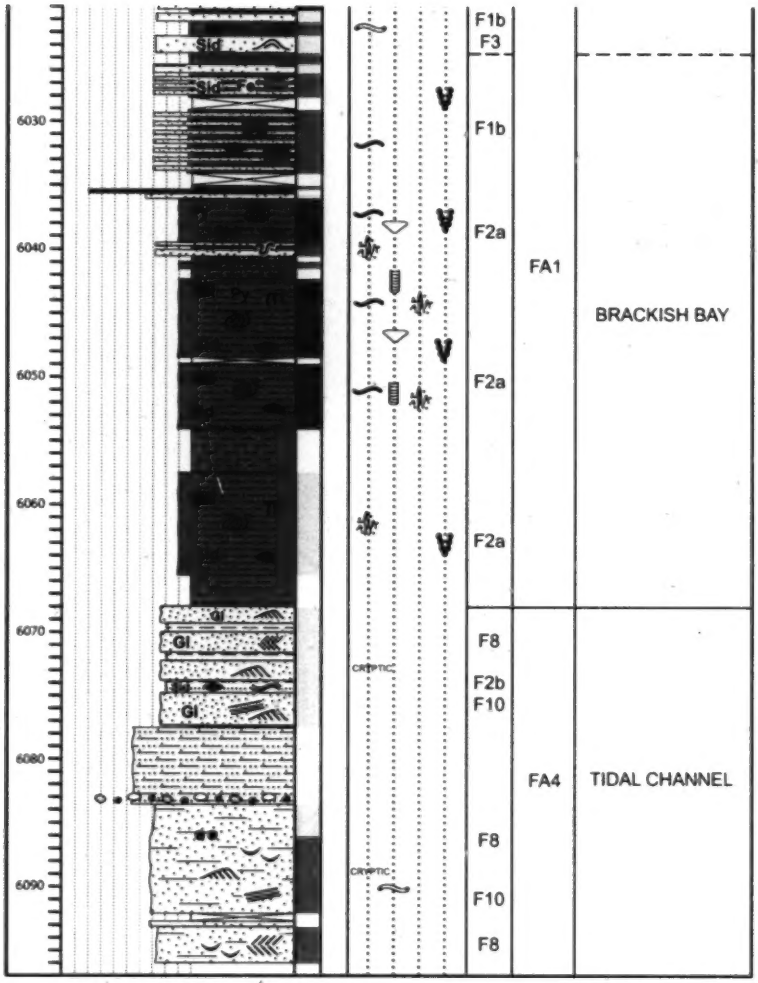
6030
6040
6050
6060
6070
6080
6090
Slcf
Slc
Gl
Gl
CRYPTIC
CRYPTIC
F1b
F3
F1b
F2a
F2a
F2a
F8
F2b
F10
F8
F10
F8
FA1
FA4
BRACKISH BAY
TIDAL CHANNEL

Salam-8

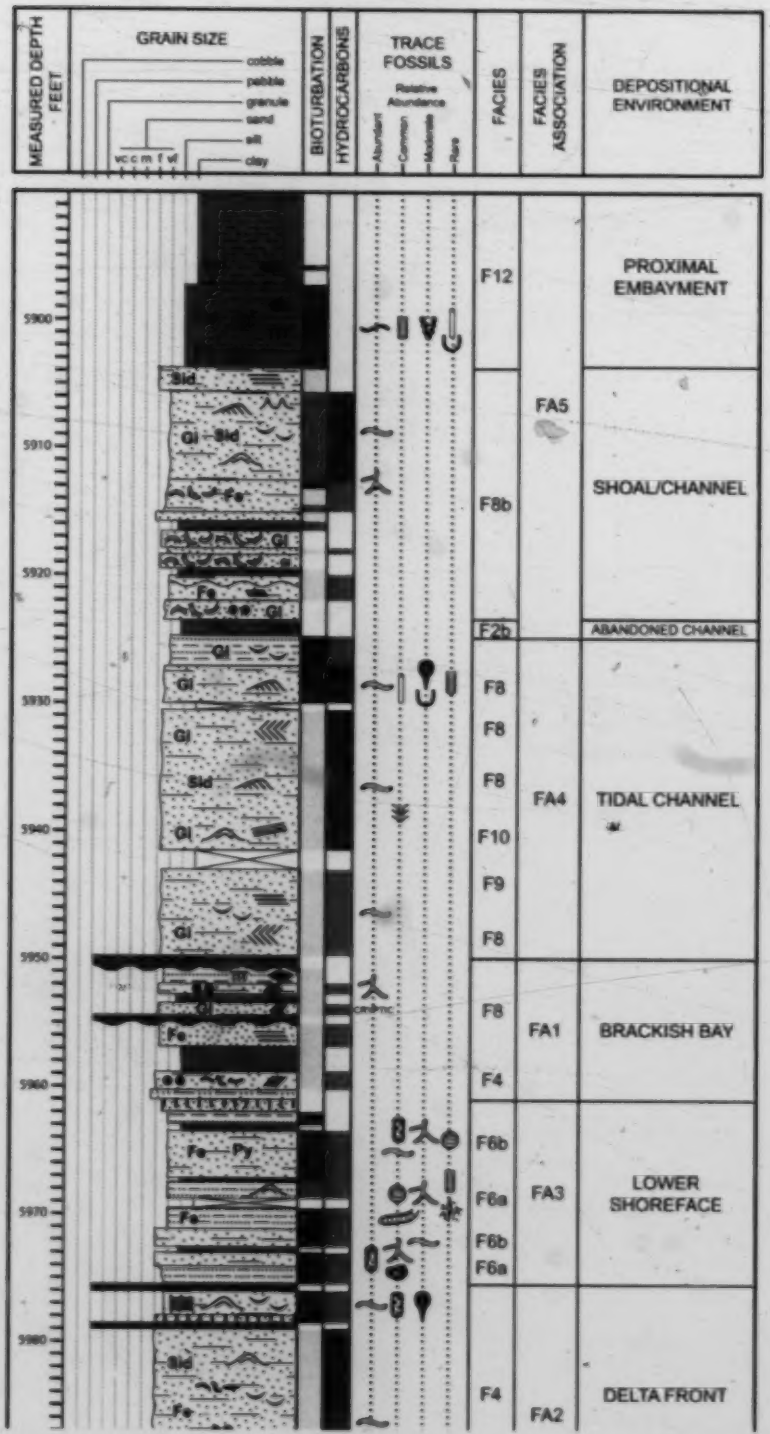
MEASURED DEPTH FEET
GRAIN SIZE
cobble
pebble
granule
sand
silt
clay
vc c m f vf
BIOTURBATION
HYDROCARBONS
TRACE FOSSILS
Relative Abundance
Abundant
Common
Moderate
Rare
FACIES
FACIES ASSOCIATION
DEPOSITIONAL ENVIRONMENT
5900
5910
5920
5930
5940
5950
5960
5970
5980
Sid
Gl
Fe
Py
F12
F8b
F2b
F8
F10
F9
F4
F6b
F6a
FA5
FA4
FA1
FA3
FA2
PROXIMAL EMBAYMENT
SHOAL/CHANNEL
ABANDONED CHANNEL
TIDAL CHANNEL
BRACKISH BAY
LOWER SHOREFACE
DELTA FRONT

Salam-8 cont.

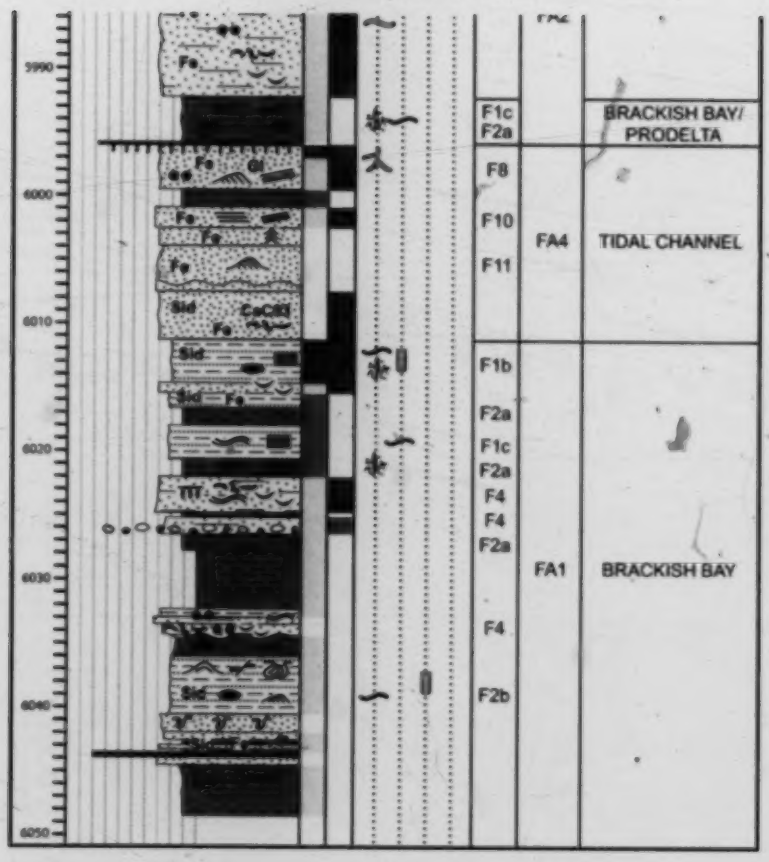
5990
6000
6010
6020
6030
6040
6050
Fe
Sid
CaCO3
F1c
F2a
F8
F10
F11
F1b
F2a
F1c
F2a
F4
F4
F2a
F4
F2b
FA4
FA1
BRACKISH BAY/
PRODELTA
TIDAL CHANNEL
BRACKISH BAY

Salam-17

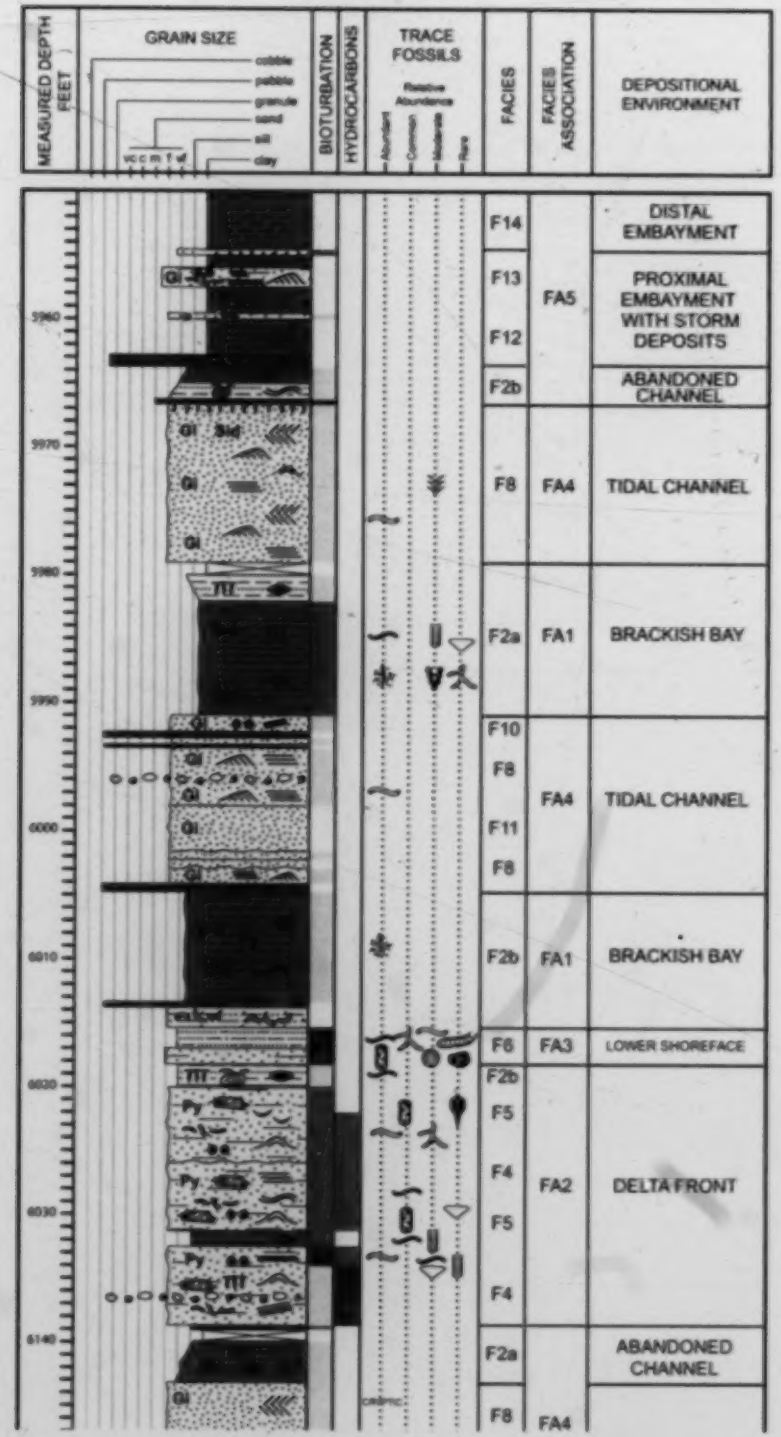
MEASURED DEPTH FEET
GRAIN SIZE
cobble
pebble
granule
sand
silt
clay
vc c m f vf
BIOTURBATION
HYDROCARBONS
TRACE FOSSILS
Relative Abundance
Abundant
Common
Moderate
Rare
FACIES
FACIES ASSOCIATION
DEPOSITIONAL ENVIRONMENT
5960
5970
5980
5990
6000
6010
6020
6030
6140
F14
DISTAL EMBAYMENT
F13
F12
FA5
PROXIMAL EMBAYMENT WITH STORM DEPOSITS
F2b
ABANDONED CHANNEL
F8
FA4
TIDAL CHANNEL
F2a
FA1
BRACKISH BAY
F10
F8
F11
F8
FA4
TIDAL CHANNEL
F2b
FA1
BRACKISH BAY
F6
FA3
LOWER SHOREFACE
F2b
F5
F4
F5
F4
FA2
DELTA FRONT
F2a
ABANDONED CHANNEL
F8
FA4

Salam-17 cont.

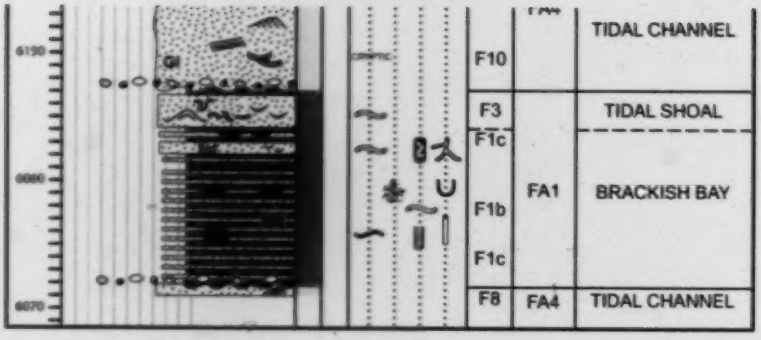

Yasser-3

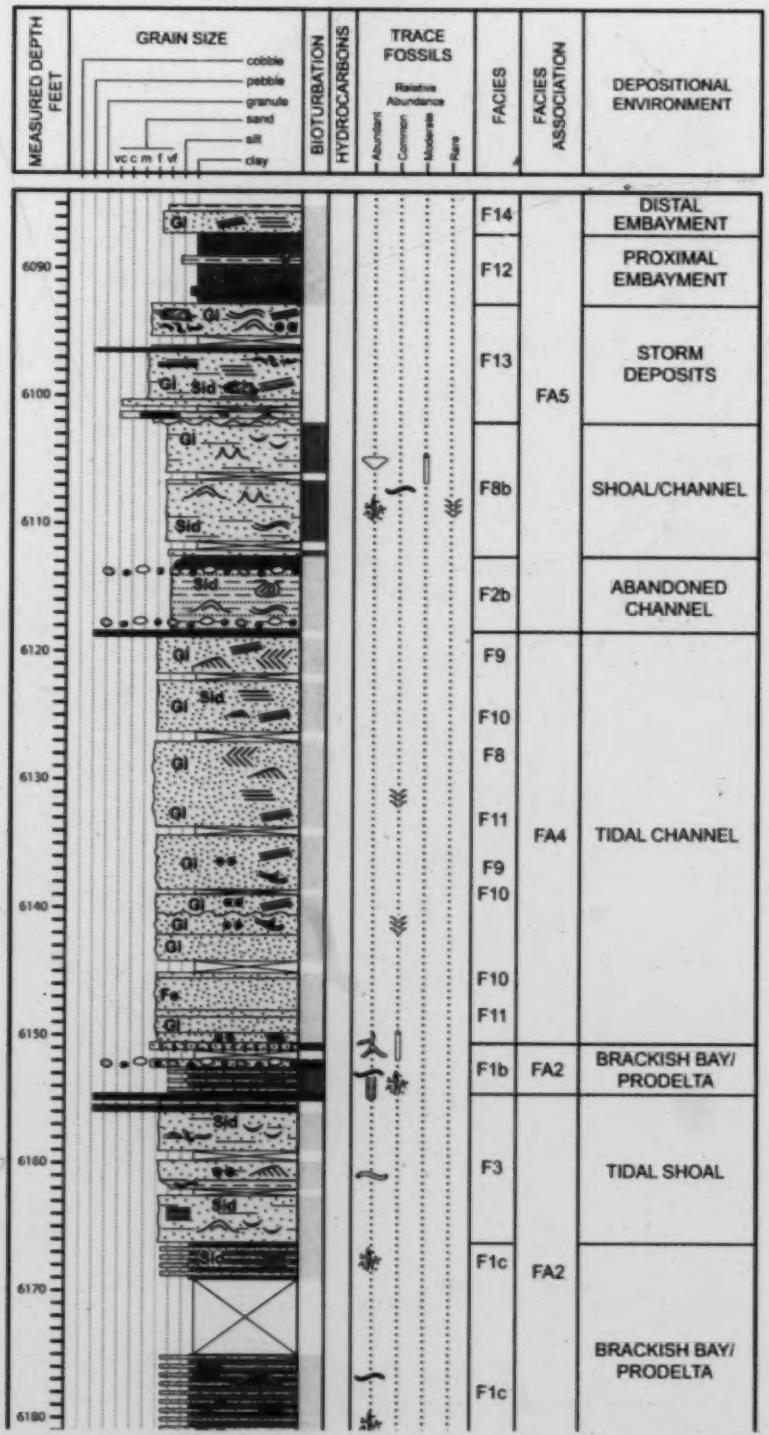
MEASURED DEPTH FEET
GRAIN SIZE
cobble
pebble
granule
sand
silt
clay
vc c m f vf
BIOTURBATION
HYDROCARBONS
TRACE FOSSILS
Relative Abundance
Abundant
Common
Moderate
Rare
FACIES
FACIES ASSOCIATION
DEPOSITIONAL ENVIRONMENT
6090
6100
6110
6120
6130
6140
6150
6160
6170
6180
Gl
Sid
Fe
F14
F12
F13
F8b
F2b
F9
F10
F8
F11
F1b
F3
F1c
FA5
FA4
FA2
DISTAL EMBAYMENT
PROXIMAL EMBAYMENT
STORM DEPOSITS
SHOAL/CHANNEL
ABANDONED CHANNEL
TIDAL CHANNEL
BRACKISH BAY/ PRODELTA
TIDAL SHOAL
BRACKISH BAY/ PRODELTA

Yasser-3 cont.

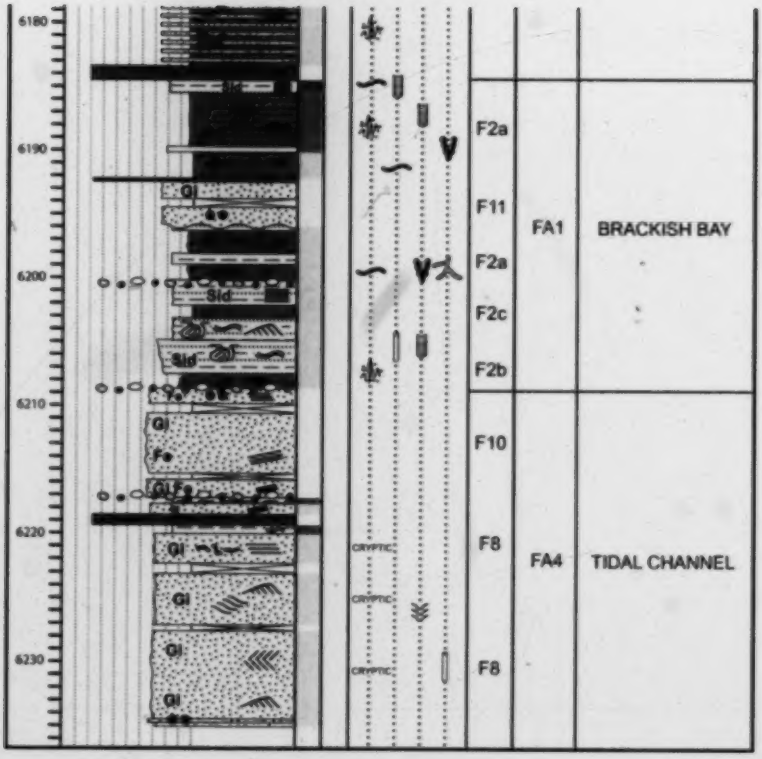

Yasser-4

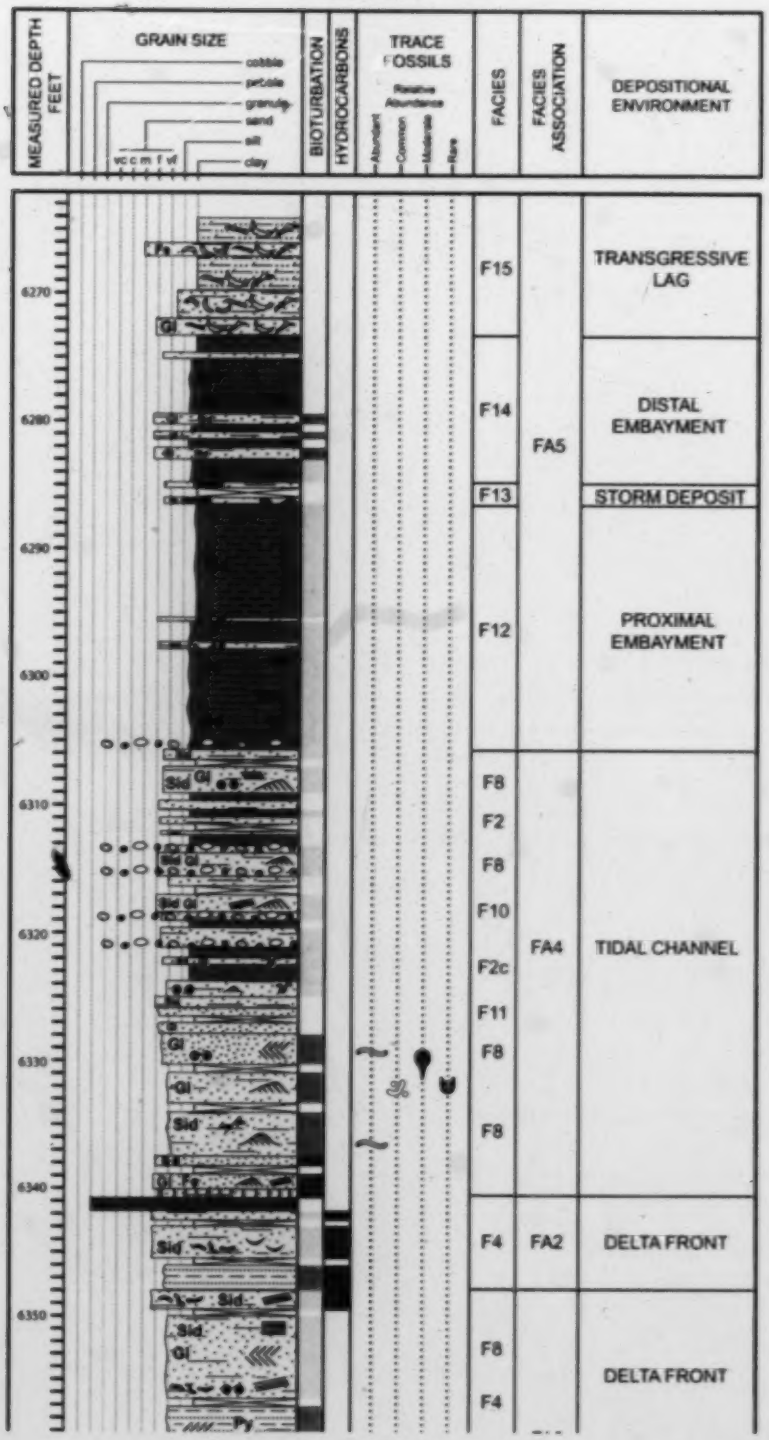
MEASURED DEPTH FEET
GRAIN SIZE
cobble
pebble
granule
sand
silt
clay
vf c m f vf
BIOTURBATION
HYDROCARBONS
TRACE FOSSILS
Relative Abundance
Abundant
Common
Moderate
Rare
FACIES
FACIES ASSOCIATION
DEPOSITIONAL ENVIRONMENT
6270
6280
6290
6300
6310
6320
6330
6340
6350
F15
TRANSGRESSIVE LAG
F14
DISTAL EMBAYMENT
FA5
F13
STORM DEPOSIT
F12
PROXIMAL EMBAYMENT
F8
F2
F8
F10
F2c
F11
F8
F8
FA4
TIDAL CHANNEL
F4
FA2
DELTA FRONT
F8
F4
DELTA FRONT
Sid
Gl
Py

Yasser-4 cont.

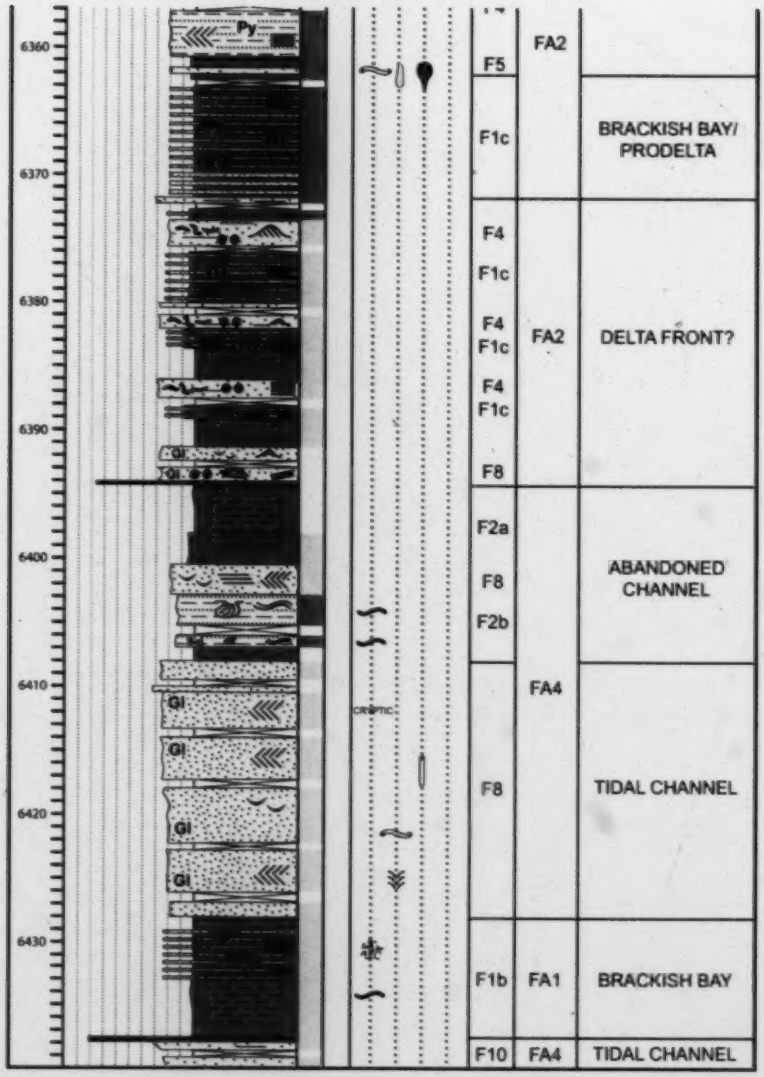

Yasser-5

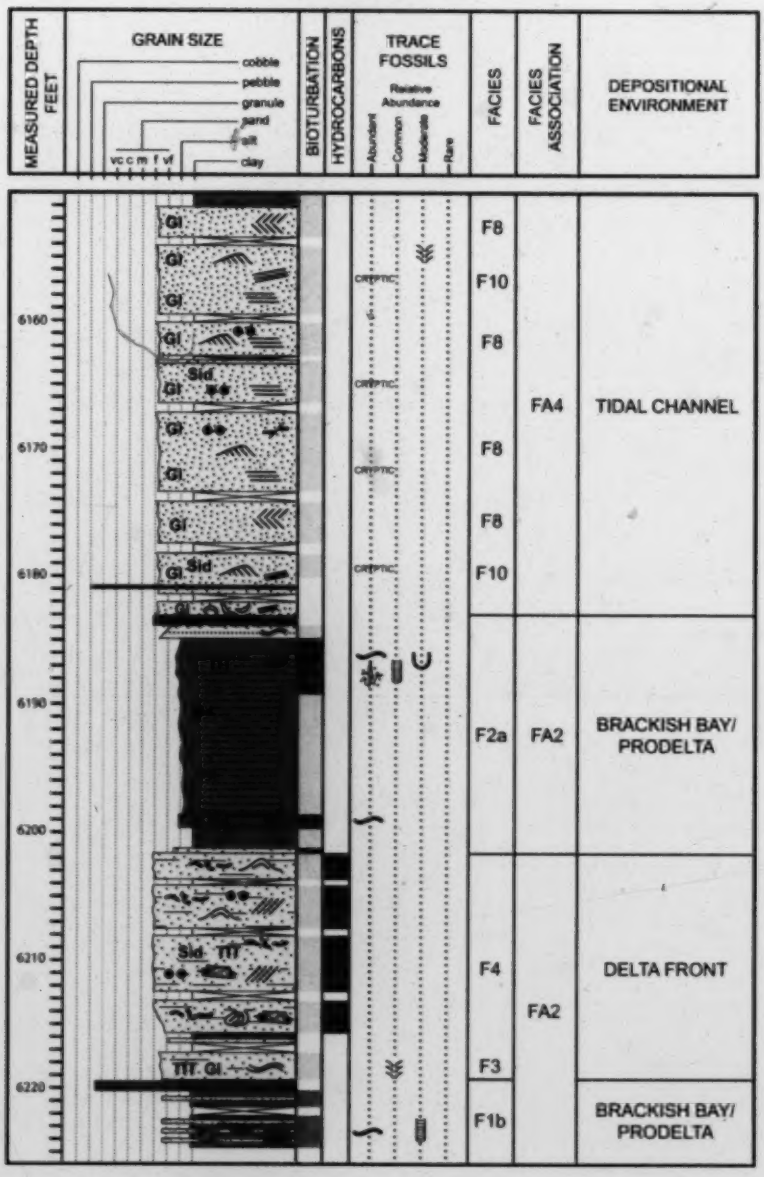
MEASURED DEPTH FEET
GRAIN SIZE
cobble
pebble
granule
sand
silt
clay
vc c m f vf
BIOTURBATION
HYDROCARBONS
TRACE FOSSILS
Relative Abundance
Abundant
Common
Moderate
Rare
FACIES
FACIES ASSOCIATION
DEPOSITIONAL ENVIRONMENT
6160
6170
6180
6190
6200
6210
6220
Gl
Sid
CRYPTIC
F8
F10
F8
F8
F8
F10
F2a
F4
F3
F1b
FA4
FA2
FA2
TIDAL CHANNEL
BRACKISH BAY/ PRODELTA
DELTA FRONT
BRACKISH BAY/ PRODELTA